

Washington University in St. Louis

Washington University Open Scholarship

All Theses and Dissertations (ETDs)

5-24-2011

Redox Homeostasis in Cyanobacteria

Jeffrey Cameron

Washington University in St. Louis

Follow this and additional works at: <https://openscholarship.wustl.edu/etd>

Recommended Citation

Cameron, Jeffrey, "Redox Homeostasis in Cyanobacteria" (2011). *All Theses and Dissertations (ETDs)*. 860.

<https://openscholarship.wustl.edu/etd/860>

This Dissertation is brought to you for free and open access by Washington University Open Scholarship. It has been accepted for inclusion in All Theses and Dissertations (ETDs) by an authorized administrator of Washington University Open Scholarship. For more information, please contact digital@wumail.wustl.edu.

WASHINGTON UNIVERSITY

Division of Biology and Biomedical Sciences

Program in Plant Biology

Dissertation Examination Committee:

Himadri B. Pakrasi, Chair

Robert E. Blankenship

Tuan-Hua David Ho

Joseph M. Jez

Robert G. Kranz

Thomas J. Smith

REDOX HOMEOSTASIS IN CYANOBACTERIA

by

Jeffrey Carlyle Cameron

A dissertation presented to the
Graduate School of Arts and Sciences
of Washington University in
partial fulfillment of the
requirements for the degree
of Doctor of Philosophy

May 2011

Saint Louis, Missouri

Copyright by
Jeffrey Carlyle Cameron
2011

ABSTRACT OF THE DISSERTATION

Redox Homeostasis in Cyanobacteria

by

Jeffrey Carlyle Cameron

Doctor of Philosophy in Biology and Biomedical Sciences (Plant Biology)

Washington University in St. Louis, 2011

Professor Himadri B. Pakrasi, Chairman

Oxygenic photosynthetic organisms utilize high-energy electron transfer chains comprised of redox active intermediates and light harvesting complexes. While oxygen is a necessary byproduct of water oxidation and the source of photosynthetic electrons, its presence is also dangerous because leakage of electrons and excitation energy can interact with molecular oxygen to generate reactive oxygen species (ROS). Elaborate antioxidant networks and redox buffering systems have evolved to protect photosynthetic organisms from the threat of ROS. Glutathione (GSH) is a multifunctional molecule that is involved in core metabolism, detoxification of xenobiotics and in maintenance of cellular redox poise. The ubiquitous nature of glutathione and its importance to cellular metabolism has been observed in many organisms, however the specific roles of glutathione in photosynthetic organisms are not fully understood. To address these questions, we have generated several mutants in the glutathione biosynthesis and degradation pathways in the model organism *Synechocystis* sp. PCC 6803 (*Synechocystis* 6803), an oxygenic photosynthetic cyanobacterium.

We utilized targeted homologous recombination to generate deletion mutants of glutamate-cysteine ligase (GshA) and glutathione synthetase (GshB) in *Synechocystis* 6803. Our results indicate that GshA activity is essential for growth in cyanobacteria because we were unable to isolate a fully segregated $\Delta gshA$ deletion mutant. We did isolate a $\Delta gshB$ mutant strain that accumulates the biosynthetic intermediate γ -glutamylcysteine (γ -EC) instead of GSH. In this work, I have characterized the physiology of the $\Delta gshB$ mutant following environmental, genetic and redox perturbations.

The results presented here also shed light on the dynamic nature of the low-molecular weight thiol pool in cyanobacteria. We quantified the levels of cellular thiols in *Synechocystis* 6803 during exposure to multiple environmental and redox perturbations and found that conditions promoting increased cellular metabolism and increased ROS production, including during high-light treatment and photomixotrophic growth, lead to higher cellular thiol levels. Furthermore, the intracellular pools of thiols decrease when the cell exhibits reduced metabolic capacity during conditions such as nutrient deprivation and dark incubation. Sulfate limitation results in dramatically decreased cellular thiol contents in a short period of time. We found that the $\Delta gshB$ strain is sensitive to sulfate limitation and exhibits delayed recovery upon sulfate repletion, indicating that GSH is important for acclimation to sulfate limiting conditions. To facilitate our understanding of GSH degradation in *Synechocystis* 6803 during sulfate limitation, we generated a mutant lacking γ -glutamyltranspeptidase (Ggt), an enzyme

with GSH degradation activity. However, the Δggt mutant still exhibited GSH degradation during sulfate depletion, indicating the presence of an alternative system or mechanism. We did find increased levels of GSH in the growth media of the Δggt strain compared to the WT, which suggests a role in GSH uptake or prevention of leakage.

Our results demonstrate that GSH is essential for protection from multiple environmental and redox perturbations in cyanobacteria. However, there are many pathways involved in maintenance of redox homeostasis in cyanobacteria. Therefore, we also aimed to determine whether these pathways function cooperatively to ameliorate damage from ROS. Several flavodiiron (Flv) proteins have been identified in *Synechocystis* 6803 that are involved in reduction of O₂ to H₂O without the formation of ROS intermediates. However, single $\Delta flv3$ mutants do not exhibit severe growth defects under normal conditions. Therefore, we generated a $\Delta gshB/\Delta flv3$ mutant to examine whether these systems cooperate to maintain redox homeostasis. Our results show that the $\Delta gshB/\Delta flv3$ mutant exhibits reduced growth than either of the single mutants when grown on solid media, suggesting a degree of interaction between these pathways in cyanobacteria.

ACKNOWLEDGEMENTS

First, I would like to thank my loving wife Jenn for her support and encouragement during my graduate career. I could not have accomplished this task without her. I would also like to thank my entire family for their support and for encouraging me to do something that I enjoy. In particular I need to thank my parents, Doug and Sally, and my siblings, Derek, Sarah and Michael for their perspectives and support over the years. I am very lucky to have wonderful grandparents that have also given me lots of support throughout my lifetime, so I would like to thank them too.

I also would like to thank my thesis advisor Himadri Pakrasi. He gave me the freedom to explore many avenues of research while successfully helping me to reach my goals. I also want to thank the past and present members of the Pakrasi lab that I have had the pleasure of interacting with over the years. It is because of these people that I enjoyed coming to work each and every day. I would especially like to thank Michelle Liberton, Kimberly Wegener and Lawrence Page for their thoughts and entertainment during our time together in room 201b.

I would also like to thank Joe Jez and the past and present members of his lab. Joe has been an excellent mentor during my time at Washington University and I have learned countless things from him.

Lastly, I would like to thank my thesis committee members for their helpful comments and discussions over the years.

I also would like to thank the funding agencies that made my research possible. This work was supported by funding from the National Science Foundation-FIBR program (EF0425749), and also from the Chemical Sciences, Geosciences and Biosciences Division, Office of Basic Energy Sciences, Office of Science, U.S. Department of Energy (DE-FG02-09ER20350).

TABLE OF CONTENTS

Abstract	ii
Acknowledgements	v
Table of Contents	vi
List of Tables	xi
List of Figures	xii

Chapter 1: Introduction

Oxygenic Photosynthesis	2
Reactive Oxygen Species.....	3
Hydroxyl Radical	4
Singlet Oxygen.....	4
Superoxide Anion Radical	5
Hydrogen Peroxide	6
Antioxidant Network	6
Redox Buffering System.....	7
Glutathione Biosynthesis and Degradation.....	8
This Work	10
References.....	15

Chapter 2: Glutathione is Essential during Environmental and Redox Perturbations

Summary	24
Introduction.....	25
Materials and Methods.....	30
Results.....	35
Discussion.....	48
Conclusions.....	54
References.....	55
Figures and Tables	67

Chapter 3: Function of γ -Glutamylcysteine during Redox and Metal Stress in *Synechocystis* sp. PCC 6803

Summary	84
Introduction.....	85
Materials and Methods.....	90
Results.....	92
Discussion.....	98
Conclusions.....	103
References.....	104
Figures.....	110

**Chapter 4: Glutathione Facilitates Antibiotic Resistance and Photosystem I Stability
during Exposure to Gentamicin in Cyanobacteria**

Summary	123
Introduction.....	124
Materials and Methods.....	128
Results.....	130
Discussion.....	133
Conclusions.....	136
References.....	137
Figures and Tables	141

Chapter 5: Characterization of the γ -Glutamyl Cycle in *Synechocystis* sp. PCC 6803

Summary	149
Introduction.....	150
Materials and Methods.....	153
Results.....	157
Discussion.....	163
Conclusions.....	166
References.....	167
Figures.....	171

**Chapter 6: Interactions between the Soluble Redox Buffering System and
Alternative Photosynthetic Electron Transport Pathways in *Synechocystis* sp. PCC**

6803

Summary.....	182
Introduction.....	183
Materials and Methods.....	186
Results.....	188
Discussion.....	193
Conclusions.....	195
References.....	196
Figures.....	199

Chapter 7: Conclusions and Future Directions

Summary and Conclusions	205
Implications of this Work	215
Future Directions	221
References.....	224
Figures.....	230

**Appendix I: Integrative Analysis of Large Scale Expression Profiles Reveals Core
Transcriptional Response and Coordination between Multiple Cellular Processes in
a Cyanobacterium**

Summary.....	233
Introduction.....	235
Materials and Methods.....	239
Results and Discussion	243
Conclusions.....	264
References.....	266
Figures.....	274

LIST OF TABLES

Chapter 2: Glutathione is Essential during Environmental and Redox Perturbations

Table 1. Primers used in this study67

Table 2. Plasmids and strains.....68

Chapter 4: Glutathione Facilitates Antibiotic Resistance and Photosystem I Stability during Exposure to Gentamicin in Cyanobacteria

Table 1. Pigment content of *Synechocystis* 6803 strains141

LIST OF FIGURES

Chapter 2: Glutathione is Essential during Environmental and Redox Perturbations

Figure 1. Disruption of glutathione biosynthesis in <i>Synechocystis</i> 6803.....	69
Figure 2. Genetic complementation of the $\Delta gshB::Gm^R$ strain and quantification of cellular thiols	70
Figure 3. Growth of WT, $\Delta gshB::Gm^R$ and $\Delta gshB::Gm^R/T2086$ strains.....	71
Figure 4. Changes in cellular thiol content after redox perturbations.....	72
Figure 5. Influence of light quality and intensity on glutathione metabolism	73
Figure 6. Cellular thiol content after addition of glucose	74
Figure 7. Affect of nutrient depletion on glutathione metabolism.....	75
Figure 8. Visual comparison of WT and $\Delta gshB::Gm^R$ cultures.....	76
Figure 9. Characterization of sulfate depletion in $\Delta gshB::Gm^R$ cells.....	77
Figure S1. Stationary phase physiology in the WT and $\Delta gshB::Gm^R$ strains.....	78
Figure S2. Chlorophyll fluorescence induction in stationary phase cultures following high light treatment	79
Figure S3. Comparison of WT and $\Delta gshB::Gm^R$ pigments during growth	80
Figure S4. 77 K fluorescence of WT and $\Delta gshB::Gm^R$ cells.....	81
Figure S5. Visual comparison of WT and the $\Delta gshB::Gm^R$ strains during recovery from sulfate depletion	82

**Chapter 3: Function of γ -Glutamylcysteine during Redox and Metal Stress in
Synechocystis sp. PCC 6803**

Figure 1. Growth in the presence of cadmium.....110

Figure 2. Growth and pigment levels during exposure to selenate.....111

Figure 3. Growth of the WT, $\Delta gshB::Gm^R$ and $\Delta gshB::Gm^R/T2086$ strains in the presence of arsenate112

Figure 4. Cellular GSH content during growth in iron deplete conditions.....113

Figure 5. Photosystem I-mediated electron transport in *Synechocystis 6803* strains114

Figure 6. PSI-mediated electron transport as a function of methyl viologen concentration in intact cells115

Figure 7. Absorption spectra of WT and the $\Delta gshB::Gm^R$ cells and isolated membranes116

Figure 8. Photosystem II activity in WT and $\Delta gshB::Gm^R$ cells117

Figure 9. Estimation of cellular ROS.....118

Figure 10. Schematic diagram of methylglyoxal pathway119

Figure 11. Growth of the WT and $\Delta gshB::Gm^R$ strains in the presence of glucose120

Figure 12. Growth of the WT and $\Delta gshB::Gm^R$ strains in the presence of glycerol121

Chapter 4: Glutathione Facilitates Antibiotic Resistance and Photosystem I Stability during Exposure to Gentamicin in Cyanobacteria

Figure 1. Growth and cellular thiol concentrations of WT *Synechocystis* 6803 following application of gentamicin at varying concentrations.....142

Figure 2. Growth of the $\Delta gshB$ and complemented $\Delta gshB::Gm^R/T2086$ strains143

Figure 3. Visualization and pigment content of strains following growth in the presence of gentamicin144

Figure 4. Immunoblot analysis of PSI (PsaA/B) and PSII (D1) core proteins145

Figure 5. Schematic diagram illustrating the role of glutathione in gentamicin resistance.....146

Chapter 5: Characterization of the γ -Glutamyl Cycle in *Synechocystis* sp. PCC 6803

Figure 1. Schematic diagram of the γ -glutamyl pathway171

Figure 2. Alignment of γ -glutamyltranspeptidase protein sequences172

Figure 3. Phylogenic relationship between Ggt proteins174

Figure 4. Disruption of γ -glutamyltranspeptidase gene in *Synechocystis* 6803.....175

Figure 5. Growth of the Δggt mutant strains at high light intensity176

Figure 6. Absorbance spectra and pigment composition during stationary phase..177

Figure 7. Cellular and extracellular GSH content in <i>Synechocystis</i> 6803 strains ...	178
Figure 8. Assay for γ -glutamyltranspeptidase (Ggt) activity in cellular extracts ...	179
Figure 9. Construction of <i>ggt-6xHis::Cm^R</i> strain and isolation of Ggt-His protein	180

Chapter 6: Interactions between the Soluble Redox Buffering System and Alternative Photosynthetic Electron Transport Pathways in *Synechocystis* sp. PCC 6803

Figure 1. Schematic diagram showing photosynthesis and ROS metabolism.....	199
Figure 2. Growth of strains on solid media.....	200
Figure 3. Growth of strains during redox perturbations	201
Figure 4. Cellular physiology of strains following high light treatment.....	202
Figure 5. Rates of P700 dark recovery following far red or green illumination.....	203

Chapter 7: Conclusions

Figure 1. Growth, GSH content and estimation of 2GSH/GSSG redox potential	230
Figure 2. Diurnal regulation of transcripts involved in GSH metabolism in <i>Cyanothece</i> 51142.....	231

Appendix I: Integrative Analysis of Large Scale Expression Profiles Reveals Core Transcriptional Response and Coordination between Multiple Cellular Processes in a Cyanobacterium

Figure 1. Differential regulation of *Synechocystis* genes across multiple perturbations274

Figure 2. Coregulation of regulatory and CTR genes.....275

Figure 3. Regulation of the functional category “Ribosome” determined from its associated genes276

Figure 4. Bayesian network for 51 KEGG pathways derived using the GES algorithm.....277

Figure 5. Coregulation of the ribosomal and ATP synthase genes.....278

Chapter 1

Introduction

BACKGROUND

Oxygenic Photosynthesis

Oxygenic photosynthesis is the process in which light energy is used to drive the oxidation of water to liberate molecular oxygen, protons and electrons. The photosynthetic electron transfer chain is comprised of numerous pigment-protein complexes and redox active intermediates involved in light harvesting and electron transport. These reactions occur within a specialized membrane system in plants, algae and most cyanobacteria called the thylakoid, which encloses an intermembrane space termed the lumen. The result of the photosynthetic reactions is the reduction of soluble electron carriers including NADP⁺ to NADPH and the generation of a trans-thylakoid electrochemical gradient used to generate ATP from ADP and P_i.

The photosynthetic electron transport chain is comprised of the integral membrane components, photosystems I (PSI) and II (PSII) and the cytochrome *b₆f* (cyt *b₆f*) complex. PSII functions as a light-driven water-plastoquinone oxidoreductase and is responsible for the generation of molecular oxygen within the cell. The cyt *b₆f* complex oxidizes the plastoquinone pool and transfers the electrons to the soluble electron carriers plastocyanin or cytochrome *c₆* and also translocates protons from the stroma to the luminal space. PSI is a light driven pigment-protein complex that oxidizes plastocyanin or cytochrome *c₆* and transfers electrons at high reducing potential to stromal components to generate the NADPH needed for reduction of CO₂ in the Calvin-Benson Cycle. The

ATP synthase complex utilizes the proton gradient generated by the oxidation of water and the proton pumping of the cyt *b₆f* complex to form ATP.

The amount of light that the cells receive is usually in excess to the amount that can be utilized for biochemical processes. Therefore, many mechanisms exist to dissipate excess energy. However, even at moderate light intensities, components of the electron transport chain, particularly PSII, can become damaged. Therefore, a dynamic cycle exists to repair and replace PSII complexes. At light intensities where the amount of damage exceeds the rate of repair, photoinhibition occurs, resulting in a rapid decline of photosynthetic activity (Nishiyama et al., 2006). If not carefully controlled, the process of photosynthesis can be very hazardous to the cell. The close proximity of redox active cofactors within the electron transfer chain with molecular oxygen generated as a byproduct of photosynthesis can result in the formation of reactive oxygen species (ROS) that have the capacity to damage cellular components.

Reactive Oxygen Species

The evolution of oxygenic photosynthesis in ancestors of modern day cyanobacteria changed the Earth's atmosphere from anoxic to oxic through the release of O₂ as a byproduct of water oxidation by PSII. While energetically, O₂ acts as an excellent electron acceptor during aerobic metabolism, these same properties make O₂ a dangerous molecule with a propensity to form reactive species that can damage cellular components.

In cyanobacteria, the respiratory and photosynthetic machinery reside in the thylakoid membrane (Cooley and Vermaas, 2001). Moreover, many of the components involved in electron transfer reactions are shared by both systems, including the plastoquinone pool. Leakage of electrons and excitation energy from these systems to O₂ can result in the formation of many distinct ROS with varying degrees of reactivity.

Hydroxyl Radical ([•]OH)

The hydroxyl radical is highly reactive and short-lived. In fact, the steady state levels of [•]OH within the cell are negligible because of the fast reactions with cellular components. Production of [•]OH is enhanced in the presence of transition metals including iron and copper through Fenton chemistry. These reactions can be enhanced through interactions with reactive thiols including cysteine (Park and Imlay, 2003). In photosynthetic organisms, uptake and storage of Fe is highly regulated to minimize these reactions (Shcolnick et al., 2009).

Singlet O₂ (¹O₂)

Photosystem II is the site of water oxidation and O₂ production and is therefore thought to be a major site for generation of ROS. Upon absorption of light energy by PSII, chlorophyll molecules are driven to an excited state. If the energy cannot be transferred to the reaction center quickly, the energy can be transferred to O₂ to generate singlet oxygen (¹O₂) (Krieger-Liszkay, 2005). ¹O₂ is much more reactive than O₂ because the spin restrictions that slow down interaction with non-radicals are removed in this excited state. Transfer of its excitation energy to another molecule can quench ¹O₂, or it can react

chemically to produce toxic peroxides. Production of $^1\text{O}_2$ within the cell elicits a specific response at the transcriptional level to mitigate the damage caused to cellular components (op den Camp et al., 2003; Ziegelhoffer et al., 2009). Photosensitizers can be used to generate $^1\text{O}_2$ within the cell. The dye rose Bengal functions as a type-II photosensitizer that transfers excitation energy following illumination to O_2 to generate $^1\text{O}_2$ (Fischer et al., 2004).

Superoxide Anion Radical (O_2^-)

Superoxide is formed through single electron donation to O_2 , creating an anion radical. The major site for superoxide formation in photosynthetic organisms is at the acceptor side of PSI (Jeanjean et al., 2008). Superoxide is not very reactive in aqueous solutions at physiological pH, however, it is much more reactive at low pH where it can be protonated to the hydroperoxyl radical ($^{\bullet}\text{HO}_2$). Superoxide is far more reactive in organic solvents and the hydrophobic interior of membrane systems, where it can react to form lipid peroxides. Superoxide also reacts with iron-sulfur clusters and can promote iron mediated Fenton chemistry and production of the highly reactive hydroxyl radical ($^{\bullet}\text{OH}$). Superoxide can be dismutated to form H_2O_2 within the cell by a variety of superoxide dismutase (SOD) enzymes. Methyl viologen (Paraquat) is an herbicide that acts by oxidizing PSI and other cellular components and donating electrons to O_2 to generate superoxide.

Hydrogen Peroxide (H₂O₂)

Hydrogen peroxide is produced within the cell through the activity of many oxidases and also through dismutation of superoxide by SOD. H₂O₂ is not very reactive with most cellular components but importantly reacts with cellular thiol (-SH) groups that can mediate cellular signaling pathways (Gutscher et al., 2009). Although H₂O₂ per se is not that reactive, it may participate in Fenton chemistry with cellular iron and copper molecules resulting in the production of the highly reactive and destructive hydroxyl radical ([•]OH).

Antioxidant Network

Photosynthetic organisms have evolved many mechanisms to protect the cellular components from ROS. In cyanobacteria, the antioxidant network is comprised of small molecules and protein components (Latifi et al., 2009). ROS can damage membranes and soluble components of the cell, therefore, there are specific antioxidant systems associated with each of these cellular locations. One layer of defense from ROS occurs near the site of generation. The photosynthetic reaction centers and membrane systems contain many different carotenoids that have the ability to quench excited state ³Chl and ROS such as ¹O₂ (Krieger-Liszkay, 2005). The soluble orange carotenoids protein may also function in quenching excess energy absorbed by the photosynthetic reaction centers (Kirilovsky, 2007). Tocopherol is another membrane soluble antioxidant compound that is important for protection from lipid peroxidation and during heterotrophic growth of cyanobacteria (Maeda et al., 2005; Sakuragi et al., 2006). Single electron reduction of oxygen results in the formation of superoxide which can be metabolized by superoxide

dismutase (SodB) in a process important for protection of PSI (Herbert et al., 1992). Cyanobacteria contain many proteins associated with metabolism of peroxides (Bernroitner et al., 2009). Among the soluble protein components, cyanobacteria contain several peroxiredoxins that are involved in metabolism of peroxides and are important for survival during high light (Kobayashi et al., 2004; Hosoya-Matsuda et al., 2005; Stork et al., 2005; Pérez-Pérez et al., 2009). Several NADPH-dependent glutathione peroxidase-like proteins have also been found in cyanobacteria (Gaber et al., 2004). Furthermore, cyanobacteria contain a catalase that functions in removal of H₂O₂ (Tichy and Vermaas, 1999). Glutathione (GSH) is an abundant, low molecular weight thiol that functions as an antioxidant and redox buffer in heterotrophic and photosynthetic organisms. GSH may also be used as a reductant during metabolism of peroxides in cyanobacteria (Hosoya-Matsuda et al., 2005). While a significant amount of work has been done regarding the functions of GSH in heterotrophic organisms, much less is known about the role of GSH in photosynthetic organisms.

Redox Buffering System

Maintenance of an appropriate cellular redox environment is essential for all organisms. This is partially due to the fact that many enzymes function optimally within a narrow range of redox potentials. In biological systems, the redox state of cellular thiol and sulfur containing compounds is important for enzymatic function, protein stability, ROS metabolism and signaling (Jacob and Anwar, 2008; Foyer et al., 2009). The cytoplasmic region of the cell is maintained in reducing conditions by numerous different soluble redox couples (Schafer and Buettner, 2001; Hu et al., 2008). Therefore, most of the redox

active thiol/disulfides within the cytoplasmic region are involved in either regulation or catalysis. Conversely, many secreted enzymes contain structural disulfides for stability. Disulfide bond formation is catalyzed by specific systems in oxidizing environments such as the periplasmic space or endoplasmic reticulum (Singh et al., 2008; Eser et al., 2009).

GSH contributes significantly to the cellular redox environment because it accumulates to high concentrations within the cell and because it forms a reversible intermolecular disulfide bond with another GSH molecule to form glutathione disulfide (GSSG). Significantly, the redox state of the 2GSH/GSSG redox couple is dependent on the total concentration and the ratio of reduced:oxidized (Schafer and Buettner, 2001). Glutaredoxins can interact with the 2GSH/GSSG couple and relay information on the redox state to other systems (Gutscher et al., 2008). Glutaredoxins are also involved in glutathionylation of proteins, a modification that may alter enzyme activity (Michelet et al., 2005; Li et al., 2007; Michelet et al., 2008; Rouhier et al., 2008; Gallogly et al., 2009).

Glutathione Biosynthesis and Degradation

Glutathione is a tripeptide comprised of glutamate, cysteine and glycine. Glutathione biosynthesis is ATP dependent and is catalyzed by the sequential action of glutamate-cysteine ligase (GshA) and glutathione synthetase (GshB). GshA catalyzes the ligation of the γ -carboxylic acid group to the amino group of cysteine to form γ -glutamylcysteine (γ -EC) (Jez et al., 2004). Furthermore, the GshA activity is redox regulated in *Arabidopsis* (Hicks et al., 2007), however there is no evidence for this type of regulation in the cyanobacterial GshA enzyme. GshB catalyzes the ligation of glycine to γ -EC to

form GSH (Jez and Cahoon, 2004). The related tripeptide, homoglutathione (hGSH), which contains alanine instead of glycine, is found in legumes and synthesized by homoglutathione synthetase (Galant et al., 2009). Bifunctional enzymes that catalyze the entire GSH biosynthetic pathway have also been reported (Vergauwen et al., 2006). Alternatively, a mutation in a proline biosynthetic enzyme has been found to result in the production of γ -EC, leading to the suppression of *gshA* mutations (Spector et al., 2001; Veeravalli et al., 2011).

GSH accumulates to high levels (mM) within the cell and therefore contains a substantial pool of reduced carbon, nitrogen and sulfur (Kopriva and Rennenberg, 2004). In fact, GSH can be catabolized as a source of amino acids (Elskens et al., 1991). Compared to the biosynthetic pathway, much less is known regarding GSH catabolism in photosynthetic organisms. Degradation of GSH first requires the removal of the γ -glutamyl residue by a γ -glutamyltranspeptidase or γ -glutamylcyclotransferase to liberate cysteinylglycine, which can be degraded by a dipeptidase (Ohkama-Ohtsu et al., 2009). The catabolic pathway is involved in degradation of GSH and GSH-conjugates involved in detoxification of xenobiotics (Ohkama-Ohtsu et al., 2007).

THIS WORK

Glutathione (GSH) has been shown to be critical for many processes in heterotrophic and photosynthetic organisms ranging from bacteria to higher plants. The ubiquitous nature of GSH is a testament to its beneficial properties. Although cyanobacterial ancestors are credited with the evolution of glutathione metabolism, there have been very few studies on the role of glutathione in cyanobacteria to date. In plants, extensive metabolic pathways and gene families have arisen that are based on the chemistry of GSH. For example, *Synechocystis* sp. PCC 6803 (hereafter *Synechocystis* 6803), a model cyanobacterium, contains three glutaredoxins, while *Arabidopsis* contains 33 (Couturier et al., 2009). Cyanobacteria offer excellent model systems to study GSH metabolism in photosynthetic organisms because of their genetic simplicity and because many of these pathways likely arose in their ancestors. *Synechocystis* 6803 has been used as a model for research on oxygenic photosynthesis. As such, there are many resources available for this organism that facilitated our research including a sequenced genome (Kaneko et al., 1996) and ease of genetic manipulation (Zang et al., 2007). In this work, we aimed to analyze the role of GSH in the maintenance of redox homeostasis in *Synechocystis* 6803.

We utilized several different strategies to investigate the role of GSH. First, we took advantage of the many omics and bioinformatics resources that are available for *Synechocystis* 6803. This information provided a foundation to understand how environmental perturbations might influence metabolic networks. We also utilized genetic and pharmacological approaches to disrupt glutathione and redox pathways in

Synechocystis 6803. The generation of mutants allowed us to probe the functional role of GSH and cooperativity between redox pathways during acclimation to many different perturbations. Finally, we utilized quantitative analytical techniques including HPLC to determine how steady-state GSH levels change as a function of growth and metabolism.

Chapter 2 describes the generation and characterization of mutants in the glutathione biosynthesis pathway in *Synechocystis* 6803. These analyses provided the building block for the rest of our studies. Our analysis suggests that the first enzyme involved in glutathione biosynthesis, GshA, is required for survival in cyanobacteria. We also utilized pharmacological approaches to disrupt activity of the GshA protein and found a significant decrease in growth rate and cellular thiol content following treatment. While this result provided insight into the essential nature of GSH, our analysis mainly focused on a mutant lacking the second and final enzyme in glutathione biosynthesis, GshB. We found that the $\Delta gshB$ mutant is no longer capable of making GSH, but instead accumulates the biosynthetic intermediate, γ -EC. Our major finding is that while the $\Delta gshB$ strain is viable under many conditions, it is extremely sensitive to conditions promoting oxidative stress. During this study, we were able to identify environmental perturbations that affect cellular GSH content. Particularly, we found that depletion of nutrients such as sulfate resulted in dramatic changes in cellular thiol content. We also found that the $\Delta gshB$ mutant exhibited reduced growth and recovery during sulfate depletion and repletion, respectively.

The $\Delta gshB$ mutant described in chapter 2 provided us with a tool to probe the role of GSH in a photosynthetic cell. We were able to capitalize on the subtle differences between GSH and γ -EC to identify conditions where GSH is absolutely essential versus conditions where a similar compound will suffice. Chapter 3 provides more insight into the role of GSH in *Synechocystis* 6803 by further exploring the physiology of the $\Delta gshB$ mutant. In these studies we examined the role of metals in perturbing redox homeostasis. We found that the $\Delta gshB$ mutant is very sensitive to Cd, but less sensitive to other compounds such as arsenate and selenate. These studies also resulted in the observation that the regulation of pigment stoichiometry appears to be altered in the $\Delta gshB$ strain compared to the WT, especially when cells were stressed. Furthermore, we analyzed the $\Delta gshB$ mutant during growth in the presence of exogenous carbon compounds. Several pathways involved in metabolism of toxic byproducts of carbon metabolism utilize GSH as a cofactor. During extensive characterization of the physiology of the $\Delta gshB$ strain, we also found that this strain could not maintain PSI-mediated electron transfer using exogenous electron donor/acceptor pairs. We speculate that this could be an artifact of increased ROS produced during this reaction in the sensitized strain.

Chapter 4 focuses on the role GSH in facilitating antibiotic resistance and PSI stability in *Synechocystis* 6803. Recent work has identified ROS as crucial components in antibiotic mediated cell death and resistance (Kohanski et al., 2007; Dwyer et al., 2009; Kohanski et al., 2010). We found that application of aminoglycoside antibiotic gentamicin (Gm), to WT cells resulted in increased levels of cellular GSH. Because the $\Delta gshB$ strain is sensitive to ROS, we investigated the sensitivity of this strain to Gm. We found that the

$\Delta gshB$ mutant is more sensitive to Gm compared to a control strain, despite the presence of a gentamicin resistance cassette. We also found that application of Gm induced a dramatic reduction in the levels of PSI. This is significant because PSI contains multiple iron-sulfur clusters that are potential mediators of ROS generation. These results imply that GSH may function to protect PSI from oxidative damage during photosynthesis.

Chapter 5 focuses on pathways thought to be involved in glutathione degradation. Interest in this area began following the observations in chapter 1 that many different conditions lead to altered cellular GSH content. Notably, we found that growth in sulfate deplete medium leads to dramatic decreases in cellular GSH content. To investigate this phenomenon, we generated a strain of *Synechocystis* 6803 that lacks γ -glutamyltransptidase (Ggt), an enzyme that catalyzes the first step in glutathione degradation. However, analysis of the Δggt strain suggests that a different pathway might be involved in degradation of cellular GSH during sulfate starvation. Our analysis suggests that Ggt is involved in uptake of GSH from the media or prevention of leakage of GSH. We did find that the Δggt mutant is less fit than the WT strain during stationary phase. It is possible that during these conditions, nutrients become limiting and GSH must be scavenged. These findings open up additional possibilities for future research into GSH degradation during nutrient limitation.

While our research identified many conditions where GSH is essential, we were surprised to find that the $\Delta gshB$ mutant did not appear to be sensitive to high-light compared to the WT. While we did find that some proxies for photosynthetic capacity (Fv/Fm) were

reduced in the $\Delta gshB$ strain in during these conditions compared to the WT, but this was not reflected in growth rate. It is possible that during high light conditions, there are many redundant pathways for detoxification and mitigation of ROS. One pathway that is particularly interesting is the water-water cycle (Asada, 1999). In this pathway, electrons derived from the oxidation of H_2O are used to reduce O_2 to H_2O , often involving ROS intermediates. In cyanobacteria, it has been reported that a significant amount of O_2 evolved by PSII can be photoreduced (Helman et al., 2005). However, earlier studies report that only small amounts of H_2O_2 accumulate during the light reactions in *Synechocystis* 6803 (Tichy and Vermaas, 1999). In *Synechocystis* 6803, several A-type flavoproteins (Flv; flavodiiron proteins) have been shown to use NADPH to reduce O_2 directly to H_2O without generating ROS intermediates (Vicente et al., 2002; Helman et al., 2003). To determine whether the GSH and the Flv proteins cooperate to maintain redox homeostasis in cyanobacteria, we combined the $\Delta flv3$ and $\Delta gshB$ mutants to create $\Delta flv3/\Delta gshB$. Our results suggest some degree of synergism between the pathways during certain conditions, but also indicate that the absence of GSH is more severe than the absence of the Flv3 protein in the conditions that we have analyzed. Further studies will be needed to fully characterize the interactions between these and other, possibly redundant pathways.

REFERENCES

- Asada K** (1999) THE WATER-WATER CYCLE IN CHLOROPLASTS: Scavenging of Active Oxygens and Dissipation of Excess Photons. *Annu Rev Plant Physiol Plant Mol Biol* **50**: 601-639
- Bernroitner M, Zamocky M, Furtmüller PG, Peschek GA, Obinger C** (2009) Occurrence, phylogeny, structure, and function of catalases and peroxidases in cyanobacteria. *J Exp Bot* **60**: 423-440
- Cooley JW, Vermaas WF** (2001) Succinate dehydrogenase and other respiratory pathways in thylakoid membranes of *Synechocystis* sp. strain PCC 6803: capacity comparisons and physiological function. *J Bacteriol* **183**: 4251-4258
- Couturier J, Jacquot J-P, Rouhier N** (2009) Evolution and diversity of glutaredoxins in photosynthetic organisms. *Cell Mol Life Sci* **66**: 2539-2557
- Dwyer DJ, Kohanski MA, Collins JJ** (2009) Role of reactive oxygen species in antibiotic action and resistance. *Curr Opin Microbiol* **12**: 482-489
- Elskens MT, Jaspers CJ, Penninckx MJ** (1991) Glutathione as an endogenous sulphur source in the yeast *Saccharomyces cerevisiae*. *J Gen Microbiol* **137**: 637-644
- Eser M, Masip L, Kadokura H, Georgiou G, Beckwith J** (2009) Disulfide bond formation by exported glutaredoxin indicates glutathione's presence in the *E. coli* periplasm. *Proc Natl Acad Sci USA* **106**: 1572-1577
- Fischer BB, Krieger-Liszkay A, Eggen RL** (2004) Photosensitizers neutral red (type I) and rose bengal (type II) cause light-dependent toxicity in *Chlamydomonas*

reinhardtii and induce the Gpxh gene via increased singlet oxygen formation.
Environ Sci Technol **38**: 6307-6313

Foyer C, Noctor G, Buchanan B, Dietz K, Pfannschmidt T (2009) Redox Regulation in Photosynthetic Organisms: Signaling, Acclimation, and Practical Implications. Antioxid Redox Signal **11**: 861-905

Gaber A, Yoshimura K, Tamoi M, Takeda T, Nakano Y, Shigeoka S (2004) Induction and functional analysis of two reduced nicotinamide adenine dinucleotide phosphate-dependent glutathione peroxidase-like proteins in *Synechocystis* PCC 6803 during the progression of oxidative stress. Plant Physiol **136**: 2855-2861

Galant A, Arkus KA, Zubieta C, Cahoon RE, Jez JM (2009) Structural basis for evolution of product diversity in soybean glutathione biosynthesis. Plant Cell **21**: 3450-3458

Gallogly M, Starke D, Mieyal J (2009) Mechanistic and Kinetic Details of Thiol-Disulfide Exchange by Glutaredoxins and Potential Mechanisms of Regulation. Antioxid Redox Signal **11**: 1059-1081

Gutscher M, Pauleau A, Marty L, Brach T, Wabnitz G, Samstag Y, Meyer A, Dick T (2008) Real-time imaging of the intracellular glutathione redox potential. Nat Methods **5**: 553-559

Gutscher M, Sobotta MC, Wabnitz GH, Ballikaya S, Meyer AJ, Samstag Y, Dick TP (2009) Proximity-based Protein Thiol Oxidation by H₂O₂-scavenging Peroxidases. J Biol Chem **284**: 31532-31540

- Helman Y, Barkan E, Eisenstadt D, Luz B, Kaplan A** (2005) Fractionation of the three stable oxygen isotopes by oxygen-producing and oxygen-consuming reactions in photosynthetic organisms. *Plant Physiol* **138**: 2292-2298
- Helman Y, Tchernov D, Reinhold L, Shibata M, Ogawa T, Schwarz R, Ohad I, Kaplan A** (2003) Genes encoding A-type flavoproteins are essential for photoreduction of O₂ in cyanobacteria. *Curr Biol* **13**: 230-235
- Herbert SK, Samson G, Fork DC, Laudenbach DE** (1992) Characterization of damage to photosystems I and II in a cyanobacterium lacking detectable iron superoxide dismutase activity. *Proc Natl Acad Sci U S A* **89**: 8716-8720
- Hicks LM, Cahoon RE, Bonner ER, Rivard RS, Sheffield J, Jez JM** (2007) Thiol-based regulation of redox-active glutamate-cysteine ligase from *Arabidopsis thaliana*. *Plant Cell* **19**: 2653-2661
- Hosoya-Matsuda N, Motohashi K, Yoshimura H, Nozaki A, Inoue K, Ohmori M, Hisabori T** (2005) Anti-oxidative stress system in cyanobacteria. Significance of type II peroxiredoxin and the role of 1-Cys peroxiredoxin in *Synechocystis* sp. strain PCC 6803. *J Biol Chem* **280**: 840-846
- Hu J, Dong L, Outten CE** (2008) The redox environment in the mitochondrial intermembrane space is maintained separately from the cytosol and matrix. *J Biol Chem* **283**: 29126-29134
- Jacob C, Anwar A** (2008) The chemistry behind redox regulation with a focus on sulphur redox systems. *Physiol Plant* **133**: 469-480
- Jeanjean R, Latifi A, Matthijs HCP, Havaux M** (2008) The PsaE subunit of photosystem I prevents light-induced formation of reduced oxygen species in the

cyanobacterium *Synechocystis* sp. PCC 6803. *Biochim Biophys Acta* **1777**: 308-316

Jez JM, Cahoon RE (2004) Kinetic mechanism of glutathione synthetase from *Arabidopsis thaliana*. *J Biol Chem* **279**: 42726-42731

Jez JM, Cahoon RE, Chen S (2004) *Arabidopsis thaliana* glutamate-cysteine ligase: functional properties, kinetic mechanism, and regulation of activity. *J Biol Chem* **279**: 33463-33470

Kaneko T, Sato S, Kotani H, Tanaka A, Asamizu E, Nakamura Y, Miyajima N, Hirosawa M, Sugiura M, Sasamoto S, Kimura T, Hosouchi T, Matsuno A, Muraki A, Nakazaki N, Naruo K, Okumura S, Shimpo S, Takeuchi C, Wada T, Watanabe A, Yamada M, Yasuda M, Tabata S (1996) Sequence analysis of the genome of the unicellular cyanobacterium *Synechocystis* sp. strain PCC6803. II. Sequence determination of the entire genome and assignment of potential protein-coding regions. *DNA Res* **3**: 109-136

Kirilovsky D (2007) Photoprotection in cyanobacteria: the orange carotenoid protein (OCP)-related non-photochemical-quenching mechanism. *Photosyn Res* **93**: 7-16

Kobayashi M, Ishizuka T, Katayama M, Kanehisa M, Bhattacharyya-Pakrasi M, Pakrasi HB, Ikeuchi M (2004) Response to oxidative stress involves a novel peroxiredoxin gene in the unicellular cyanobacterium *Synechocystis* sp. PCC 6803. *Plant Cell Physiol* **45**: 290-299

Kohanski MA, DePristo MA, Collins JJ (2010) Sublethal antibiotic treatment leads to multidrug resistance via radical-induced mutagenesis. *Mol Cell* **37**: 311-320

- Kohanski MA, Dwyer DJ, Hayete B, Lawrence CA, Collins JJ** (2007) A common mechanism of cellular death induced by bactericidal antibiotics. *Cell* **130**: 797-810
- Kopriva S, Rennenberg H** (2004) Control of sulphate assimilation and glutathione synthesis: interaction with N and C metabolism. *J Exp Bot* **55**: 1831-1842
- Krieger-Liszkay A** (2005) Singlet oxygen production in photosynthesis. *J Exp Bot* **56**: 337-346
- Latifi A, Ruiz M, Zhang C-C** (2009) Oxidative stress in cyanobacteria. *FEMS Microbiol Rev* **33**: 258-278
- Li M, Yang Q, Zhang L, Li H, Cui Y, Wu Q** (2007) Identification of novel targets of cyanobacterial glutaredoxin. *Arch Biochem Biophys* **458**: 220-228
- Maeda H, Sakuragi Y, Bryant DA, Dellapenna D** (2005) Tocopherols Protect *Synechocystis* sp. Strain PCC 6803 from Lipid Peroxidation. *Plant Physiol* **138**: 1422-1435
- Michelet L, Zaffagnini M, Marchand C, Collin V, Decottignies P, Tsan P, Lancelin J-M, Trost P, Miginiac-Maslow M, Noctor G, Lemaire SD** (2005) Glutathionylation of chloroplast thioredoxin f is a redox signaling mechanism in plants. *Proc Natl Acad Sci USA* **102**: 16478-16483
- Michelet L, Zaffagnini M, Vanacker H, Le Maréchal P, Marchand C, Schroda M, Lemaire SD, Decottignies P** (2008) In vivo targets of S-thiolation in *Chlamydomonas reinhardtii*. *J Biol Chem* **283**: 21571-21578

- Nishiyama Y, Allakhverdiev SI, Murata N** (2006) A new paradigm for the action of reactive oxygen species in the photoinhibition of photosystem II. *Biochim Biophys Acta* **1757**: 742-749
- Ohkama-Ohtsu N, Fukuyama K, Oliver D** (2009) Roles of γ -Glutamyl Transpeptidase and γ -Glutamyl Cyclotransferase in Glutathione and Glutathione-Conjugate Metabolism in Plants. *Adv Bot Res* **52**: 87-113
- Ohkama-Ohtsu N, Zhao P, Xiang C, Oliver DJ** (2007) Glutathione conjugates in the vacuole are degraded by γ -glutamyl transpeptidase GGT3 in Arabidopsis. *Plant J* **49**: 878-888
- op den Camp R, Przybyla D, Ochsenein C, Laloi C, Kim C, Danon A, Wagner D, Hideg É, Göbel C, Feussner I** (2003) Rapid induction of distinct stress responses after the release of singlet oxygen in Arabidopsis. *Plant Cell* **15**: 2320-2332
- Park S, Imlay J** (2003) High Levels of Intracellular Cysteine Promote Oxidative DNA Damage by Driving the Fenton Reaction. *J Bacteriol* **185**: 1942-1950
- Pérez-Pérez M, Mata-Cabana A, Sánchez-Riego A, Lindahl M, Florencio F** (2009) A comprehensive analysis of the peroxiredoxin reduction system in the cyanobacterium *Synechocystis* sp. PCC 6803 reveals that all five peroxiredoxins are thioredoxin dependent. *J Bacteriol* **191**: 7477-7489
- Rouhier N, Lemaire S, Jacquot J** (2008) The Role of Glutathione in Photosynthetic Organisms: Emerging Functions for Glutaredoxins and Glutathionylation. *Annual review of plant biology* **59**: 143-166
- Sakuragi Y, Maeda H, Dellapenna D, Bryant DA** (2006) α -Tocopherol plays a role in photosynthesis and macronutrient homeostasis of the cyanobacterium

- Synechocystis* sp. PCC 6803 that is independent of its antioxidant function. Plant Physiol **141**: 508-521
- Schafer FQ, Buettner GR** (2001) Redox environment of the cell as viewed through the redox state of the glutathione disulfide/glutathione couple. Free Radic Biol Med **30**: 1191-1212
- Shcolnick S, Summerfield TC, Reytman L, Sherman LA, Keren N** (2009) The mechanism of iron homeostasis in the unicellular cyanobacterium *Synechocystis* sp. PCC 6803 and its relationship to oxidative stress. Plant Physiol **150**: 2045-2056
- Singh AK, Bhattacharyya-Pakrasi M, Pakrasi HB** (2008) Identification of an atypical membrane protein involved in the formation of protein disulfide bonds in oxygenic photosynthetic organisms. J Biol Chem **283**: 15762-15770
- Spector D, Labarre J, Toledano MB** (2001) A genetic investigation of the essential role of glutathione: mutations in the proline biosynthesis pathway are the only suppressors of glutathione auxotrophy in yeast. J Biol Chem **276**: 7011-7016
- Stork T, Michel K-P, Pistorius E, Dietz K-J** (2005) Bioinformatic analysis of the genomes of the cyanobacteria *Synechocystis* sp. PCC 6803 and *Synechococcus elongatus* PCC 7942 for the presence of peroxiredoxins and their transcript regulation under stress. J Exp Bot **56**: 3193-3206
- Tichy M, Vermaas W** (1999) In vivo role of catalase-peroxidase in *Synechocystis* sp. strain PCC 6803. J Bacteriol **181**: 1875-1882

- Veeravalli K, Boyd D, Iverson BL, Beckwith J, Georgiou G** (2011) Laboratory evolution of glutathione biosynthesis reveals natural compensatory pathways. *Nat Chem Biol* **7**: 101-105
- Vergauwen B, De Vos D, Van Beeumen JJ** (2006) Characterization of the bifunctional gamma-glutamate-cysteine ligase/glutathione synthetase (GshF) of *Pasteurella multocida*. *J Biol Chem* **281**: 4380-4394
- Vicente J, Gomes C, Wasserfallen A, Teixeira M** (2002) Module fusion in an A-type flavoprotein from the cyanobacterium *Synechocystis* condenses a multiple-component pathway in a single polypeptide chain. *Biochem Biophys Res Commun* **294**: 82-87
- Zang X, Liu B, Liu S, Arunakumara KKIU, Zhang X** (2007) Optimum conditions for transformation of *Synechocystis* sp. PCC 6803. *J Microbiol* **45**: 241-245
- Ziegelhoffer EC, Ziegelhoffer EC, Donohue TJ, Donohue TJ** (2009) Bacterial responses to photo-oxidative stress. *Nat Rev Microbiol* **7**: 856

Chapter 2

Glutathione is Essential during Environmental and Redox Perturbations

This chapter was adapted from:

Jeffrey C. Cameron and Himadri B. Pakrasi (2010) Essential Role of Glutathione in Acclimation to Environmental and Redox Perturbations in the Cyanobacterium *Synechocystis* sp. PCC 6803. *Plant Physiology* **154**: 1672-1685

Copyright © American Society of Plant Biologists

SUMMARY

Glutathione, a non-ribosomal thiol tripeptide, has been shown to be critical for many processes in plants. Much less is known about the roles of glutathione in cyanobacteria, oxygenic photosynthetic prokaryotes that are the evolutionary precursor of the chloroplast. An understanding of glutathione metabolism in cyanobacteria is expected to provide novel insight into the evolution of the elaborate and extensive pathways that utilize glutathione in photosynthetic organisms. To investigate the function of glutathione in cyanobacteria, we generated deletion mutants of glutamate-cysteine ligase (*gshA*) and glutathione synthetase (*gshB*) in *Synechocystis* sp. PCC 6803. Complete segregation of the Δ *gshA* mutation was not achieved, suggesting that GshA activity is essential for growth. In contrast, fully segregated Δ *gshB* mutants were isolated and characterized. The Δ *gshB* strain lacks glutathione (GSH), but instead accumulates the precursor compound, γ -glutamylcysteine (γ -EC). The Δ *gshB* strain grows slower than the wild type (WT) strain under favorable conditions, and exhibits extremely reduced growth or death when subjected to conditions promoting oxidative stress. Furthermore, we analyzed thiol contents in WT and the Δ *gshB* mutant after subjecting the strains to multiple environmental and redox perturbations. We found that conditions promoting growth stimulate glutathione biosynthesis. We also determined that cellular GSH and γ -EC content decline following exposure to dark, blue light and during photoheterotrophic growth. Moreover, a rapid depletion of GSH and γ -EC is observed in WT and the Δ *gshB* strain, respectively, when cells are starved for nitrate or sulfate.

INTRODUCTION

Photosynthetic organisms are constantly faced with the threat of reactive oxygen species (ROS) generated as a byproduct of photosynthesis and cellular metabolism (Asada, 1999). To overcome these challenges, photosynthetic organisms have developed robust antioxidant and redox buffering systems comprised of enzymatic and small molecule components (Latifi et al., 2009). Glutathione is a small, ubiquitous molecule that is involved in a plethora of cellular processes in addition to its role as an antioxidant and maintenance of cellular redox homeostasis (Schafer and Buettner, 2001). Compared to heterotrophic organisms such as yeast (Penninckx, 2000) and *E. coli* (Masip et al., 2006), less is known regarding the roles of glutathione in photosynthetic organisms, despite an array of studies performed in plants (Meyer, 2008; Rouhier et al., 2008; Foyer et al., 2009). The disparity is likely due to the extensive diversity of pathways involving glutathione metabolism in photoautotrophs compared to heterotrophs (Meyer and Hell, 2005). Surprisingly, even less is known about the functions of glutathione in cyanobacteria. This is especially significant given that glutathione metabolism likely evolved with the advent of oxygenic photosynthesis in cyanobacterial ancestors (Copley and Dhillon, 2002). There are many similarities between processes involving glutathione in plants and cyanobacteria. Cyanobacteria have smaller gene families involving glutathione metabolism compared to plants (Rouhier et al., 2008) making them excellent candidates for the study of glutathione metabolism in a photosynthetic organisms. In this

study, we investigated the role of glutathione in the cyanobacterium *Synechocystis* sp. PCC 6803 (hereafter *Synechocystis* 6803), a model photosynthetic organism.

Glutathione (L- γ -glutamyl-L-cysteinyl-glycine) is a low molecular weight thiol tripeptide that is synthesized through two sequential ATP dependent steps catalyzed by glutamate-cysteine ligase (GshA) and glutathione synthetase (GshB) (Fig. 1A). GshA catalyzes the ligation of cysteine with the γ -carboxyl group of glutamate to form γ -glutamylcysteine (γ -EC). GshB ligates glycine to the cysteine residue of γ -EC to form glutathione. The glutamate-cysteine ligase (Gsh1) in *Arabidopsis thaliana* (*Arabidopsis*) has been extensively characterized and shown to be redox regulated (Jez et al., 2004; Hicks et al., 2007). GshA from the cyanobacteria *Anabaena* sp. PCC 7120 has been biochemically characterized but there is no evidence that its activity is redox modulated (Ashida et al., 2005). The kinetic mechanism of glutathione synthetase (Gsh2) from *Arabidopsis* has been described (Jez and Cahoon, 2004) and enzymatic activity has been demonstrated for the GshB protein in the cyanobacterium *Synechococcus* sp. PCC 7942 (Okumura et al., 1997).

Glutathione accumulates to millimolar levels within the cell, primarily in the reduced form (GSH). GSH can undergo intermolecular oxidation to form glutathione disulfide (GSSG), a process that can be reversed enzymatically by glutathione reductase through NADPH dependent reduction of the disulfide (Serrano et al., 1984). The reduction potential of the 2GSH/GSSG redox couple is dependent on the absolute concentration

and the ratio of reduced to oxidized glutathione and it has been proposed that this redox couple contributes significantly to the cellular redox environment (Schafer and Buettner, 2001). Changes to the glutathione redox state have been proposed to be involved in cellular signaling pathways in plants (Meyer, 2008). However, analysis of the cellular redox environment is complicated by the fact that even within a single cell, different cellular organelles may maintain the glutathione couple at different reducing potentials (Meyer et al., 2007; Wolf et al., 2008). The comparative simplicity of the cyanobacterial cell makes biochemical interpretations more clear, potentially providing insight into the functions of glutathione within the plant chloroplast.

In plants, glutathione is critical for many cellular functions (Mullineaux and Rausch, 2005; Rouhier et al., 2008; Foyer et al., 2009). Genetic perturbation of glutathione biosynthesis in *Arabidopsis* has dramatic consequences to cellular development, hampering genetic studies of glutathione deficiency in fully developed plants. Weak alleles of *gsh1* (glutamate-cysteine ligase) in *Arabidopsis* result in cadmium sensitivity due to the role of GSH in phytochelatin synthesis and heavy metal detoxification (Howden et al., 1995). Strong alleles of *gsh1* result in seedlings lacking a root meristem and null alleles are embryo lethal (Vernoux et al., 2000; Cairns et al., 2006). Null mutations in *gsh2* result in a seedling lethal phenotype in *Arabidopsis*. Homozygous *gsh2* mutant ovules accumulate high levels of the glutathione precursor, γ -glutamylcysteine (γ -EC), which is presumably exported from the chloroplast into the cytoplasm (Pasternak et al., 2008). In plants and algae, ascorbate and glutathione function in a glutathione-

ascorbate cycle and comprise the major soluble antioxidant network for degradation of H₂O₂ (Asada, 1999) in combination with other cellular components including glutathione reductase and catalase (Mhamdi et al., 2010). However, ascorbate concentrations in cyanobacteria are about 250 times lower than that reported for plant chloroplasts and while ascorbate peroxidase activity have been reported for *Nostoc muscorum* 7119 and *Synechococcus* 6311 and 7942 (Tel-Or et al., 1985; Mittler and Tel-Or, 1991), recent genome analysis has not identified a gene with similarity to a plant-like ascorbate peroxidase in *Synechocystis* 6803 (Stork et al., 2005). Therefore, glutathione appears to be the major water-soluble antioxidant in cyanobacteria.

It has been known for some time that cyanobacteria contain high levels of glutathione (Fahey et al., 1978; Tel-Or et al., 1985). Furthermore, it has been demonstrated that addition of the precursor amino acid cysteine to *Synechocystis* 6803 results in increased glutathione accumulation (Suginaka et al., 1998) and increased heat tolerance (Suginaka et al., 1999). Recently, immunocytochemical methods were used to identify the subcellular localization of glutathione and cysteine in *Synechocystis* 6803 (Zechmann et al., 2010). This report also claimed that glutathione and cysteine levels are reduced when cells are grown in sulfate deplete medium, a phenomenon also observed in yeast (Elskens et al., 1991) that likely involves degradation by γ -glutamyltranspeptidase. To date, there has been a single report of the genetic deletion of a glutathione biosynthesis gene in cyanobacteria. (Okumura et al., 1997) isolated a *gshB* mutant strain from a screen for pigment biosynthesis mutants in *Synechococcus* 7942 and found that the mutant appeared

more yellow in color compared to WT, but had similar growth under photoautotrophic conditions. However, this report did not extensively characterize the mutant phenotypes under adverse conditions. Recently there have been some exciting studies showing the importance of glutaredoxins in *Synechocystis* 6803, leading to the discovery of a novel pathway for selenate tolerance (Marteyn et al., 2008), insight in to their potential role in iron-sulfur cluster delivery (Picciocchi et al., 2007; Iwema et al., 2009) and in arsenate reduction and detoxification (Lopez-Maury et al., 2009). While these studies have shed light on some aspects of the roles of glutathione, it is not known how glutathione levels change in response to cellular perturbations and what role glutathione plays during oxidative stress in cyanobacteria.

In this work, we have investigated the role of glutathione in the model cyanobacterium *Synechocystis* 6803 by generating deletion mutations of *gshA* and *gshB*. We find that glutathione is beneficial to *Synechocystis* 6803 during acclimation to both environmental and redox perturbations and is essential during extreme oxidative stress. We found that many diverse conditions commonly utilized to probe cellular physiology have dramatic affects on glutathione levels. Furthermore, we found a strong connection between glutathione metabolism and photosynthetic electron transport, in particular, photosystem II activity, emphasizing the importance of glutathione in oxygenic photosynthetic organisms.

MATERIALS AND METHODS

Culture Conditions

Synechocystis sp. PCC 6803 strains were grown in liquid BG11 (Allan and Stanier, 1968) medium at 30°C under continuous illumination by cool white fluorescent lights under 30 $\mu\text{mol photons m}^{-2} \text{ s}^{-1}$, unless otherwise indicated. Mutant strains were maintained on solid BG11 agar plates supplemented with 40 $\mu\text{g ml}^{-1}$ kanamycin, 5 $\mu\text{g ml}^{-1}$ gentamicin or a combination of 40 $\mu\text{g ml}^{-1}$ kanamycin and 5 $\mu\text{g ml}^{-1}$ gentamicin for $\Delta\text{gshA}::\text{Km}^{\text{R}}$, $\Delta\text{gshB}::\text{Gm}^{\text{R}}$ and $\Delta\text{gshA}::\text{Km}^{\text{R}}/\Delta\text{gshB}::\text{Gm}^{\text{R}}$ strains, respectively; and 5 $\mu\text{g ml}^{-1}$ gentamicin plus 10 $\mu\text{g ml}^{-1}$ chloramphenicol for the $\Delta\text{gshB}::\text{Gm}^{\text{R}}/\text{T2086}$ strain. All experiments were performed using media without antibiotics added, as the strains lacking glutathione ($\Delta\text{gshB}::\text{Gm}^{\text{R}}$ and $\Delta\text{gshA}::\text{Km}^{\text{R}}/\Delta\text{gshB}::\text{Gm}^{\text{R}}$) were sensitive to low concentrations of aminoglycoside antibiotics present in liquid medium, despite the expression of a functional resistance gene (data not shown). For growth assays, cells were grown to mid-log phase and harvested by centrifugation. The cells were washed in fresh BG11, centrifuged to pellet, and the cell pellets were resuspended in the appropriate media. The cells were diluted to an $\text{OD}_{730 \text{ nm}} = 0.05$ in BG11 without antibiotics and grown with shaking (200 rpm). The $\text{OD}_{730 \text{ nm}}$ was measured every 24 h on a μQuant Microplate spectrophotometer (Biotek Instruments, Inc., Winooski, VT). When indicated, DL-buthionine-S,R-sulfoximine (BSO), H_2O_2 , Rose Bengal, or methyl viologen was added at concentrations specified in “Results”. For nutrient deprivation, cells were washed and resuspended in appropriate deplete medium (at $\text{OD}_{730 \text{ nm}} \approx 0.04$), transferred

to 400 ml square flasks and bubbled with air under continuous illumination under 40 $\mu\text{mol photons m}^{-2} \text{ s}^{-1}$. After 6 days growth, deplete cells were harvested by centrifugation, resuspended in BG11 to $\text{OD}_{730 \text{ nm}} = 0.05$ and transferred to 250 ml shake flasks for an additional 6 days. Glucose (5 mM) and DCMU (10 μM) were added when specified. For growth in orange-red and blue light, cells grown in shake flasks at 40 $\mu\text{mol photons m}^{-2} \text{ s}^{-1}$ were transferred to 3 cm diameter test tubes in a water bath maintained at 30°C and bubbled with air. Illumination was provided by a custom LED panel at approximately 10 $\mu\text{mol photons m}^{-2} \text{ s}^{-1}$ as previously described (Singh et al., 2009).

Construction of Mutant Strains

The open reading frame of *gshA* (*slr0990*) was replaced with a modified kanamycin gene lacking a transcriptional terminator sequence. Primer pairs GshA1 + GshA2 and GshA3 + GshA4 were used to amplify a 498 bp region upstream and a 499 bp region downstream of *gshA*, respectively. Upstream and downstream fragments were cloned into pUC18 flanking a kanamycin resistance cassette (Km^{R}) and the resulting plasmid is pSL2083. The *gshB* (*slr1238*) reading frame was replaced with a gentamicin resistance cassette (Gm^{R}). Primer pairs GshB1 + GshB2 and GshB3 + GshB4 were used to amplify a 529 bp region upstream and a 505 bp region downstream of *gshB*, respectively. Upstream and downstream PCR products were cloned into the pUC18 plasmid on either side of a gentamicin resistance gene to create pSL2085. WT *Synechocystis* 6803 was transformed with pSL2083 and pSL2085 to make $\Delta\text{gshA}::\text{Km}^{\text{R}}$ and $\Delta\text{gshB}::\text{Gm}^{\text{R}}$, respectively. The

$\Delta gshA::Km^R/\Delta gshB::Gm^R$ double mutant was obtained by transforming $\Delta gshA::Km^R$ with pSL2085. To genetically complement $\Delta gshB::Gm^R$, primers GshB8 + GshB9 containing *NdeI* and *HpaI* restriction sites, respectively, were used to amplify the coding region of *gshB*. The product of this reaction was cloned into plasmid pTCP2031V (Sato et al., 2001; Muramatsu et al., 2009) and the resulting plasmid is pSL2086 (Fig. 2A and Table II). This plasmid was transformed into $\Delta gshB::Gm^R$ and the resulting strain is designated $\Delta gshB::Gm^R/T2086$. Segregation of mutant alleles was determined by PCR as shown in Figure 1 and Figure 2. All primers used in study are listed in Table I.

Measurement of Cellular Thiols

Thiols were extracted from *Synechocystis* 6803, derivatized with monobromobimane and analyzed essentially as described (Newton and Fahey, 1995). Thiols were separated using a ZORBAX XDB-C18 (4.6 x 250 mm, 5 μ m) column on an Agilent 1200 series HPLC (Agilent Technologies, Santa Clara, CA). Fluorescent bimane-thiol conjugates were detected on an Agilent 1200 series fluorescence detector (380 nm excitation, 480 nm emission). HPLC run conditions were as follows: Solvent A is 0.1% trifluoroacetic acid in deionized H₂O, Solvent B is 100% methanol. Flow rates were maintained at 1.2 ml/min and linear gradients were used for separation (0 min., 10% B; 2 min., 15% B; 8 min., 20% B; 14 min., 40% B; 16 min., 100% B; 18 min., 100% B; 20 min., 10% B; 30 min., 10% B, reinjection). Comparison of peak areas to those of authentic standards was used to quantify thiols. Measurement of reduced and oxidized forms of glutathione and γ -EC were measured essentially as described (Fey et al., 2005) with the following

modifications. In the extraction buffer, we utilized 50 % acetonitrile instead of 50% methanol, and we buffered with 20 mM HEPES, pH 8.0 instead of 100 mM phosphate, pH 7.1. Separation of thiols was conducted as above. GSH concentration after growth in BSO (Fig. 1) was measured by the glutathione reductase-DTNB recycling assay as described (Queval and Noctor, 2007) after extraction of thiols from cells in 0.2 N HCl. Intracellular concentrations were estimated using an average *Synechocystis* 6803 cellular volume of 4.4×10^{-15} L. The cellular volume was calculated based on an average cell diameter of $2.0 (\pm 0.2) \mu\text{m}$ ($n = 300$) and assuming a spherical cell. Cell diameter was determined using light microscopy (Nikon eclipse 80i) and analyzed using MetaVue software (version 6.3).

Measurement of Photosynthetic Electron Transfer Reactions

Whole chain oxygen evolution activity (H_2O to HCO_3^-) was measured with a Clark-type electrode at a light intensity of $8250 \mu\text{mol photons m}^{-2} \text{s}^{-1}$ (orange-red) using cells suspended in BG11 medium at a chlorophyll concentration of $5 \mu\text{g/ml}$.

Fluorescence Measurements

Measurement of chlorophyll fluorescence induction kinetics (Kautsky) was performed on a FL-200 dual modulation kinetic fluorometer (PSI, Brno, CZ) using cells at a chlorophyll concentration of $5 \mu\text{g/ml}$ that were dark adapted for 5 minutes. Low temperature (77K) fluorescence emission spectra were measured on a Fluoromax-2 fluorometer (Jobin Yvon) using an excitation wavelength of 435 nm or 600 nm.

DCFH-DA Assay for Estimation of ROS

Cells grown in BG11, sulfate-deplete or replete media were transferred to opaque black 96 well plates (Costar). DCFH-DA (2 mM in 100% ethanol) was added directly to the cells at a final concentration of 10 μ M. Cells were incubated in the dark with intermittent shaking for 1 h at room temperature. Fluorescence was measured at 525 nm after excitation at 488 nm every 20 minutes for the duration of the incubation on a Synergy Mx fluorescence plate reader (Biotek Instruments, Inc., Winooski, VT). Three sample replicates were measured for each of the three biological replicates. Fluorescence intensity was normalized to OD_{730 nm} and is presented as relative fluorescence.

Chemicals

All chemicals and thiol standards were purchased from Sigma (St. Louis, MO).

RESULTS

Disruption of the Glutathione Biosynthetic Pathway

The *slr1238* gene product is annotated as glutathione synthetase (GshB), whereas, the gene encoding GshA in *Synechocystis* 6803 is not annotated in KEGG Pathways (Ogata et al., 1999) or on Cyanobase (<http://genome.kazusa.or.jp/cyanobase/>). Identification of a putative *gshA* gene (*slr0990*) is based on 64% sequence identity to the *Anabaena* sp. PCC 7120 gene (*alr3351*), the product of which has been biochemically characterized as having glutamate-cysteine ligase activity (Ashida et al., 2005). The *slr1238* gene exhibits 64.4% sequence identity to the functionally characterized *gshB* gene (*Synpcc7942_2324*) in *Synechococcus elongatus* PCC 7942 (Okumura et al., 1997). To study the function of glutathione in *Synechocystis* 6803, we generated deletion mutations of *slr0990* ($\Delta gshA::Km^R$) and *slr1238* ($\Delta gshB::Gm^R$) (Fig. 1). Because *Synechocystis* 6803 maintains approximately ten copies of its chromosome under normal conditions (Labarre et al., 1989), it is necessary to passage the culture through several generations to allow for full segregation of genomic insertions. After multiple passages on kanamycin containing plates, we were unable to obtain fully segregated colonies of $\Delta gshA::Km^R$, but instead obtained colonies maintaining approximately 50% wild type DNA at the *gshA* locus as determined by PCR (Fig. 1C), suggesting that this gene is essential for survival. Further attempts to segregate the mutant on media containing kanamycin (40 μ g/ml) and 1 mM GSH were also unsuccessful (data not shown). This strain contains approximately 30% less GSH compared to WT under normal growth conditions, which further supports the

notion that *slr0990* encodes GshA. Complete segregation of the $\Delta gshB::Gm^R$ mutant was confirmed by PCR (Fig. 1E). The $\Delta gshA::Km^R/\Delta gshB::Gm^R$ double mutant was also constructed. As in each single mutant, full segregation of $\Delta gshB::Gm^R$, but not of $\Delta gshA::Km^R$ was observed (data not shown). Because we were unable to obtain fully segregated $\Delta gshA::Km^R$ mutants, we also utilized a pharmacological approach to disrupt glutathione biosynthesis, by applying the specific GshA inhibitor DL-buthionine-S,R-sulfoximine (BSO), the L-form being active, (Griffith and Meister, 1979) to cell cultures. We found a concentration dependent growth reduction (Fig. 1E) and decrease in GSH levels (Fig. 1F) in the presence of BSO. This finding supports our hypothesis that GshA activity is required for growth. The unusually high concentrations required for growth reduction likely result from the decreased sensitivity of cyanobacterial GshA to BSO ($K_i = 29.3$ mM) (Ashida et al., 2005) compared to the Arabidopsis protein ($K_i = 1.2$ mM) (Jez et al., 2004). Due to the inherent problems in analyzing the partially segregated $\Delta gshA::Km^R$ mutant, our subsequent analysis mainly focused on the fully segregated $\Delta gshB::Gm^R$ mutant strain.

Characterization and Genetic Complementation of $\Delta gshB::Gm^R$

To verify the function of GshB, we generated a vector designed to express the *gshB* gene (pSL2086) in the $\Delta gshB::Gm^R$ strain using the strategy shown in Figure 2A. Integration of pSL2086 containing the *gshB* gene into the $\Delta gshB::Gm^R$ mutant strain was confirmed by PCR (Fig. 2B). Cellular thiol content was analyzed in the resulting strain, $\Delta gshB::Gm^R/T2086$, and compared to WT and $\Delta gshB::Gm^R$ (Fig. 2C-F). Reduced

glutathione is the predominant species in WT (2.7 ± 0.05 mM) and $\Delta gshB::Gm^R/T2086$ (5.1 ± 0.07 mM). In contrast, the $\Delta gshB::Gm^R$ mutant does not contain detectable amounts of glutathione but instead accumulates high levels of γ -EC (12 ± 0.25 mM). γ -EC levels in the $\Delta gshB::Gm^R$ mutant are significantly higher than those in WT (0.17 ± 0.005 mM) and $\Delta gshB::Gm^R/T2086$ (0.21 ± 0.012 mM) strains. In fact, these levels are over 4 fold higher than that of GSH in WT, a phenomenon observed in bacteria and yeast *gshB* mutants (Grant et al., 1997; Harrison et al., 2005). In contrast, the seedling lethal Arabidopsis *gsh2* mutant ovules accumulate γ -EC over ten fold higher than GSH levels in WT plants (Pasternak et al., 2008). Cysteine levels are also increased in $\Delta gshB::Gm^R$ (62 ± 5 μ M) compared to WT (39 ± 3 μ M) and $\Delta gshB::Gm^R/T2086$ (51 ± 0.7 μ M). Similar accumulation of cysteine is also observed in embryos of the Arabidopsis *gsh2* mutant (Pasternak et al., 2008). While we did not focus on the oxidation state of the thiols in this work, preliminary data indicate that in WT cells, GSSG does not represent more than 10% of the total glutathione pool under normal conditions and is typically maintained under 5%.

$\Delta gshB::Gm^R$ is Sensitive to Redox Perturbations

Glutathione is known to function as a redox buffer and cellular antioxidant. Therefore we tested growth of the $\Delta gshB::Gm^R$ strain, which does not contain glutathione, in conditions predicted to induce oxidative stress. The $\Delta gshB::Gm^R$ mutant is able to grow photoautotrophically, however growth is slower compared to WT and $\Delta gshB::Gm^R/T2086$ strains (Fig. 3A). At all light intensities tested (20-1000 μ mol

photons $\text{m}^{-1} \text{s}^{-1}$), as well as under light/dark regimes the $\Delta\text{gshB}::\text{Gm}^{\text{R}}$ strain was able to grow, albeit at a slower rate than WT. After extended growth in batch culture, the $\Delta\text{gshB}::\text{Gm}^{\text{R}}$ mutant consistently bleached and died before WT suggesting a role for GSH in maintenance of cellular viability during stationary phase in *Synechocystis* 6803. In *E. coli*, glutathione content increases during transition to stationary phase (Fahey et al., 1978) and the requirement of antioxidant enzymes during stationary phase has been observed in yeast (Longo et al., 1996). To further examine the physiology of the $\Delta\text{gshB}::\text{Gm}^{\text{R}}$ strain, we measured chlorophyll fluorescence induction and whole chain oxygen evolution during growth in linear and stationary phase (Fig. S1). During the linear growth phase, the $\Delta\text{gshB}::\text{Gm}^{\text{R}}$ strain exhibited slightly increased oxygen evolution compared to WT. Reduced photosynthetic activity was observed during stationary phase in the WT and $\Delta\text{gshB}::\text{Gm}^{\text{R}}$ strains compared to during linear phase, however the $\Delta\text{gshB}::\text{Gm}^{\text{R}}$ strain evolved O_2 at only 50% of the WT rate. Fluorescence induction kinetics also demonstrate that the $\Delta\text{gshB}::\text{Gm}^{\text{R}}$ strain exhibits reduced photosynthetic capacity during stationary phase compared to WT. We also found that stationary phase $\Delta\text{gshB}::\text{Gm}^{\text{R}}$ cells were less resistant to high light stress compared to WT cells of the same age using chlorophyll induction as a proxy for photosynthetic capacity (Fig. S2). Furthermore, we measured chlorophyll-a (Chl-a) and phycocyanin (PC) content during the growth phase and found that the $\Delta\text{gshB}::\text{Gm}^{\text{R}}$ strain maintains a higher Chl-a:PC ratio than WT, a feature that is exaggerated during stationary phase (Fig. S3). While the ratio of PSI:PSII remains similar according to 77K fluorescence spectra using an excitation of 435 nm (Fig. S4A), there appears to be more energy transfer from the phycobilisomes to

PSI and PSII compared to WT using an excitation of 600 nm (Fig. S4B). Growth in the $\Delta gshB::Gm^R$ strain was also examined in conditions promoting extreme oxidative stress. H_2O_2 is known to oxidize cellular thiols (Gutscher et al., 2009) and elicit expression of genes involved in oxidative stress in *Synechocystis* 6803 (Li et al., 2004; Singh et al., 2004). The $\Delta gshB::Gm^R$ strain exhibited severe growth retardation in the presence of H_2O_2 at concentrations that did not affect WT or the complemented strain (Fig. 3B). To determine whether this response was specific to H_2O_2 or if it was a general sensitivity to ROS, we grew the mutant in the presence of the type II photosensitizer Rose Bengal (RB) and the herbicide methyl viologen (MV). RB absorbs visible light and transfers excitation energy to molecular oxygen to generate singlet oxygen (1O_2) (Fischer et al., 2004). On the other hand, MV accepts electrons from the reducing side of photosystem I and donates the electrons to molecular oxygen to generate the superoxide anion radical (O_2^-). The $\Delta gshB::Gm^R$ mutant was extremely sensitive to RB and MV at concentrations that did not significantly reduce the growth of wild type (Fig. 3, B and C). When started at low culture densities ($OD_{730nm} = 0.05$; 2.4×10^7 cells/ml) there was no growth of this mutant strain in the presence of 1 μM MV. Even at higher cell densities ($>10^8$ cells/ml), this concentration of MV led to a reduction of cellular chlorophyll and resulted in cell death (data not shown). Titration of MV in the growth media indicated that the $\Delta gshB::Gm^R$ mutant cannot grow at levels $\geq 0.5 \mu M$, whereas WT could grow in the presence of 2.0 μM MV.

To further examine the cellular response to MV, RB and H₂O₂, we measured GSH and γ -EC levels after 3 h exposure to each of the compounds at the indicated concentrations (Fig. 4). After exposure to 1 μ M MV, GSH, but not γ -EC levels decreased by approximately 30%. A decrease in foliar GSH levels following MV treatment has also been observed in plants (Iturbe-Ormaetxe et al., 1998). Treatment with 1 mM H₂O₂ resulted an approximately 10% increase of GSH and γ -EC levels. Stimulation of glutathione biosynthesis by oxidants such as hydrogen peroxide is a well-studied phenomenon in plants (May and Leaver, 1993; Queval et al., 2009; Mhamdi et al., 2010). No increase in GSH or γ -EC was observed after treatment with 5 μ M RB, however a role for GSH in response to RB is not unlikely given that increased glutathione peroxidase transcript abundance has been observed in *Chlamydomonas* following RB treatment (Fischer et al., 2004). These results highlight the importance of GSH as an antioxidant in cyanobacteria during oxidative stress. During MV treatment, the decrease in GSH levels might indicate that it was being utilized to protect the cells, whereas γ -EC levels did not change to a great extent. Because we only measured reduced thiols in this assay, the decrease might also reflect oxidation of GSH to GSSG. Additionally, many factors including concentration of compound, duration of exposure, light intensity and cell density will likely influence the outcome of the experiment. In summary, these results indicate that while γ -EC appears to functionally replace GSH under favorable conditions, it is not sufficient during severe redox perturbations. Moreover, GSH is critical for protection against diverse ROS species including H₂O₂, ¹O₂ and O₂⁻.

Light Intensity and Quality Affect Glutathione Metabolism

Photosynthetic organisms depend on energy obtained from light to drive cellular metabolism and carbon fixation. Therefore, it is crucial that cyanobacteria are able to balance light harvesting and energy transduction with demands at the metabolic level. Our lab recently found through transcriptional profiling that changes in light intensity (Aurora et al., 2007; Singh et al., 2008) and quality (Singh et al., 2009) have major effects on cellular physiology and primary metabolism, especially carbon, nitrogen and sulfur metabolism.

We examined the primary thiol concentration in WT (GSH) and $\Delta gshB::Gm^R$ (γ -EC) cells after exposure to different light conditions (Fig. 5). Singh et al. (2009) found that *gshA* and *gshB* genes are differentially expressed in response to preferential illumination of PSI (blue light) or PSII (orange-red light). The differential illumination of the photosystems is primarily due to the large pigment-protein antennae complex, the phycobilisome, thought to be mostly associated with photosystem II (Mullineaux, 2008). Blue light excites chlorophyll in PSI. When cells are exposed to PSII light, *gshB* expression is upregulated compared to PSII light. In contrast, *gshA* expression is decreased in PSII vs. PSI light. In concordance with these results, we found that illumination with orange-red or blue light affected GSH and γ -EC levels in the opposite direction. Blue light led to a 25% decrease in GSH levels and only a slight decline in γ -EC levels, whereas red light led to a 30% increase in WT GSH levels and a 20% decline in γ -EC levels. In both WT and $\Delta gshB::Gm^R$ cells, HL led to increased thiol

concentration, however, GSH levels increased by 200% while γ -EC levels increased by only 15%. Exposure to dark led to an approximately 20% decline in both GSH and γ -EC levels. It is important to note that initial γ -EC levels (approximately 10 mM) in the $\Delta gshB::Gm^R$ mutant LL control were about 6 fold higher than the GSH levels in WT (approximately 1.5 mM).

These results demonstrate the interplay between photosynthetic electron transfer on glutathione metabolism. Linear photosynthetic electron transport does not occur during illumination with blue light or in the dark, and these conditions both led to a substantial decrease in GSH and γ -EC levels. Additionally, these conditions do not promote growth in *Synechocystis* 6803 (Singh et al., 2009). Exposure to orange-red light and high light both promote growth, oxygen evolution and linear photosynthetic electron transport, and resulted in significant increases in GSH levels. Furthermore, transcriptional activation of *gshB* is coordinated with conditions promoting production of reductant and ATP needed for the biosynthesis of GSH and precursors including glutamate and cysteine. These results emphasize a role for GSH during increased growth and metabolism and conditions promoting oxidative stress. However, the ability of the $\Delta gshB::Gm^R$ strain to grow at all light intensities tested suggests that many factors in addition to glutathione are responsible for acclimation to high light conditions as concluded from transcriptomics studies (Hihara et al., 2001; Singh et al., 2008).

Affect of Glucose on Glutathione Metabolism

Synechocystis 6803 is able to grow photoautotrophically (PA), photomixotrophically (PM) in the presence of glucose and photoheterotrophically (PH) in the presence of glucose and the photosystem II inhibitor, DCMU. During PM growth, glucose is catabolized via glycolysis and the oxidative pentose phosphate pathway and high rates of photosynthetic and respiratory electron transport are observed (Takahashi et al., 2008). Increased electron transfer reactions during PM growth could result in increased ROS production compared to PA or PH growth. During PH growth, the linear photosynthetic electron transport chain is blocked and glucose catabolism is utilized for energy production. We analyzed the primary thiol component in WT (GSH) and $\Delta gshB::Gm^R$ (γ -EC) cells after 24 h in PA, PM and PH conditions (Fig. 6), and compared them to the levels in control cultures prior to transfer to experimental conditions. We found that PM growth led to increased thiol levels, while PH growth led to decreased thiol levels in both WT and $\Delta gshB::Gm^R$ cells. PM conditions also resulted increased growth compared to the other conditions. These results agree with the data presented above which indicates that increased photosynthetic electron transport and conditions promoting rapid growth are correlated with high cellular glutathione content.

Glutathione is involved in Acclimation to Nutritional Perturbations

Cyanobacteria are continually faced with environmental challenges such as nutrient limitation. To overcome these challenges, they must adjust their physiology and metabolism (Schwarz and Forchhammer, 2005). While many responses appear to be specific to a particular stress, there are also many general stress responses elicited during a perturbation. Using integrated analysis of large-scale transcriptome datasets, our lab recently determined that oxidative stress is a general phenomenon underlying numerous perturbations in *Synechocystis* 6803 (Singh et al., 2010). In plants, biotic and abiotic perturbations lead to oxidative stress and signaling through production of ROS and changes in the glutathione redox potential (Mittler, 2002; Foyer and Noctor, 2008; Meyer, 2008).

To probe the role of glutathione during physiologically important perturbations, we deprived WT and $\Delta gshB::Gm^R$ cells of nitrate, sulfate or phosphate. These three nutrients play critical roles in growth and photosynthesis in cyanobacteria and plants, therefore limitation of any one of these seriously impacts cellular physiology (Richaud et al., 2001; Schwarz and Forchhammer, 2005; Schachtman and Shin, 2007; Adams et al., 2008). Furthermore, GSH represents a large portion of reduced sulfur within the cell, and contains glutamate, a central player in nitrogen metabolism. Thus, there must be strict coordination between nutrient assimilation and glutathione biosynthesis (Kopriva and Rennenberg, 2004). To test the affect of nutrient availability on the glutathione pool, we measured cellular thiols during nutrient depletion and repletion in WT and the

$\Delta gshB::Gm^R$ strain (Fig. 7). For depletion, cells were transferred to BG11 media lacking nitrate, sulfate or phosphate and grown for 6 days. For repletion, cells were transferred from deplete conditions to BG11, and allowed to recover for 6 days. GSH and γ -EC levels were measured in WT and $\Delta gshB::Gm^R$ strains, respectively. After 6 days of growth in BG11, GSH and γ -EC levels increased (Fig. 7A). Upon dilution into fresh BG11, GSH and γ -EC concentrations decreased. After 6 days growth in the replete conditions, γ -EC levels increased significantly in the $\Delta gshB::Gm^R$ strain. During phosphate depletion, γ -EC levels in the $\Delta gshB::Gm^R$ mutant strain increased, while GSH in WT transiently decreased after 24 h and then increased slightly during the duration of the nutrient depletion. Following phosphate repletion, γ -EC levels in the $\Delta gshB::Gm^R$ mutant transiently decreased during the first 24 h and then increased, while GSH levels in WT increased slightly after 24 h and then decreased for the duration of the time course (Fig. 7B). Nitrate limitation led to a 50% decrease of GSH in WT within 24 h. γ -EC levels were also reduced by approximately 50% in $\Delta gshB::Gm^R$ after 6 days growth. After 24 h in replete media, levels of both GSH and γ -EC increased and continued to rise in the $\Delta gshB::Gm^R$ strain (Fig. 7C). Sulfate depletion led to a dramatic reduction of both GSH and γ -EC within 24 h that was exaggerated after 6 days (Fig. 7D). Other experiments have shown that the depletion occurs in less than 12 h after transfer to sulfate deplete media (data not shown). After transfer to complete media, WT GSH levels surpassed control values within 24 h and then returned near control levels, while γ -EC levels in the $\Delta gshB::Gm^R$ mutant did not fully recover to control levels during this time-course. Cultures of both WT and $\Delta gshB::Gm^R$ strains visually appeared similar after

24 h depletion (Figure 8). The large and dynamic changes in glutathione and γ -EC levels during sulfate and nitrate depletion and repletion suggest that glutathione and γ -EC can be catabolized as a source of sulfur and nitrogen during adverse conditions in cyanobacteria.

Reduced Growth and Fitness of $\Delta gshB::Gm^R$ strain during Sulfate Starvation and Recovery

When WT and $\Delta gshB::Gm^R$ cells were transferred to media lacking sulfate, growth stopped within 24 h, and both GSH and γ -EC levels were depleted. In order to more thoroughly investigate the role of GSH in adaptation to sulfate deprivation, we grew cells in BG11 (control) or in media containing 1/10 the sulfate concentration of BG11 (30.3 μ M vs. 303 μ M) (Fig. 9A). The growth rates of all cultures remained similar for the first 100 h. After 100 h $\Delta gshB::Gm^R$ cells entered a stationary phase in sulfate deplete media, followed by WT. However, WT maintained a higher cell density throughout the experiment. After 264 h of growth, cells were transferred to fresh BG11 media and growth was monitored (Fig. 9B). WT cells from sulfate deplete media grew similar to the BG11 grown controls, but sulfur-deprived $\Delta gshB::Gm^R$ cells recovered very slowly. Sulfur starved cells exhibited reduced pigment content and appeared lighter in color compared to cells grown in BG11 (Fig. 8). After transfer from sulfate deplete media to sulfur replete media, WT cells quickly recovered pigments and grew, while $\Delta gshB::Gm^R$ cells stayed light green for several days (Fig. S5). After several day's growth, $\Delta gshB::Gm^R$ cells were usually able to recover, however sometimes the cells

progressively bleached to white and died. During the time course, GSH levels and γ -EC levels were measured for WT and $\Delta gshB::Gm^R$ strains, respectively (Fig. 9C) and ROS production was measured using the cell permeable fluorescent probe DCFH-DA (Fig. 9D). Increased DCF fluorescence during sulfate starvation in $\Delta gshB::Gm^R$ cells compared to WT indicates oxidative stress in the mutant cells during sulfate depletion. The oxidation state of GSH and γ -EC was also determined during growth in BG11 or after 24 h sulfate starvation. In WT, the GSSG levels increased from approximately 2.5% (GSH to GSSG ratio = 38) to 4% (GSH to GSSG ratio = 26) of the glutathione pool during sulfate starvation. In the $\Delta gshB::Gm^R$ strain, bis- γ -glutamylcystine levels rose from about 2% (γ -EC to $(\gamma$ -EC)₂ ratio = 43) to 7 % (γ -EC to $(\gamma$ -EC)₂ ratio = 14) of the γ -EC pool during sulfate starvation. Together, these data suggest that during sulfate starvation, the $\Delta gshB::Gm^R$ mutant is experiencing more oxidative stress than WT and provides evidence that GSH is important in acclimation to nutrient deplete conditions. Consistent with our previous results, the $\Delta gshB::Gm^R$ strain is able to survive under normal conditions, but not when faced with extreme environmental and redox perturbations.

DISCUSSION

In this study we have utilized $\Delta gshA$ and $\Delta gshB$ deletion mutants in *Synechocystis* 6803 to investigate the functions of glutathione in cyanobacteria. Furthermore, we analyzed thiol compounds in WT and the $\Delta gshB$ strain during exposure to environmental and redox perturbations commonly utilized to study cyanobacterial physiology. Our findings demonstrate that glutathione metabolism is invoked under multiple conditions, suggesting a role in the acclimation response to many diverse perturbations. Furthermore, we find that γ -EC is able to functionally replace GSH under favorable conditions, but not during conditions promoting extreme oxidative stress.

Our findings suggest that GshA activity is essential in *Synechocystis* 6803 because we were unable to isolate fully segregated $\Delta gshA::Km^R$ mutants. In Arabidopsis, *gsh1* mutant plants are embryo lethal (Cairns et al., 2006) and *gshA* mutants in yeast require either DTT or GSH supplemented in the media for growth (Spector et al., 2001). However, in *E. coli*, glutathione is dispensable, because redundancy exists between the glutathione and thioredoxin systems (Prinz et al., 1997). This indicates more specialized roles of GSH in photosynthetic microbes compared to heterotrophic bacteria. In fact, glutathione may be involved in the regulation of many processes in cyanobacteria through glutathionylation (Li et al., 2007).

We were able to generate a fully segregated $\Delta gshB::Gm^R$ mutant that lacks glutathione and instead accumulate γ -EC. In Arabidopsis, mutations in *gsh2* result in a seedling lethal phenotype that can be rescued by expressing *gsh2* in the cytoplasm alone (Pasternak et al., 2008). In some organisms, such as halobacteria, γ -EC is the naturally occurring primary thiol due to its increased stability in high salt concentrations (Sundquist and Fahey, 1989). The $\Delta gshB::Gm^R$ strain accumulates γ -EC to levels over 4 fold higher than GSH in WT. The redox state of the 2GSH/GSSG couple is dependent on the ratio of reduced and oxidized glutathione in addition to the reducing capacity (absolute concentration) (Schafer and Buettner, 2001). This means that changes in the total GSH pool can have dramatic consequences on the cellular redox state. Furthermore, high levels of glutathione increase the buffering capacity of the of the GSH/GSSH redox couple. The high levels of γ -EC in the $\Delta gshB::Gm^R$ may be required to maintain redox poise in the absence of GSH or could represent a decreased efficiency of γ -EC in feedback regulation of GshA compared to GSH. Feedback inhibition of GshA by GSH has been reported for purified *Anabaena* 7120 (Ashida et al., 2005) and Arabidopsis (Jez et al., 2004) enzymes. γ -EC also inhibits Arabidopsis GshA, but to a lower degree than GSH; At 10 mM γ -EC, GshA activity was reduced to only 34% of the control compared to 21% with GSH (Pasternak et al., 2008).

Changes in light quality and intensity is thought to modulate the cellular redox environment in photosynthetic organisms. Our results show that increased photosynthetic electron transfer directly impacts cellular glutathione levels. While

increased GSH biosynthesis has been observed in response to high light treatment in plants (Ogawa et al., 2004), our results suggest that PSII illumination, and not PSI illumination leads to increased GSH biosynthesis. In *Synechocystis* 6803, thiols increased during high light and orange-red light treatments, and during photomixotrophic growth (Fig. 5 and 6). Furthermore, glutathione levels decrease in conditions where linear photosynthetic electron transport is inactive. This is observed during photoheterotrophic growth (Fig. 6), in the dark and during illumination with blue light (Fig. 5). Singh et al., (2009) concluded that preferential illumination of PSI with blue light leads to cyclic electron transfer for generation of ATP, and stimulation of respiration for generation of reducing equivalents. While it is possible that increased electron flow surrounding PSI results in increased ROS, thereby oxidizing the glutathione pool, it has been demonstrated that photoreduction of O₂ to water in *Synechocystis* 6803 is mediated by two A-type flavoproteins and does not generate substantial ROS (Helman et al., 2003). This is also supported by the finding that only 1% of photosynthetic electron transport results in production of H₂O₂ in *Synechocystis* 6803 (Tichy and Vermaas, 1999). All of the conditions promoting increased cellular glutathione content also result in increased PSII mediated oxygen evolution and therefore provide evidence for the role of GSH in the detoxification of ROS.

Photosynthetic electron transport also shuttles electrons into regulatory networks such as those controlled by thioredoxin (Schürmann and Buchanan, 2008). The glutathione system also plays critical roles in the coordination of cellular processes with

photosynthetic activity (Foyer et al., 2009). High light is known to promote oxidative stress and result in many changes at the physiological and transcriptional level in *Synechocystis* 6803 including decreasing photosystem content and phycobilisomes and inducing genes involved in cellular protection (Hihara et al., 2001; Singh et al., 2008). It is surprising that the $\Delta gshB::Gm^R$ is able to grow at all light intensities tested. While growth of $\Delta gshB::Gm^R$ is consistently reduced compared to WT, high light resulted in a proportional decrease in both WT and $\Delta gshB::Gm^R$ growth. Multiple protective mechanisms are responsible for acclimation to high light in *Synechocystis* 6803. Induction of peroxiredoxin genes (*slr1198* and *sll1621*) as well as the NADPH dependent glutathione peroxidase-like (*slr1992*) are observed following high light treatment (Singh et al., 2008). In *Synechocystis* 6803, production of H_2O_2 under high light intensity is considerably lower than that observed in isolated chloroplasts (Tichy and Vermaas, 1999).

Cyanobacteria contain several enzymatic antioxidant systems which metabolize ROS including superoxide dismutase (SodB), catalase (KatG) and multiple peroxiredoxins (Perez-Perez et al., 2009). While $\Delta katG$ is not sensitive to methyl viologen or H_2O_2 (Tichy and Vermaas, 1999), $\Delta sodB$ mutants are extremely sensitive to methyl viologen treatment (Thomas et al., 1998). Additional protection from ROS is provided by the membrane soluble tocopherol, which has been shown to be important during mixotrophic growth in cyanobacteria (Sakuragi et al., 2006). Our results show that GSH plays a critical role in the protection from multiple ROS species in cyanobacteria despite the

presence of other specialized systems. While glutathione appears to play a critical role in protection from ROS, many systems for detoxification of ROS exist within cyanobacteria (Perelman et al., 2003) and each system may function under a particular condition.

We observe large changes in cellular thiol pools after nitrate, sulfate and phosphate depletion in WT and the $\Delta gshB::Gm^R$ mutant strain. During nitrate and sulfur starvation, GSH and γ -EC are depleted and could be catabolized for amino acids as seen in yeast (Elskens et al., 1991; Mehdi and Penninckx, 1997) during nutrient deficiency. In plants, a significant shift in cellular metabolism is observed following sulfur deprivation leading to decreased glutathione, protein and chlorophyll content (Nikiforova et al., 2005). We hypothesize that the increased sensitivity of the $\Delta gshB::Gm^R$ mutant to sulfate starvation and recovery emphasizes reflects increase oxidative stress in the mutant during these conditions. It is possible that recovery of $\Delta gshB::Gm^R$ could reflect defects in sulfate uptake or assimilation. However, γ -EC biosynthesis rates following transfer to sulfate replete conditions are similar to those of WT, and eventually γ -EC levels exceed the levels of GSH in WT. In plants, GSH serves as a reductant to convert adenosine 5' phosphosulfate (APS) into sulfite by APS reductase but γ -EC can replace GSH in this process (Bick et al., 1998). In *Synechocystis* 6803, APS is phosphorylated to 3'-phospho-5'-adenylylsulfate (PAPS) by APS kinase and subsequently reduced to sulfite by PAPS reductase (Schmidt, 1977), an enzyme thought to be redox regulated by the glutathione/glutaredoxin system in *E. coli* (Lillig et al., 2003). There are still many outstanding questions regarding the regulatory components involved in sulfate

assimilation and integration with carbon and nitrogen metabolism, nutrients critical for glutathione metabolism.

CONCLUSIONS

In summary, our analysis of glutathione metabolism in cyanobacteria reveals that cellular glutathione content is highly responsive to changes in light quality, quantity and nutrient availability. Dynamic changes in cellular thiol content requires significant amounts of energy and resources, and therefore these changes must be beneficial for acclimation to changing environmental conditions. Furthermore, our data indicates that GshA activity is essential in cyanobacteria because we were unable to obtain fully segregated $\Delta gshA::Km^R$ mutants. In addition, we find that while the glutathione precursor γ -EC can function during normal growth, GSH is essential for protection against redox stress.

REFERENCES

- Adams MM, Gomez-Garcia MR, Grossman AR, Bhaya D** (2008) Phosphorus deprivation responses and phosphonate utilization in a thermophilic *Synechococcus* sp. from microbial mats. *J Bacteriol* **190**: 8171-8184
- Asada K** (1999) THE WATER-WATER CYCLE IN CHLOROPLASTS: Scavenging of Active Oxygens and Dissipation of Excess Photons. *Annu Rev Plant Physiol Plant Mol Biol* **50**: 601-639
- Ashida H, Sawa Y, Shibata H** (2005) Cloning, biochemical and phylogenetic characterizations of gamma-glutamylcysteine synthetase from *Anabaena* sp. PCC 7120. *Plant Cell Physiol* **46**: 557-562
- Aurora R, Hihara Y, Singh AK, Pakrasi HB** (2007) A Network of Genes Regulated by Light in Cyanobacteria. *OMICS* **11**: 166-185
- Bick JA, Aslund F, Chen Y, Leustek T** (1998) Glutaredoxin function for the carboxyl-terminal domain of the plant-type 5'-adenylsulfate reductase. *Proc Natl Acad Sci USA* **95**: 8404-8409
- Cairns NG, Pasternak M, Wachter A, Cobbett CS, Meyer AJ** (2006) Maturation of Arabidopsis seeds is dependent on glutathione biosynthesis within the embryo. *Plant Physiol* **141**: 446-455
- Copley SD, Dhillon JK** (2002) Lateral gene transfer and parallel evolution in the history of glutathione biosynthesis genes. *Genome Biol* **3**: 25.1-25.16

- Elskens MT, Jaspers CJ, Penninckx MJ** (1991) Glutathione as an endogenous sulphur source in the yeast *Saccharomyces cerevisiae*. *J Gen Microbiol* **137**: 637-644
- Fahey RC, Brown WC, Adams WB, Worsham MB** (1978) Occurrence of glutathione in bacteria. *J Bacteriol* **133**: 1126-1129
- Fey V, Wagner R, Braütigam K, Wirtz M, Hell R, Dietzmann A, Leister D, Oelmüller R, Pfannschmidt T** (2005) Retrograde plastid redox signals in the expression of nuclear genes for chloroplast proteins of *Arabidopsis thaliana*. *J Biol Chem* **280**: 5318-5328
- Fischer BB, Krieger-Liszkay A, Eggen RL** (2004) Photosensitizers neutral red (type I) and rose bengal (type II) cause light-dependent toxicity in *Chlamydomonas reinhardtii* and induce the Gpxh gene via increased singlet oxygen formation. *Environ Sci Technol* **38**: 6307-6313
- Foyer CH, Noctor G, Buchanan B, Dietz KJ, Pfannschmidt T** (2009) Redox Regulation in Photosynthetic Organisms: Signaling, Acclimation, and Practical Implications. *Antioxid Redox Signal* **11**: 861-905
- Grant CM, MacIver FH, Dawes IW** (1997) Glutathione synthetase is dispensable for growth under both normal and oxidative stress conditions in the yeast *Saccharomyces cerevisiae* due to an accumulation of the dipeptide gamma-glutamylcysteine. *Mol Biol Cell* **8**: 1699-1707
- Griffith OW, Meister A** (1979) Potent and specific inhibition of glutathione synthesis by buthionine sulfoximine (S-n-butyl homocysteine sulfoximine). *J Biol Chem* **254**: 7558-7560

- Gutscher M, Sobotta M, Wabnitz G, Ballikaya S, Meyer A, Samstag Y, Dick T** (2009) Proximity-based Protein Thiol Oxidation by H₂O₂-scavenging Peroxidases. *J Biol Chem* **284**: 31532-31540
- Harrison J, Jamet A, Muglia CI, Van de Sype G, Aguilar OM, Puppo A, Frendo P** (2005) Glutathione plays a fundamental role in growth and symbiotic capacity of *Sinorhizobium meliloti*. *J Bacteriol* **187**: 168-174
- Helman Y, Tchernov D, Reinhold L, Shibata M, Ogawa T, Schwarz R, Ohad I, Kaplan A** (2003) Genes encoding A-type flavoproteins are essential for photoreduction of O₂ in cyanobacteria. *Curr Biol* **13**: 230-235
- Hicks LM, Cahoon RE, Bonner ER, Rivard RS, Sheffield J, Jez JM** (2007) Thiol-based regulation of redox-active glutamate-cysteine ligase from *Arabidopsis thaliana*. *Plant Cell* **19**: 2653-2661
- Hihara Y, Kamei A, Kanehisa M, Kaplan A, Ikeuchi M** (2001) DNA microarray analysis of cyanobacterial gene expression during acclimation to high light. *Plant Cell* **13**: 793-806
- Howden R, Andersen CR, Goldsbrough PB, Cobbett CS** (1995) A cadmium-sensitive, glutathione-deficient mutant of *Arabidopsis thaliana*. *Plant Physiol* **107**: 1067-1073
- Iturbe-Ormaetxe I, Escuredo P, Arrese-Igor C, Becana M** (1998) Oxidative Damage in Pea Plants Exposed to Water Deficit or Paraquat. *Plant Physiol* **116**: 173-181

- Iwema T, Picciocchi A, Traore DA, Ferrer JL, Chauvat F, Jacquamet L (2009)** Structural basis for delivery of the intact [Fe₂S₂] cluster by monothiol glutaredoxin. *Biochemistry* **48**: 6041-6043
- Jez JM, Cahoon RE (2004)** Kinetic mechanism of glutathione synthetase from *Arabidopsis thaliana*. *J Biol Chem* **279**: 42726-42731
- Jez JM, Cahoon RE, Chen S (2004)** *Arabidopsis thaliana* glutamate-cysteine ligase: functional properties, kinetic mechanism, and regulation of activity. *J Biol Chem* **279**: 33463-33470
- Kopriva S, Rennenberg H (2004)** Control of sulphate assimilation and glutathione synthesis: interaction with N and C metabolism. *J Exp Bot* **55**: 1831-1842
- Labarre J, Chauvat F, Thuriaux P (1989)** Insertional mutagenesis by random cloning of antibiotic resistance genes into the genome of the cyanobacterium *Synechocystis* strain PCC 6803. *J Bacteriol* **171**: 3449-3457
- Latifi A, Ruiz M, Zhang CC (2009)** Oxidative stress in cyanobacteria. *FEMS Microbiol Rev* **33**: 258-278
- Li H, Singh AK, McIntyre LM, Sherman LA (2004)** Differential gene expression in response to hydrogen peroxide and the putative PerR regulon of *Synechocystis* sp. strain PCC 6803. *J Bacteriol* **186**: 3331-3345
- Li M, Yang Q, Zhang L, Li H, Cui Y, Wu Q (2007)** Identification of novel targets of cyanobacterial glutaredoxin. *Arch Biochem Biophys* **458**: 220-228

- Lillig C, Potamitou A, Schwenn J, Vlamis-Gardikas A, Holmgren A** (2003) Redox regulation of 3'-phosphoadenylylsulfate reductase from *Escherichia coli* by glutathione and glutaredoxins. *J Biol Chem* **278**: 22325-22330
- Longo V, Gralla E, Valentine J** (1996) Superoxide dismutase activity is essential for stationary phase survival in *Saccharomyces cerevisiae*. *J Biol Chem* **271**: 12275-12280
- Lopez-Maury L, Sanchez-Riego AM, Reyes JC, Florencio FJ** (2009) Glutathione/glutaredoxin system is essential for arsenate reduction in *Synechocystis* sp. PCC 6803. *J Bacteriol* **191**: 3534-3543
- Marteyn B, Domain F, Legrain P, Chauvat F, Cassier-Chauvat C** (2008) The thioredoxin reductase-glutaredoxins-ferredoxin crossroad pathway for selenate tolerance in *Synechocystis* PCC6803. *Mol Microbiol* **71**: 520-532
- Masip L, Veeravalli K, Georgiou G** (2006) The many faces of glutathione in bacteria. *Antioxid Redox Signal* **8**: 753-762
- May M, Leaver C** (1993) Oxidative stimulation of glutathione synthesis in *Arabidopsis thaliana* suspension cultures. *Plant Physiol* **103**: 621-627
- Mehdi K, Penninckx MJ** (1997) An important role for glutathione and gamma-glutamyltranspeptidase in the supply of growth requirements during nitrogen starvation of the yeast *Saccharomyces cerevisiae*. *Microbiology* **143**: 1885-1889
- Meyer A** (2008) The integration of glutathione homeostasis and redox signaling. *J Plant Physiol* **165**: 1390-1403

- Meyer AJ, Brach T, Marty L, Kreye S, Rouhier N, Jacquot JP, Hell R** (2007) Redox-sensitive GFP in *Arabidopsis thaliana* is a quantitative biosensor for the redox potential of the cellular glutathione redox buffer. *Plant J* **52**: 973-986
- Meyer AJ, Hell R** (2005) Glutathione homeostasis and redox-regulation by sulfhydryl groups. *Photosyn Res* **86**: 435-457
- Mhamdi A, Hager J, Chaouch S, Queval G, Han Y, Taconnat L, Saindrenan P, Gouia H, Issakidis-Bourguet E, Renou J-P, Noctor G** (2010) Arabidopsis GLUTATHIONE REDUCTASE1 Plays a Crucial Role in Leaf Responses to Intracellular Hydrogen Peroxide and in Ensuring Appropriate Gene Expression through Both Salicylic Acid and Jasmonic Acid Signaling Pathways. *Plant Physiol* **153**: 1144-1160
- Mittler R** (2002) Oxidative stress, antioxidants and stress tolerance. *Trends Plant Sci* **7**: 405-410
- Mittler R, Tel-Or E** (1991) Oxidative stress responses in the unicellular cyanobacterium *Synechococcus* PCC 7942. *Free Radical Res* **13**: 845-850
- Mullineaux CW** (2008) Phycobilisome-reaction centre interaction in cyanobacteria. *Photosynth Res* **95**: 175-182
- Mullineaux PM, Rausch T** (2005) Glutathione, photosynthesis and the redox regulation of stress-responsive gene expression. *Photosynth Res* **86**: 459-474
- Muramatsu M, Sonoike K, Hihara Y** (2009) Mechanism of downregulation of photosystem I content under high-light conditions in the cyanobacterium *Synechocystis* sp. PCC 6803. *Microbiology* **155**: 989-996

- Newton GL, Fahey RC** (1995) Determination of biothiols by bromobimane labeling and high-performance liquid chromatography. *Meth Enzymol* **251**: 148-166
- Nikiforova VJ, Kopka J, Tolstikov V, Fiehn O, Hopkins L, Hawkesford MJ, Hesse H, Hoefgen R** (2005) Systems rebalancing of metabolism in response to sulfur deprivation, as revealed by metabolome analysis of *Arabidopsis* plants. *Plant Physiol* **138**: 304-318
- Ogata H, Goto S, Sato K, Fujibuchi W, Bono H, Kanehisa M** (1999) KEGG: Kyoto Encyclopedia of Genes and Genomes. *Nucleic Acids Res* **27**: 29-34
- Ogawa K, Hatano-Iwasaki A, Yanagida M, Iwabuchi M** (2004) Level of glutathione is regulated by ATP-dependent ligation of glutamate and cysteine through photosynthesis in *Arabidopsis thaliana*: mechanism of strong interaction of light intensity with flowering. *Plant Cell Physiol* **45**: 1-8
- Okumura N, Masamoto K, Wada H** (1997) The *gshB* gene in the cyanobacterium *Synechococcus* sp. PCC 7942 encodes a functional glutathione synthetase. *Microbiology* **143**: 2883-2890
- Pasternak M, Lim B, Wirtz M, Hell R, Cobbett CS, Meyer AJ** (2008) Restricting glutathione biosynthesis to the cytosol is sufficient for normal plant development. *Plant J* **53**: 999-1012
- Penninckx M** (2000) A short review on the role of glutathione in the response of yeasts to nutritional, environmental, and oxidative stresses. *Enzyme Microb Tech* **26**: 737-742

- Perelman A, Uzan A, Hacoen D, Schwarz R** (2003) Oxidative stress in *Synechococcus* sp. strain PCC 7942: various mechanisms for H₂O₂ detoxification with different physiological roles. *J Bacteriol* **185**: 3654-3660
- Perez-Perez ME, Mata-Cabana A, Sanchez-Riego AM, Lindahl M, Florencio FJ** (2009) A comprehensive analysis of the peroxiredoxin reduction system in the cyanobacterium *Synechocystis* sp. PCC 6803 reveals that all five peroxiredoxins are thioredoxin dependent. *J Bacteriol* **191**: 7477-7489
- Picciochi A, Saguez C, Boussac A, Cassier-Chauvat C, Chauvat F** (2007) CGFS-type monothiol glutaredoxins from the cyanobacterium *Synechocystis* PCC6803 and other evolutionary distant model organisms possess a glutathione-ligated [2Fe-2S] cluster. *Biochemistry* **46**: 15018-15026
- Prinz WA, Aslund F, Holmgren A, Beckwith J** (1997) The role of the thioredoxin and glutaredoxin pathways in reducing protein disulfide bonds in the *Escherichia coli* cytoplasm. *J Biol Chem* **272**: 15661-15667
- Queval G, Noctor G** (2007) A plate reader method for the measurement of NAD, NADP, glutathione, and ascorbate in tissue extracts: Application to redox profiling during *Arabidopsis* rosette development. *Anal Biochem* **363**: 58-69
- Queval G, Thominet D, Vanacker H, Miginiac-Maslow M, Gakiere B, Noctor G** (2009) H₂O₂-activated up-regulation of glutathione in *Arabidopsis* involves induction of genes encoding enzymes involved in cysteine synthesis in the chloroplast. *Mol Plant* **2**: 344-356

- Richaud C, Zabulon G, Joder A, Thomas JC** (2001) Nitrogen or sulfur starvation differentially affects phycobilisome degradation and expression of the *nblA* gene in *Synechocystis* strain PCC 6803. *J Bacteriol* **183**: 2989-2994
- Rouhier N, Lemaire SD, Jacquot JP** (2008) The Role of Glutathione in Photosynthetic Organisms: Emerging Functions for Glutaredoxins and Glutathionylation. *Ann Rev Plant Biol* **59**: 143-166
- Sakuragi Y, Maeda H, Dellapenna D, Bryant DA** (2006) alpha-Tocopherol plays a role in photosynthesis and macronutrient homeostasis of the cyanobacterium *Synechocystis* sp. PCC 6803 that is independent of its antioxidant function. *Plant Physiol* **141**: 508-521
- Satoh S, Ikeuchi M, Mimuro M, Tanaka A** (2001) Chlorophyll b expressed in Cyanobacteria functions as a light-harvesting antenna in photosystem I through flexibility of the proteins. *J Biol Chem* **276**: 4293-4297
- Schachtman D, Shin R** (2007) Nutrient sensing and signaling: NPKS. *Annu Rev Plant Biol* **58**: 47-69
- Schafer FQ, Buettner GR** (2001) Redox environment of the cell as viewed through the redox state of the glutathione disulfide/glutathione couple. *Free Radic Biol Med* **30**: 1191-1212
- Schmidt A** (1977) Assimilatory sulfate reduction via 3'-phosphoadenosine-5'-phosphosulfate (PAPS) and adenosine-5'-phosphosulfate (APS) in blue-green algae. *FEMS Microbiol Lett* **1**: 137-140

- Schürmann P, Buchanan BB** (2008) The ferredoxin/thioredoxin system of oxygenic photosynthesis. *Antioxid Redox Signal* **10**: 1235-1274
- Schwarz R, Forchhammer K** (2005) Acclimation of unicellular cyanobacteria to macronutrient deficiency: emergence of a complex network of cellular responses. *Microbiology* **151**: 2503-2514
- Serrano A, Rivas J, Losada M** (1984) Purification and properties of glutathione reductase from the cyanobacterium *Anabaena* sp. strain 7119. *J Bacteriol* **158**: 317-324
- Singh AK, Elvitigala T, Cameron JC, Ghosh BK, Bhattacharyya-Pakrasi M, Pakrasi HB** (2010) Integrative analysis of large scale expression profiles reveals core transcriptional response and coordination between multiple cellular processes in a cyanobacterium. *BMC Syst Biol* **4**:105
- Singh AK, Bhattacharyya-Pakrasi M, Elvitigala T, Ghosh B, Aurora R, Pakrasi HB** (2009) A systems-level analysis of the effects of light quality on the metabolism of a cyanobacterium. *Plant Physiol* **151**: 1596-1608
- Singh AK, Elvitigala T, Bhattacharyya-Pakrasi M, Aurora R, Ghosh B, Pakrasi HB** (2008) Integration of carbon and nitrogen metabolism with energy production is crucial to light acclimation in the cyanobacterium *Synechocystis*. *Plant Physiol* **148**: 467-478
- Singh AK, Li H, Sherman LA** (2004) Microarray analysis and redox control of gene expression in the cyanobacterium *Synechocystis* sp. PCC 6803. *Physiol Plant* **120**: 27-35

- Spector D, Labarre J, Toledano MB** (2001) A genetic investigation of the essential role of glutathione: mutations in the proline biosynthesis pathway are the only suppressors of glutathione auxotrophy in yeast. *J Biol Chem* **276**: 7011-7016
- Stork T, Michel K, Pistorius EK, Dietz K** (2005) Bioinformatic analysis of the genomes of the cyanobacteria *Synechocystis* sp. PCC 6803 and *Synechococcus elongatus* PCC 7942 for the presence of peroxiredoxins and their transcript regulation under stress. *J Exp Bot* **56**: 3193-3206
- Suginaka K, Yamamoto K, Ashida H, Sawa Y** (1999) Effect of Intracellular Glutathione on Heat-induced Cell Death in the Cyanobacterium, *Synechocystis* PCC 6803. *Biosci Biotechnol Biochem* **63**: 1112-1115
- Suginaka K, Yamamoto K, Ashida H, Kono Y** (1998) Cysteine uptake for accumulation of glutathione by the cyanobacterium *Synechocystis* PCC 6803. *Biosci Biotechnol Biochem* **62**: 424-428
- Sundquist A, Fahey R** (1989) The function of gamma-glutamylcysteine and bis-gamma-glutamylcystine reductase in *Halobacterium halobium*. *J Biol Chem* **264**: 719-725
- Takahashi H, Uchimiya H, Hihara Y** (2008) Difference in metabolite levels between photoautotrophic and photomixotrophic cultures of *Synechocystis* sp. PCC 6803 examined by capillary electrophoresis electrospray ionization mass spectrometry. *J Exp Bot* **59**: 3009-3018
- Tel-Or E, Huflejt M, Packer L** (1985) The role of glutathione and ascorbate in hydroperoxide removal in cyanobacteria. *Biochem Biophys Res Commun* **132**: 533-539

- Thomas DJ, Avenson TJ, Thomas JB, Herbert SK** (1998) A Cyanobacterium Lacking Iron Superoxide Dismutase Is Sensitized to Oxidative Stress Induced with Methyl Viologen but Is Not Sensitized to Oxidative Stress Induced with Norflurazon. *Plant Physiol* **116**: 1593-1602
- Tichy M, Vermaas W** (1999) In vivo role of catalase-peroxidase in *Synechocystis* sp. strain PCC 6803. *J Bacteriol* **181**: 1875-1882
- Vernoux T, Wilson RC, Seeley KA, Reichheld JP, Muroy S, Brown S, Maughan SC, Cobbett CS, Van Montagu M, Inzé D, May MJ, Sung ZR** (2000) The *ROOT MERISTEMLESS1/CADMIUM SENSITIVE2* gene defines a glutathione-dependent pathway involved in initiation and maintenance of cell division during postembryonic root development. *Plant Cell* **12**: 97-110
- Wolf AM, Asoh S, Ohsawa I, Ohta S** (2008) Imaging mitochondrial redox environment and oxidative stress using a redox-sensitive fluorescent protein. *J Nippon Med Sch* **75**: 66-67
- Zechmann B, Tomašić A, Horvat L, Fulgosi H** (2010) Subcellular distribution of glutathione and cysteine in cyanobacteria. *Protoplasma* **246**:15-24

Table I**Primers used in this study.**

Forward (F) and reverse (R) primers were used to amplify upstream (up) and downstream (dn) regions of indicated genes for generation of transformation plasmids shown in parenthesis and Table II or for segregation analysis (seg). Bold font indicates restriction sites used for cloning.

Primer	Description	Sequence (5'-3')
GshA1	F: up. <i>gshA</i> (pSL2083)	TCTGGATCCGAAACCGGTTGTGTCAGTT
GshA2	R: up. <i>gshA</i> (pSL2083)	TCTCTGCAGGCACTGCACTCGCCTCTTTA
GshA3	F: dn. <i>gshA</i> (pSL2083)	TCTCTGCAGCTGCTTACCCCTGAGCAAAG
GshA4	R: dn. <i>gshA</i> (pSL2083)	TCTAAGCTTAATCCGTGGATTGGTAGGTG
GshA5	F: Seg. of $\Delta gshA::Km^R$	CCACTGTTTCTGGTGGTCT
GshA6	R: Seg. of $\Delta gshA::Km^R$	CCCTCGGCAAAAGTTTATGA
GshB1	F: up. <i>gshB</i> (pSL2085)	TCTGGATCCGACTTTCGTGGCGAAATGGT
GshB2	R: up. <i>gshB</i> (pSL2085)	TCTCTGCAGCAGGGTCAATATCCTTGGGA
GshB3	F: dn. <i>gshB</i> (pSL2085)	TCTCTGCAGCCTGGGATCAAGACAGCTCAA
GshB4	R: dn. <i>gshB</i> (pSL2085)	TCTAAGCTTGTCCCTGTACTGGCACATTG
GshB5	F: Seg. of $\Delta gshB::Gm^R$	GGAAACCATGGGTCTGCTTA
GshB6	R: Seg. of $\Delta gshB::Gm^R$	TTTTCATTGGCTTCCCCTAG
GshB7	R: Seg. of $\Delta gshB::Gm^R$	TCACCGTAATCTGCTTGCAC
GshB8	F: <i>gshB</i> ORF (pSL2086)	TCTCATATGAACTGGCTTTTATTATCGAT
GshB9	R: <i>gshB</i> ORF (pSL2086)	TCTGTTAACCTAAAATTGTTTTTCCAACCA
GshB10	R: Seg. of T2086	CTCGCTTCTTGGATGACCTC
GshB11	R: Seg. of T2086	ATATAAGCGGCCCACTTCT

Table II
Plasmids and Strains

Plasmids were constructed as described in “Materials and Methods” and used to generate strains analyzed in this study.

Plasmid	Description (strain)	Reference
pSL2083	For generation of ($\Delta gshA::Km^R$)	This Study
pSL2085	For generation of ($\Delta gshB::Gm^R$)	This Study
pTCP2031v	Contains Cm^R , <i>psbA2</i> promoter and <i>slr2031</i> targeting sequences.	(Sato et al, 2001; Muramatsu et al, 2009)
pSL2086	<i>gshB</i> cloned in pTCP2031v (T2086) for generation of ($\Delta gshB::Gm^R/T2086$)	This Study

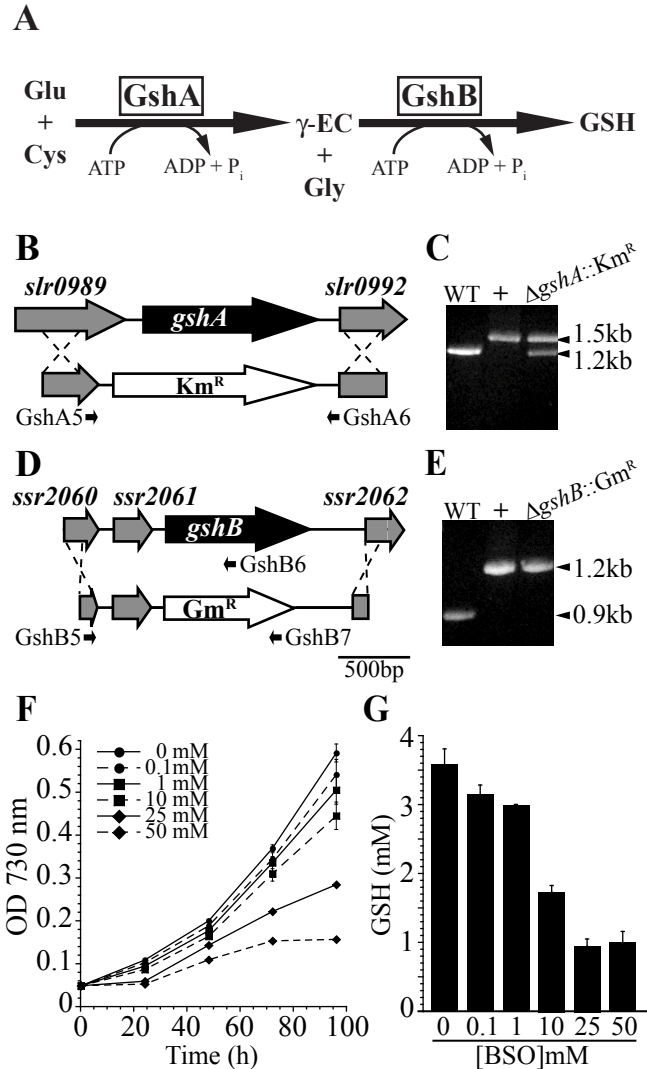


Figure 1. Disruption of glutathione biosynthesis in *Synechocystis* 6803.

(A) Diagram of glutathione biosynthetic pathway. (B) The entire ORF of the *gshA* gene was replaced with a kanamycin resistance cassette (Km^R) to generate the $\Delta gshA::Km^R$ strain. (C) Segregation of $\Delta gshA::Km^R$ was tested by PCR using primers GshA5 and GshA6 shown in (A). Lanes: WT genomic DNA, pSL2083 (+), $\Delta gshA::Km^R$ genomic DNA. (D) The *gshB* gene was replaced with a gentamicin resistance cassette (Gm^R). (E) Segregation of $\Delta gshB::Gm^R$ was confirmed by PCR using primers GshB5, GshB6 and GshB7 shown in (D). Lanes: WT genomic DNA, pSL2085 (+), $\Delta gshB::Gm^R$ genomic DNA. (F) Growth of WT cells in the presence of GshA inhibitor, BSO. (G) Cellular GSH concentration after 96 h growth in the presence of BSO. Values represent mean of three cultures and error bars represent SE. Primer sequences used in cloning and segregation analysis are shown in Table I. GSH, glutathione; γ -EC, γ -glutamylcysteine; BSO, DL-buthionine-S,R-sulfoximine.

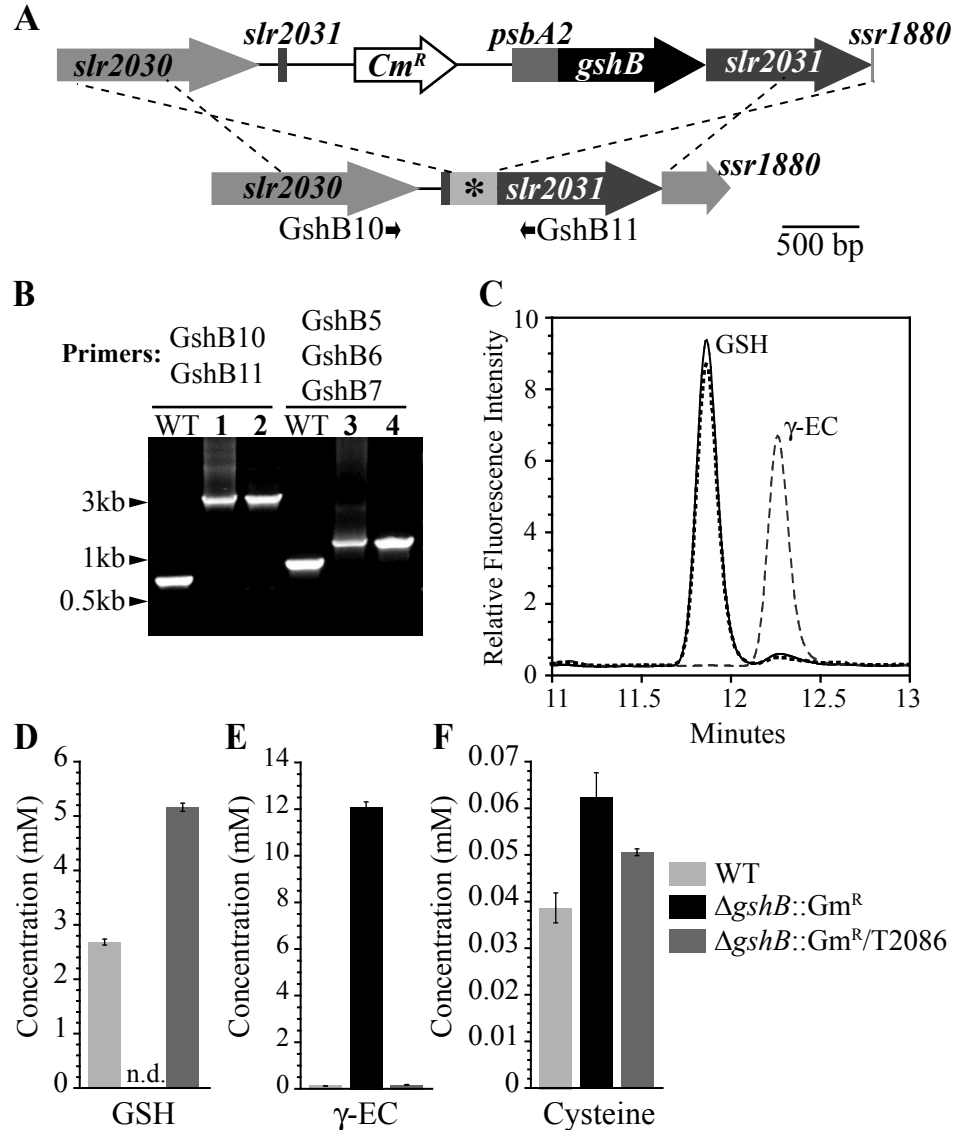


Figure 2. Genetic complementation of the $\Delta gshB::Gm^R$ strain and quantification of cellular thiols. (A) The *gshB* gene was cloned into the pTCP2031V (Sato et al, 2001; Muramatsu et al, 2009) vector under the control of the *psbA2* promoter (top) and targeted to the *slr2031* site (*) in the $\Delta gshB::Gm^R$ mutant; the resulting strain is $\Delta gshB::Gm^R/T2086$. (B) Segregation of $\Delta gshB::Gm^R/T2086$ was confirmed by PCR using primers shown in (A) and Figure 1C. Lanes: WT genomic DNA; 1, pSL2086; 2 and 4, $\Delta gshB::Gm^R/T2086$ genomic DNA; 3, pSL2085. (C) HPLC elution profile of monobromobimane derivatized thiols extracted from WT (solid), $\Delta gshB::Gm^R$ (dashed) and $\Delta gshB::Gm^R/T2086$ (dotted) cells. Quantification of cellular (D) GSH, (E) γ -EC and (F) cysteine levels. GSH, reduced glutathione; γ -EC, γ -glutamylcysteine. Data are mean of three independent cultures \pm SE. Intracellular concentrations are based on an estimated cellular volume of *Synechocystis* 6803 equal to 4.4×10^{-15} L; See “Materials and Methods” for details. n.d., not detected.

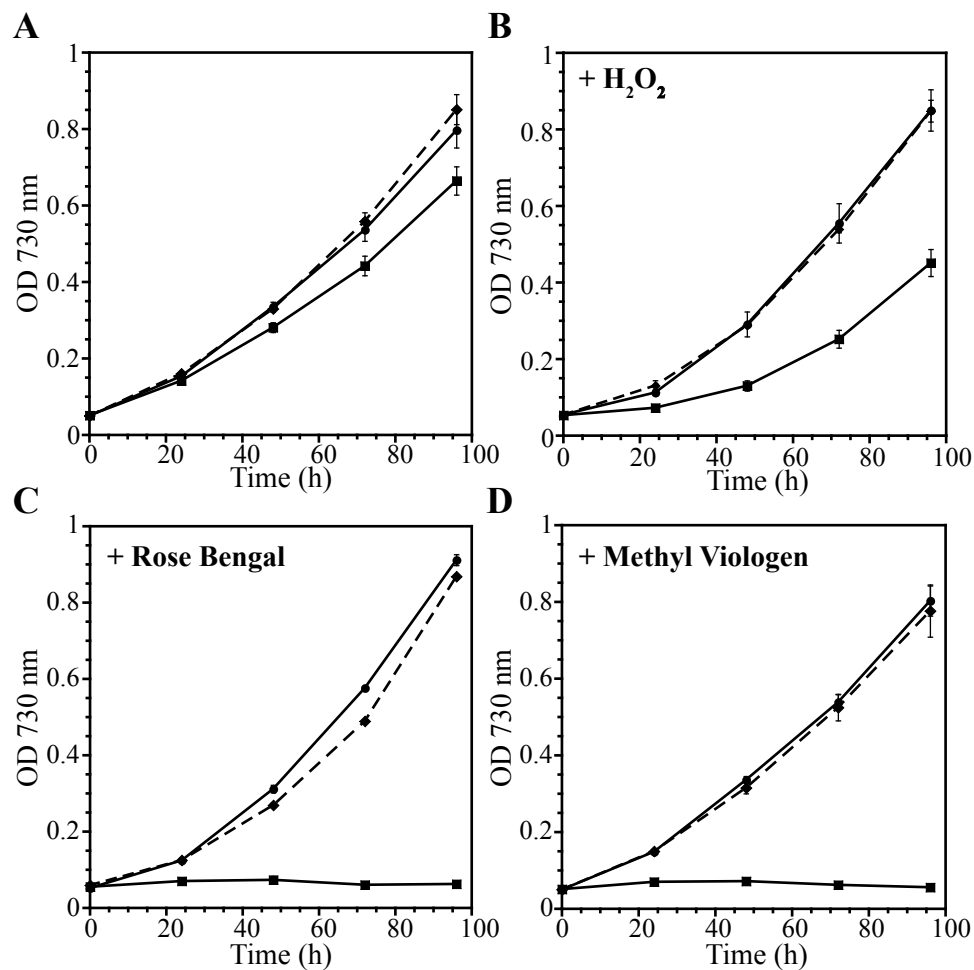


Figure 3. Growth of WT, $\Delta gshB::Gm^R$ and $\Delta gshB::Gm^R/T2086$ strains.

(A) Photoautotrophic; (B) 1.5 mM H_2O_2 ; (C) 5 μM Rose Bengal; (D) 1 μM methyl viologen. WT (circle, solid); $\Delta gshB::Gm^R$ (square, solid); $\Delta gshB::Gm^R/T2086$ (diamond, dashed). Cells were grown with continuous illumination of 30 $\mu mol photons m^{-2} s^{-1}$. Growth was monitored as turbidity at 730 nm. Error bars represent SE of three independent cultures.

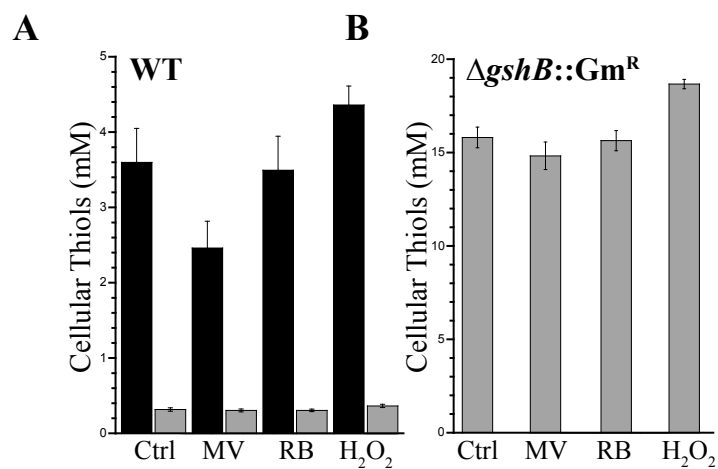


Figure 4. Changes in cellular thiol content after redox perturbations.

GSH (black bar) and γ -EC (grey bar) were measured in untreated WT (A) and $\Delta gshB::Gm^R$ (B) cells (Ctrl) or cells exposed to 1 μ M methyl viologen, 5 μ M Rose Bengal or 1 mM H₂O₂ for 3 h under continuous illumination at 30 μ mol photons m⁻² s⁻¹. Each bar represents the mean of three independent cultures and error bars represent SE.

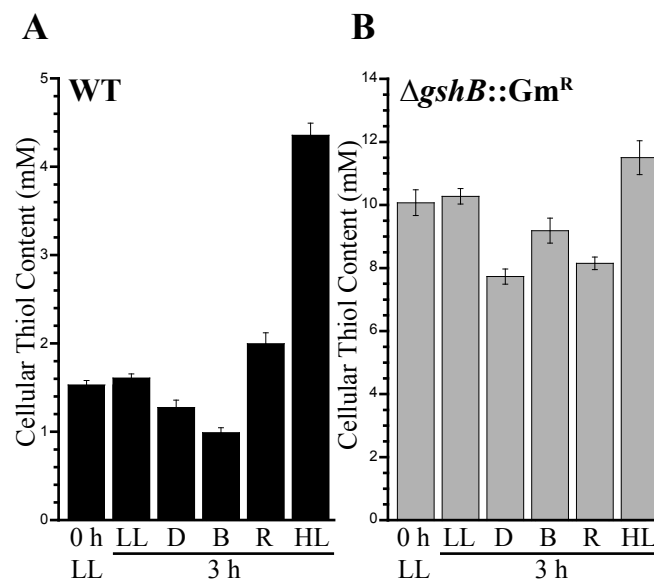


Figure 5. Influence of light quality and intensity on glutathione metabolism.

The major cellular thiol was measured in (A) WT (GSH; black bar) and (B) $\Delta gshB::Gm^R$ (γ -EC; grey bar) after exposure to different light conditions. Low light (LL; $20 \mu\text{mol photons m}^{-2} \text{s}^{-1}$) grown cells were transferred to LL, dark (D), blue (B), orange-red (R) or high light (HL, $150 \mu\text{mol photons m}^{-2} \text{s}^{-1}$) for 3 hours. Thiols were then analyzed by HPLC. Each bar represents the mean of three independent cultures and error bars represent SE. See “Materials and Methods” section for further details.

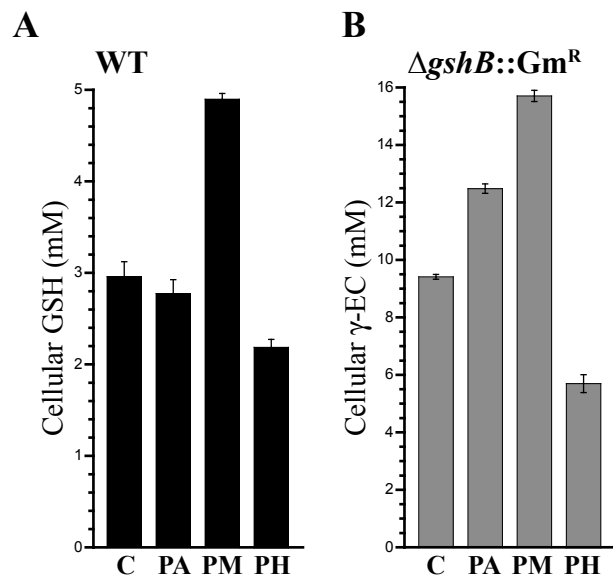


Figure 6. Cellular thiol content after addition of glucose.

The major cellular thiol was measured in (A) WT (GSH; black bars) and (B) the $\Delta gshB::Gm^R$ strain (γ -EC; grey bars) grown photoautotrophically (PA), photomixotrophically (PM) in the presence of 5 mM glucose, or photoheterotrophically (PH) in the presence of 5 mM glucose and 10 μ M DCMU for 24 hours. Values for preculture cells used as the inoculum for the experiment are also shown (C). Error bars represent SE of two separate measurements each from two independent cultures.

DCMU; 3-(3,4-dichlorophenyl)-1,1-dimethylurea

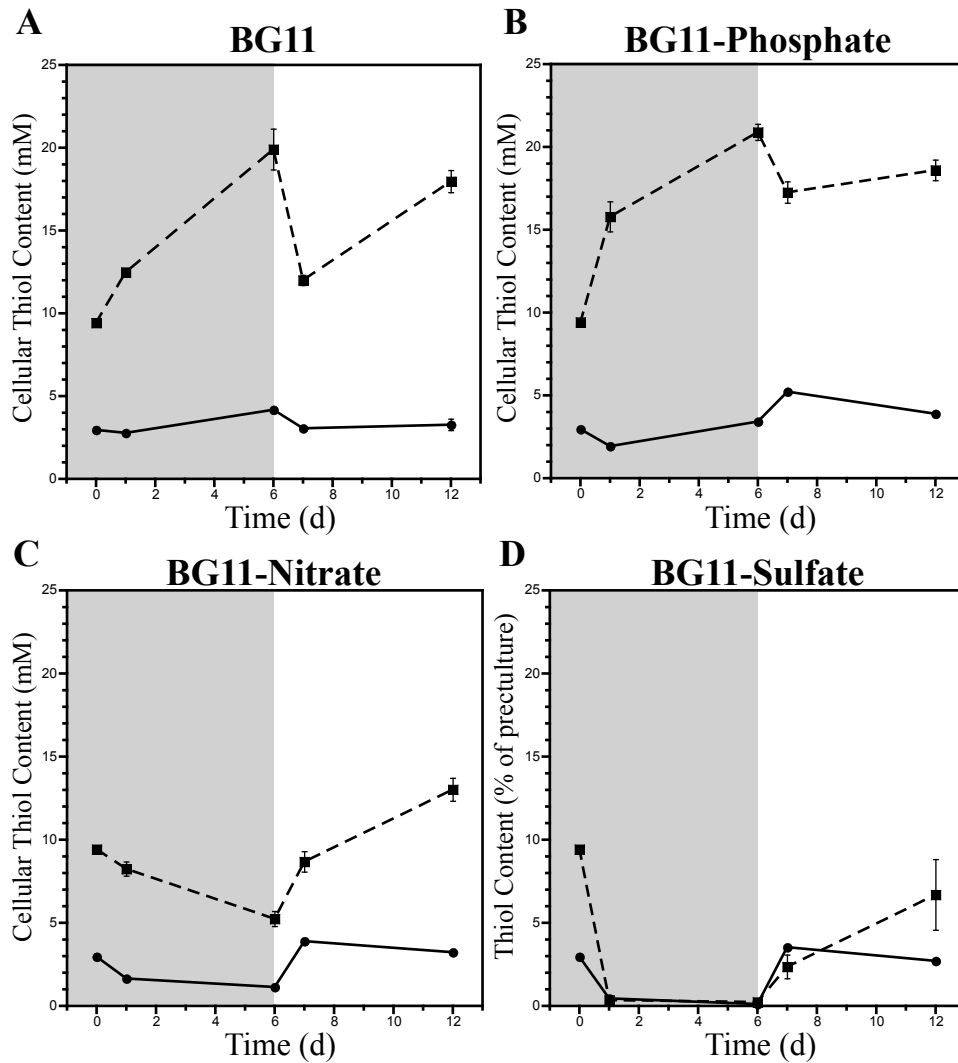


Figure 7. Affect of nutrient depletion on glutathione metabolism.

The major primary thiol was measured in WT (GSH; solid line; circle) and the $\Delta gshB::Gm^R$ strain (γ -EC; dashed line; square) over the course of 12 days in deplete (shaded) and replete (white) conditions. Cells were precultured in BG11 media (0 d) prior to transfer to (A) BG11 or BG11 lacking (B) nitrate, (C) sulfate or (D) phosphate for 6 days. After 6 days of growth in deplete conditions, cells were transferred to fresh BG11 media and grown for an additional 6 days. Error bars represent SE of two measurements each from two independent cultures.

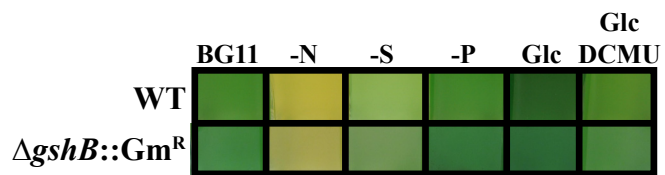


Figure 8. Visual comparison of WT and $\Delta gshB::Gm^R$ cultures.

Photographs of cultures after 24 h growth in BG11 medium lacking nitrate (-N), sulfate (-S), phosphate (-P) or with the addition of 5 mM glucose (Glc) with or without 10 μ M DCMU.

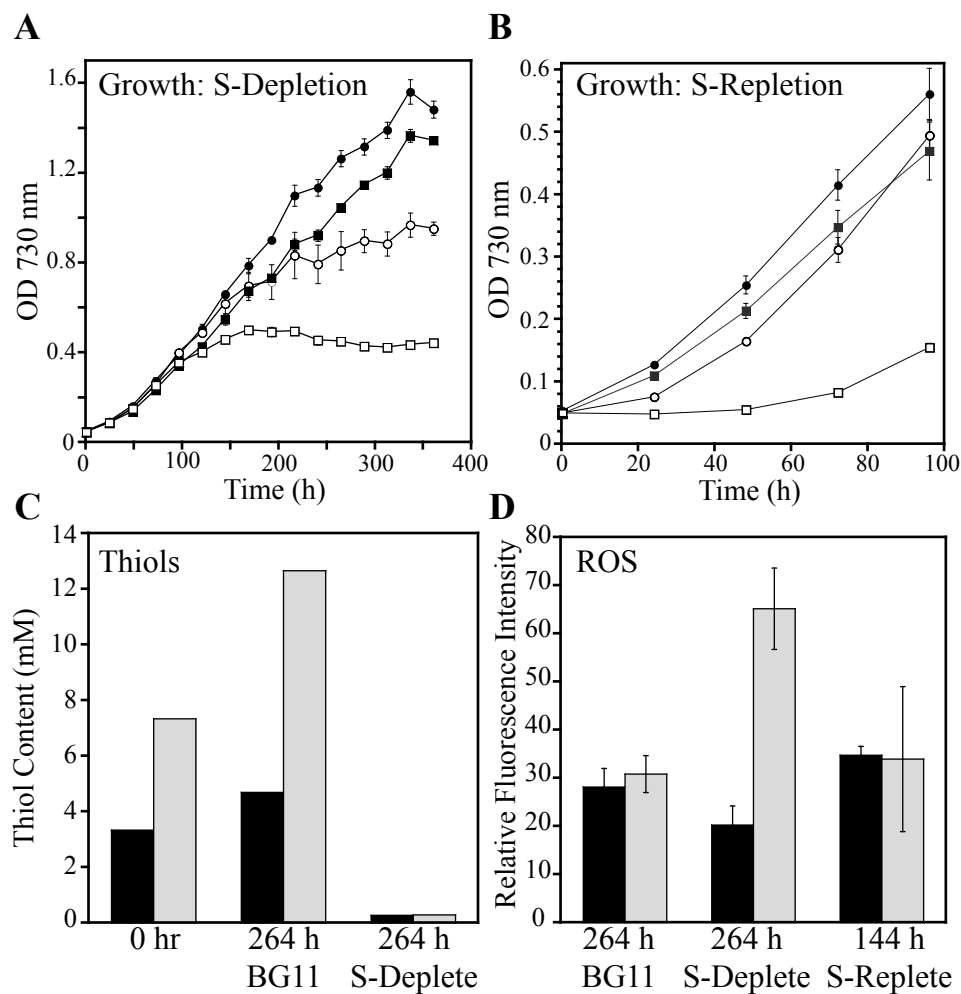


Figure 9. Characterization of sulfate depletion in $\Delta gshB::Gm^R$ cells. (A) Growth of WT (circle) and $\Delta gshB::Gm^R$ (square) in BG11 (filled symbol) or BG11 containing 10% sulfate (30.3 μ M) (open symbol). Values represent mean \pm SE (n = 3). (B) Growth of WT (circle) and $\Delta gshB::Gm^R$ (square) in BG11 after 264 hours growth in S-deplete (open symbol) or BG11 (filled symbol). Values are the mean \pm SE of three cultures. (C) The major cellular thiol in WT (GSH; black bar) and $\Delta gshB::Gm^R$ (γ -EC; grey bar) was quantified by HPLC prior to S-depletion (0 hr), after 264 hours of growth in BG11 or in sulfate deplete media. Each value represents a single measurement and is consistent with results of at least three independent experiments. (D) ROS accumulation of WT (black) and $\Delta gshB::Gm^R$ (grey) after 264 hours growth in BG11 or S-deplete, and after 144 hours recovery in BG11 media. Error bars represent SE of three measurements each from three independent cultures.

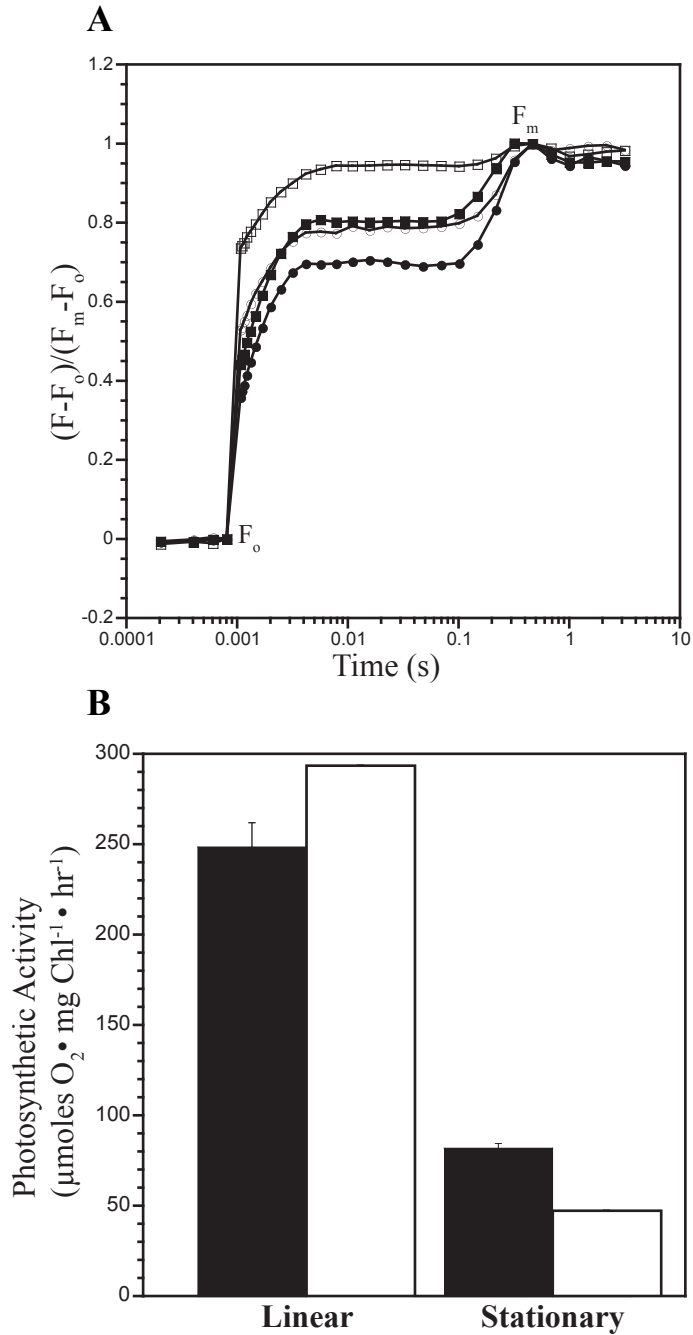


Figure S1. Stationary phase physiology in the WT and $\Delta gshB::Gm^R$ strains.

(A) Chlorophyll fluorescence induction kinetics were measured during linear (8 days; solid shape) and stationary growth phases (15 days; open shape) in WT (circles) and $\Delta gshB::Gm^R$ (squares). (B) Whole chain oxygen evolution activity was measured using same cultures as in (A) in the presence of 10 mM HCO_3^- with saturating light ($8250 \mu\text{mol photons m}^{-2} \text{s}^{-2}$) on a Clark-type electrode. WT, black bars; $\Delta gshB::Gm^R$, white bars.

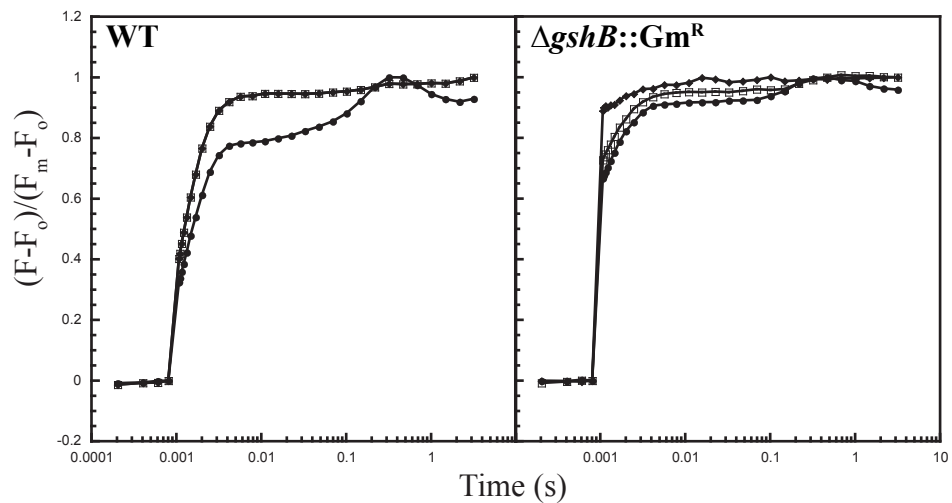


Figure S2. Chlorophyll fluorescence induction in stationary phase cultures following high light treatment.

Stationary phase cultures (15 day old) of the WT and the $\Delta gshB::Gm^R$ strains were exposed to high light ($500 \mu\text{mol photons m}^{-2} \text{s}^{-1}$ RGB LED's) in a Fytoscope (Photon Systems Instruments, Brno, Czech Republic) chamber at 30°C . Fluorescence induction was measured after 0 h (closed circles), 3 h (open squares) and 24 h (closed diamonds).

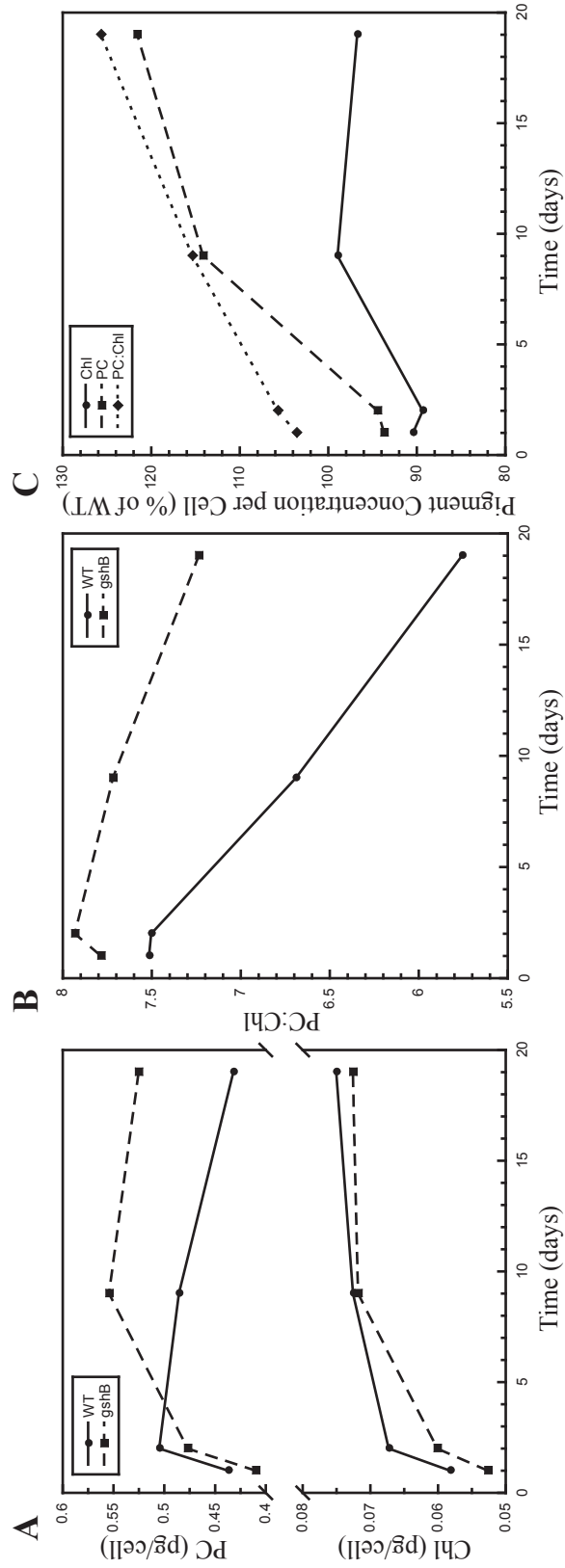


Figure S3. Comparison of WT and $\Delta gshB::Gm^R$ pigments during growth.

(A) Chlorophyll-a and phycocyanin concentrations were measured in shake-flask batch cultures for 19 days in the WT (circle, line) and $\Delta gshB::Gm^R$ (square, dotted) strains. (B) PC to Chl ratio during growth. (C) Presentation of data shown in A and B as % of WT at each time-point. Pigment concentrations were estimated using whole cell absorption spectra as described in “Methods” section of Chapter 4 in this dissertation.

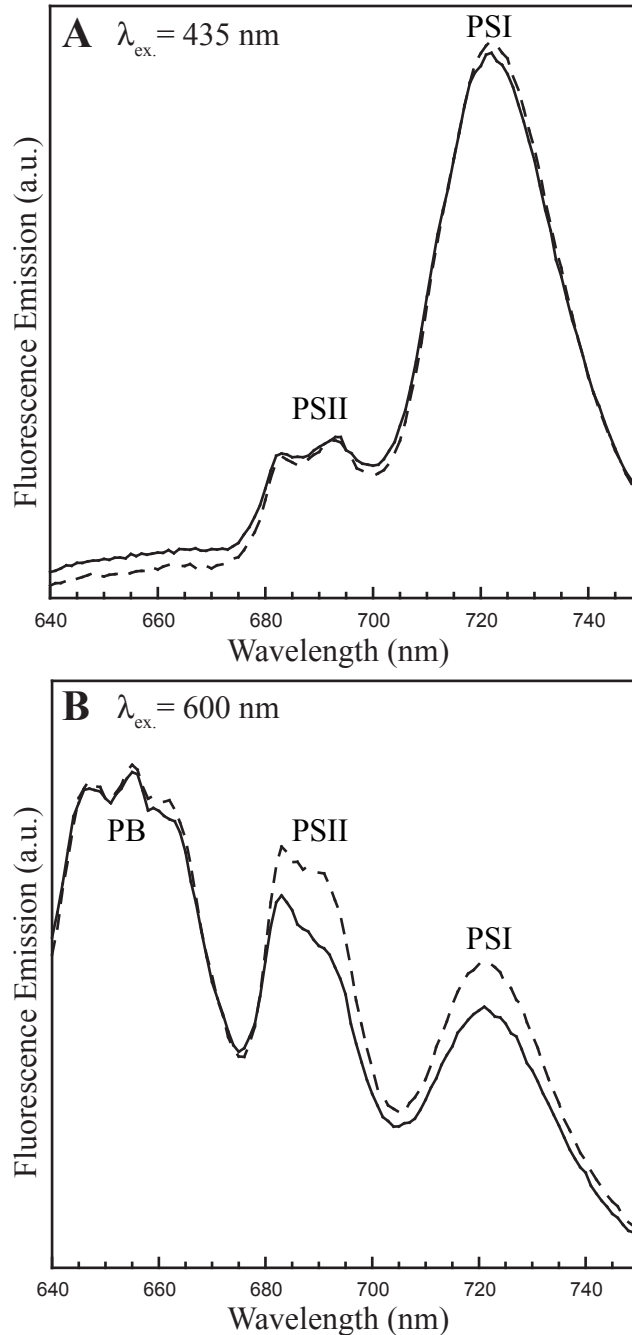


Figure S4. 77 K fluorescence of WT and $\Delta gshB::Gm^R$ Cells.

Low temperature (77 K) fluorescence emission spectra were measured following excitation of chlorophyll at 435 nm (A) or phycocyanin at 600 nm (B). Emission spectra were normalized to the peak at 695 nm (A) or 650 nm (B). Emission peaks corresponding to photosystem I (PSI), photosystem II (PSII) and phycobilisome (PB) are labeled. Measurements were performed on cells suspended at a chlorophyll concentration of 5 $\mu\text{g/ml}$ in BG11 medium. Arbitrary units (a.u.).

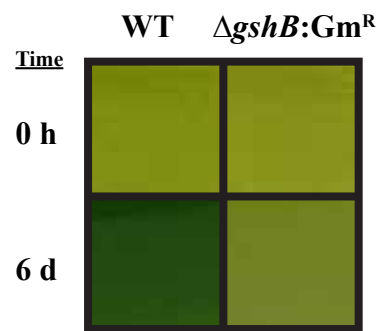


Figure S5. Visual comparison of WT and the $\Delta gshB::Gm^R$ strains during recovery from sulfate depletion.

Cells were transferred from sulfate deplete media into fresh BG11 containing 303 μM sulfate (0 h) and grown for 6 days.

Chapter 3

Function of γ -Glutamylcysteine during Redox and Metal Stress in *Synechocystis* sp. PCC 6803

This chapter was adapted from:

Jeffrey C. Cameron and Himadri B. Pakrasi (2011). Glutathione in *Synechocystis* 6803: A closer look into the physiology of a $\Delta gshB$ mutant. *Plant Signaling and Behavior* **6**: 89-92

SUMMARY

Glutathione (GSH) is a low molecular weight thiol compound that plays many roles in photosynthetic organisms. We utilized a $\Delta gshB$ (glutathione synthetase) mutant strain as a tool to evaluate the role of GSH in the cyanobacterium *Synechocystis* sp. PCC 6803 (hereafter *Synechocystis* 6803), a model photosynthetic organism. The $\Delta gshB$ mutant does not synthesize glutathione, but instead accumulates the GSH precursor, γ -glutamylcysteine (γ -EC), to millimolar levels. We found that γ -EC was sufficient to permit cellular proliferation during optimal conditions, but not when cells were exposed to conditions promoting oxidative stress. Furthermore, we found that many factors affecting growth rate and photosynthetic activities strongly influenced cellular thiol content. Here, we are providing some additional insights into the role of GSH and γ -EC in *Synechocystis* 6803 during conditions promoting oxidative stress and altered metabolism.

INTRODUCTION

Maintenance of cellular redox homeostasis is critical for the functions of cellular processes. This is especially important in when cells are exposed to environmental perturbations that promote the formation of reactive oxygen species (ROS). In photosynthetic organisms, many perturbations can lead to increased generation of ROS due to the close proximity of the oxygen evolving complex of photosystem II (PSII) and the many redox active cofactors that participate in photosynthesis and respiration. Therefore, photosynthetic organism have developed intricate mechanisms to alleviate the stress of ROS that include many protein and small molecule antioxidants (Latifi et al., 2009).

Glutathione, a small thiol tripeptide, is crucial for maintenance of redox homeostasis during many environmental perturbations in cyanobacteria (Cameron and Pakrasi, 2011). Glutathione is comprised of the amino acids glutamate, cysteine and glycine. The tripeptide is generated through two sequential ATP dependent steps by glutatamate-cysteine ligase (GshA) and glutathione synthetase (GshB). We have previously generated mutants of the *gshA* and *gshB* genes *Synechocystis* sp. PCC 6803 (hereafter *Synechocystis* 6803). We found that GshA activity is essential for growth, while the Δ *gshB* strain is viable under normal laboratory conditions (Cameron and Pakrasi, 2011). The Δ *gshB* strain is unable to synthesize GSH, but accumulates the biosynthetic intermediate, γ -glutamylcysteine (γ -EC). Our results demonstrated that while the Δ *gshB*

strain grows photoautotrophically in many conditions, it does not tolerate conditions promoting oxidative stress. While these results demonstrate that GSH is critical as an antioxidant in *Synechocystis* 6803, despite the presence of other antioxidant systems, it also suggests that γ -EC can functionally replace GSH in some metabolic processes in cyanobacteria. This is not completely unfounded, as it has been shown that γ -EC is the main soluble thiol in Halobacteria, presumably due to its increased stability compared to GSH in high salt concentrations (Sundquist and Fahey, 1989).

Glutathione has become ubiquitous in nature due to its versatile properties that allow it to function as a redox buffer, electron donor and antioxidant. However, it also plays many roles in the maintenance of metal homeostasis. GSH has been shown to be important for metal tolerance in diverse organisms including bacteria and plants (Howden et al., 1995; Helbig et al., 2008). While many metals are crucial to the function of diverse proteins, they also have the capacity to damage cellular components if their storage, handling or transport mechanisms malfunction. In addition, metals such as cadmium and selenium are often encountered in the environment and have the ability to perturb many aspects of cellular metabolism. GSH has also been found to play important roles in detoxification of cadmium in bacteria and eukaryotic organisms (Helbig et al., 2008; Preveral et al., 2009). In plants, algae and yeast, phytochelatin, a polymer of GSH, is produced during exposure to heavy metals such as cadmium (Kobayashi et al., 2006; Mendoza-Cózatl et al., 2008; Mendoza-Cozatl et al., 2010). Further, *Arabidopsis* mutants with altered GshA activity have been shown to be sensitive to cadmium (Howden et al., 1995; Vernoux et al., 2000).

These polymers can bind cadmium and facilitate transport out of the cell or into storage/degradation vacuoles to prevent disruption of cellular processes. Although some cyanobacteria contain proteins with similarities to phytochelatin synthase cyanobacteria are not known to synthesize phytochelatin (Harada et al., 2004).

In photosynthetic organisms, acquisition and storage of metals is critical for the function of the many photosynthetic complexes. In fact, cyanobacterial cells contain an order of magnitude more iron within their cells than *Escherichia coli* (Shcolnick et al., 2009). However, transition metals such as iron and copper are highly reactive and can promote the generation of ROS within the cell if homeostasis is perturbed. This further necessitates a robust antioxidant network in photosynthetic cells. Recently, GSH has been implicated in iron-sulfur cluster metabolism in *Synechocystis* 6803 (Picciocchi et al., 2007; Iwema et al., 2009), suggesting a role as an antioxidant and in metal homeostasis. The glutaredoxin system has also been implicated in detoxification of arsenate (Lopez-Maury et al., 2009) and selenate (Marteyn et al., 2008) in *Synechocystis* 6803.

The photosynthetic reaction centers utilize light energy to drive electrons derived from the oxidation of H₂O to high redox potentials. The terminal component of the photosynthetic electron transport chain, photosystem I (PSI), contains several iron-sulfur clusters involved in transferring electrons to stromal components for the generation of NADPH and reduction of CO₂ to carbohydrates. If there becomes a limitation of

preferred electron acceptors, such as NADP^+ and CO_2 , damage can occur to components of the electron transfer chain (Sonoike, 2006). O_2 is an excellent electron acceptor and can therefore be reduced by PSI if the preferred substrates are over-reduced (Endo and Asada, 2006). The ROS generated through this mechanism can likely damage cellular components and create a chain-reaction of destruction throughout the cell. High levels of GSH at the stromal side of photosynthesis likely buffer these reactions and prevent damage to the sensitive photosynthetic reaction centers during these conditions.

GSH also participates in many central pathways including the detoxification of methylglyoxal, a reactive aldehyde derived from dihydroxyacetone phosphate (DHAP) during carbon metabolism (Masip et al., 2006). This pathway has been well studied in heterotrophic organisms, but not in photosynthetic microbes. Production of methylglyoxal has been detected in *Synechococcus* sp. 7002 during growth on glycerol (Xu et al., 2006).

In this work, we utilized the $\Delta gshB$ strain to examine the role of GSH in metal homeostasis in *Synechocystis* 6803. We found that the $\Delta gshB$ is extremely sensitive to cadmium, but does not appear to be hypersensitive to selenate or arsenate. We also found that the $\Delta gshB$ strain exhibits severely reduced PSI-mediated electron transport activity in whole-cell assays utilizing artificial electron donor/acceptor pairs. Finally, we show that the $\Delta gshB$ strain exhibits reduced growth in the presence of glucose and glycerol,

possibly reflecting a decreased affinity of γ -EC by the enzymes involved in methylglyoxal detoxification.

MATERIALS AND METHODS

Growth of Strains

Strains of *Synechocystis* sp. PCC 6803 were maintained on solid BG11 (Allen, 1968) with the appropriate antibiotic (WT, no antibiotic; $\Delta gshB$ and $\Delta gshB/T2086$, 5 $\mu\text{g/ml}$ gentamicin). For growth experiments, strains were grown in BG11 and illuminated with cool-white fluorescent lights at an intensity of 30 $\mu\text{mol photons m}^{-2} \text{ s}^{-1}$. For growth assays, cells were grown to mid-log phase and harvested by centrifugation. The cells were washed in fresh BG11, centrifuged to pellet, and the cell pellets were resuspended in fresh BG11. The cells were diluted to an $\text{OD}_{730 \text{ nm}} = 0.05$ in BG11 without antibiotics and grown with shaking (200 rpm) after addition of the indicated compound. The $\text{OD}_{730 \text{ nm}}$ was measured every 24 h on a μQuant Microplate spectrophotometer (Biotek Instruments, Inc., Winooski, VT).

Measurement of Cellular Thiols

Cellular thiols were simultaneously extracted from cells and derivatized with monobromobimane before being separated by HPLC as described (Cameron and Pakrasi, 2011). Quantification of cellular thiol concentration was accomplished by comparison of peak areas to those of authentic standards.

Optical Measurements

Absorption spectra were obtained using a DW2000 spectrophotometer (SLM-Aminco, Urbana, IL). Chlorophyll and phycocyanin concentrations were estimated using whole cell absorption spectra as described (Arnon et al, 1974).

Measurement of Electron Transport Rates

Electron transport rates were measured on a Clark-type electrode in a chamber maintained at 30°C using saturating orange-red light (8250 $\mu\text{mol photons m}^{-2} \text{s}^{-1}$) as previously described (Mannan and Pakrasi, 1993). For measurements, cells or membranes were diluted to a chlorophyll concentration of 5 $\mu\text{g/ml}$. Chl-a concentration was measured in methanolic extracts as described (Porra et al, 1989).

Estimation of ROS

Estimation of ROS was performed as previously described (Cameron and Pakrasi, 2011). Briefly, DCFH-DA (2 mM in 100% ethanol) was added directly to the cells at a final concentration of 10 μM . Fluorescence was measured at 525 nm after excitation at 488 nm on a Synergy Mx fluorescence plate reader (Biotek Instruments, Inc., Winooski, VT). Fluorescence intensity was normalized to $\text{OD}_{730 \text{ nm}}$ and is presented as relative fluorescence.

RESULTS

Role of Glutathione in Metal Homeostasis

Cadmium

Cadmium is known to stimulate production of ROS and affect sulfur metabolism within the cell (Houot et al., 2007). We hypothesized that the $\Delta gshB$ mutant would exhibit increased sensitivity to Cd. To test this, we grew WT and the $\Delta gshB$ strains in the presence or absence of 10 μ M CdCl₂ (Fig. 1). At this concentration, WT does exhibit reduced growth compared to the control. However, it is able to recover from this perturbation, while the $\Delta gshB$ cannot.

Selenium

Selenium is a redox active element with many properties similar to sulfur. In fact, many organisms contain an intricate system for uptake and incorporation of selenate into the amino acid selenocysteine and subsequently into proteins (Stadtman, 1996). While this system is found in eukaryotic algae, selenocysteine has not been identified in cyanobacteria. In fact, selenate may disrupt cellular processes in cyanobacteria. Recently, the glutaredoxin system has been implicated in redox-based detoxification of selenate (Marteyn et al., 2008). We therefore tested whether the $\Delta gshB$ strain was more sensitive to selenate than the WT.

Figure 2 shows some physiological changes of the WT and $\Delta gshB$ strains during growth in the presence of 20 μM NaSeO_4 . The presence of selenate does appear to inhibit growth in both strains to a similar extent (Fig. 2A). This suggests that the absence of GSH in the $\Delta gshB$ strain does not impair the pathways required for resistance to selenate. We also compared pigment content of the WT and $\Delta gshB$ strains following 96 h of growth in the presence of different concentrations of NaSeO_4 . We observed a sharp decrease in the chlorophyll-a (Chl) content of both strains during growth at high concentrations of NaSeO_4 ; however, the reduction was less in the $\Delta gshB$ strain (Fig. 2B). In WT, a decrease in Chl concentration often occurs concomitantly with a reduction in the light-harvesting pigment phycocyanin (PC) (Fig. 2C). This decrease was not observed in the $\Delta gshB$ strain, resulting in a remarkable blue appearance in the culture. Throughout the treatment, the $\Delta gshB$ maintained a higher PC:Chl ratio that was exaggerated at the highest concentrations of NaSeO_4 (Fig. 2D).

Arsenate

In a similar fashion to that of selenate, arsenate detoxification is thought to involve the glutaredoxin system (Lopez-Maury et al., 2009). Therefore, we also tested the sensitivity of the WT, $\Delta gshB$ and $\Delta gshB/T2086$ strains to Na_2HAsO_4 (Fig. 3). However, the response to arsenate is complicated by its chemical similarity with phosphate. Therefore, it is necessary to grow cyanobacteria in phosphate free medium for them to uptake a significant amount of arsenate. Surprisingly, all of the strains grow fairly well in the presence of 100 mM Na_2HAsO_4 (Fig. 3B). Therefore, we have also compared growth in

phosphate deplete medium in the absence (Fig. 3C) or presence (Fig. 3D) of 100 mM Na_2HAsO_4 . While there appears to be a slight decrease in growth of the $\Delta gshB$ strain during phosphate depletion in the presence of 100 mM Na_2HAsO_4 (Fig. 3D), it is not clear whether this represents a significant difference considering that the $\Delta gshB$ strain consistently exhibits decreased growth compared to the WT strain in BG11 medium (Fig. 3A).

Iron

Iron is an important transition metal that plays many roles as a redox cofactor in photosynthetic organisms. The process of acquisition and storage of iron is highly regulated in cyanobacteria (Shcolnick et al., 2009). Disruption of this system can perturb cellular redox homeostasis and generate intracellular ROS. We therefore examined whether cellular glutathione concentration changes during exposure to iron-limiting conditions in WT cells (Fig. 4). GSH levels increased after 24 h following iron-limitation. After 72 h, there was a dramatic increase in cellular GSH levels. These findings suggest that increased GSH is required during iron-limitation. While we do not have evidence that the $\Delta gshB$ strain is more sensitive to iron-limitation, we predict that the $\Delta gshB$ strain would have reduced fitness in these conditions compared to the WT.

Maintenance of Redox Homeostasis During Photosynthetic Electron Transport

To characterize the physiology of *Synechocystis* 6803 strains, we routinely assay their photosynthetic activities using spectroscopic and biochemical methods. We commonly

utilize a Clark-type electrode to directly measure dissolved oxygen concentrations, the byproduct of photosynthetic water splitting and substrate of respiration and Mehler reactions. Specifically, using artificial electron donor/acceptor pairs, we are able to characterize the activities of photosystem I (PSI) and photosystem II (PSII) complexes as a function of light intensity.

We were somewhat surprised to determine that the $\Delta gshB$ strain exhibited extremely low PSI-mediated electron transport activity in intact cell assays using ascorbate/3,6-diaminodurene (DAD) as the electron donors and methyl viologen (MV) as the electron acceptor (Fig. 5A). In this assay, we first measure respiratory consumption of oxygen in the dark as a baseline, and then illuminate the samples with varying light intensity to determine the net oxygen consumption due to electron flow through PSI. Following titration of MV in the reaction mixture, we still observed a decreased rate of PSI-mediated electron transport in the $\Delta gshB$ strain (Fig. 6).

To further investigate this phenomenon, we isolated membrane fractions from WT, $\Delta gshB$ and the complemented $\Delta gshB/T2086$ strains, and assayed their PSI-mediated electron transfer reactions at saturating light intensity ($8250 \mu\text{mol photons m}^{-2} \text{s}^{-1}$) (Fig. 5B). We consistently found, using several sets of independently isolated membranes, that the activity of the $\Delta gshB$ membranes was significantly enhanced compared to the WT and $\Delta gshB/T2086$ strains, in an apparent contradiction to the whole cell data. We did, however, notice a slight color difference between the WT and the $\Delta gshB$ membranes.

We examined this by taking absorbance spectra of whole-cells and isolated membranes utilized in the previous assay (Fig. 7). The decreased absorbance at approximately 500 nm could reflect a difference in the level or composition of carotenoids between the strains. Furthermore, previous measurements of whole chain oxygen evolution (H₂O to CO₂) and PSII measurements using 1 mM potassium ferricyanide and 0.5 mM 2,6-dichloro-*p*-benzoquinone did not indicate a deficiency in electron transport Figure (Fig. 8).

Based on the previous findings that the $\Delta gshB$ strain is extremely sensitive to treatment with MV, we hypothesized that increased ROS following addition of MV could be negatively affecting the assay results. To test the hypothesis that increased ROS generation is responsible for the observed low PSI-mediated electron transport activity in the $\Delta gshB$ strain, we utilized the fluorescent ROS indicator 2',7'-dichlorofluoresceine diacetate as described (Cameron and Pakrasi, 2010) to monitor ROS production in cells following 30 minutes of MV treatment at varying concentrations (Fig. 9). At 1 mM MV, the WT strain exhibited <2 fold increase in fluorescence compared to the untreated, while the $\Delta gshB$ strain exhibited a >4 fold increase compared to the control. These data suggest that increased ROS production in cells upon MV treatment might lead to the inhibition of the PSI mediated electron transport in the $\Delta gshB$ strain.

Role of GSH in Carbon Metabolism

Synechocystis 6803 grows photoautotrophically (PA) and utilizes CO₂ as a carbon source for building biomass. However, *Synechocystis* 6803 is also able to utilize glucose for growth. Cells can be grown photomixotrophically (PM) in the presence of glucose and photoheterotrophically (PH) in the presence of glucose and the PSII inhibitor, DCMU (Fig. 10). The utilization of externally added reduced carbon compounds leads to many changes in cellular metabolism and redox poise (Sakuragi et al., 2006; Takahashi et al., 2008). Increased carbon metabolism can also result in the formation of the toxic metabolite, methylglyoxal. This toxic compound is produced during carbon metabolism via the removal of phosphate from DHAP. Metabolism of glycerol leads to the accumulation of DHAP and enhanced production of methylglyoxal (Fig. 10). Therefore, we tested whether the $\Delta gshB$ mutant is more sensitive to growth in the presence of glucose (Fig. 11) and glycerol (Fig. 12). During PM conditions growth is significantly enhanced compared to PA and PH conditions. Under all of the tested conditions, the $\Delta gshB$ strain shows reduced growth (Fig. 11). It is possible that accumulation of toxic metabolites results in decreased growth of the $\Delta gshB$ strain. We also observe a significant decrease in growth of the $\Delta gshB$ mutant upon addition of glycerol at 1 and 5 mM (Fig. 12). Growth was reduced slightly in the WT following the same treatments. However, it is not clear whether the glycerol actually entered the cells and was metabolized.

DISCUSSION

We found that the $\Delta gshB$ strain is extremely sensitive to growth in the presence of $CdCl_2$ compared to the wild type (WT) strain (Fig. 1), similar to findings with *Escherichia coli* and yeast (Helbig et al., 2008; Preveral et al., 2009). In *Synechocystis* 6803, cadmium elicits many similar responses to those to H_2O_2 , resulting in the down-regulation of processes involved in energy metabolism and upregulation of processes involved in iron homeostasis and oxidative stress (Houot et al., 2007).

We have previously concluded that reactive oxygen species (ROS) are generated during many environmental perturbations (Singh et al., 2010). Moreover, recent work has implicated GSH and the glutaredoxin system in selenate (Marteyn et al., 2008) and arsenate (Lopez-Maury et al., 2009) detoxification in *Synechocystis* 6803. However, the role of GSH as an electron donor in these pathways *in vivo* remains unclear. Marteyn *et al.* have shown that Grx1 and Grx2 function in a electron transfer cascade to reduce selenate (Marteyn et al., 2008). We found that the $\Delta gshB$ strain behaves similar to WT during growth in the presence of $NaSeO_4$ at concentrations as high as $20 \mu M$, with both strains exhibiting reduced growth (Fig. 2). Similarly, we only observed a slight decrease in growth of the $\Delta gshB$ strain compared to WT in phosphate deplete BG11 medium containing 100 mM Na-As^V (Fig. 3). Taken together, these data suggest that GSH, *per se* is not required for defense against arsenate and selenate in *Synechocystis* 6803. Further, they support the notion that while Grx1 and Grx2 have GSH-dependent disulfide

oxidoreductase activity, GSH is likely not required for their function *in vivo* as they are able to receive electrons from NADPH-dependent thioredoxin reductase and a ferredoxin (Marteyn et al., 2008). It is also possible that γ -EC, if present at high concentrations, is able to functionally replace GSH (Bick et al., 1998).

Our results also suggest the involvement of GSH during conditions of iron limitation (Fig. 4). During iron limitation, iron is sequestered intracellularly in bacterioferritin (Shcolnick et al., 2009). This process results in the generation of hydrogen peroxide. It is possible that the stimulation of glutathione biosynthesis during growth in limiting iron is a result of this process. Further, it could also be involved in sensing iron limitation and coordinating iron-sulfur biogenesis (Picciocchi et al., 2007; Iwema et al., 2009).

While attempting to determine PSI-mediated electron transfer rates using artificial electron donor/acceptor pairs, we found that the $\Delta gshB$ strain is unable to support the whole-cell assay (Fig. 5 and 6). We previously found that the $\Delta gshB$ strain is extremely sensitive to growth in the presence of MV at concentrations $>0.5 \mu\text{M}$ (Cameron and Pakrasi, 2010). The PSI assay utilizes lethal concentrations of MV as a PSI electron acceptor, however the overall duration of the measurement is in minutes. It is possible, though unlikely, that in this time frame, sufficient reactive oxygen species (ROS) are generated to damage the functional PSI complexes and prevent accurate measurement of activity. Studies on a cyanobacterial superoxide dismutase mutant claim that MV primarily damages PSI compared to PSII (Herbert et al., 1992). While less studied than

PSII photoinhibition, PSI photoinhibition has been observed in plants following cold treatment, and ROS mediated loss of Fe-S clusters is the likely cause (Sonoike, 1996; Sonoike, 2006). In the WT strain, it is possible that endogenous ROS scavenging mechanisms are sufficient to overcome the amount of ROS produced and artificial electron transfer through PSI can proceed. Membranes were measured in a buffered reaction mix containing superoxide dismutase as a scavenger of the superoxide anion radical formed upon single electron reduction of O₂. While superoxide is not likely the direct cause of PSI inactivation, Fenton reactions involving the product of superoxide dismutation, H₂O₂, and Fe-S clusters of PSI result in formation of the hydroxyl radical that will inactivate PSI (Sonoike, 2006). In this artificial system using membranes, we are able to observe PSI mediated electron transport, though it has been found that methyl viologen is able to accept electron from damaged PSI complexes (Terashima et al., 1994). The nature of the enhanced activity of the $\Delta gshB$ membranes is currently not known. We did not find significant differences in the amounts of the PSI P700 reaction centers in the $\Delta gshB$ mutant compared to WT. It is possible that damage or alterations to the donor side of PSI could increase MV access sites of electron transfer components, thereby enhancing the apparent rate of reaction, however we have no data to support this in our case. Additionally, we cannot rule out the possibility that other components of the photosynthetic electron transport chain contribute to oxygen reduction in this assay (Khorobrykh et al., 2004).

Besides functioning as a redox buffer, GSH also participates in some metabolic reactions as a cofactor. One such pathway involves the conversion of methylglyoxal to lactate through a lactoyl-glutathione intermediate (Fig. 10). Methylglyoxal is a toxic metabolite that generated as a side product during glycolysis through phosphate elimination of DHAP or GAP. Feeding cells glycerol as a carbon source can significantly increase the production of methylglyoxal, leading to cytotoxicity (Xu et al., 2006). Our results suggest that γ -EC is not as efficient in detoxification of methylglyoxal, as growth is reduced in the $\Delta gshB$ strain following addition of glucose (Fig. 11) and glycerol (Fig. 12). It should be noted however, that in the WT strain, growth is not enhanced by the addition of glycerol. Therefore, it is not clear whether glycerol is utilized as a carbon source in *Synechocystis* 6803, a trait observed in other cyanobacteria such as *Synechococcus* 7002 (Xu et al., 2006) and *Cyanothece* 51142 (Feng et al., 2010). It is possible that the resulting decrease in growth upon addition of glycerol is a result of changes in the osmotic properties in the medium. In fact, glutathione has been proposed to be involved in osmoadaptation in other bacteria (Masip et al., 2006). We did find that addition of glucose led to a rapid increase of glutathione and γ -EC in the WT and $\Delta gshB$ strains, respectively (Cameron and Pakrasi, 2011). Glucose metabolism could also promote methylglyoxal formation in *Synechocystis* 6803 and require higher levels of cellular thiols to increase detoxification.

These results highlight the multi-functionality of GSH in *Synechocystis* 6803. While γ -EC is able to function under ideal conditions, it is not sufficient under conditions that

greatly disturb the cellular redox balance. It is interesting to note, however, that γ -EC is the primary thiol in halobacteria (Sundquist and Fahey, 1989). Therefore it is likely that the subtle differences between these molecules and the co-evolution of the intricate pathways they participate in will dictate the cellular responses to many environmental perturbations.

CONCLUSIONS

Our results suggest that γ -EC is able to functionally replace GSH during many conditions. However, during conditions leading to extreme redox stress, GSH is essential. This could be due to the decreased stability of γ -EC compared to GSH. Further, there are many subtle phenotypes in the $\Delta gshB$ mutant that could be the result of altered signaling or metabolism that is dependent on glutathione. Analysis of these phenotypes could shed light on the role of GSH in photosynthetic microbes and lead to novel insight in the role of GSH in higher plants.

REFERENCES

- Allen MM** (1968) Simple conditions for growth of unicellular blue-green algae on plates. *J of Phycol* **4**: 1-4
- Arnon, D. I., B. D. McSwain, H. Y. Tsujimoto, and K. Wada.** 1974. Photochemical activity and components of membrane preparations from blue-green algae. I. Coexistence of two photosystems in relation to chlorophyll a and removal of phycocyanin. *Biochim Biophys Acta* **357**:231-345.
- Bick JA, Aslund F, Chen Y, Leustek T** (1998) Glutaredoxin function for the carboxyl-terminal domain of the plant-type 5'-adenylylsulfate reductase. *Proc Natl Acad Sci USA* **95**: 8404-8409
- Cameron JC, Pakrasi HB** (2010) Essential role of glutathione in acclimation to environmental and redox perturbations in the cyanobacterium *Synechocystis* sp. PCC 6803. *Plant Physiol* **154**: 1672-1685
- Cameron JC, Pakrasi HB** (2011) Glutathione in *Synechocystis* 6803: A closer look into the physiology of a $\Delta gshB$ mutant. *Plant Signal Behav* **6**: 89-92
- Endo T, Asada K** (2006) Photosystem I and photoprotection: cyclic electron flow and water-water cycle. In: Demmig-Adams B, Adams WW III and Mattoo AK (eds) *Photoprotection, Photoinhibition, Gene Regulation, and Environment* pp 205-221. Springer.

- Feng X, Bandyopadhyay A, Berla B, Page L, Wu B, Pakrasi HB, Tang YJ** (2010) Mixotrophic and photoheterotrophic metabolism in *Cyanothece* sp. ATCC 51142 under continuous light. *Microbiology* **156**: 2566-2574
- Harada E, von Roepenack-Lahaye E, Clemens S** (2004) A cyanobacterial protein with similarity to phytochelatase catalyzes the conversion of glutathione to gamma-glutamylcysteine and lacks phytochelatase activity. *Phytochemistry* **65**: 3179-3185
- Helbig K, Bleuel C, Krauss G, Nies D** (2008) Glutathione and transition metal homeostasis in *Escherichia coli*. *J Bacteriol* **190**: 5431-5438
- Helbig K, Grosse C, Nies D** (2008) Cadmium Toxicity in Glutathione Mutants of *Escherichia coli* *The Journal of Bacteriology* **190**: 5439-5454
- Herbert SK, Samson G, Fork DC, Laudénbach DE** (1992) Characterization of damage to photosystems I and II in a cyanobacterium lacking detectable iron superoxide dismutase activity. *Proc Natl Acad Sci U S A* **89**: 8716-8720
- Houot L, Floutier M, Marteyn B, Michaut M, Picciocchi A, Legrain P, Aude J-C, Cassier-Chauvat C, Chauvat F** (2007) Cadmium triggers an integrated reprogramming of the metabolism of *Synechocystis* PCC6803, under the control of the Slr1738 regulator. *BMC Genomics* **8**: 350
- Howden R, Andersen CR, Goldsbrough PB, Cobbett CS** (1995) A cadmium-sensitive, glutathione-deficient mutant of *Arabidopsis thaliana*. *Plant Physiol* **107**: 1067-1073

- Iwema T, Picciocchi A, Traore DAK, Ferrer J-L, Chauvat F, Jacquamet L (2009)**
Structural basis for delivery of the intact [Fe₂S₂] cluster by monothiol glutaredoxin. *Biochemistry* **48**: 6041-6043
- Khorobrykh S, Mubarakshina M, Ivanov B (2004)** Photosystem I is not solely responsible for oxygen reduction in isolated thylakoids. *Biochim Biophys Acta* **1657**: 164-167
- Kobayashi I, Fujiwara S, Saegusa H, Inouhe M, Matsumoto H, Tsuzuki M (2006)**
Relief of arsenate toxicity by Cd-stimulated phytochelatin synthesis in the green alga *Chlamydomonas reinhardtii*. *Mar Biotechnol* **8**: 94-101
- Latifi A, Ruiz M, Zhang C-C (2009)** Oxidative stress in cyanobacteria. *FEMS Microbiol Rev* **33**: 258-278
- Lopez-Maury L, Sanchez-Riego A, Reyes J, Florencio F (2009)**
Glutathione/glutaredoxin system is essential for arsenate reduction in *Synechocystis* sp. PCC 6803. *J of Bacteriol* **191**: 3534-3543
- Mannan R, Pakrasi H (1993)** Dark Heterotrophic Growth Conditions Result in an Increase in the Content of Photosystem II Units in the Filamentous Cyanobacterium *Anabaena variabilis* ATCC 29413. *Plant Physiol* **103**: 971
- Marteyn B, Domain F, Legrain P, Chauvat F, Cassier-Chauvat C (2008)** The thioredoxin reductase-glutaredoxins-ferredoxin crossroad pathway for selenate tolerance in *Synechocystis* PCC6803. *Mol Microbiol* **71**: 520-532
- Masip L, Veeravalli K, Georgiou G (2006)** The many faces of glutathione in bacteria. *Antioxid Redox Signal* **8**: 753-762

- Mendoza-Cózatl DG, Butko E, Springer F, Torpey JW, Komives EA, Kehr J, Schroeder JI** (2008) Identification of high levels of phytochelatin, glutathione and cadmium in the phloem sap of *Brassica napus*. A role for thiol-peptides in the long-distance transport of cadmium and the effect of cadmium on iron translocation. *Plant J* **54**: 249-259
- Mendoza-Cozatl DG, Zhai Z, Jobe TO, Akmakjian GZ, Song WY, Limbo O, Russell MR, Kozlovskyy VI, Martinoia E, Vatamaniuk OK, Russell P, Schroeder JI** (2010) Tonoplast-localized Abc2 transporter mediates phytochelatin accumulation in vacuoles and confers cadmium tolerance. *J Biol Chem* **285**: 40416-40426
- Picciochi A, Saguez C, Boussac A, Cassier-Chauvat C, Chauvat F** (2007) CGFS-type monothiol glutaredoxins from the cyanobacterium *Synechocystis* PCC6803 and other evolutionary distant model organisms possess a glutathione-ligated [2Fe-2S] cluster. *Biochemistry* **46**: 15018-15026
- Porra RJ, Thompson WA, Kriedmann PE.** (1989) Determination of accurate extinction coefficients and simultaneous equations for assaying chlorophylls *a* and *b* extracted with four different solvents: verification of the concentration of chlorophyll standards by atomic absorption spectroscopy. *Biochim Biophys Acta* **975**: 384-394
- Preveral S, Gayet L, Moldes C, Hoffmann J, Mounicou S, Gruet A, Reynaud F, Lobinski R, Verbavatz J-M, Vavasseur A, Forestier C** (2009) A Common Highly Conserved Cadmium Detoxification Mechanism from Bacteria to Humans: HEAVY METAL TOLERANCE CONFERRED BY THE ATP-

BINDING CASSETTE (ABC) TRANSPORTER SpHMT1 REQUIRES GLUTATHIONE BUT NOT METAL-CHELATING PHYTOCHELATIN PEPTIDES. *J Biol Chem* **284**: 4936-4943

Sakuragi Y, Maeda H, Dellapenna D, Bryant DA (2006) alpha-Tocopherol plays a role in photosynthesis and macronutrient homeostasis of the cyanobacterium *Synechocystis* sp. PCC 6803 that is independent of its antioxidant function. *Plant Physiol* **141**: 508-521

Shcolnick S, Summerfield TC, Reytman L, Sherman LA, Keren N (2009) The mechanism of iron homeostasis in the unicellular cyanobacterium *Synechocystis* sp. PCC 6803 and its relationship to oxidative stress. *Plant Physiol* **150**: 2045-2056

Singh AK, Elvitigala T, Cameron JC, Ghosh BK, Bhattacharyya-Pakrasi M, Pakrasi HB (2010) Integrative analysis of large scale expression profiles reveals core transcriptional response and coordination between multiple cellular processes in a cyanobacterium. *BMC systems biology* **4**: 105

Sonoike K (1996) Photoinhibition of Photosystem I: Its Physiological Significance in the Chilling Sensitivity of Plants. *Plant and Cell Physiology* **37**: 239-247

Sonoike K (2006) Photoinhibition and Protection of Photosystem I. In: John H. Golbeck (ed): *Photosystem I: The Light-Driven Plastocyanin:Ferredoxin Oxidoreductase*, pg. 657-668. Springer.

Stadtman TC (1996) Selenocysteine. *Annu Rev Biochem* **65**: 83-100

- Sundquist A, Fahey R** (1989) The function of gamma-glutamylcysteine and bis-gamma-glutamylcysteine reductase in *Halobacterium halobium*. J Biol Chem **264**: 719-725
- Takahashi H, Uchimiya H, Hihara Y** (2008) Difference in metabolite levels between photoautotrophic and photomixotrophic cultures of *Synechocystis* sp. PCC 6803 examined by capillary electrophoresis electrospray ionization mass spectrometry. J Exp Bot **59**: 3009-3018
- Terashima I, Funayama S, Sonoike K** (1994) The site of photoinhibition in leaves of *Cucumis sativus* L. at low temperatures is photosystem I, not photosystem II. Planta **193**: 300-306
- Vernoux T, Wilson RC, Seeley KA, Reichheld JP, Muroy S, Brown S, Maughan SC, Cobbett CS, Van Montagu M, Inzé D, May MJ, Sung ZR** (2000) The ROOT MERISTEMLESS1/CADMIUM SENSITIVE2 gene defines a glutathione-dependent pathway involved in initiation and maintenance of cell division during postembryonic root development. Plant Cell **12**: 97-110
- Xu D, Liu X, Guo C, Zhao J** (2006) Methylglyoxal detoxification by an aldo-keto reductase in the cyanobacterium *Synechococcus* sp. PCC 7002. Microbiology **152**: 2013-2021

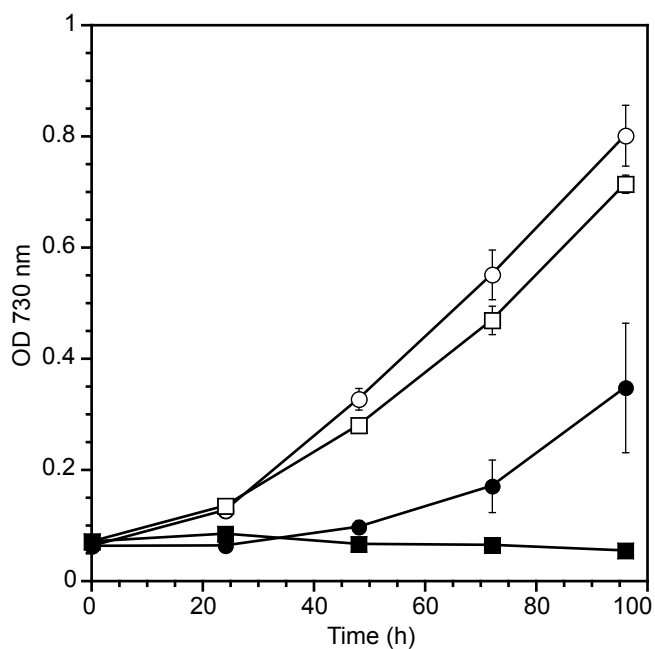


Figure 1. Growth in the presence of cadmium.

WT (circles) and $\Delta gshB$ strains (squares) were grown in the absence (open symbols) or presence of $10 \mu\text{M CdCl}_2$ (closed symbols) at a light intensity of $30 \mu\text{mol photons m}^{-2} \text{s}^{-1}$. Growth was measured as optical density (OD) at 730 nm on a microtiter plate spectrophotometer (BioTek, Winooksi, VT). Error bars represent SE of three replicates.

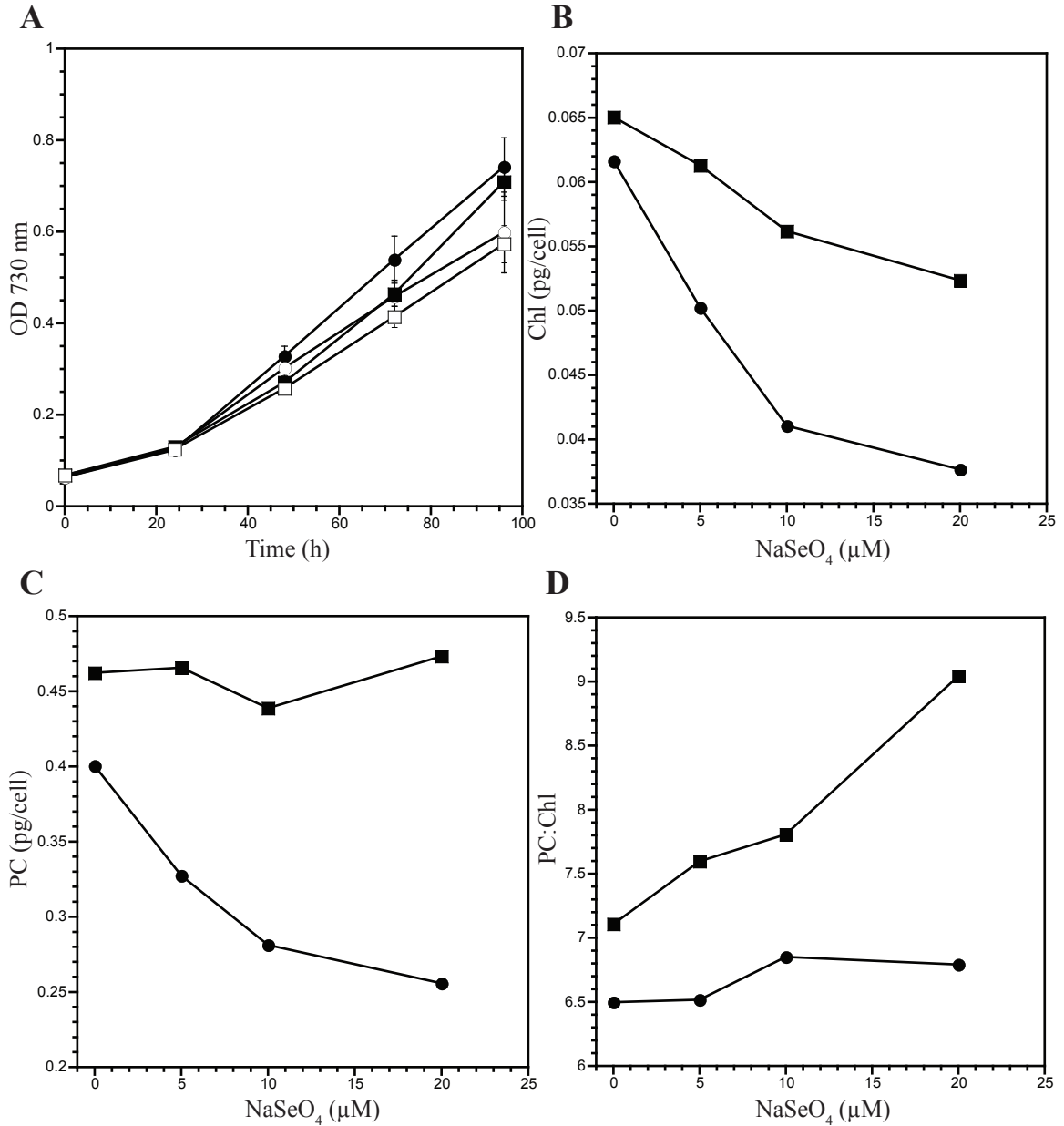


Figure 2. Growth and pigment levels during exposure to selenate.

(A) WT (circles) and $\Delta gshB$ (squares) cells were diluted to an OD 730 nm = 0.05 in BG11 medium (closed symbols) or in medium containing 20 μM NaSeO₄. Cells were grown with shaking at 30°C and illuminated with fluorescent white lights at an intensity of 30 $\mu\text{mol photons m}^{-2} \text{s}^{-1}$. Error bars represent SE of three replicates. Chlorophyll (A) and phycocyanin (B) concentrations were estimated from whole cell absorption spectra after 96 h growth in presence of increasing amounts of NaSeO₄. (C) The ratio of PC/Chl was calculated from the values shown in (B) and (C).

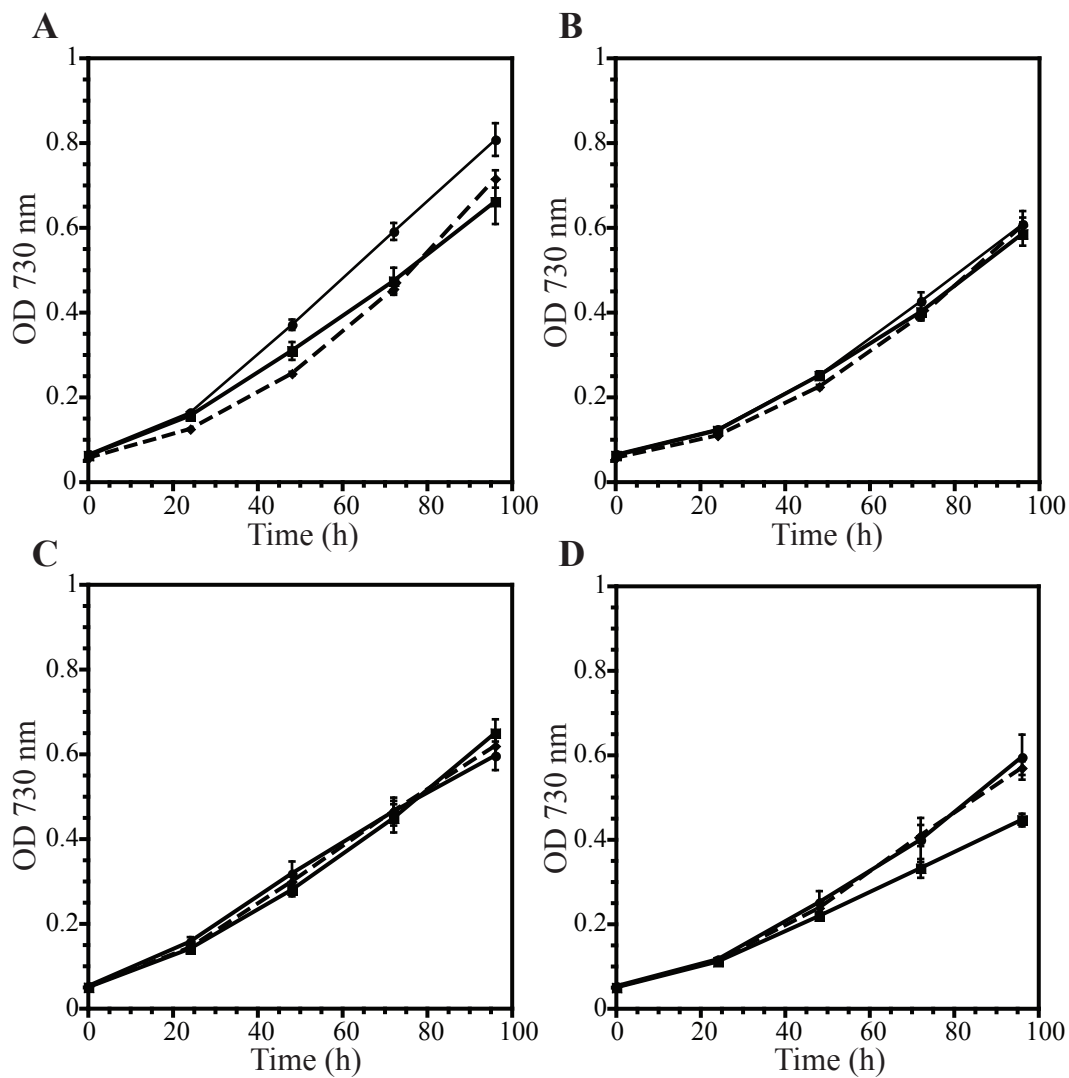


Figure 3. Growth of the WT, $\Delta gshB$ and $\Delta gshB/T2086$ strains in the presence of arsenate.

WT (circle), $\Delta gshB$ (square) and $\Delta gshB/T2086$ (diamond, dashed) cells were washed and diluted to an OD 730 nm = 0.05 in the appropriate medium and grown with shaking at 30°C with illumination at an intensity of 30 $\mu\text{mol photons m}^{-2} \text{s}^{-1}$. (A) Control growth in BG11 medium. (B) Growth in BG11 medium containing 100 mM Na_2HAsO_4 . (C) Growth in BG11 medium lacking phosphate. (D) Growth in BG11 medium lacking phosphate and containing 100 mM Na_2HAsO_4 . Error bars represent SE of three replicates.

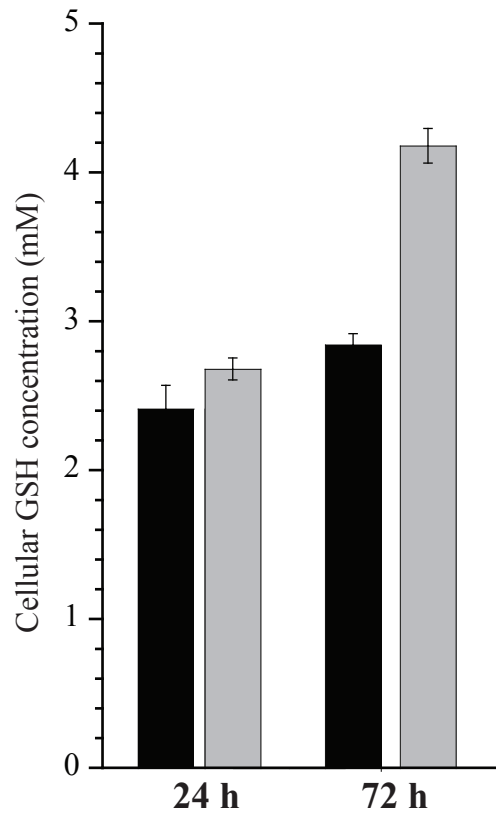


Figure 4. Cellular GSH content during growth in iron deplete conditions.

GSH was measured in WT *Synechocystis* 6803 cells by HPLC following growth for 24 and 72 h in BG11 medium (black) or BG11 lacking iron (grey). For iron depletion, cells were washed twice in BG11 medium lacking iron and then diluted to an OD 730 = 0.05. Control cells were washed in BG11 and diluted to the same density. Error bars represent SE of

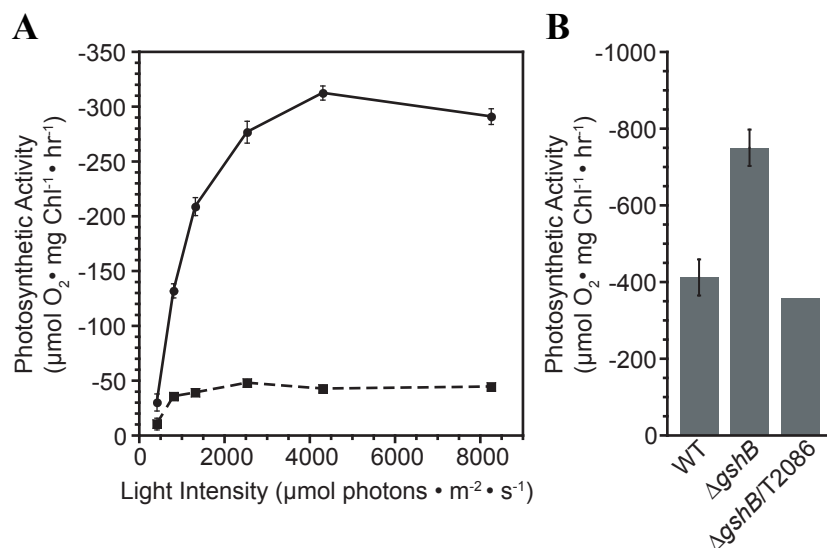


Figure 5. Photosystem I-mediated electron transport in *Synechocystis* 6803 strains. Oxygen consumption was monitored on a Clark-type electrode in whole cells (A) or in isolated membranes (B) adjusted to a chlorophyll concentration of 5 $\mu\text{g/ml}$. WT (circle, line) and ΔgshB (square, dashed) cells were suspended in BG11 medium and measured in the presence of 20 μM 3-(3,4-dichlorophenyl)-1,1-dimethylurea (DCMU), 1 mM sodium ascorbate, 2 mM methyl viologen and 1 mM 3,6-diaminodurene at varying light intensities using neutral density filters (A). (B) Membranes from WT, ΔgshB and the complemented $\Delta\text{gshB/T2086}$ strain were harvested from cells following breakage and centrifugation. Oxygen consumption was measured at a saturating light intensity of 8250 $\mu\text{mol photons m}^{-2} \text{s}^{-1}$ orange-red light. Membranes were suspended in measuring buffer consisting of 50 mM Hepes (pH 7.5), 10 mM NaCl, 5 mM MgCl_2 , 1 mM KCN, 20 μM DCMU, 10 $\mu\text{g/ml}$ superoxide dismutase (Sigma), 0.1 mM dichlorophenolindolphenol and 1 mM methyl viologen (B). Error bars represent SE of three measurements for whole cells and from three independent membrane preparations for WT and ΔgshB . The $\Delta\text{gshB/T2086}$ value represents a single measurement.

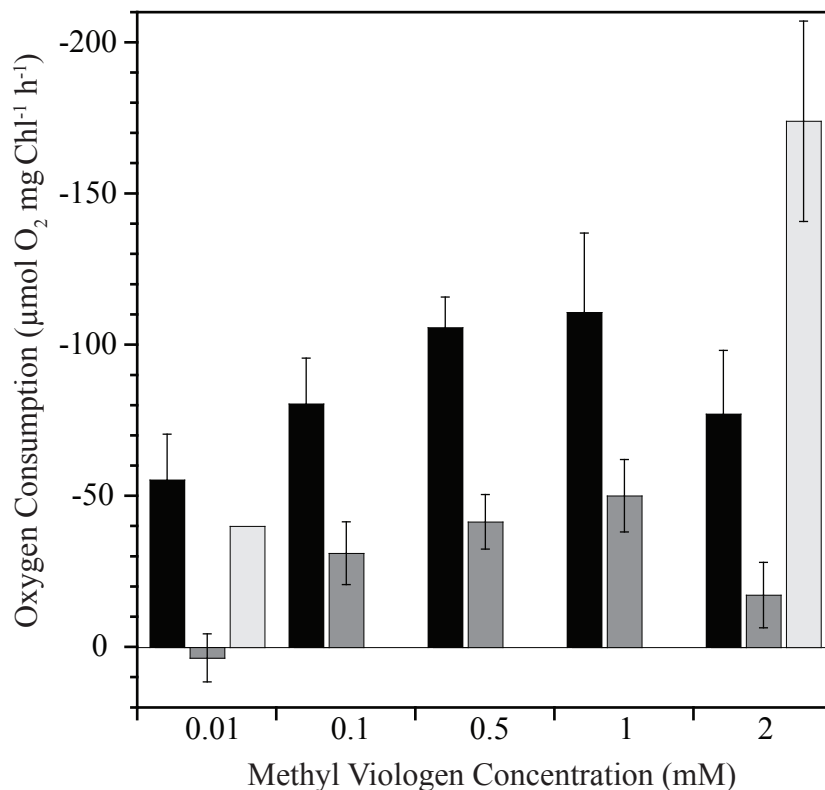


Figure 6. PSI-mediated electron transport as a function of methyl viologen concentration in intact cells.

WT (black), $\Delta gshB$ (dark grey) and $\Delta gshB/T2086$ (light grey) cells were suspended in BG11 medium at a chlorophyll concentration of 5 $\mu\text{g/ml}$ prior to measurements. Oxygen consumption was measured on a Clark-type electrode in the presence of 20 μM 3-(3,4-dichlorophenyl)-1,1-dimethylurea (DCMU), 1 mM sodium ascorbate, 1 mM 3,6-diaminodurene and methyl viologen at the indicated concentration. Cells were maintained at 30°C and illuminated with saturating orange-red light at an intensity of 8250 $\mu\text{mol photons m}^{-2} \text{s}^{-1}$.

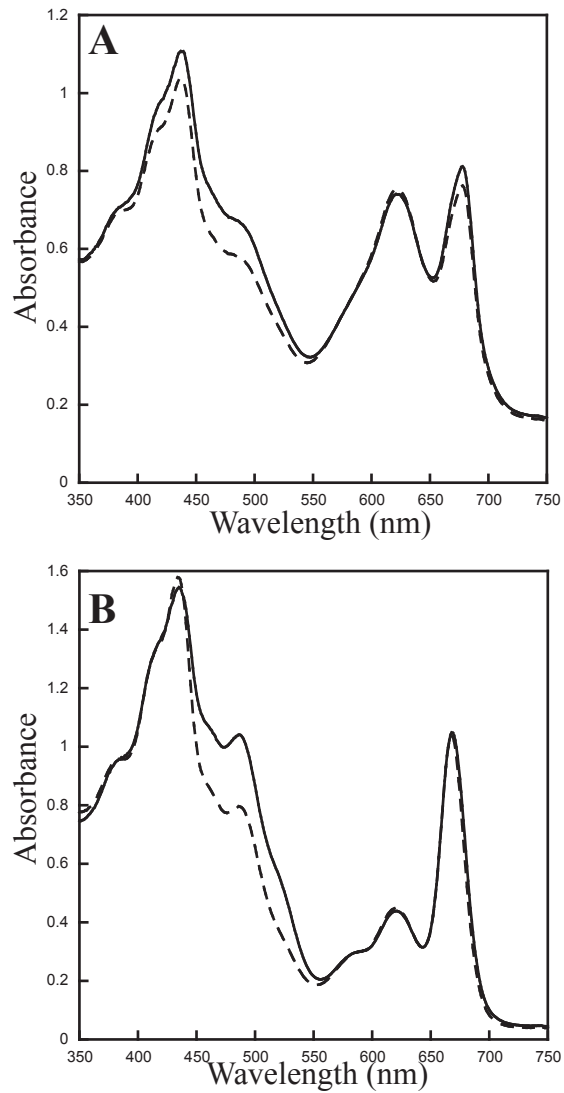


Figure 7. Absorption spectra of WT and $\Delta gshB$ cells and isolated membranes. Absorption spectra using intact cell suspensions (A) and isolated membranes (B) from WT (line) and $\Delta gshB$ (dashed) strains.

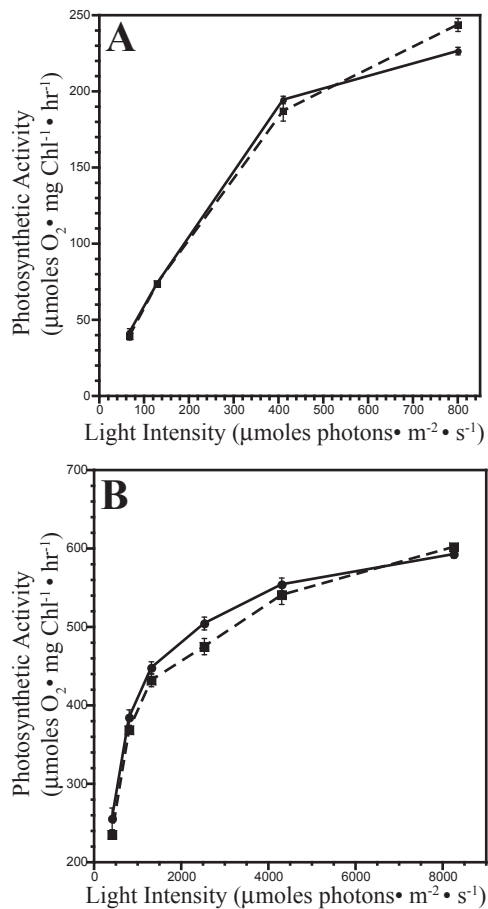


Figure 8. Photosystem II activity in WT and ΔgshB cells

Oxygen evolution activity was measured on a Clark-type electrode as a function of light intensity in WT (line) and ΔgshB (dashed) cells. (A) Whole-chain oxygen evolution (H_2O to HCO_3^-). (B) Photosystem II activity in the presence of the electron acceptors 2,6-dichloro-*p*-benzoquinone (0.5 mM) and potassium ferricyanide (1 mM). Error bars represent SE of three measurements.

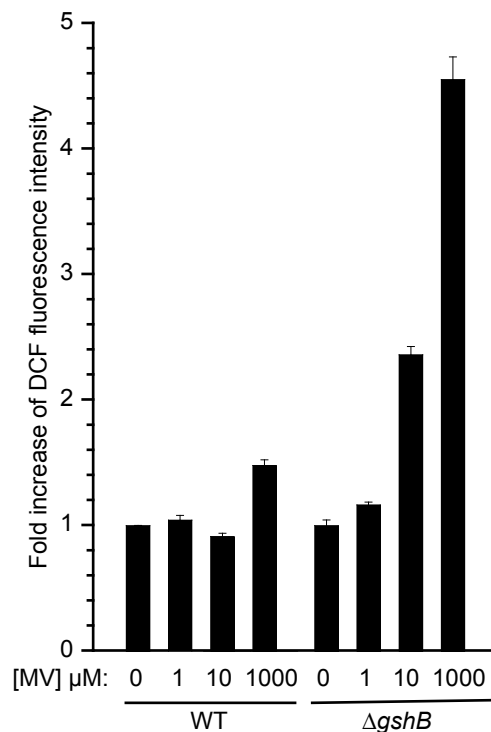


Figure 9. Estimation of cellular ROS.

WT and the ΔgshB strains were incubated at 30°C and illuminated with 30 $\mu\text{mol photons m}^{-2} \text{s}^{-1}$ for 0.5 h with varying amounts of methyl viologen (MV). 2',7'-dichlorofluorescein diacetate (DCF; Sigma) was added to cells at a concentration of 10 μM . Fluorescence intensity at 525 nm was monitored following 488 excitation using a Synergy Mx fluorescence platereader (Biotek, Winooski, VT). Fluorescence intensity was normalized to cell density and is represented as fold increase compared to control (0 μM MV). Error bars represent SE of four measurements.

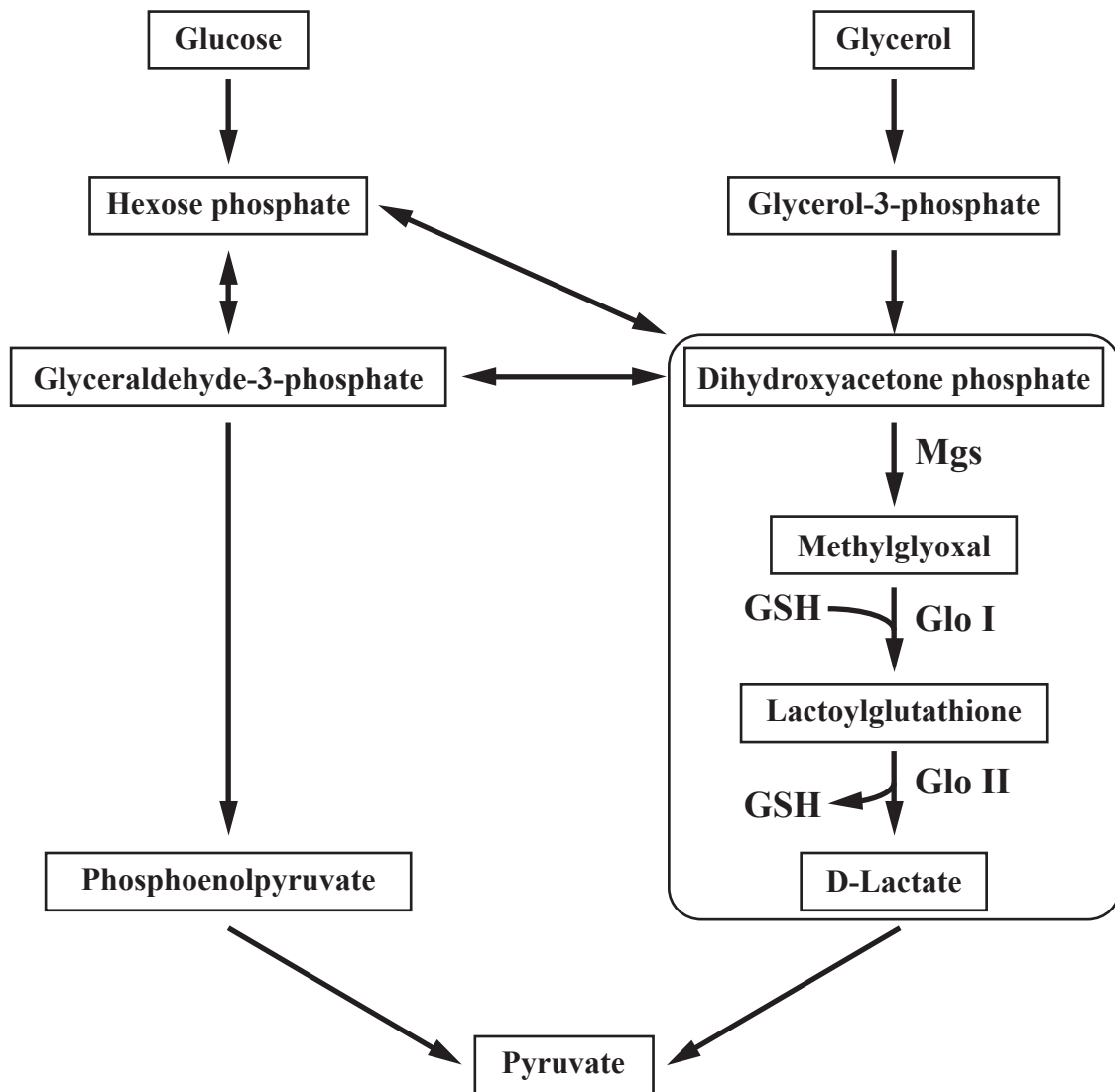


Figure 10. Schematic diagram of methylglyoxal pathway.

Glucose and glycerol metabolism lead to increased triose phosphate concentrations. Methylglyoxal synthase (Mgs) converts dihydroxyacetone phosphate into methylglyoxal, a toxic metabolite. Methylglyoxal is detoxified by glyoxylase I (Glo I) and II (Glo II) using a glutathione (GSH) conjugated intermediate, forming D-lactate. This pathway is activated during conditions of low inorganic phosphate resulting from accumulation of triose phosphates. Only enzymes in the methylglyoxal pathway are shown for clarity.

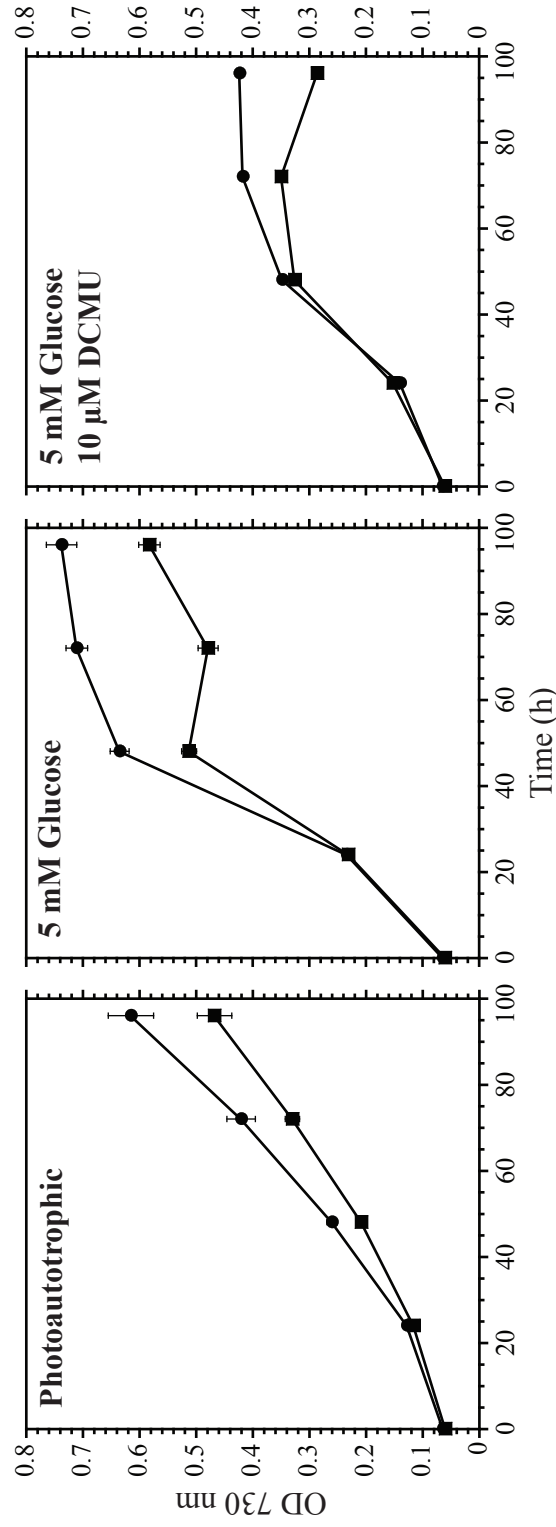


Figure 11. Growth of the WT and $\Delta gshB$ strains in the presence of glucose. WT (circles) and $\Delta gshB$ (squares) cells were diluted to an OD 730 nm = 0.05 in BG11 medium alone (Photoautotrophic), with the addition of 5 mM glucose (photomixotrophic) or 5 mM glucose + 10 μ M DCMU (photoheterotrophic). Cells were grown with shaking at 30°C and illuminated with fluorescent white lights at an intensity of 30 μ mol photons $m^{-2} s^{-1}$. Error bars represent SE of three replicates.

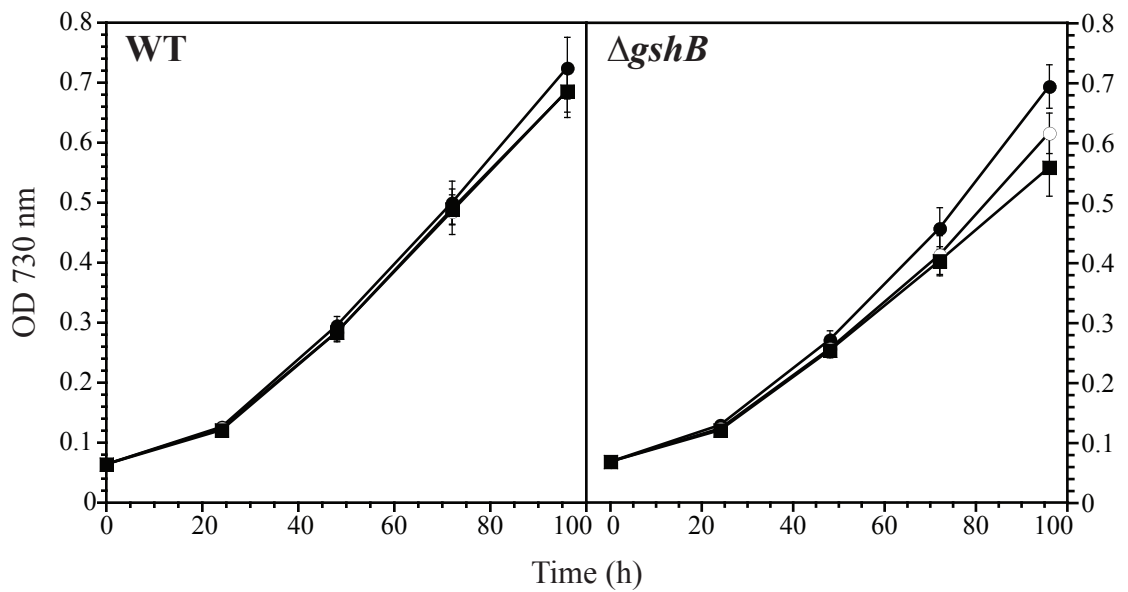


Figure 12. Growth of the WT and $\Delta gshB$ strains in the presence of glycerol.

Cells were diluted to an OD 730 nm = 0.05 in BG11 medium alone (filled circles) or with the addition of 1 mM (open circle) or 5 mM (filled square) glycerol. Cells were grown with shaking at 30°C and illuminated with fluorescent white lights at an intensity of 30 $\mu\text{mol photons m}^{-2} \text{s}^{-1}$. Error bars represent SE of three replicates.

Chapter 4

Glutathione Facilitates Antibiotic Resistance and Photosystem I Stability during Exposure to Gentamicin in Cyanobacteria

This chapter was adapted from:

Jeffrey C. Cameron and Himadri B. Pakrasi (2011). Glutathione facilitates antibiotic resistance and photosystem I stability during exposure to gentamicin in cyanobacteria.

Applied and Environmental Microbiology. doi:10.1128/AEM.02542-10

Copyright © American Society for Microbiology

SUMMARY

Understanding mechanisms of antibiotic resistance is important to the fields of biology and medicine. We find that glutathione contributes to antibiotic resistance in the cyanobacterium *Synechocystis* sp. PCC 6803. Our results also suggest that glutathione protects photosystem I from oxidative damage resulting from growth in the presence of gentamicin.

INTRODUCTION

The discovery, production and implementation of antibiotics has dramatically improved life for humans (Demain, 2009). However, as antibiotic resistance is inevitable, the search for novel compounds and targets is ongoing (Singh and Barrett, 2006). Recent work has found that there are vast natural reservoirs of antibiotic resistance genes (Dantas et al., 2008; Sommer et al., 2009). Therefore a detailed understanding of antibiotic resistance mechanisms and mode of action will facilitate development and discovery of novel antibiotics.

Antibiotics target a broad array of cellular metabolic functions to inhibit growth or cause death. Bactericidal antibiotics primarily target cellular integrity, DNA replication and translation (Kohanski et al., 2010). It has been demonstrated that reactive oxygen species (ROS) produced following antibiotic treatment lead to cell death (Kohanski et al., 2007; Kohanski et al., 2008; Dwyer et al., 2009). Additionally, antibiotics such as the aminoglycoside gentamicin (Gm) may be directly involved in production of ROS (Priuska and Schacht, 1995). Antibiotic resistance can be manifested in many ways by the cell through enzymatic antibiotic modification, exclusion, export and modulation of core metabolic pathways (Benveniste and Davies, 1973; Wright, 2005). Due to the formation of ROS following exposure to bactericidal antibiotics, the cellular antioxidant network likely plays a critical role in antibiotic resistance.

Glutathione is a multifunctional molecule that is involved in core metabolic pathways, detoxification of xenobiotics and in maintenance of cellular redox poise. Many of these properties may come into play when the cell is challenged with an antibiotic. Glutathione S-transferases catalyze the addition of glutathione to xenobiotics to reduce toxicity and facilitate export (Allocati et al., 2009). Further, GSH could also function in moderating the toxicity of ROS generated as a byproduct of antibiotic toxicity. GSH and related thiols have also been suggested to modulate antibiotic sensitivity in non-photosynthetic organisms (Rawat et al., 2002; Turnbull and Surette, 2008, 2010).

Glutathione biosynthesis proceeds through the ATP-dependent ligation of glutamate and cysteine to form the intermediate γ -glutamylcysteine (γ -EC) by the enzyme glutamate-cysteine ligase (GshA). Finally, glutathione synthetase (GshB) catalyzes the ATP-dependent ligation of glycine and γ -EC to form GSH. As glutathione biosynthesis likely evolved in ancestors of cyanobacteria during the evolution of oxygenic photosynthesis and was then transferred to many other organisms through lateral gene transfer (Copley and Dhillon, 2002), it is interesting to consider the role of cyanobacteria in modulating antibiotic resistance mechanisms across Kingdoms.

Cyanobacteria are photosynthetic microbes that utilize light energy to oxidize water and generate reduced compounds and ATP for reduction of CO₂ into carbohydrates. This process is facilitated by the light-driven protein-pigment complexes, photosystem I (PSI) and II (PSII). The formation of O₂ as a byproduct of photosynthesis in close proximity to

many redox active cofactors increases the chances of ROS production and necessitates a robust antioxidant network and redox buffering system. The antioxidant system is comprised of many small molecules and proteins that interact to prevent cellular damage in the presence of ROS (Latifi et al., 2009). We recently found that glutathione is essential in the cyanobacterium *Synechocystis* sp. PCC 6803 (hereafter *Synechocystis* 6803) for acclimation to various cellular perturbations eliciting oxidative stress (Cameron and Pakrasi, 2010). Our results also demonstrated that the glutathione biosynthetic intermediate, γ -EC, is able to function in place of GSH during growth under optimal conditions, but not during extreme oxidative stress.

While little is known regarding the antibiotic resistance mechanisms in cyanobacteria, their ability to biosynthesize a variety of toxic compounds is well recognized (Li et al., 2010). In fact, blooms of cyanobacteria and the toxic compounds released during these events have a large socioeconomic impact and may become more prevalent in the future as temperatures rise and eutrophication of water sources increase (Paerl et al., 2001; Paerl and Scott, 2010). Although we are not aware of a specific study that focused on the molecular mechanism of antibiotic resistance in cyanobacteria, there have been many excellent reports documenting the nature of antibiotic resistance in heterotrophic bacteria (Kaufmann and Hung, 2010; Kohanski et al., 2010). While these reports have provided some insight, there are many differences between autotrophic and heterotrophic metabolism that could modulate the mechanism of antibiotic toxicity. Foremost are the large amount of electron transfer reactions and pigment-protein complexes within the

specialized thylakoid membrane system and the intracellular generation of molecular oxygen.

In this study, we report that glutathione is important for protection from Gm toxicity in *Synechocystis* 6803. Further, our results suggest that glutathione facilitates photosystem I (PSI) stability during exposure to Gm.

MATERIALS AND METHODS

Culture conditions

Strains of *Synechocystis* sp. PCC 6803 were grown in BG11 medium (Allen, 1968) in the absence or presence of gentamicin (5 $\mu\text{g/ml}$). Growth was performed in 250 ml shake-flasks (150 rpm shaking) filled with 50 ml liquid medium at 30°C with continuous illumination (30 $\mu\text{mol photons m}^{-2} \text{ s}^{-1}$). The $\text{OD}_{730 \text{ nm}}$ was measured every 24 h on a μQuant Microplate spectrophotometer (Biotek Instruments, Inc., Winooski, VT).

Measurement of Cellular Thiols

Cellular GSH and $\gamma\text{-EC}$ were separated and quantified using HPLC as described (Cameron and Pakrasi, 2011). Briefly, thiols were extracted and derivatized in a reaction mixture containing 50% acetonitrile and 100 mM monobromobimane buffered with 20 mM HEPES (pH 8.0) at 60°C in the dark. Thiol-bimane derivatives were separated by RP-HPLC on a C18 Zorbax Eclipse XDB (4.6 x 250 mm, 5 μm ; Agilent) column using a gradient of methanol in 0.1% trifluoroacetic acid on a 1200 series HPLC (Agilent) and using a fluorescence detector (380 nm excitation, 480 nm emission; Agilent). Quantification of cellular thiol concentration was accomplished by comparison of peak areas to those of authentic standards.

Optical Measurements

Optical measurements were performed on a DW2000 spectrophotometer (SLM-Aminco, Urbana, IL). For pigment analysis chlorophyll and phycocyanin concentrations were

estimated using whole cell absorption spectra as described (Arnon et al., 1974). P700 concentrations were determined from chemical difference spectra (potassium ferricyanide oxidized – ascorbate reduced) as described (Mannan and Pakrasi, 1993) using isolated membranes at a Chl-a concentration of at 15-25 $\mu\text{g/ml}$. For these measurements, Chl-a concentration was measured in methanolic extracts as described (Porra, 1989).

Protein separation and visualization

Proteins were separated by SDS-PAGE on 16% polyacrylamide gels containing 6 M urea and then transferred to 0.22 μm nitrocellulose membranes using a semi-dry transfer apparatus (Bio-Rad, Hercules, CA). Specific antibodies were used to detect PsaA/B and D1 proteins following reaction with peroxidase-conjugated antiserum (Pierce) developed in West Pico (Pierce). After blots were incubated in the substrate, they were imaged on a Fujifilm LAS-1000plus imager (Fujifilm, Stamford, CT) and the signal intensity was quantified using ImageJ software.

RESULTS

Increased cellular glutathione content following application of gentamicin

We utilized wild type (WT) *Synechocystis* 6803 cells to test whether glutathione is involved in protection from application of Gm. We found that growth in liquid BG11 (Allen, 1968) medium is quickly inhibited in such cells following application of Gm at various concentrations (Fig. 1A). We also measured cellular GSH (Fig. 1B) and the GSH precursor γ -glutamylcysteine (γ -EC; Fig. 1C) content by HPLC as described (Cameron and Pakrasi, 2010) after 11 h of gentamicin treatment. Evidently glutathione biosynthesis is stimulated in WT *Synechocystis* 6803 cells following addition of Gm, suggesting a role in cellular protection from this antibiotic.

The $\Delta gshB$ strain exhibits increased sensitivity to gentamicin

To further test the role of glutathione in protection from Gm, we utilized a glutathione synthetase ($\Delta gshB$) mutant that we have previously characterized (Cameron and Pakrasi, 2010). The $\Delta gshB$ strain does not contain glutathione, but instead accumulates γ -EC. We noticed that the $\Delta gshB$ is extremely sensitive to growth in liquid media in the presence of Gm, despite the fact that the *gshB* gene was replaced with a Gm resistance cassette (Gm^R) in this strain (Cameron and Pakrasi, 2010). To further examine this phenotype, we compared growth of the $\Delta gshB$ and $\Delta gshB/T2086$ strains in the presence of Gm (5 μ g/ml; Fig. 2). The $\Delta gshB/T2086$ strain was constructed by fusing the *gshB* coding region to the *psbA2* promoter and expressing it at a second site in the genome of the $\Delta gshB$ mutant (Cameron and Pakrasi, 2010). While both strains contain a Gm^R cassette replacing the

native *gshB* gene, the $\Delta gshB/T2086$ strain is able to produce GSH. In the presence of Gm, the $\Delta gshB$ strain did not grow while the $\Delta gshB/T2086$ strain could (Fig. 2). Furthermore, using the broth dilution method and an initial cell concentration of approximately 9×10^7 cells/ml, the MIC for Gm ($\mu\text{g/ml}$) was determined to be 5 and 7.5 for the $\Delta gshB$ and $\Delta gshB/T2086$ strains, respectively. The MIC for WT *Synechocystis* 6803, which does not contain a Gm^R gene, was $0.5 \mu\text{g/ml}$. We also utilized a control strain, HT47-Gm, which harbors a Gm^R gene in addition to a histidine tag on the CP47 gene of PSII (Roose, 2008), and found the MIC to be $7.5 \mu\text{g/ml}$. These data suggest that GSH and the Gm^R cassette are essential for Gm resistance in *Synechocystis* 6803.

Depletion of photosystem I upon exposure to gentamicin

Following application of Gm to $\Delta gshB$ liquid cultures, we noticed that the cultures would turn a bluish color compared to WT. To further investigate this phenomenon, we analyzed the cellular pigment composition in WT cells and in the $\Delta gshB$ strain grown in the absence or presence of Gm ($5 \mu\text{g/ml}$) using whole cell absorption spectra as described (Arnon et al., 1974) (Table I and Fig. 3). As a majority of the chlorophyll in cyanobacteria is found in PSI, we also quantified the amount of P700 reaction centers by chemical difference spectroscopy (potassium ferricyanide oxidized - ascorbate reduced) using isolated membranes at a chlorophyll-*a* concentration of $15\text{-}25 \mu\text{g/ml}$ as described (Mannan and Pakrasi, 1993). We found similar Chl:P700 ratios in WT and the $\Delta gshB$ strain during growth in the absence of Gm. However, in the presence of Gm, a significant increase in the Chl:P700 ratio was observed in the $\Delta gshB$ strain, suggesting a depletion of PSI (Table I).

Next, we analyzed the content of PSI and photosystem II (PSII) reaction center proteins in isolated membranes. Figure 4 shows immunoblots of WT and the $\Delta gshB$ samples probed with antibodies raised against the PSI and PSII reaction center proteins, PsaA/B and D1, respectively. The intensities of the cross-reacting bands were also quantified by densitometry using ImageJ software (Fig. 4B). We determined that the PsaA/B proteins were significantly reduced in the $\Delta gshB$ strain grown in the presence of Gm. However, the levels of D1 did not decrease following Gm treatment.

DISCUSSION

The results presented here show that glutathione is a critical player in Gm resistance mechanisms in *Synechocystis* 6803. Furthermore, GSH is required for resistance even when cells contain a functional Gm^R cassette. Our results also show that PSI, but not PSII, content is severely reduced in the $\Delta gshB$ strain following application of Gm.

Recently it has been shown that diverse classes of antibiotics result in the formation of ROS in Gram-positive and Gram-negative bacteria despite the differences in primary targets (Kohanski et al., 2007; Kohanski et al., 2008; Dwyer et al., 2009). Kohanski et al. (2008) demonstrate that aminoglycoside antibiotics such as kanamycin and gentamicin stimulate oxidation of NADPH that is generated by the TCA-cycle. The resulting increase in respiratory activity generates superoxide (O_2^-) that is converted into H_2O_2 by superoxide dismutase. Superoxide and H_2O_2 are able to react with and liberate enzyme-bound iron-sulfur and promote Fenton reactions that result in the formation of the highly reactive hydroxyl radical ($\bullet\text{OH}$; Fig. 5). It has been suggested that iron-mediated Fenton reactions play a role in the cell-killing ability of many bactericidal antibiotics (Priuska and Schacht, 1995; Kohanski et al., 2007; Kohanski et al., 2008; Dwyer et al., 2009; Kohanski et al., 2010; Kohanski et al., 2010). In fact, it was shown that alterations in import of iron or disruption of iron-sulfur cluster biogenesis could reduce the killing-efficiency of aminoglycoside antibiotics (Kohanski et al., 2008). Therefore, increased cellular iron content could play a significant role in susceptibility to antibiotic induced death.

Compared to heterotrophic bacteria, cyanobacteria contain at least an order of magnitude more iron within their cells (Shcolnick et al., 2009) in order to supply the components of the photosynthetic and respiratory electron transfer chains, which reside in the same internal membrane system (Cooley and Vermaas, 2001). PSI, the terminal component of the photosynthetic electron transfer chain contains multiple iron-sulfur clusters that participate in electron transfer reactions (Chitnis, 2001). Therefore, PSI could be contributing to the ROS production following Gm application (Fig. 5). Our results suggest that glutathione plays a critical role in facilitating the removal of ROS and in the protection of PSI from oxidative damage. Depletion of PSI could be a consequence of ROS production and removal of iron-sulfur clusters, or it could represent an acclimation mechanism to increased ROS in a similar way that cells reduce PSI content following high-light treatment (Muramatsu et al., 2009).

While there are striking differences in the metabolism of cyanobacteria and heterotrophic bacteria, a common thread is the necessity to ameliorate potential damage by ROS. Ancestors of modern day cyanobacteria developed robust antioxidant networks and redox buffering systems as a necessity due to the generation of molecular oxygen within the cell as a byproduct of photosynthesis. These same mechanisms have been transferred to other bacteria and eukaryotes and have been elaborated upon to facilitate many aspects of cellular metabolism. Glutathione is a multifunctional molecule that is used by a plethora of organisms to prevent oxidative damage and also for detoxification of hazardous

compounds. Therefore, it is likely that glutathione could play a role in resistance from multiple antibiotics in diverse organisms.

CONCLUSIONS

In this report, we have shown that glutathione likely contributes to PSI stability during exposure to Gm in cyanobacteria by protecting terminal components from oxidative damage. While our results suggest that glutathione biosynthesis is stimulated during exposure to Gm in WT *Synechocystis* 6803, eventually the defense is overcome and the cells die. When Gm is applied to a strain containing a functional Gm^R gene, there exists a balance between Gm inactivation and Gm induced ROS formation. During these conditions, glutathione is necessary for full resistance to Gm.

REFERENCES

- Allen MM** (1968) Simple conditions for growth of unicellular blue-green algae on plates. *J Phycol* **4**: 1-4
- Allocati N, Federici L, Masulli M, Di Ilio C** (2009) Glutathione transferases in bacteria. *FEBS J* **276**: 58-75
- Arnon DI, McSwain BD, Tsujimoto HY, Wada K** (1974) Photochemical activity and components of membrane preparations from blue-green algae. I. Coexistence of two photosystems in relation to chlorophyll a and removal of phycocyanin. *Biochim Biophys Acta* **357**: 231-245
- Benveniste R, Davies J** (1973) Mechanisms of antibiotic resistance in bacteria. *Annu Rev Biochem* **42**: 471-506
- Cameron JC, Pakrasi HB** (2010) Essential role of glutathione in acclimation to environmental and redox perturbations in the cyanobacterium *Synechocystis* sp. PCC 6803. *Plant Physiol* **154**: 1672-1685
- Cameron JC, Pakrasi HB** (2011) Glutathione in *Synechocystis* 6803: A closer look into the physiology of a $\Delta gshB$ mutant. *Plant Signal Behav* **6**: 89-92
- Chitnis P** (2001) PHOTOSYSTEM I: Function and Physiology. *Annu Rev Plant Physiol Plant Mol Biol* **52**: 593-626
- Cooley JW, Vermaas WF** (2001) Succinate dehydrogenase and other respiratory pathways in thylakoid membranes of *Synechocystis* sp. strain PCC 6803: capacity comparisons and physiological function. *J Bacteriol* **183**: 4251-4258

- Copley SD, Dhillon JK** (2002) Lateral gene transfer and parallel evolution in the history of glutathione biosynthesis genes. *Genome Biol* **3**: 25.1-25.16
- Dantas G, Sommer MO, Oluwasegun RD, Church GM** (2008) Bacteria subsisting on antibiotics. *Science* **320**: 100-103
- Demain AL** (2009) Antibiotics: natural products essential to human health. *Med Res Rev* **29**: 821-842
- Dwyer DJ, Kohanski MA, Collins JJ** (2009) Role of reactive oxygen species in antibiotic action and resistance. *Curr Opin Microbiol* **12**: 482-489
- Kaufmann BB, Hung DT** (2010) The fast track to multidrug resistance. *Mol Cell* **37**: 297-298
- Kohanski MA, DePristo MA, Collins JJ** (2010) Sublethal antibiotic treatment leads to multidrug resistance via radical-induced mutagenesis. *Mol Cell* **37**: 311-320
- Kohanski MA, Dwyer DJ, Collins JJ** (2010) How antibiotics kill bacteria: from targets to networks. *Nat Rev Microbiol* **8**: 423-435
- Kohanski MA, Dwyer DJ, Hayete B, Lawrence CA, Collins JJ** (2007) A common mechanism of cellular death induced by bactericidal antibiotics. *Cell* **130**: 797-810
- Kohanski MA, Dwyer DJ, Wierzbowski J, Cottarel G, Collins JJ** (2008) Mistranslation of membrane proteins and two-component system activation trigger antibiotic-mediated cell death. *Cell* **135**: 679-690
- Latifi A, Ruiz M, Zhang C-C** (2009) Oxidative stress in cyanobacteria. *FEMS Microbiol Rev* **33**: 258-278

- Li B, Sher D, Kelly L, Shi Y, Huang K, Knerr PJ, Joewono I, Rusch D, Chisholm SW, van der Donk WA** (2010) Catalytic promiscuity in the biosynthesis of cyclic peptide secondary metabolites in planktonic marine cyanobacteria. *Proc Natl Acad Sci U S A* **107**: 10430-10435
- Mannan R, Pakrasi H** (1993) Dark Heterotrophic Growth Conditions Result in an Increase in the Content of Photosystem II Units in the Filamentous Cyanobacterium *Anabaena variabilis* ATCC 29413. *Plant Physiol* **103**: 971-977
- Muramatsu M, Sonoike K, Hihara Y** (2009) Mechanism of downregulation of photosystem I content under high-light conditions in the cyanobacterium *Synechocystis* sp. PCC 6803. *Microbiology* **155**: 989-996
- Paerl HW, Fulton RS, 3rd, Moisander PH, Dyle J** (2001) Harmful freshwater algal blooms, with an emphasis on cyanobacteria. *ScientificWorldJournal* **1**: 76-113
- Paerl HW, Scott JT** (2010) Throwing fuel on the fire: synergistic effects of excessive nitrogen inputs and global warming on harmful algal blooms. *Environ Sci Technol* **44**: 7756-7758
- Porra RJ, Thompson, W.A., Kriedmann, P.E.** (1989) Determination of accurate extinction coefficients and simultaneous equations for assaying chlorophylls *a* and *b* extracted with four different solvents: verification of the concentration of chlorophyll standards by atomic absorption spectroscopy. *Biochim Biophys Acta* **975**: 384-394
- Priuska E, Schacht J** (1995) Formation of free radicals by gentamicin and iron and evidence for an iron/gentamicin complex. *Biochemical Pharmacology* **50**: 1749-1752

- Rawat M, Newton GL, Ko M, Martinez GJ, Fahey RC, Av-Gay Y** (2002) Mycothiol-deficient *Mycobacterium smegmatis* mutants are hypersensitive to alkylating agents, free radicals, and antibiotics. *Antimicrob Agents Chemother* **46**: 3348-3355
- Roose JL** (2008) Assembly and function of cyanobacterial photosystem II. Thesis Document, Washington University in St. Louis, MO
- Shcolnick S, Summerfield TC, Reytman L, Sherman LA, Keren N** (2009) The mechanism of iron homeostasis in the unicellular cyanobacterium *Synechocystis* sp. PCC 6803 and its relationship to oxidative stress. *Plant Physiol* **150**: 2045-2056
- Singh SB, Barrett JF** (2006) Empirical antibacterial drug discovery--foundation in natural products. *Biochem Pharmacol* **71**: 1006-1015
- Sommer MO, Dantas G, Church GM** (2009) Functional characterization of the antibiotic resistance reservoir in the human microflora. *Science* **325**: 1128-1131
- Turnbull AL, Surette MG** (2008) L-Cysteine is required for induced antibiotic resistance in actively swarming *Salmonella enterica* serovar Typhimurium. *Microbiology* **154**: 3410-3419
- Turnbull AL, Surette MG** (2010) Cysteine biosynthesis, oxidative stress and antibiotic resistance in *Salmonella typhimurium*. *Res Microbiol* **161**: 643-650
- Wright G** (2005) Bacterial resistance to antibiotics: enzymatic degradation and modification. *Adv Drug Deliv Rev* **57**: 1451-1470

Table I
Pigment Content of *Synechocystis* 6803 Strains

Chl a, chlorophyll a; PC, phycocyanin; Gm (5 $\mu\text{g/ml}$), gentamicin.

Pigments	Strain		
	WT	$\Delta gshB$	$\Delta gshB + \text{Gm}$
Chl (pg/cell) ^a	0.063 \pm 0.0018	0.058 \pm 0.0021	0.042 \pm 0.0011
PC (pg/cell) ^a	0.45 \pm 0.017	0.44 \pm 0.018	0.35 \pm 0.021
PC:Chl ^a	7.18 \pm 0.22	7.65 \pm 0.18	8.42 \pm 0.52
Chl:P700 (mol/mol) ^b	136.9 \pm 6.9	132.8 \pm 4.6	177.1 \pm 10.3

Values represent mean \pm standard error from at least three independent experiments. ^a Values obtained from whole cell absorption spectra. ^b Calculated from chemical difference spectroscopy.

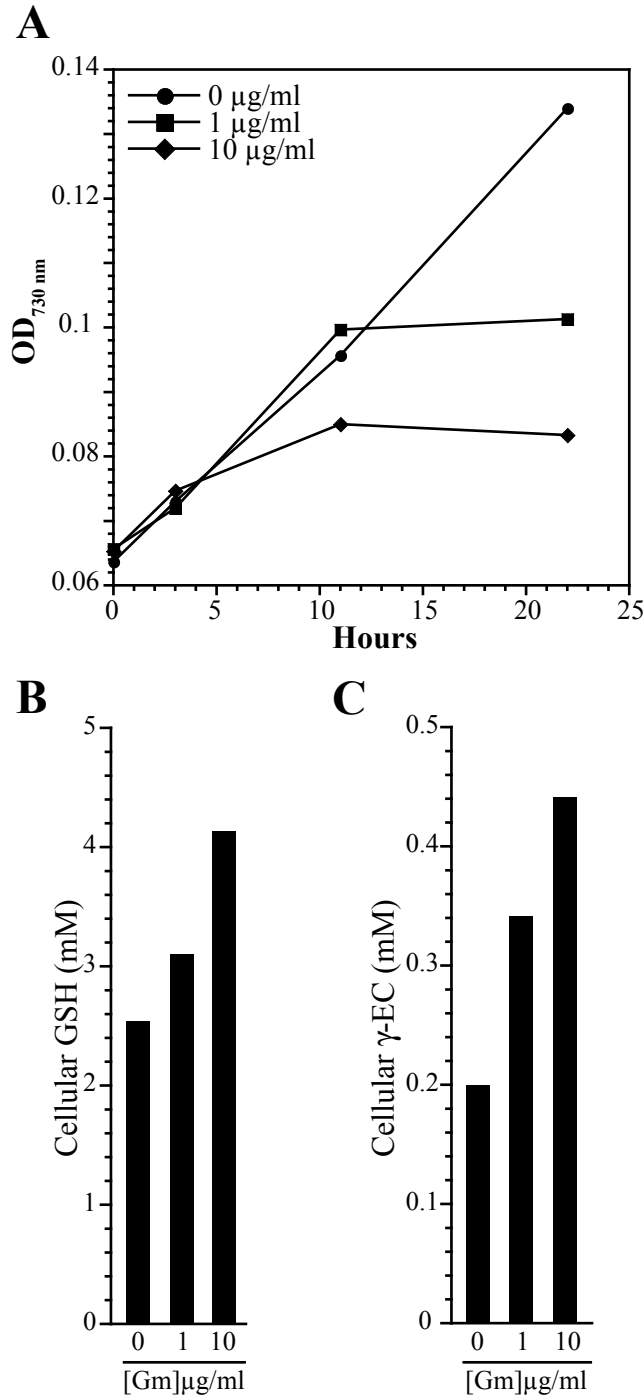


Figure 1. Growth and cellular thiol concentrations of WT *Synechocystis* 6803 following application of gentamicin at varying concentrations.

Growth (A) was monitored as turbidity at 730 nm for 24 h. The cellular GSH (B) and γ -EC (C) concentration was measured by HPLC after 11 h growth in presence of gentamicin.

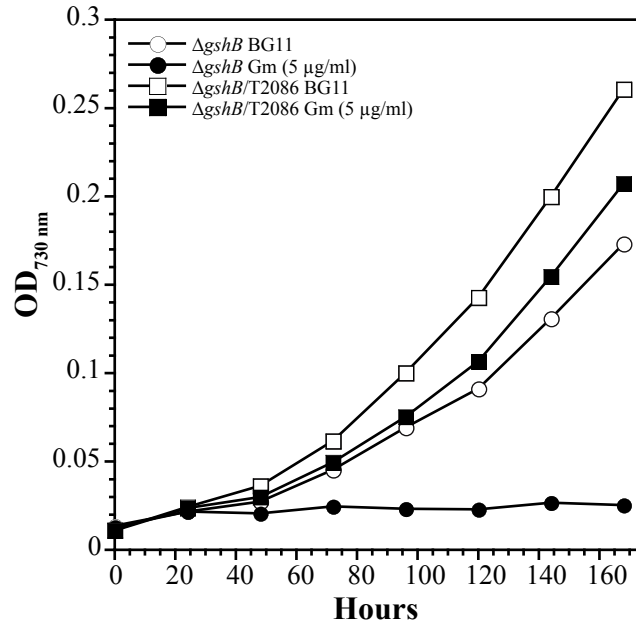


Figure 2. Growth of the $\Delta gshB$ and complemented $\Delta gshB/T2086$ strains.

The $\Delta gshB$ (circles) and $\Delta gshB/T2096$ (squares) strains were diluted to an OD 730 nm = 0.01 in BG11 medium in the presence (filled symbol) or absence (open symbol) of gentamicin (5 $\mu\text{g/ml}$).

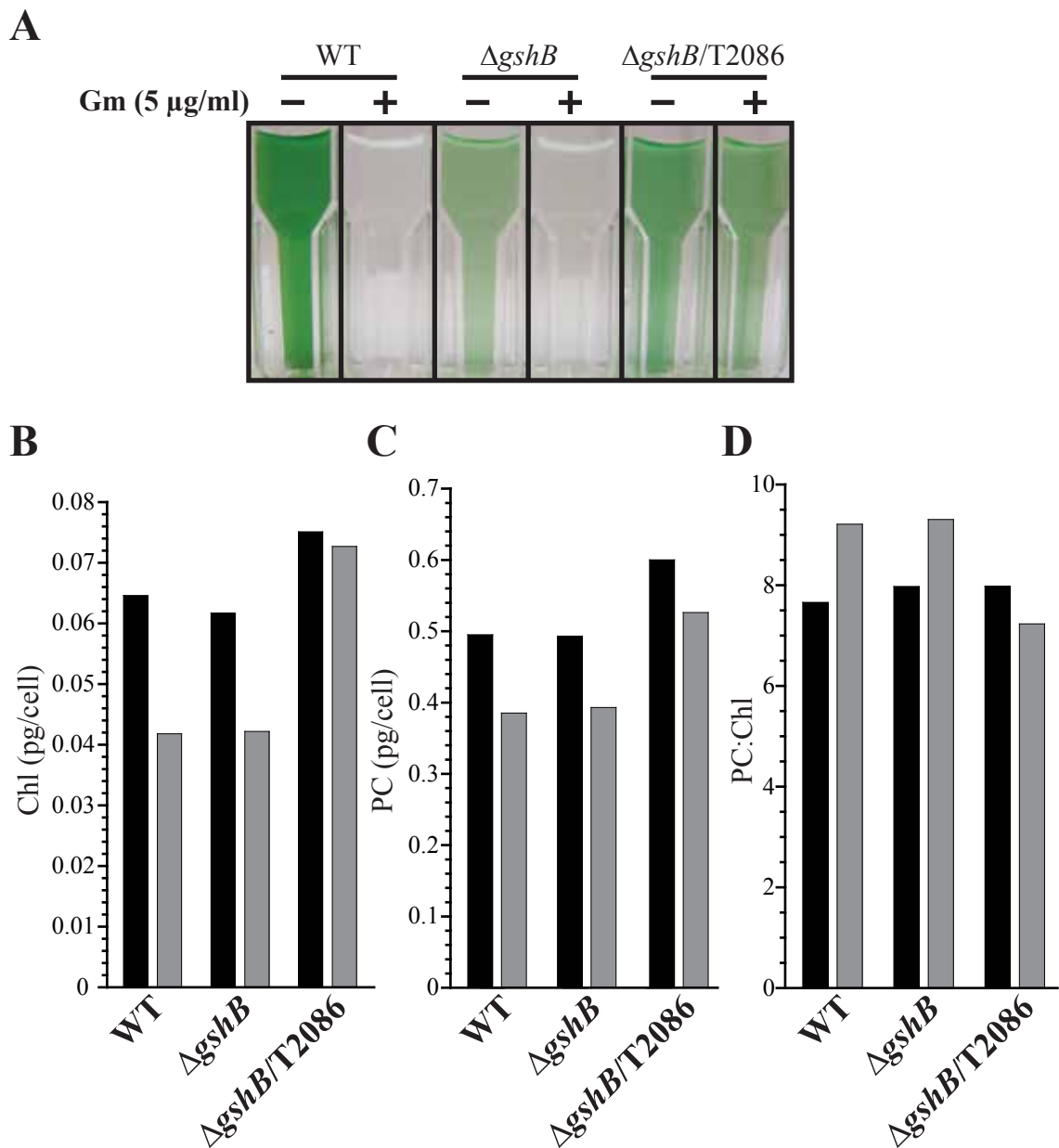


Figure 3. Visualization and pigment content of strains following growth in presence of gentamicin.

(A) Cells were imaged after approximately 160 h growth in the absence or presence of gentamicin (5 μ g/ml). Chlorophyll (Chl; B) and phycocyanin (PC; C) concentrations were estimated from absorption spectra taken from cells grown in the absence (black) or presence (5 μ g/ml) of gentamicin shown in (A). (D) Ratio of Chl to PC in strains.

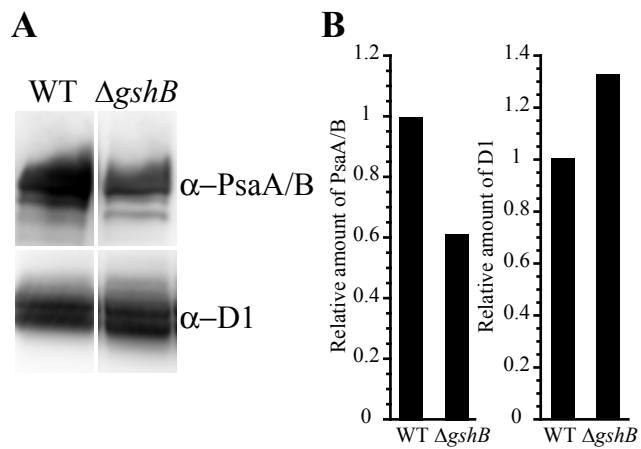


Figure 4. Immunoblot analysis of PSI (PsaA/B) and PSII (D1) core proteins.

(A) Isolated membranes from WT or $\Delta gshB$ were loaded based on equal chlorophyll (2.5 μg Chl/lane) and separated by SDS-PAGE on a 16% gel. The $\Delta gshB$ strain was grown in the presence of Gm (5 $\mu\text{g}/\text{ml}$) prior to harvesting. (B) Immunoblot band intensity was quantified densitometrically using ImageJ software.

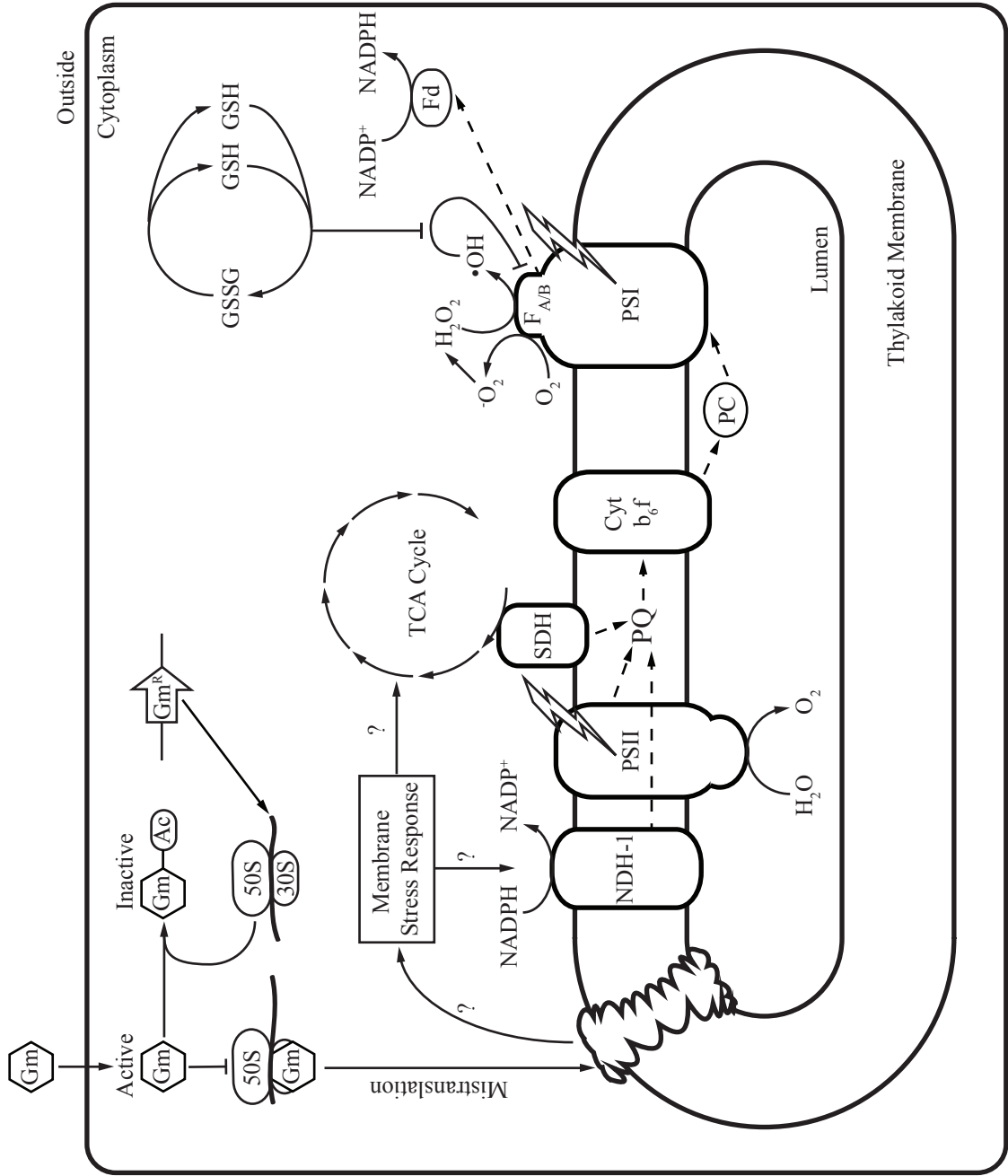


Figure 5. Schematic diagram illustrating the role of glutathione in gentamicin resistance.

Once gentamicin has entered the cell, it can be acetylated and detoxified by the product of the Gm^R gene or bind to the 30S subunit of the ribosome and cause mistranslation of proteins. Mistranslated proteins stimulate the membrane stress response, resulting in alteration of respiration and TCA cycle components. In cyanobacteria, the TCA cycle is incomplete. Stimulation of NADPH oxidation results in increased flow through the photosynthetic and respiratory electron transfer pathways. The terminal iron-sulfur clusters of photosystem I (PSI; $F_{A/B}$) can mediate Fenton chemistry and generation of the reactive hydroxyl radical ($\bullet OH$). Glutathione (GSH) participates in ROS metabolism and can become oxidized to glutathione disulfide (GSSG).

Chapter 5

Characterization of the γ -Glutamyl Cycle in *Synechocystis* sp. PCC 6803

SUMMARY

We recently demonstrated that GSH is essential for acclimation to multiple perturbations in *Synechocystis* sp. PCC 6803, a model photosynthetic cyanobacterium (Cameron and Pakrasi, 2010). In this study, we found that cellular GSH is rapidly depleted when cells are subjected to sulfate and nitrate starvation. In this study we examined the pathways involved in GSH catabolism. We have generated deletion mutants in the γ -glutamyltranspeptidase (*ggt*) gene. Ggt has been shown to be involved in degradation of GSH and other γ -glutamyl compounds in systems including bacteria, plants and mammals. Our results show that the *ggt* gene is not required for growth, but that Ggt activity is likely involved in maintenance of cell viability during stationary phase. We also found that Δ *ggt* strains contained more GSH in the media compared to the WT strain, suggesting that the function may be involved in uptake of GSH or prevention of cellular leakage. To facilitate functional analysis of this pathway, we also generated a strain containing a histidine tag fused to the native *ggt* gene.

INTRODUCTION

Glutathione (GSH; γ -Glu-Cys-Gly) is a ubiquitous low molecular weight thiol compound that is found in Gram-negative bacteria and eukaryotes. Importantly, GSH functions as an antioxidant and is a major component of the soluble redox buffering system (Schafer and Buettner, 2001). Besides maintenance of cellular redox poise, GSH also participates in many cellular pathways. Among the many critical roles, GSH is utilized as a substrate by glutathione S-transferases for the detoxification of xenobiotics and has been implicated in regulation of several enzymes through glutathionylation (Rouhier et al., 2008).

The enzymes and regulation of GSH biosynthesis have been well characterized. In *Arabidopsis thaliana* (hereafter Arabidopsis), Glutamate-cysteine ligase (GshA), a redox regulated enzyme (Hicks et al., 2007), catalyzes the ligation of the γ -carboxylic acid of group of glutamate to cysteine to make γ -glutamylcysteine (γ -EC) (Jez et al., 2004). Glutathione synthetase (GshB) catalyzes the ligation of glycine to the cysteine residue of γ -EC to form GSH (Jez and Cahoon, 2004). Although there has been significant progress in understanding GSH metabolism in plants, much less is known about the role of GSH in photosynthetic microbes such as cyanobacteria. Cyanobacterial ancestors are credited with the evolution of glutathione metabolism during the advent of oxygenic photosynthesis (Copley and Dhillon, 2002) and are the evolutionary precursors of plant chloroplasts. Therefore knowledge of GSH metabolism in cyanobacteria will likely

provide important insights into the diverse roles of GSH in higher plants. We recently found that GSH is essential for acclimation to many environmental perturbations in the model photosynthetic microbe *Synechocystis* sp. PCC 6803 (hereafter *Synechocystis* 6803) (Cameron and Pakrasi, 2010).

Glutathione catabolism also plays important roles in cellular metabolism. GSH degradation involves several different enzymes that comprise the γ -glutamyl cycle (Fig. 1). In this pathway, γ -glutamyltranspeptidase (Ggt) catalyzes the removal of glutamate from glutathione by cleaving the γ -glutamyl bond, resulting in the formation of cysteinylglycine, which can be metabolized by a dipeptidase. Alternatively, a γ -glutamylcyclotransferase (GGC) can convert the γ -glutamyl residue into 5-oxoproline (5-OP). 5-OPase converts 5-OP to glutamate. While this pathway has been studied extensively in mammalian systems due to its importance in human health (Enoiu et al., 2000; Heisterkamp et al., 2008) and in model organisms such as *E. coli*, less is known about this pathway in photosynthetic organisms. Recently, there has been significant progress on the understanding of glutathione catabolism in plants (Martin et al., 2007; Ohkama-Ohtsu et al., 2007; Ohkama-Ohtsu et al., 2008; Ohkama-Ohtsu et al., 2009). The Arabidopsis genome encodes four genes annotated as GGTs. GGT1 and GGT2 are localized to the apoplastic space while GGT4 is localized to the vacuole and is involved in degradation of GSH-xenobiotic conjugates (Grzam et al., 2007; Martin et al., 2007; Ohkama-Ohtsu et al., 2007; Ohkama-Ohtsu et al., 2007). While depletion of glutathione under conditions of nutrient depletion has been observed in cyanobacteria (Cameron and

Pakrasi, 2010; Zechmann et al., 2010), the pathways for glutathione degradation have not yet been characterized. The *Synechocystis* 6803 genome encodes a single gene annotated as a *ggt* (*slr1269*). Among the four GGTs annotated in Arabidopsis, the *Synechocystis* 6803 Ggt that has the highest similarity to GGT4.

In this work, we have generated deletion mutants of *ggt* in the cyanobacterium *Synechocystis* 6803. Our results suggest that Ggt mainly functions in maintenance of cellular fitness during stationary phase and is involved in uptake of GSH from the culture medium. Our results also implicate another independent pathway for intracellular depletion of GSH observed during sulfate limitation.

MATERIALS AND METHODS

Alignment of Protein Sequences and Construction of Phylogenetic Tree

Protein sequences were aligned using ClustalW software. An unrooted tree was constructed by the Neighbor-Joining method using ClustalW.

Growth and Maintenance of *Synechocystis* 6803 Strains

Strains of *Synechocystis* sp. PCC 6803 were maintained on solid BG11 (Allen, 1968) with the appropriate antibiotic (WT, no antibiotic; $\Delta ggt::Km^R$, 20 μ g/ml kanamicin; $\Delta ggt::Cm^R$ and $ggt-6xHis::Cm^R$, 10 μ g/ml chloramphenicol). Strains were grown in BG11 at 30°C and illuminated with cool-white fluorescent lights at an intensity of 30 μ mol photons $m^{-2} s^{-1}$. The high light experiment was performed at 30°C in a Fytoscope chamber containing red, green and blue (RGB) LED's at a light intensity 500 μ mol photons $m^{-2} s^{-1}$ (Photon Systems Instruments, Brno, Czech Republic). Growth was monitored as optical density (OD) at 730 nm on a μ Quant Microplate spectrophotometer (Biotek Instruments, Inc., Winooski, VT).

Construction of the $\Delta ggt::Km^R$, $\Delta ggt::Cm^R$ and $ggt-6xHis::Cm^R$ Strains

To construct the deletion mutants, we first cloned sequences upstream and downstream of the *slr1269* open reading frame into the pUC18 plasmid using restriction sites encoded in the primers. To generate the *slr1269* upstream sequence (606 bp) we utilized forward (5'-TCTAAGCTTGACAAGTATTTCCATCCGGGACT-3') and reverse (5'-

TCTCTGCAGAGAAAGTTTCGATAACAATTG-3') primers containing a PstI and HindIII restriction site, respectively. To generate the *slr1269* downstream sequence (600bp), we utilized forward (5'-TCTCTGCAGCATTGGTTACAATTCTTAGGGC-3') and reverse (5'-TCTGGATCCTTGATTCTGGTTGGCAATGA-3') primers containing a PstI and BamHI restriction site, respectively. We then cloned a Km or Cm resistance cassette between the upstream and downstream sequences using the PstI site. This plasmid (pUC18-*Aggt*::Km^R and pUC18-*Aggt*::Cm^R) was used to transform the WT *Synechocystis* 6803 strain. To generate the *ggt*-6xHis::Cm^R strain, we replaced the upstream fragment of pUC18-*Aggt*::Cm^R with 487 bp fragment containing the 3' end of the *slr1269* gene without the stop codon and with a 6x-His gene fusion encoded in the reverse primer. This product was generated using forward (5'-TCTAAGCTTGGGGGAAGAAGACCTCAATC-3') and reverse (5'-AGACTGCAGTTAGTGGTGATGGTGATGATGTTCCAGACTGTAGGCCACGG-3') primers that contain a HindIII and PstI site, respectively. Transformations were plated on selective media and transformants were isolated and screened for segregation of the insert by PCR using a combination of upstream and downstream primers.

Optical Measurements

Absorption spectra were obtained using a DW2000 spectrophotometer (SLM-Aminco, Urbana, IL). Chlorophyll and phycocyanin concentrations were estimated using whole cell absorption spectra as described (Arnon et al, 1974).

Measurement of Cellular Thiols

Cellular thiols were simultaneously extracted from cells and derivatized with monobromobimane before being separated by HPLC as described (Cameron and Pakrasi, 2011). Quantification of cellular thiol concentration was accomplished by comparison of peak areas to those of authentic standards. For measurement of GSH in the medium, we replaced the water in the extraction buffer with filtered culture medium after cells were removed by centrifugation. HPLC analysis of culture medium following derivatization was the same as for cellular thiols.

Ggt Activity Assay

Ggt activity was measured in cellular extracts of *Arabidopsis* (ecotype Columbia) rosette leaf tissue (4 week old) exactly as described (Martin et al., 2007). For *Synechocystis*, we also utilized the same assay, with a few modifications. We lysed the cells with glass beads (0.15 mm) on ice in buffer A containing 100 mM Tris-Cl (pH 8.0), 1 mM EDTA and protease inhibitor cocktail (Sigma). For activity assays, we utilized a 96 well microtiter plate and a reaction volume of 100 μ l. The reaction mix contained 100 mM Tris-Cl, 10 μ l extract, 5 mM γ -glutamyl-*p*-nitroanilide (γ -GPNA) and 20 mM glycylglycine. Formation of *p*-nitroaniline was measured spectrophotometrically at 405 nm on μ Quant Microplate spectrophotometer (Biotek Instruments, Inc., Winooski, VT). In *Arabidopsis*, the highest Ggt activity was found after washing the insoluble pellet with buffer A containing 1 M NaCl. In *Synechocystis* 6803 cells, the highest activity was

found in the soluble fraction. Activity of *Synechocystis* 6803 extracts was not enhanced in the presence of NaCl.

Protein Purification

Synechocystis 6803 *ggt-6xHis::Cm^R* cells were harvested by centrifugation and the supernatant was removed. The cells were suspended in ice-cold 20 mM Tris-Cl (pH 8.0). Cell breakage was achieved by vortexing in the presence of glass beads on ice (0.15 mm). The cell lysate was centrifuged for 5 minutes at 16.1 x g at 4°C. The supernatant was transferred to a new microfuge tube. The membrane fraction was re-suspended in equal volume of supernatant fraction. Isolation of his-tagged proteins was accomplished using a Ni-NTA spin column (Qiagen) according to manufacturers instructions. Proteins were separated by SDS-PAGE on 16% polyacrylamide gels containing 6 M urea and then transferred to 0.22 µm nitrocellulose membranes using a semi-dry transfer apparatus (Bio-Rad, Hercules, CA). Anti-His antibodies were used to detect his-tagged proteins following reaction with peroxidase-conjugated antiserum (Pierce) developed in West Pico (Pierce). After blots were incubated in the substrate, they were imaged on a Fujifilm LAS-1000plus imager (Fujifilm, Stamford, CT).

RESULTS

Comparison of Plant and Bacterial Ggt Proteins

The *Synechocystis* 6803 genome contains a single gene annotated as a γ -glutamyltranspeptidase (*slr1269*). The gene encodes a 518 amino acid protein with a molecular weight of 55.9 kDa. The N-terminus contains a putative 19 amino acid signal peptide. Based on similarities to the *Escherichia coli* protein, it is likely that the *slr1269* gene product is proteolytically processed into a large (34.6 kDa) and small (19.5 kDa) subunit. The small subunit contains the catalytic residues. The Arabidopsis genome contains four genes annotated as Ggt, with GGT1 possessing most of the measured cellular activity (Ohkama-Ohtsu et al., 2009). Figure 2 shows a protein alignment of Arabidopsis, *Synechocystis* 6803 and *E. coli* Ggt proteins that was performed using ClustalW. The amino acids that contact the γ -glutamyl substrate in *E. coli* have been highlighted in the protein alignment (Fig. 2) (Okada et al., 2006). Figure 3 is an unrooted Neighbor-Joining tree showing the relationships between the protein sequences in figure 2. As expected, most of the conservation among the proteins occurs in the small, catalytic subunit.

Genetic Disruption of the *ggt* Gene in *Synechocystis* sp. PCC 6803

To facilitate functional characterization of the γ -glutamyl pathway (Fig. 1) in *Synechocystis* 6803 we generated two Δggt deletion mutants of the *slr1269* gene using targeted homologous recombination (Fig. 4). The entire ORF was replaced with a Kan^R

or Cm^R antibiotic resistance cassette. Two separate lines were generated to facilitate the functional analysis and provide flexibility in generation of combinatorial mutant lines. Transformants were selected on the appropriate medium and routinely streaked to fresh selective medium to facilitate segregation of the insertion. Segregation of the strains was confirmed by PCR (Fig. 4B and C) using specific primers that flanked the insert.

Analysis of Growth and Pigment Content in Δggt Strains

The fact that the *ggt* gene could be completely deleted indicates that it is not essential for growth in standard laboratory conditions. Therefore, we investigated the growth and physiological characteristics of the Δggt mutants during multiple environmental perturbations. We did not observe a significant growth defect of these strains under any perturbation. We tested growth at different light intensities, in the presence of H₂O₂, and in media lacking nitrate and sulfate. However, the strains resembled the WT under all of the conditions. We did notice a slight reduction of growth after an extended period of time under high-light (500 $\mu\text{mol photons m}^{-2} \text{s}^{-1}$) conditions (Fig. 5A). Furthermore, after extended growth (17 days) at a medium light intensity (30 $\mu\text{mol photons m}^{-2} \text{s}^{-1}$), the Δggt strains contained less pigment compared to the WT strain (Fig. 5). In fact, these cultures eventually bleached completely, while the WT strain maintained a green color for several weeks. We have observed a similar phenotype in the $\Delta gshB$ strain, which lacks GSH, but accumulates the biosynthetic intermediate γ -glutamylcysteine (Cameron and Pakrasi, 2010). This suggests that the Ggt activity is necessary for maintenance of cellular functions during stationary phase.

Quantification of Cellular and Extracellular GSH in Δggt Strains

We have previously shown that GSH levels decrease rapidly following transfer of cells to sulfate deplete medium (Cameron and Pakrasi, 2010). We hypothesized that the GSH was being degraded in a process facilitated by the *ggt* gene product. Therefore, we predicted that GSH would not be depleted in the Δggt mutant strains following sulfate depletion. We measured cellular and extracellular GSH content following 300 h growth in BG11 media or BG11 media lacking sulfate by HPLC (Fig. 7). We found that the Δggt strains contained more GSH during growth in BG11. During growth in sulfate free medium, however, we observed a rapid decline of cellular GSH levels in the Δggt and WT strains. We also measured the GSH content of the media after sedimentation of the cells by centrifugation. We found that the Δggt strains excreted significantly more GSH into the media compared to the WT strain in sulfur sufficient conditions. During sulfate deplete conditions, there was not a large difference between the GSH content of the medium in all of the strains.

Characterization of Ggt Enzymatic Activity

Analysis of cellular GSH content suggests that the Ggt protein might be involved in retention or uptake of GSH. The Ggt enzyme utilizes a variety of substrates and donors, resulting in transfer of the γ -glutamyl residue to an amino acid or peptide, or hydrolysis of the γ -glutamyl bond to release glutamate (Fig. 1 and 8A). To facilitate detection of Ggt activity in crude extracts of *Synechocystis* 6803, we utilized an artificial γ -glutamyl

donor, γ -glutamyl-*p*-nitroanilide (γ -GPNA), and acceptor, glycylglycine (Fig. 8). In this assay, the transfer of the γ -glutamyl from γ -GPNA to glycylglycine results in stoichiometric release of *p*-nitroaniline. Formation of *p*-nitroaniline is monitored at 410 nm ($\epsilon = 8.8 \text{ mM}^{-1} \text{ cm}^{-1}$).

In *Arabidopsis*, the GGT1 protein is responsible for most of the activity in leaf tissue. The highest activity fractions are obtained in the supernatant after the insoluble pellet containing cell wall material is washed with 1 M NaCl (Martin et al., 2007). To facilitate our understanding the Ggt protein in *Synechocystis* 6803, we separated the cells into soluble and membrane fractions. We also washed the insoluble membranes with 1 M NaCl. The highest levels of enzymatic activity were found in the soluble fraction (Fig. 8C). The membrane fraction and NaCl wash only exhibited residual activity (data not shown). We included 1 M NaCl extracts from a similar amount of *Arabidopsis thaliana* tissue (500 mg) in the assay for comparison (Fig. 8C). The kinetics of *p*-nitroaniline formation was much faster in the *Arabidopsis* extract compared to the *Synechocystis* 6803 extract. After several minutes, color change (yellow) was visible by eye in the wells containing *Arabidopsis* extract. However, activity of the *Synechocystis* 6803 extract was only noticeable after several hours of incubation. A more detailed analysis of the Ggt protein will likely provide insight into function of the γ -glutamyl cycle in *Synechocystis* 6803.

Generation of *ggt*-6xHis Tagged Strain in *Synechocystis* 6803

Analysis of microarray data suggests that the *ggt* gene is not differentially regulated during most conditions (Singh et al., 2010). Furthermore, we could only detect low levels of enzymatic activity in the WT strain. Therefore, a *ggt*-6xHis::Cm^R epitope tagged strain was generated in order to detect Ggt protein levels under different conditions (Fig. 9). The resulting strain has a 6xHis tag fused to the 3' end of the native *ggt* gene, which is driven by the native promoter. We were able to confirm segregation of the insertion using PCR with primers that flanked the insertion site (Fig. 9B). Next, we aimed to analyze the expression of the Ggt-6xHis protein in cellular extracts. We lysed the *ggt*-6xHis::Cm^R cells using glass beads at 4°C and then separated the soluble and membrane fractions by centrifugation. Whole cell lysates and individual soluble and membrane fractions were subjected to a nickel spin column (Qiagen) and the flow through and elution fractions were collected. The fractions were separated by SDS-PAGE on a 16% acrylamide gel (Fig. 9C). In other organisms, the Ggt protein is translated as a single polypeptide (56 kDa) with a 19 AA signal peptide that is proteolytically processed into a large (35 kDa) and small subunit (20 kDa). The C-terminal His-tag is located on the small subunit. Therefore, we expected a size of either 20 or 55 kDa, depending on whether the protein was processed. A single strong band corresponding to a molecular weight of approximately 45 kDa was observed in the first elution of whole cell lysate and soluble fractions, but not of the membrane fraction. We were able to detect some bands that cross-reacted with the anti-His antibody by Western blot analysis (Fig. 9D). The intense band corresponding to a molecular weight of

approximately 45 kDa was only detected in the elution fractions. We have not verified the identity of the cross-reacting bands. It is therefore possible that all of these bands are a consequence of non-specific cross-reactivity of the antibody.

DISCUSSION

The results presented here suggest that Ggt activity is not necessary for photoautotrophic growth *Synechocystis* 6803. We found that while *ggt* is not necessary for growth, the Δggt mutants exhibited reduced cell density (Fig. 5) and pigment composition (Fig. 6) during stationary phase. In *E. coli*, Ggt activity is maximal during stationary phase (Suzuki et al., 1986). Further, increased leakage of GSH has been observed in Δggt mutants of *E. coli* (Suzuki et al., 1987) and following inhibition of Ggt activity in *P. mirabilis* (Nakayama et al., 1984). In *E. coli*, GSH accumulates in the media during growth until the stationary phase, where it is re-absorbed by the cells. The Δggt mutants of *E. coli* leaked more GSH into the media during growth and uptake during stationary phase was reduced (Suzuki et al., 1987). Furthermore, Ggt activity was shown to be critical for utilization of γ -glutamyl amino acids in *E. coli* (Suzuki et al., 1993). We also found increased cellular and extracellular GSH in the *Synechocystis* 6803 Δggt mutants. Therefore it is possible that the uptake of GSH is critical for cellular maintenance in *Synechocystis* 6803 during stationary phase.

In a previous report, we hypothesized that the depletion of GSH content during sulfate limitation was dependent on Ggt activity in *Synechocystis* 6803 (Cameron and Pakrasi, 2010). In the current study we found that the GSH content also decreased in the Δggt mutants following sulfur starvation. Therefore, another mechanism must be involved in depletion of intracellular GSH following nutrient starvation. In *Arabidopsis*, a *ggt*

independent pathway for degradation of GSH has been reported (Ohkama-Ohtsu et al., 2008). In this pathway, an unidentified enzyme with γ -glutamylcyclotransferase (GGC) activity converts the γ -glutamyl residue into 5-oxoproline (5-OP). 5-OP is subsequently converted to glutamate by 5-OPase. The *Synechocystis* 6803 genome encodes a gene annotated as 5-OPase (*slr0697*), however to date there have been no reports describing this pathway in cyanobacteria.

We were able to measure low levels of Ggt transpeptidation in crude extracts of WT *Synechocystis* 6803 cells. We found the highest activity was associated with soluble fractions. This is in agreement with the finding that Ggt activity is highest in the periplasm in *E. coli* (Suzuki et al., 1986). Unlike in *E. coli*, we were unable to detect activity in whole cell assays using *Synechocystis* 6803 cells. As a control in our assay, we utilized extracts of Arabidopsis. In Arabidopsis, 80% of Ggt activity in leaf tissue is associated with GGT1. We found significantly lower activity in *Synechocystis* 6803 extracts versus Arabidopsis. However, the artificial substrates and acceptor molecules used in the assay might not reflect the activity in vivo. In fact, the transpeptidation reaction of purified Ggt from *Proteus mirabilis* was reduced by 80% with γ -GNPA as the donor compared to GSH (Nakayama et al., 1984).

It is possible that the genomic context of *ggt* (*slr1269*) might provide clues to the function of Ggt in cyanobacteria. The *ggt* gene is in close proximity (97bp) to *slr1270*, the product of which is related to the bacterial efflux protein channel, TolC. TolC is the

outer membrane component of a channel that spans the inner and outer membranes of Gram-negative bacteria and is important for multidrug resistance (Zgurskaya and Nikaido, 2000). In fact, synteny between *ggt* and *tolC* is conserved in several cyanobacterial genomes. It is possible that GSH-conjugated species are exported from the cell, and the Ggt protein facilitates recovery of the lost GSH molecule. In Arabidopsis, GGT4 facilitates degradation of GSH-xenobiotic conjugates in the vacuole (Grzam et al., 2007). Among the four GGT proteins in Arabidopsis, the *Synechocystis* 6803 Ggt has the highest homology with GGT4 (Fig. 2 and 3).

As a tool to monitor expression of the Ggt protein in *Synechocystis* 6803 cells during growth and after exposure to environmental perturbations, we constructed a histidine tagged version of the *ggt* gene that is expressed in the native locus under control of the native promoter (Fig. 9). In crude extracts we were unable to identify a specific band that cross-reacted with the anti-His antibody. It is possible that the Ggt protein is expressed at low levels or only at specific times during growth. We also utilized a Ni-NTA resin column in an attempt to purify the Ggt-6xHis protein. While we were able to detect a band in the elution fraction, we were unable to confirm its identity.

CONCLUSIONS

While there have been many studies focused on the biosynthesis of GSH, much less is known regarding its degradation. The γ -glutamyl cycle has been shown to be important for uptake of γ -glutamyl amino acids from the media in other Gram-negative bacteria. Therefore, we generated Δggt mutants in the cyanobacterium *Synechocystis* 6803 to determine whether these strains were still able to degrade intracellular GSH during sulfate starvation. We did not find a difference in cellular thiol contents between the WT and Δggt strains during sulfate depletion. However, we did observe increased GSH content in the media of Δggt strains compared to the WT. While our results suggest that *ggt* activity is not critical for growth, they do implicate Ggt activity in maintenance of cellular fitness during stationary phase, possibly by recovering GSH that was lost from the cell during growth.

REFERENCES

- Allen MM** (1968) Simple conditions for growth of unicellular blue-green algae on plates. J Phycol **4**: 1-4
- Cameron JC, Pakrasi HB** (2010) Essential role of glutathione in acclimation to environmental and redox perturbations in the cyanobacterium *Synechocystis* sp. PCC 6803. Plant Physiol **154**: 1672-1685
- Cameron JC, Pakrasi HB** (2011) Glutathione in *Synechocystis* 6803: A closer look into the physiology of a $\Delta gshB$ mutant. Plant Signal Behav **6**: 89-92
- Copley SD, Dhillon JK** (2002) Lateral gene transfer and parallel evolution in the history of glutathione biosynthesis genes. Genome Biol **3**: 25.1-25.16
- Enoiu M, Aberkane H, Salazar JF, Leroy P, Groffen J, Siest G, Wellman M** (2000) Evidence for the pro-oxidant effect of gamma-glutamyltranspeptidase-related enzyme. Free Radic Biol Med **29**: 825-833
- Grzam A, Martin MN, Hell R, Meyer AJ** (2007) gamma-Glutamyl transpeptidase GGT4 initiates vacuolar degradation of glutathione S-conjugates in Arabidopsis. FEBS Lett **581**: 3131-3138
- Heisterkamp N, Groffen J, Warburton D, Sneddon TP** (2008) The human gamma-glutamyltransferase gene family. Hum Genet **123**: 321-332
- Hicks LM, Cahoon RE, Bonner ER, Rivard RS, Sheffield J, Jez JM** (2007) Thiol-based regulation of redox-active glutamate-cysteine ligase from *Arabidopsis thaliana*. Plant Cell **19**: 2653-2661

- Jez JM, Cahoon RE, Chen S** (2004) *Arabidopsis thaliana* glutamate-cysteine ligase: functional properties, kinetic mechanism, and regulation of activity. *J Biol Chem* **279**: 33463-33470
- Martin MN, Saladores PH, Lambert E, Hudson AO, Leustek T** (2007) Localization of members of the gamma-glutamyl transpeptidase family identifies sites of glutathione and glutathione S-conjugate hydrolysis. *Plant Physiol* **144**: 1715-1732
- Nakayama R, Kumagai H, Tochikura T** (1984) Leakage of glutathione from bacterial cells caused by inhibition of gamma-glutamyltranspeptidase. *Appl Environ Microbiol* **47**: 653-657
- Nakayama R, Kumagai H, Tochikura T** (1984) Purification and properties of gamma-glutamyltranspeptidase from *Proteus mirabilis*. *J Bacteriol* **160**: 341-346
- Ohkama-Ohtsu N, Fukuyama K, Oliver D** (2009) Roles of γ -Glutamyl Transpeptidase and γ -Glutamyl Cyclotransferase in Glutathione and Glutathione-Conjugate Metabolism in Plants. *Adv Bot Res* **52**: 87-113
- Ohkama-Ohtsu N, Oikawa A, Zhao P, Xiang C, Saito K, Oliver DJ** (2008) A γ -glutamyl transpeptidase-independent pathway of glutathione catabolism to glutamate via 5-oxoproline in *Arabidopsis*. *Plant Physiol* **148**: 1603-1613
- Ohkama-Ohtsu N, Radwan S, Peterson A, Zhao P, Badr AF, Xiang C, Oliver DJ** (2007) Characterization of the extracellular γ -glutamyl transpeptidases, GGT1 and GGT2, in *Arabidopsis*. *Plant J* **49**: 865-877

- Ohkama-Ohtsu N, Zhao P, Xiang C, Oliver DJ** (2007) Glutathione conjugates in the vacuole are degraded by γ -glutamyl transpeptidase GGT3 in Arabidopsis. *Plant J* **49**: 878-888
- Okada T, Suzuki H, Wada K, Kumagai H, Fukuyama K** (2006) Crystal structures of γ -glutamyltranspeptidase from *Escherichia coli*, a key enzyme in glutathione metabolism, and its reaction intermediate. *Proc Natl Acad Sci USA* **103**: 6471-6476
- Rouhier N, Lemaire S, Jacquot J** (2008) The Role of Glutathione in Photosynthetic Organisms: Emerging Functions for Glutaredoxins and Glutathionylation. *Annu Rev Plant Biol* **59**: 143-166
- Schafer FQ, Buettner GR** (2001) Redox environment of the cell as viewed through the redox state of the glutathione disulfide/glutathione couple. *Free Radic Biol Med* **30**: 1191-1212
- Singh AK, Elvitigala T, Cameron JC, Ghosh BK, Bhattacharyya-Pakrasi M, Pakrasi HB** (2010) Integrative analysis of large scale expression profiles reveals core transcriptional response and coordination between multiple cellular processes in a cyanobacterium. *BMC Sys Biol* **4**: 105
- Suzuki H, Hashimoto W, Kumagai H** (1993) *Escherichia coli* K-12 can utilize an exogenous γ -glutamyl peptide as an amino acid source, for which γ -glutamyltranspeptidase is essential. *J Bacteriol* **175**: 6038-6040
- Suzuki H, Kumagai H, Tochikura T** (1986) γ -Glutamyltranspeptidase from *Escherichia coli* K-12: formation and localization. *J Bacteriol* **168**: 1332-1335

- Suzuki H, Kumagai H, Tochikura T** (1987) Isolation, genetic mapping, and characterization of *Escherichia coli* K-12 mutants lacking γ -glutamyltranspeptidase. *J Bacteriol* **169**: 3926-3931
- Zechmann B, Tomašić A, Horvat L, Fulgosi H** (2010) Subcellular distribution of glutathione and cysteine in cyanobacteria. *Protoplasma* **246**: 65-72
- Zgurskaya HI, Nikaido H** (2000) Multidrug resistance mechanisms: drug efflux across two membranes. *Mol Microbiol* **37**: 219-225

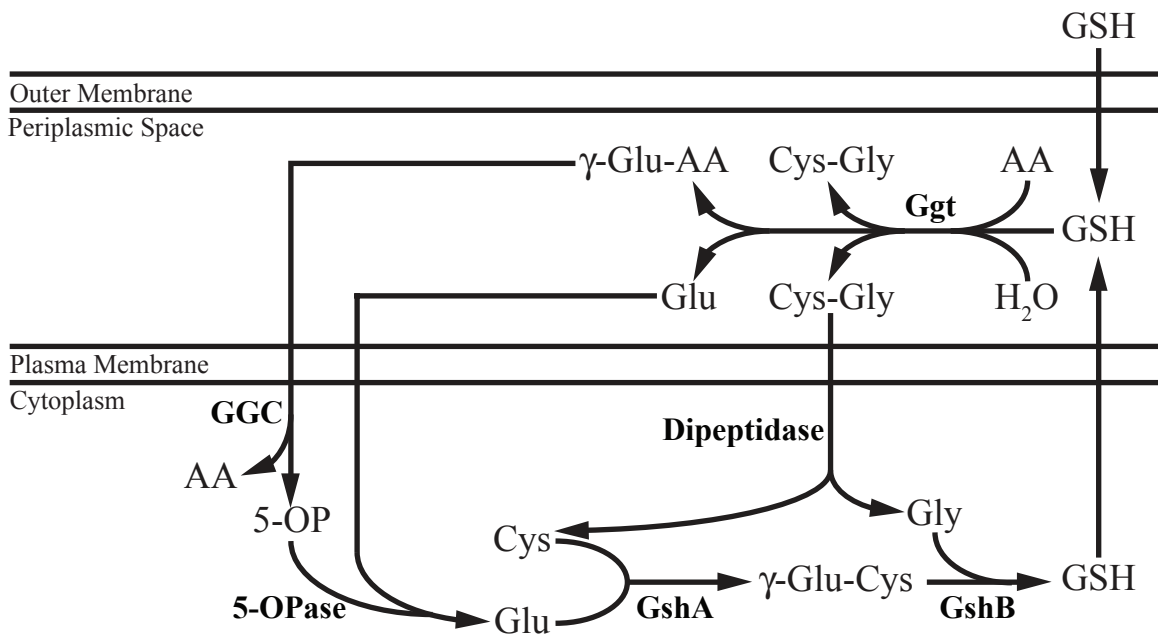


Figure 1. Schematic diagram of the γ -glutamyl pathway.

Glutathione (GSH) biosynthesis occurs in the cytoplasmic space. GSH can be exported or taken up into the periplasmic space where degradation is facilitated by γ -glutamyltranspeptidase (Ggt). Ggt catalyzes the transfer of γ -glutamate to an amino acid (AA) or to H₂O. γ -glutamyl-AA's are metabolized by γ -glutamylcyclotransferase (GGC) and 5-oxoprolinase to release AA and Glu. Cys-Gly is cleaved into constitutive amino acids by a dipeptidase. Enzymes are shown in bold.

Figure 2. Alignment of γ -glutamyltranspeptidase protein sequences.

Protein sequences from *Arabidopsis thaliana*, *Escherichia coli* and *Synechocystis* sp. PCC 6803 (Slr1269) were aligned using ClustalW. The γ -glutamyltranspeptidase protein is translated into a single polypeptide and then processed into a large (blue underline) and small subunit (green underline). A 19 amino acid signal peptide with cleavage site was predicted for the Slr1269 protein using SignalP (red underline). *E. coli* active site residues contacting the γ -glutamyl substrate are boxed in red.

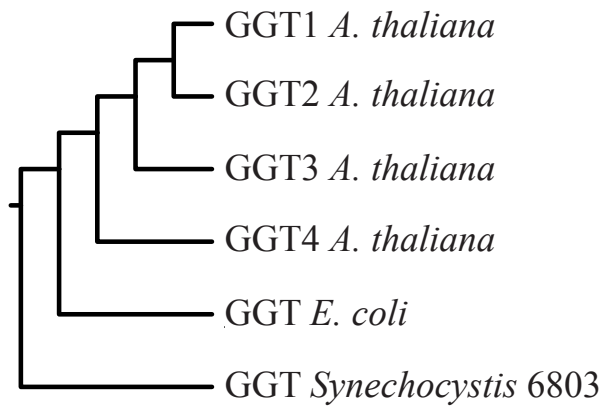


Figure 3. Phylogenetic relationship between Ggt proteins

The protein sequences shown in figure 2 were used to generate this unrooted tree using the Neighbor-Joining method on ClustalW.

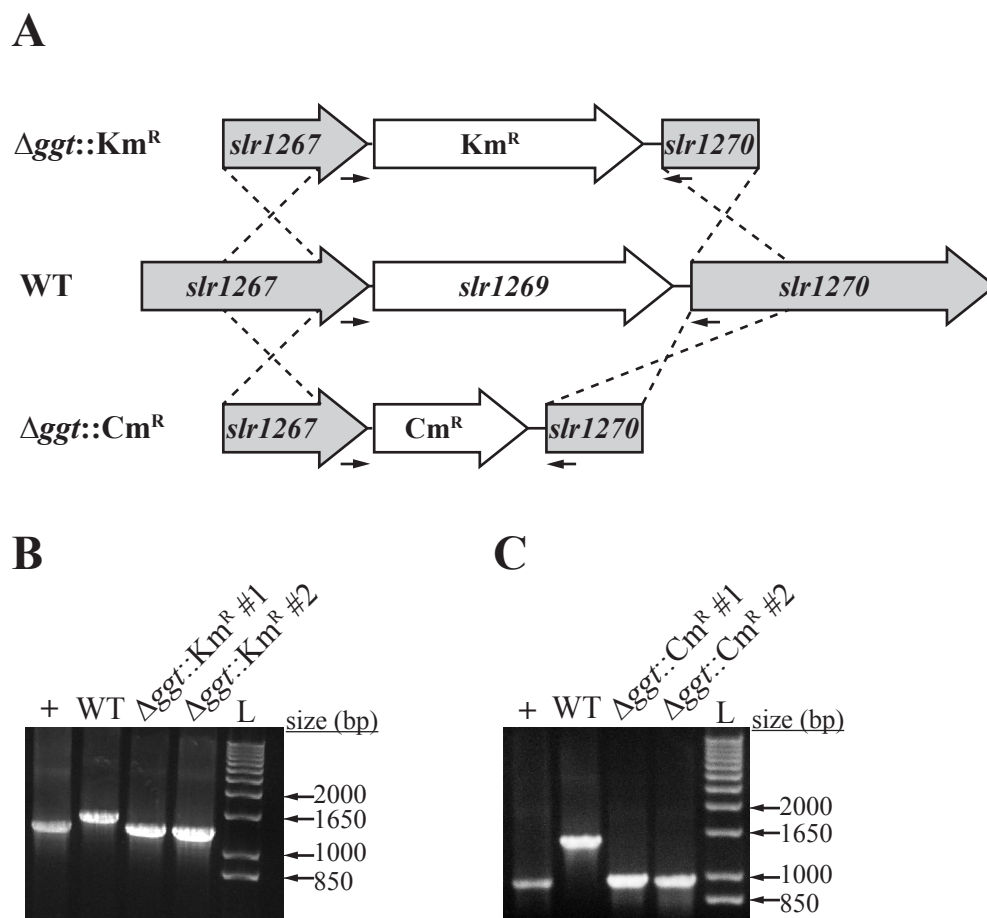


Figure 4. Disruption of γ -glutamyltranspeptidase gene in *Synechocystis* 6803.

(A) Diagram of the wild-type (WT) *Synechocystis* 6803 genomic region containing the γ -glutamyltranspeptidase gene (*sly1269*; *ggt*) and strategy for gene deletion. The entire *sly1269* open reading frame was replaced with a Km^R or Cm^R resistance gene using homologous recombination that was directed by fragments homologous to upstream and downstream regions of the gene. Arrow indicate locations of primers used in segregation analysis and dotted lines represent homologous recombination. Segregation analysis of the $\Delta ggt::Km^R$ (B) and $\Delta ggt::Cm^R$ (C) strains by PCR using primers shown in (A). The plasmid used to transform the strain was used as the positive control (+), and wild-type *Synechocystis* 6803 genomic DNA was used as the negative control (WT). A 1kb ladder (L) was used to determine the size of PCR products.

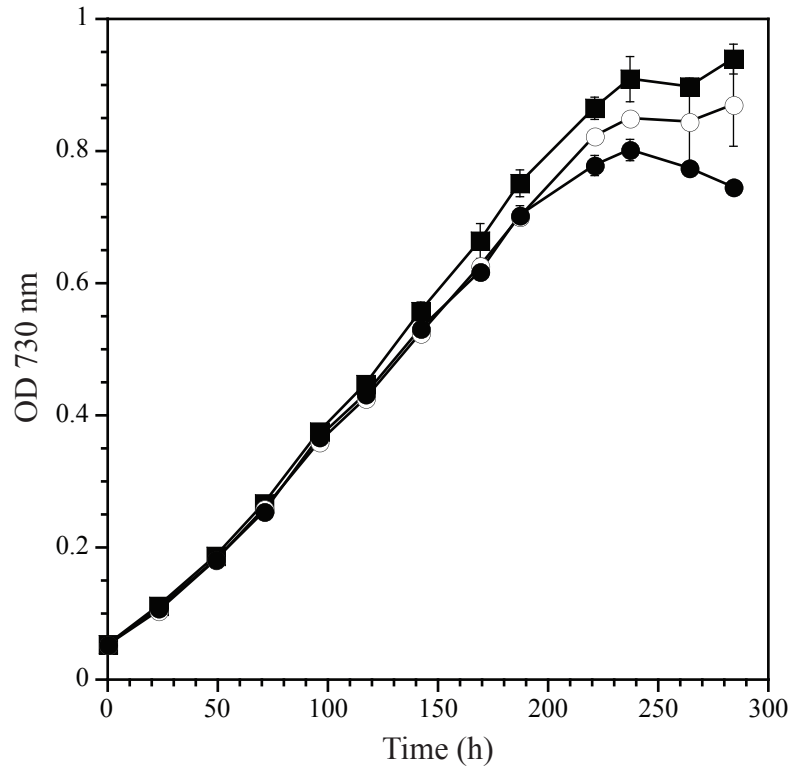


Figure 5. Growth of Δggt mutant strains at high light intensity.

The WT (squares), $\Delta ggt::Cm^R$ (open circle) and $\Delta ggt::Km^R$ (filled circle) strains were diluted to an OD 730 nm = 0.05 in BG11 media. The strains were grown in shake flasks at 30 °C and illuminated with RGB LED's at a light intensity of 500 $\mu\text{mol photons m}^{-2} \text{s}^{-1}$ (40% RGB, Fytoscope, PSI, Brno, Czech Republic). Each value represents the mean from two independent cultures and error bars represent SE.

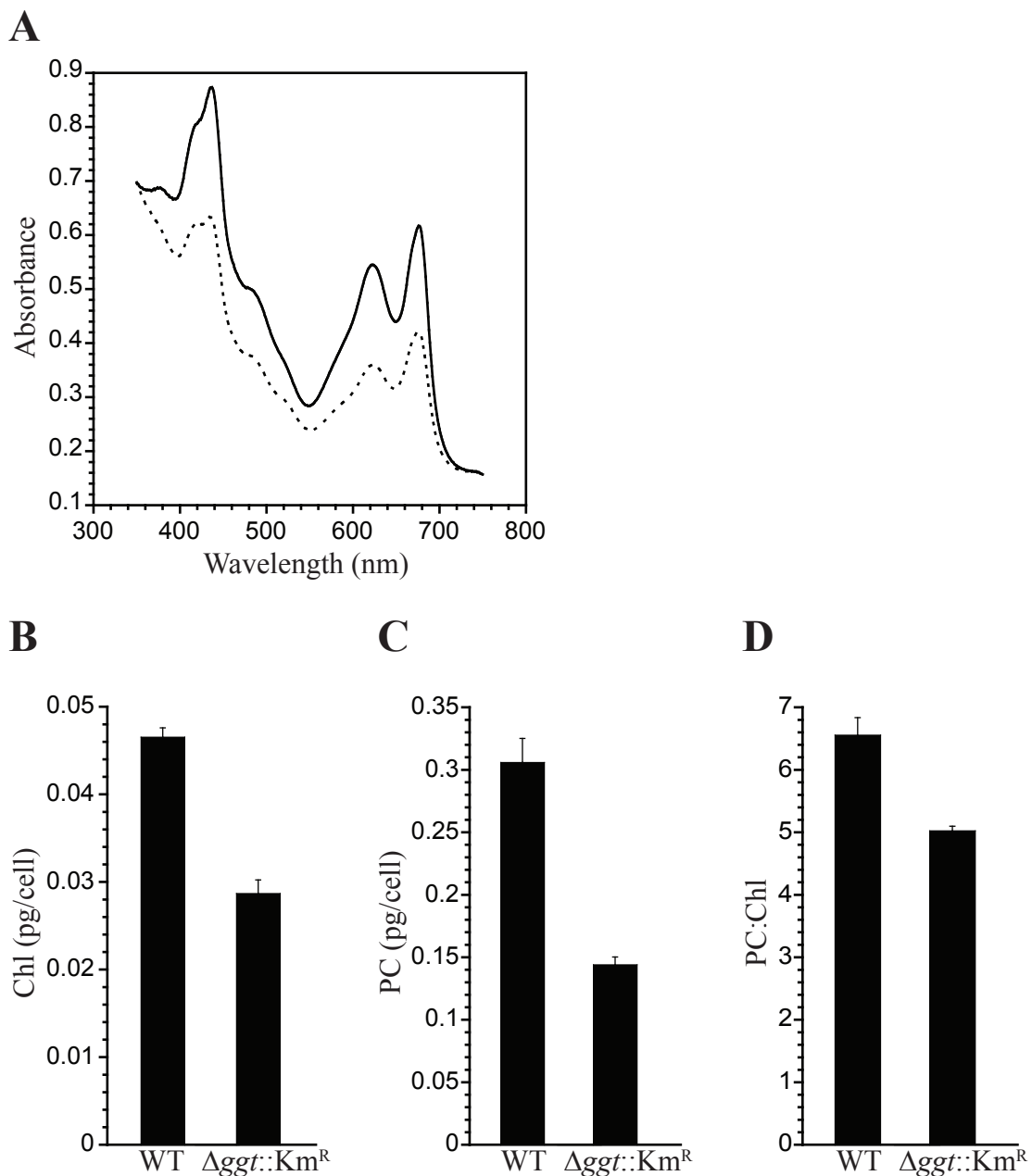


Figure 6. Absorbance spectra and pigment composition during stationary phase.

WT and $\Delta ggt::Km^R$ strains were grown for 17 days in BG11 media at 30°C with illumination provided by fluorescent lights at an intensity of 30 $\mu\text{mol photons m}^{-2} \text{s}^{-1}$. Representative absorbance spectra of WT (line) and $\Delta ggt::Km^R$ (dotted) strains are shown in (A). Chlorophyll-a (Chl; B) and phycocyanin (PC; C) pigment concentrations were estimated from absorption spectra. The ratio of PC:Chl was also calculated (D). Error bars represent SE from three separate cultures.

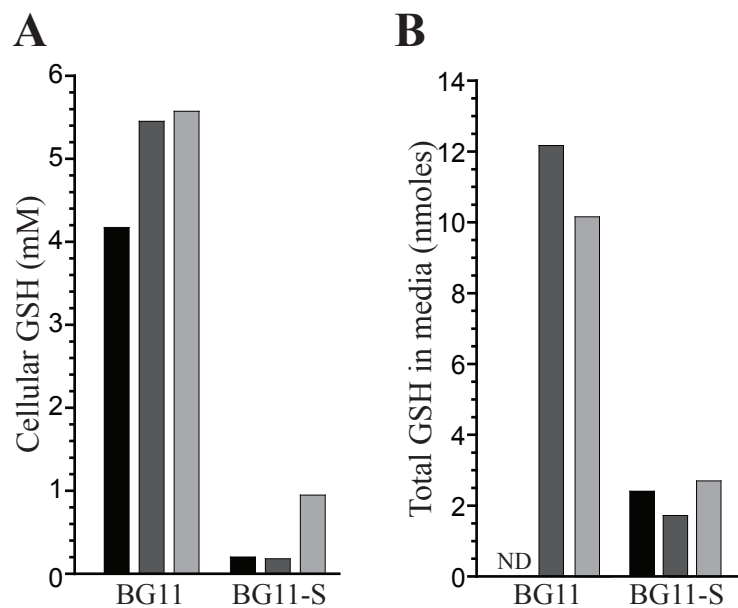
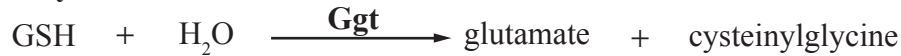
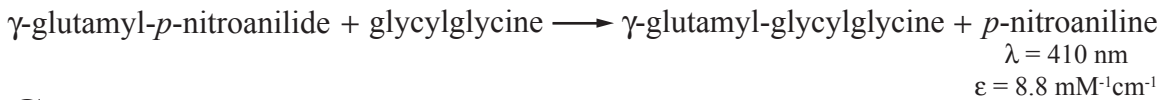
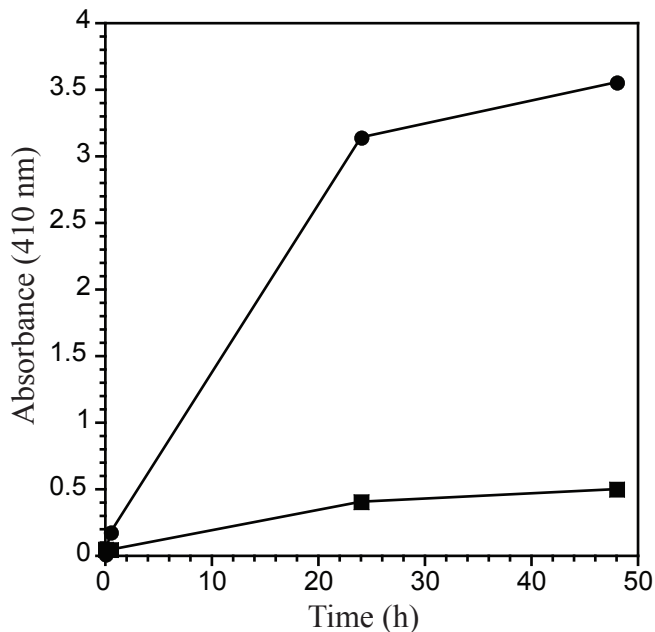
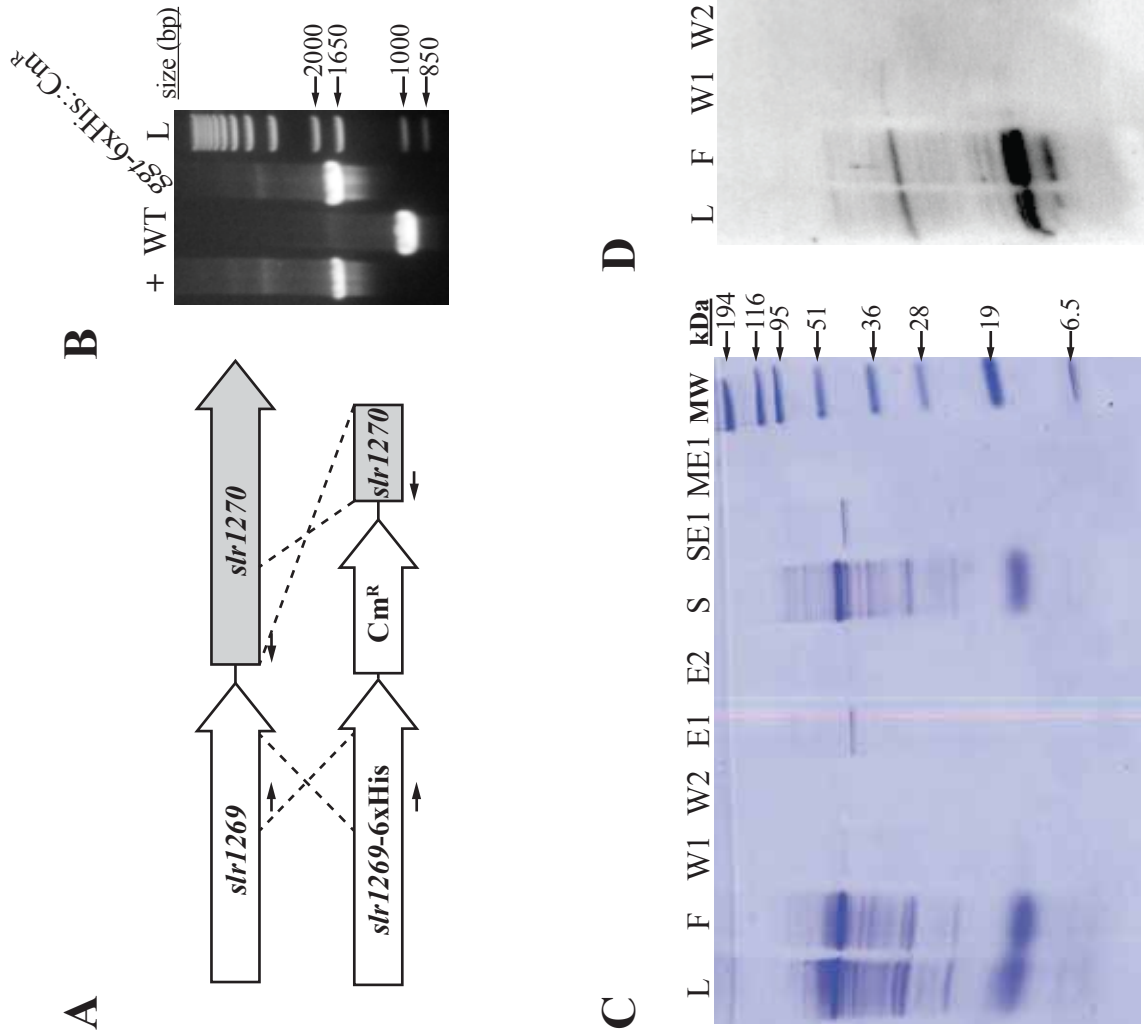


Figure 7. Cellular and extracellular GSH content in *Synechocystis* 6803 strains. (A) GSH was extracted from WT (black), $\Delta ggt::Cm^R$ (dark grey) and $\Delta ggt::Km^R$ (light grey) cells and quantified by HPLC following derivatization with monobromobimane after 300 h growth in BG11 or BG11 media lacking sulfate (BG11-S). (B) GSH was measured in media after cells were harvested by centrifugation.

A**Transferase****Hydrolysis****B****C****Figure 8. Assay for γ -glutamyltranspeptidase (Ggt) activity in cellular extracts.**

(A) Reactions catalyzed by Ggt. Ggt is able to catalyze the transfer of a γ -glutamyl residue to an acceptor substrate ($\text{NH}_2\text{-R}$) such as an amino acid or peptide. Ggt can also hydrolyze the γ -glutamyl peptide bond, using H_2O as an acceptor. (B) Ggt activity was quantified using γ -glutamyl-*p*-nitroaniline as the donor and glycylglycine as the acceptor. The release of *p*-nitroaniline resulting from cleavage of the γ -glutamyl residue was monitored spectroscopically at 410 nm. (C) Activity of WT *Synechocystis* 6803 (square) and *Arabidopsis thaliana* (circle) extracts. For the assay, soluble fractions from *Synechocystis* 6803 were used. For the *Arabidopsis* sample, the insoluble pellet following grinding of leaf tissue was washed in 1 M NaCl. The NaCl wash was used in this assay. GSH, γ -glutamyl-cysteinylglycine.

Figure 9. Construction of *ggt-6xHis::Cm^R* strain and isolation of Ggt-His protein.
 (A) Strategy used to create *ggt-6xHis::Cm^R* strain using targeted homologous recombination. The 6xHis tag was fused to the 3' (C-terminus) end of the gene. Arrows indicate primers used in segregation. (B) Segregation of insert was analyzed by PCR using WT genomic DNA (WT) and control plasmid (+). (C) Coomassie stained gel showing Ggt-His fractions from Ni-NTA column. (D) Fractions were probed with anti-His antibody. L, cell lysate; F, flowthrough; W, wash; E, elute, MW, molecular weight marker.



Chapter 6

Interaction Between the Soluble Redox Buffering System and Alternative Photosynthetic Electron Transport Pathways in *Synechocystis* sp. PCC 6803

SUMMARY

Photosynthetic organisms must overcome the dangers associated with the production of reactive oxygen species (ROS) generated as a byproduct of photosynthesis and cellular metabolism. In order to maintain redox homeostasis during environmental perturbations, cyanobacteria utilize a robust redox buffering system. Glutathione is a low molecular weight thiol that participates in the redox buffering system and also as an antioxidant. Besides metabolism of ROS through the antioxidant system, cyanobacteria also utilize flavodiiron proteins to directly reduce O₂ to water without generating ROS. In this paper we determined whether these pathways function together during conditions promoting oxidative stress by analyzing single ($\Delta flv3$ and $\Delta gshB$) and double mutants $\Delta flv3/\Delta gshB$ involved in glutathione biosynthesis and the photoreduction of O₂. We find that while the $\Delta flv3/\Delta gshB$ mutant is more sensitive under some conditions, the $\Delta gshB$ mutation appears to contribute more to the phenotype.

INTRODUCTION

Photosynthesis is inherently a dangerous process for the cell. Photosynthesis operates at extreme redox potentials and produces O₂ as a byproduct of water oxidation by photosystem II (PSII). O₂ is an efficient electron acceptor that can interact with many redox active intermediates, forming reactive oxygen species (ROS) that can damage cellular components (Fig. 1). Photosynthetic organisms have therefore developed many systems to minimize the formation of ROS, prevent damage, and repair cellular components that are damaged by ROS (Foyer et al., 2009).

Ancestors of modern day cyanobacteria evolved oxygenic photosynthesis, resulting in the conversion of earth from anoxic to oxic (Hohmann-Marriott and Blankenship, 2011). During the evolution of oxygenic photosynthesis, cyanobacteria ancestors also developed a series of protein and small molecule antioxidants (Latifi et al., 2009). Among them, glutathione (GSH) has become ubiquitous among bacteria and eukarotes (Copley and Dhillon, 2002). GSH is a low molecular weight thiol compound comprised of glutamate, cysteine and glycine. Biosynthesis of GSH requires ATP and is catalyzed by glutamate-cysteine ligase (GshA) and glutathione synthetase (GshB) (Jez and Cahoon, 2004; Jez et al., 2004). We have previously generated and characterized a $\Delta gshB$ mutant in the model photosynthetic cyanobacterium *Synechocystis* sp. PCC 6803 (Cameron and Pakrasi, 2010, 2011). We found that the $\Delta gshB$ strain no longer makes GSH, but instead accumulates

the GSH precursor, γ -glutamylcysteine (γ -EC). We also found that the $\Delta gshB$ strain is viable, but is sensitive to conditions promoting oxidative stress.

Besides an elaborate system of soluble antioxidants, cyanobacteria have also developed intricate pathways to balance electron transport pathways with the needs of cellular metabolism (Singh et al., 2008; Singh et al., 2009; Wegener et al., 2010). During linear electron flow, electrons generated from PSII result in the formation of NADPH, which is used during carbon fixation and nutrient assimilation. Alternatively, cyclic electron transport around photosystem I can be used to produce ATP instead of reducing equivalents. The amount of linear versus cyclic electron flow maintains the appropriate ratio of NADPH to ATP needed for carbon fixation (Alric et al., 2010). The cyclic pathway may also be involved in protection from photoinhibition (Takahashi et al., 2009). Besides the linear and cyclic pathways, electrons can also be used to reduce O_2 to H_2O , in a so-called water-water cycle (Asada, 1999). It has been reported that as much as 40% of the O_2 evolved by PSII can be photoreduced (Helman et al., 2005). While single electron reduction of O_2 results in the formation of ROS, cyanobacteria also contain several A-type flavoproteins (flavodiiron protein; Flv) involved in reduction of O_2 . In this process, electrons are apparently transferred from NADPH to O_2 to form H_2O , without the production of a ROS intermediate (Helman et al., 2003). The *Synechocystis* 6803 genome encodes four Flv proteins (Wasserfallen et al., 1998). Flv1 and Flv3 are involved in photoreduction of O_2 (Vicente et al., 2002; Helman et al., 2003), though it has been suggested that Flv1 may be involved in nitrosative stress in *Synechocystis* 6803

(Goncalves et al., 2011). The Flv2 and Flv4 proteins have been reported to contribute to PSII photoprotection (Zhang et al., 2009). Increased expression of the *flv3* gene (Eisenhut et al., 2007) and protein (Zhang et al., 2009) has been observed following exposure to low CO₂. Moreover, Flv3 has been shown to be important during conditions promoting photorespiration in *Synechocystis* 6803 (Hackenberg et al., 2009).

Despite the report that large fluxes of PSII derived electrons end up reducing O₂ in *Synechocystis* 6803 (Helman et al., 2005), the $\Delta flv3$ mutant does not exhibit a severe growth defect (Helman et al., 2003) except during extreme conditions promoting photorespiration (Hackenberg et al., 2009). We found that the $\Delta gshB$ mutant exhibits slightly reduced growth during optimal conditions and severe retardation of growth during conditions promoting oxidative stress (Cameron and Pakrasi, 2010). Therefore, in this study we aimed to test whether the soluble redox buffering system and the water-water cycle are synergistic during environmental perturbations. To facilitate the study, we have generated and characterized a $\Delta flv3/\Delta gshB$ double mutant and the individual single mutants. Our results suggest that both pathways contribute to acclimation to conditions that promote oxidative stress, but the glutathione system appears to contribute more under the conditions tested.

MATERIALS AND METHODS

Growth and Maintenance of Strains

Strains were grown in BG11 (Allen, 1968) medium at 30°C and illuminated with fluorescent white lights or a custom LED panel (Photon Systems Instruments, Brno, Czech Republic) that has been described (Singh et al., 2009). Growth was monitored as optical density at 730 nm on a μ Quant Microplate spectrophotometer (Biotek Instruments, Inc., Winooski, VT). Strains were maintained on solid BG11 medium containing antibiotics (WT, none; $\Delta gshB$, 5 μ g/ml gentamicin (Gm); $\Delta flv3$, 10 μ g/ml spectinomycin (Sp); $\Delta flv3/\Delta gshB$, 5 μ g/ml Gm plus 10 μ g/ml Sp). Antibiotics were not used for growth experiments.

Generation of Strains

The $\Delta gshB$ strain contains a Gm^R cassette that replaces the entire *slr1238* ORF and has been described in detail (Cameron and Pakrasi, 2010). The $\Delta flv3$ strain contains a Sp^R cassette inserted in the ORF of the *sl10550* gene as described (Helman et al., 2003). The $\Delta flv3/\Delta gshB$ strain was constructed by transforming the $\Delta flv3$ strain with the construct used to generate the $\Delta gshB$ strain. Transformants were selected on solid BG11 medium containing 2 μ g/ml Gm and 5 μ g/ml Sp.

Optical Analysis

Pigment concentrations were estimated from whole-cell absorption spectra using formulas that have been previously described (Arnon et al., 1974). Absorption spectra were obtained using a DW2000 spectrophotometer (SLM-Aminco, Urbana, IL).

Fluorescence Analysis

Fluorescence induction kinetics were measured on a dual-modulation kinetic fluorometer (FL-100, Photon Systems Instruments, Brno, Czech Republic).

P700 Redox Kinetics

P700 redox kinetics were monitored at 705 nm using an LED-based pulse-probe spectrophotometer (JTS-10, Biologic, France) with appropriate filters. Actinic illumination was provided by far-red or green LEDs at the intensity indicated. Cells were illuminated for 10 s and then the measurement was continued in the dark for 20 s. Cells were suspended in BG11 medium at a chlorophyll concentration of 10 μ g/ml for the measurements in the presence of 10 mM NaHCO₃.

RESULTS

Generation of $\Delta flv3/\Delta gshB$ Double Mutant

In order to maintain redox homeostasis during environmental perturbations, photosynthetic organisms have developed intricate antioxidant networks, redox buffering systems and metabolic flexibility. Some of this flexibility is due to redundancy between pathways, allowing a cell to function even when a particular system is absent or disrupted. Metabolism of oxygen and reactive oxygen species (ROS) is critical for photosynthetic cells. In this study, we aimed to determine the relationship between the soluble redox buffering system and pathways involved in the photoreduction of O_2 . In cyanobacteria, GSH functions as a major component of the redox buffering system, and Flv3, a flavodiiron protein contributes to photoreduction of O_2 . Therefore, we generated a strain harboring mutations in the glutathione synthetase and *flv3* genes ($\Delta flv3/\Delta gshB$) by transforming the $\Delta flv3$ strain with the plasmid used to generate the $\Delta gshB$ strain (Cameron and Pakrasi, 2010). To confirm segregation of the $\Delta gshB$ mutation, we analyzed the cellular thiol contents by HPLC as described (Cameron and Pakrasi, 2010). We found that the $\Delta flv3/\Delta gshB$ strain no longer accumulated GSH, but instead accumulates γ -EC like the $\Delta gshB$ mutant, indicating an absence of the *gshB* gene. The WT and $\Delta flv3$ strains contained similar amounts of GSH (data not shown).

Growth Characteristics of Mutant Strains

In order to assess the whether the pathways involving glutathione and reduction of O₂ function cooperatively, we compared growth of the WT, $\Delta gshB$, $\Delta flv3$ and $\Delta flv3/\Delta gshB$ strains. First, we compared growth of the strains solid media (Fig. 2). The cells were suspended at the same cell density and then serially diluted. The plate was incubated for 72 h at a light intensity of 40 $\mu\text{mol photons m}^{-2} \text{s}^{-1}$ provided by white fluorescent lights. We found that the WT and $\Delta flv3$ strains grew similarly to each other at all dilutions. The $\Delta gshB$ strain was visually lighter green and grew slightly less than the WT and $\Delta flv3$ strains. The $\Delta flv3/\Delta gshB$ mutant grew very poorly compared to the other strains, especially at the higher dilutions. This could indicate that the $\Delta flv3/\Delta gshB$ strain is more sensitive to the effectively higher light intensities that penetrate dilute cultures.

We also tested growth of the strains in liquid culture and in the presence of various redox agents (Fig. 3). During photoautotrophic growth in liquid culture (30 $\mu\text{mol photons m}^{-2} \text{s}^{-1}$) we observed that the $\Delta gshB$ strain grew slightly worse than the $\Delta flv3/\Delta gshB$ strain, whereas the WT and $\Delta flv3$ strains grew at similar rates. We also grew the strains in the presence of 5 μM rose Bengal (RB), a photosensitizer that results in the formation of singlet O₂ (¹O₂) (Fischer et al., 2004). We have previously shown that the $\Delta gshB$ strain is sensitive to this perturbation (Cameron and Pakrasi, 2010). In this case, we found the $\Delta flv3/\Delta gshB$ strain was extremely sensitive to this condition (Fig. 3B). It is possible that more ¹O₂ is produced in this strain due to the absence of O₂ photoreduction in this strain compared to the $\Delta gshB$ strain alone. The addition of 1 μM methyl viologen (MV)

resulted in death for the $\Delta gshB$ and $\Delta flv3/\Delta gshB$ strains (Fig. 3C). The $\Delta flv3$ strain appeared to be slightly less sensitive to MV compared to the WT strain.

Acclimation of Strains to High Light

During photosynthesis, PSII undergoes constant damage and repair cycles. During exposure to high light, the rate of PSII damage can exceed rate of repair, leading to photoinhibition and increased production of ROS (Nishiyama et al., 2006). The flavodiiron proteins have the capacity to oxidize the NADPH pool and reduce O_2 to H_2O . These reactions simultaneously increase the pool of electron acceptors ($NADP^+$) while decreasing the pool of O_2 , which can be converted into ROS during these conditions. GSH has the ability to facilitate metabolism of ROS during these conditions, and we have previously reported that GSH levels increase dramatically following exposure to high light but $\Delta gshB$ mutant grows similarly to WT during exposure to high light (Cameron and Pakrasi, 2010). Therefore, we tested to see whether the absence of Flv3 would increase the sensitivity of the $\Delta gshB$ strain to high light. We exposed cells to monochromatic blue (455 nm) and red light (627 nm) at an intensity of approximately $200 \mu\text{mol photons m}^{-2} \text{s}^{-1}$ for 24 h. During this time, we measured chlorophyll induction kinetics to assay the relative photosynthetic capacity of the cells (F_v/F_m) (Fig. 4A,B,C). We found that the F_v/F_m decreased rapidly during the first three hours but then began to increase over the time course (Fig. 4C). We found that the $\Delta gshB$ mutant exhibited the slowest recovery, followed by the $\Delta flv3/\Delta gshB$ strain. We also measured the ratio of phycocyanin (PC) to chlorophyll (Chl) in the strains during the treatment (Fig. 4D). The

ΔgshB and *Δflv3/ΔgshB* strains maintained a higher PC:Chl ratio throughout the treatment. During the end of the treatment, the PC:Chl ratio decreased significantly in the WT and the *Δflv3* strains, however, it increased in the *ΔgshB* and *Δflv3/ΔgshB* strains. This could suggest altered regulation of phycobilisome to photosystem stoichiometry in the absence of GSH.

Altered P700 Redox Kinetics in *ΔgshB* and *Δflv3/ΔgshB* Strains

To probe the mechanism of electron flow in the various strains, we utilized a pulse-probe spectrophotometer to measure the redox state of the PSI reaction center (P700) during actinic illumination and upon darkness (Fig. 5). Figure 5 shows the $t_{1/2}$ (ms) for P700 recovery in the dark following illumination with either far red light (PSI actinic) or green light (PSI and PSII actinic). We also utilized specific inhibitors of electron transport pathways. DCMU blocks electrons from PSII into the plastoquinone (PQ) pool. MV oxidizes PSI and prevents cyclic electron transport from occurring (Figure 1). Using these compounds and preferential illumination of the photosystems, it is possible to estimate the amount of linear and cyclic electron flow around PSI. Following oxidation of P700 to P700⁺ with far red light, we found significantly faster P700 recovery in the *ΔgshB* and *Δflv3/ΔgshB* strains compared to the WT and *Δflv3* strains. Addition of MV results in slower recovery kinetics because it efficiently oxidizes the acceptor side of PSI (Fig. 5B). The presence of DCMU did not have much of an effect in the samples illuminated with FR light because PSII is not activated during these conditions (Fig. 5C). Following illumination with green light in the absence (Fig. 5A) or presence (Fig. 5B) of

MV, the P700 recovery rate was much faster than after FR illumination due to the contribution of electrons from the oxidation of H₂O by PSII. Although we observe faster P700 recovery in the $\Delta gshB$ and $\Delta flv3/\Delta gshB$ strains compared to the WT and $\Delta flv3$ strains after green illumination in the presence of DCMU (Fig. 5C) and DCMU + MV (Fig. 5D), the difference is less in the latter case.

DISCUSSION

In this report, we investigated whether the soluble redox buffering system and oxygen reduction systems function cooperatively to prevent cellular damage during conditions promoting ROS formation. We found that under certain conditions, the $\Delta flv3/\Delta gshB$ strain is more sensitive than either of the single mutants or the WT strain. This was most apparent during growth on solid media when cells were started very dilute. In liquid media, at a lower light intensity, the $\Delta gshB$ and $\Delta gshB/\Delta flv3$ strains grew at similar rates. However we find that the double mutant is more sensitive to rose Bengal. This could result from decreased resistance to oxidative stress because of the lack of glutathione, and increased cellular O₂ concentration due to the lack of Flv3 activity.

Our results suggest that the $\Delta gshB$ mutation contributes more to the phenotype of the double mutant than the $\Delta flv3$ mutation. During exposure to high light, the $\Delta flv3$ mutant behaved very similar to the WT strain (Fig. 4), while the $\Delta gshB$ and $\Delta flv3/\Delta gshB$ mutant appeared quite similar. In fact, the $\Delta gshB$ mutant seems to result in altered ratios of PC to Chl. It is possible that glutathione is involved in regulation of the phycobilisome through glutathionylation in *Synechocystis* 6803 (Li et al., 2007). Further supporting this conclusion is the observation that the $\Delta gshB$ mutation leads to increased rates of P700 recovery in the dark in the $\Delta flv3/\Delta gshB$ strain (Fig. 5). It is possible that this is the result of increased cyclic electron transport in the $\Delta gshB$ mutant. It could also reflect differences in the oxidation state at the acceptor side of PSI. We have previously

reported that the $\Delta gshB$ mutant exhibits altered PSI-mediated electron to oxygen using an artificial system (Cameron and Pakrasi, 2011), however, it is not know whether these observations are directly related. Further experiments will be required to fully elucidate the mechanism behind these observations.

CONCLUSIONS

We conclude that although the $\Delta flv3/\Delta gshB$ mutant exhibits reduced growth compared to the single mutants, the $\Delta gshB$ mutation appears to contribute more to the observed phenotypes than the $\Delta flv3$ mutation. However, we have not yet tested the growth of the double mutant in conditions that could lead to increased requirements for the $\Delta flv3$ mutant, including transition from high to low carbon. Therefore, it remains to be seen the full extent of cooperation among these pathways.

REFERENCES

- Allen MM** (1968) Simple conditions for growth of unicellular blue-green algae on plates. *Journal of Phycology* **4**: 1-4
- Alric J, Lavergne J, Rappaport F** (2010) Redox and ATP control of photosynthetic cyclic electron flow in *Chlamydomonas reinhardtii* (I) aerobic conditions. *Biochim Biophys Acta* **1797**: 44-51
- Arnon DI, McSwain BD, Tsujimoto HY, Wada K** (1974) Photochemical activity and components of membrane preparations from blue-green algae. I. Coexistence of two photosystems in relation to chlorophyll a and removal of phycocyanin. *Biochim Biophys Acta* **357**: 231-245
- Asada K** (1999) THE WATER-WATER CYCLE IN CHLOROPLASTS: Scavenging of Active Oxygens and Dissipation of Excess Photons. *Annu Rev Plant Physiol Plant Mol Biol* **50**: 601-639
- Cameron JC, Pakrasi HB** (2010) Essential role of glutathione in acclimation to environmental and redox perturbations in the cyanobacterium *Synechocystis* sp. PCC 6803. *Plant Physiol* **154**: 1672-1685
- Cameron JC, Pakrasi HB** (2011) Glutathione in *Synechocystis* 6803: A closer look into the physiology of a $\Delta gshB$ mutant. *Plant Signal Behav* **6**: 89-92
- Copley SD, Dhillon JK** (2002) Lateral gene transfer and parallel evolution in the history of glutathione biosynthesis genes. *Genome Biol* **3**: 25.1-25.16

- Eisenhut M, von Wobeser EA, Jonas L, Schubert H, Ibelings BW, Bauwe H, Matthijs HCP, Hagemann M** (2007) Long-term response toward inorganic carbon limitation in wild type and glycolate turnover mutants of the cyanobacterium *Synechocystis* sp. strain PCC 6803. *Plant Physiol* **144**: 1946-1959
- Fischer BB, Krieger-Liszkay A, Eggen RL** (2004) Photosensitizers neutral red (type I) and rose bengal (type II) cause light-dependent toxicity in *Chlamydomonas reinhardtii* and induce the Gpxh gene via increased singlet oxygen formation. *Environ Sci Technol* **38**: 6307-6313
- Foyer C, Noctor G, Buchanan B, Dietz K, Pfannschmidt T** (2009) Redox Regulation in Photosynthetic Organisms: Signaling, Acclimation, and Practical Implications. *Antioxid Redox Signal* **11**: 861-905
- Goncalves VL, Saraiva LM, Teixeira M** (2011) Gene expression study of the flavodi-iron proteins from the cyanobacterium *Synechocystis* sp. PCC6803. *Biochem Soc Trans* **39**: 216-218
- Hackenberg C, Engelhardt A, Matthijs HC, Wittink F, Bauwe H, Kaplan A, Hagemann M** (2009) Photorespiratory 2-phosphoglycolate metabolism and photoreduction of O₂ cooperate in high-light acclimation of *Synechocystis* sp. strain PCC 6803. *Planta* **230**: 625-637
- Helman Y, Barkan E, Eisenstadt D, Luz B, Kaplan A** (2005) Fractionation of the three stable oxygen isotopes by oxygen-producing and oxygen-consuming reactions in photosynthetic organisms. *Plant Physiol* **138**: 2292-2298

- Helman Y, Tchernov D, Reinhold L, Shibata M, Ogawa T, Schwarz R, Ohad I, Kaplan A** (2003) Genes encoding A-type flavoproteins are essential for photoreduction of O₂ in cyanobacteria. *Curr Biol* **13**: 230-235
- Hohmann-Marriott MF, Blankenship RE** (2011) Evolution of Photosynthesis. *Annu Rev Plant Biol* **62**: 20.21-20.34
- Jez JM, Cahoon RE** (2004) Kinetic mechanism of glutathione synthetase from *Arabidopsis thaliana*. *J Biol Chem* **279**: 42726-42731
- Jez JM, Cahoon RE, Chen S** (2004) *Arabidopsis thaliana* glutamate-cysteine ligase: functional properties, kinetic mechanism, and regulation of activity. *J Biol Chem* **279**: 33463-33470
- Latifi A, Ruiz M, Zhang C-C** (2009) Oxidative stress in cyanobacteria. *FEMS Microbiol Rev* **33**: 258-278
- Li M, Yang Q, Zhang L, Li H, Cui Y, Wu Q** (2007) Identification of novel targets of cyanobacterial glutaredoxin. *Arch Biochem Biophys* **458**: 220-228
- Nishiyama Y, Allakhverdiev SI, Murata N** (2006) A new paradigm for the action of reactive oxygen species in the photoinhibition of photosystem II. *Biochim Biophys Acta* **1757**: 742-749
- Singh A, Elvitigala T, Bhattacharyya-Pakrasi M, Aurora R, Ghosh B, Pakrasi H** (2008) Integration of carbon and nitrogen metabolism with energy production is crucial to light acclimation in the cyanobacterium *Synechocystis*. *Plant Physiol* **148**: 467-478

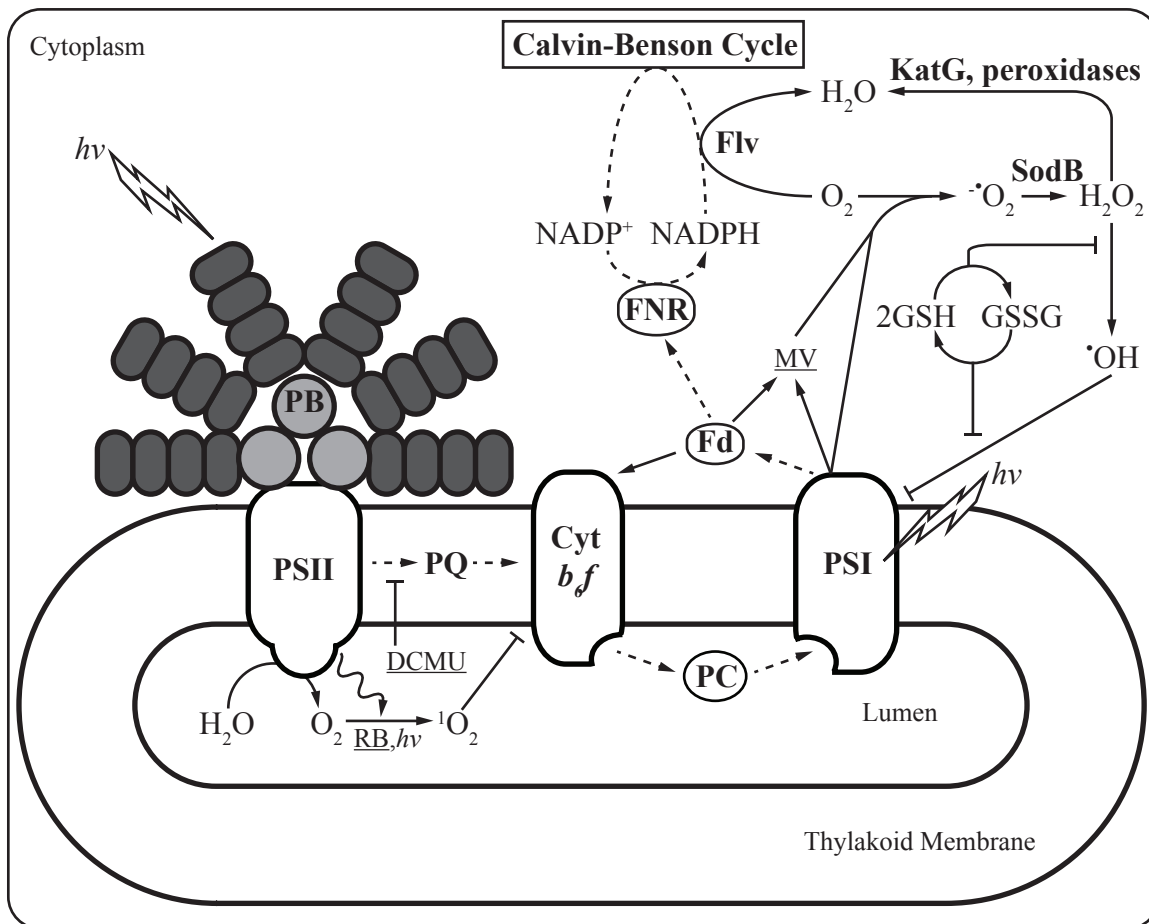


Figure 1. Schematic diagram showing photosynthesis and ROS metabolism.

Photosystem II (PSII) oxidizes water and reduces the plastoquinone pool (PQ) using light energy captured by the light harvesting complex (PB; phycobilisome). ^3Chl in PSII and the photosensitizer rose Bengal (RB) can transfer energy to O_2 and generate singlet 1O_2 . The Cytochrome b_6/f complex (Cyt b_6/f) oxidizes the PQ pool and reduces plastocyanin (PC). Photosystem I (PSI) uses light energy to oxidize PC and reduce ferredoxin (Fd). Reduced Fd participates in cyclic electron transfer with the Cyt b_6/f complex and in generation of NADPH by Fd:NADP⁺ reductase (FNR). Direct reduction of O_2 by PSI generates the superoxide anion radical ($\cdot O_2^-$). Superoxide can be dismutated to hydrogen peroxide (H_2O_2) by superoxide dismutase (SodB). H_2O_2 can be metabolized by catalase (KatG) or a variety of cellular peroxidases. H_2O_2 can also be converted into the destructive hydroxyl radical ($\cdot OH$). Alternatively, flavodiiron proteins (Flv) can facilitate the reduction of O_2 to H_2O without the production of ROS intermediates. Reduced glutathione (GSH) can be reversibly oxidized to glutathione disulfide (GSSG). The 2GSH/GSSG redox couple is a soluble redox buffer and participates in metabolism of ROS. Methyl viologen (MV) accepts electrons from PSI and Fd and reduces O_2 to $\cdot O_2^-$. DCMU (3-(3',4'-dichlorophenyl)-1,1-dimethylurea) blocks electron flow from PSII to PQ. Linear electron flow is represented by dotted arrows. Reactive oxygen species, ROS.

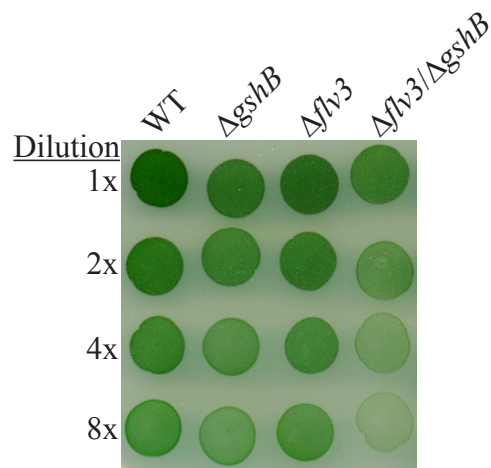


Figure 2. Growth of strains on solid media.

Cells were harvested and suspended at approximately the same initial cell concentration (2.8×10^8 cells/ml) and then serially diluted. 15 μ l of each dilution was plated on solid BG11 medium and cells were grown for 72 h at 30°C with an illumination of 40 μ mol photons $m^{-2} s^{-1}$ provided by fluorescent lights.

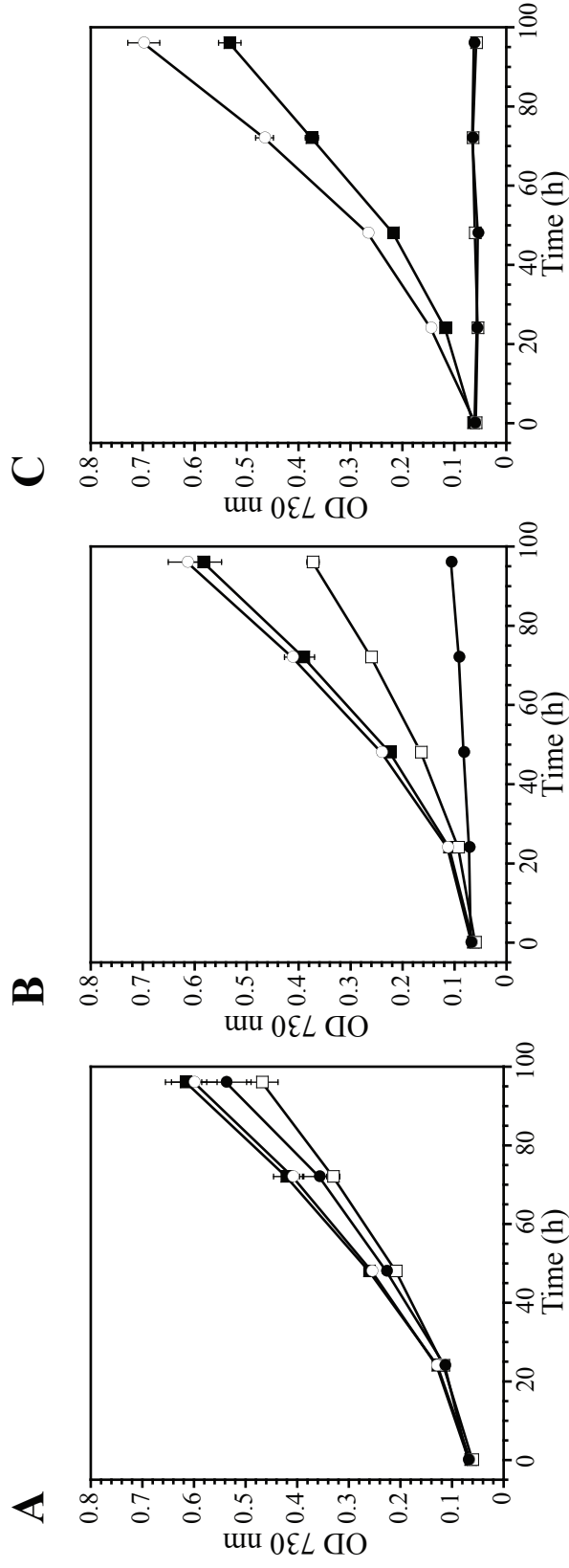


Figure 3. Growth of strains during redox perturbation.

WT (black square), $\Delta gshB$ (white square), $\Delta fiv3$ (white circle) and $\Delta fiv3/\Delta gshB$ (black circle) strains were grown in BG11 (A) media with the addition of 5 μM rose Bengal (B) or 1 μM methyl viologen. Illumination was provided by fluorescent light at an intensity of 30 $\mu\text{mol photons m}^{-2} \text{s}^{-1}$. Error bars represent SE from three cultures.

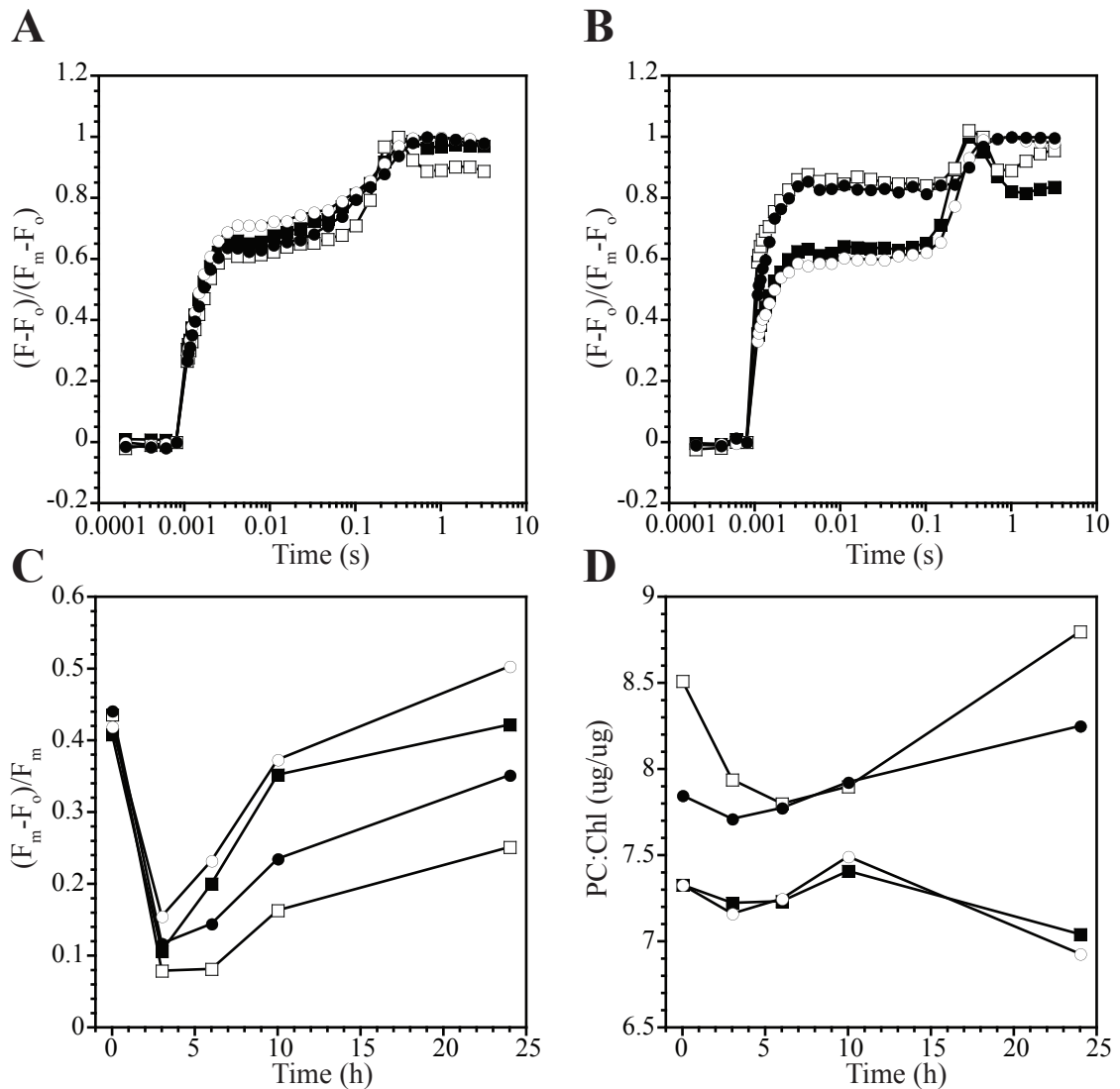


Figure 4. Cellular physiology of strains following high light treatment.

WT (black square), $\Delta gshB$ (white square), $\Delta flv3$ (white circle) and $\Delta flv3/\Delta gshB$ (black circle) cells were diluted to an OD 730 nm = 0.02 (1.5×10^7 cells/ml) and then transferred to 3 cm diameter culture tubes that were bubbled with air and maintained at 30°C in a water bath. Cells were exposed to monochromatic red (455 nm) and blue light (627 nm) at an intensity of approximately $200 \mu\text{mol photons m}^{-2} \text{s}^{-1}$ for 24 h. Fluorescence induction kinetics were measured throughout the course of the treatment. Kinetic traces for the 0 h (A) and 10 h (B) time-points are shown. (C) Relative photosynthetic capacity ($F_v/F_m = (F_m - F_0)/F_m$) following high light treatment. (D) Ratio of phycocyanin (PC) to chlorophyll (Chl) following high light treatment was calculated from whole cell absorption spectra.

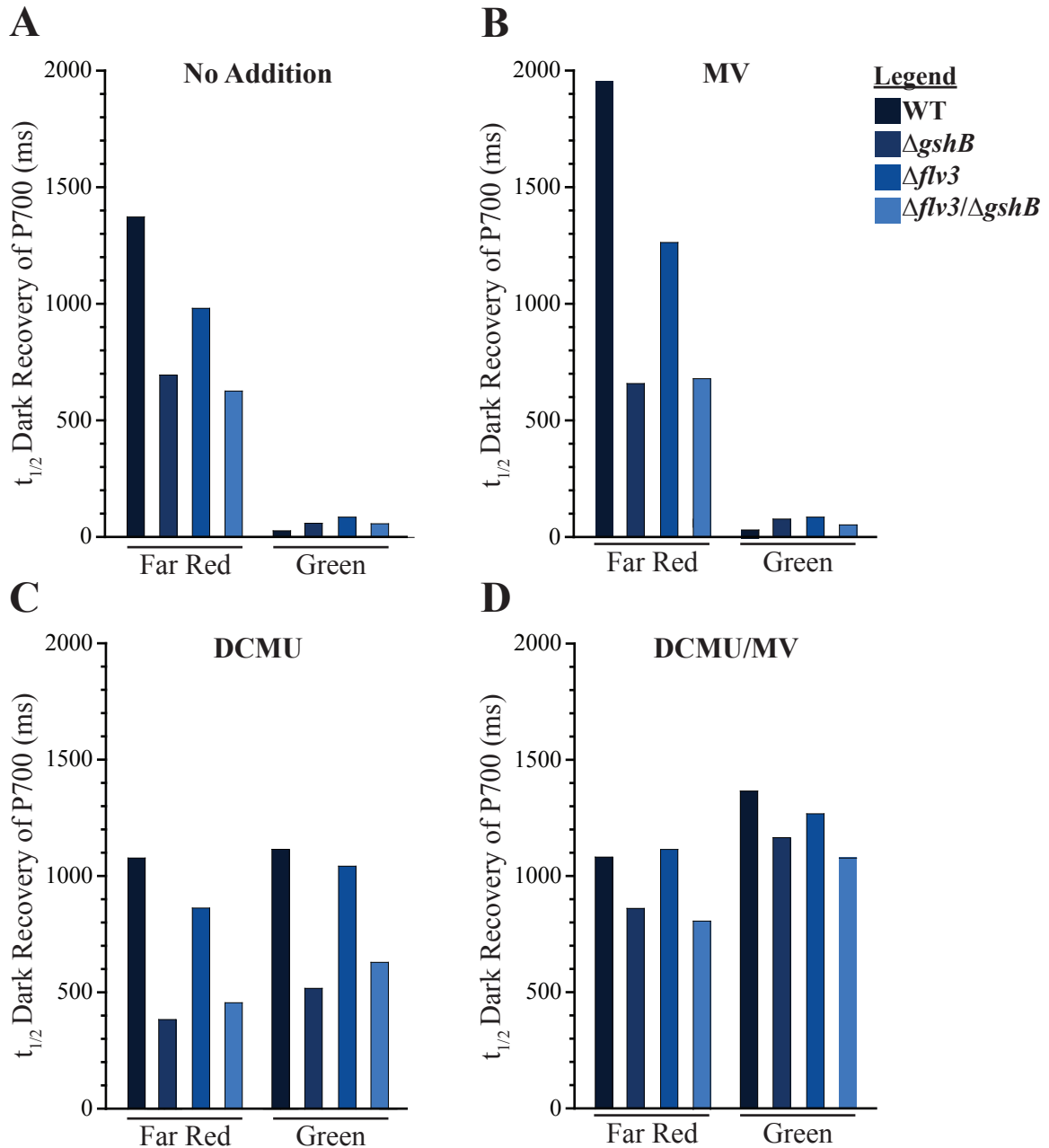


Figure 5. Rates of P700 dark recovery following far red or green illumination.

P700 recovery in the dark was measured at 705 nm following illumination with far red ($2500 \mu\text{mol photons m}^{-2} \text{s}^{-1}$) or green ($590 \mu\text{mol photons m}^{-2} \text{s}^{-1}$) actinic light for 10 s. Measurements were performed without any addition of inhibitors (A), with 1 mM MV (B), 20 μM DCMU (C) or with 1 mM MV and 20 μM DCMU (D). Cells were suspended in BG11 media at a chlorophyll concentration of 10 $\mu\text{g/ml}$ for all measurements.

Chapter 7
Conclusions and Future Directions

SUMMARY AND CONCLUSIONS

The goal of this work was to investigate mechanisms of redox homeostasis in photosynthetic organisms. Prior to this investigation, there was little information regarding the role of GSH in maintenance of redox homeostasis in cyanobacteria, organisms whose relatives are responsible for the advent of oxygenic photosynthesis and the development of GSH. Our findings have shed light on the role of GSH in redox homeostasis and acclimation to environmental perturbations in cyanobacteria. We found many factors influence the cellular GSH content, which in turn could dramatically influence the cellular redox environment. Our results also demonstrate that GSH is essential for protection from diverse species of ROS, despite the presence of many independent antioxidant systems.

Cellular GSH Content is Dynamic

GSH is a multifunctional molecule that has been recruited by many cellular pathways and processes. Among the many attributes of GSH is the ability to form a reversible disulfide bond with another GSH molecule to make glutathione disulfide (GSSG; Equation 1).



This reversible reduction:oxidation reaction allows the 2GSH/GSSG redox couple to function as a redox buffer. Moreover, the 2GSH/GSSG couple is thought to contribute significantly to the cellular redox environment (Schafer and Buettner, 2001). Importantly, the redox state of the 2GSH/GSSG couple is a factor of the ratio of

reduced:oxidized species and the molar concentration, or capacitance of the system. Therefore, changes in the amount of GSSG and in the total pool size can influence the cellular redox environment. We find that in *Synechocystis* 6803, the majority of the glutathione within the cell (>90%) is maintained in the GSH (reduced) form. However, our results also demonstrate the total amount of cellular GSH is not static. In fact, we find that the GSH levels can shift drastically following many environmental perturbations. This implies that the cellular redox environment also changes during these conditions. Further, proteins like glutaredoxin are able to relay information about the cellular redox state (Gutscher et al., 2008). These changes can influence cellular transcriptional profiles and also may influence cell cycle and cell fate decisions (Schafer and Buettner, 2001).

Photosynthetic organisms utilize light energy to generate ATP and reducing power needed for cellular metabolism. Therefore, it is not surprising that the transcriptional and metabolic profiles of cyanobacterial cells change in response to altered light levels and light quality (Hihara et al., 2001; Aurora et al., 2007; Singh et al., 2008; Singh et al., 2009). We found that the cellular GSH content is responsive to changes in light quality and light quantity (Chapter 1, Figure 5). In summary of these results, we find that conditions that lead to increased oxygen evolution and increased photosynthetic electron transport also result in increased cellular GSH content. We also found a correlation between changes in transcriptional regulation of GSH biosynthetic genes and cellular thiol content. Many genes have been shown to be differentially abundant upon

illumination of either photosystems I (PSI) or II (PSII) using orange-red or blue light, respectively (Singh et al., 2009). The expression of the *gshB* gene, encoding glutathione synthetase, is upregulated during illumination of PSII compared to PSI. We also found that GSH levels increase during PSII versus PSI illumination. Physiologically, illumination of PSII results in the production of O₂ by splitting of water and subsequent transfer of electrons through the photosynthetic electron transport chain to support growth. Similarly, we found the GSH levels increase dramatically following high light treatment, in agreement with the observation that sulfate uptake and demand increases during these conditions (Aurora et al., 2007). Both of these conditions lead to production of O₂, ATP and reducing equivalents and likely result in the production of ROS. In contrast, when cells were transferred to the dark or when PSI was preferentially illuminated with blue light, the cellular GSH content decreased. Both of these conditions do not support growth of *Synechocystis* 6803 and do not result in the production of O₂. To further dissect whether photosynthesis *per se* influences the observed changes in cellular thiol content, we also compared strains grown photoautotrophically (PA), photoheterotrophically (PH; glucose) and photomixotrophically (PM; glucose + DCMU). Our results suggest that PSII activity is crucial because we found that GSH levels increased in PM conditions upon addition of glucose, but not in PH conditions where glucose was provided but PSII was inhibited by DCMU (Chapter 2, Figure 6).

Our data demonstrates a correlation between growth and cellular GSH content. This likely reflects the fact that GSH biosynthesis and growth require ATP production and

reducing equivalents for assimilation of inorganic nutrients such as nitrate, sulfate and CO₂. In fact, coordination between these assimilatory processes are crucial during for the biosynthesis GSH (Kopriva and Rennenberg, 2004). We found a strong connection between availability of nitrate and sulfate and cellular GSH content. Strikingly, we found that cellular GSH content declined rapidly upon transfer to sulfate deplete medium (Chapter 2, Figures 7 and 9). This suggests that GSH is utilized as a nutrient reservoir, but also implies a change in the cellular redox status. In concordance with our previous findings, this rapid depletion of GSH also correlates with a decline in photosynthetic activity and growth rate. Upon sulfur repletion, we find that the GSH levels increase along with photosynthetic capacity and growth rate. We also subjected the $\Delta gshB$ mutant to sulfate depletion and repletion and found that this strain could not acclimate to these conditions. This emphasizes the essential nature of GSH during acclimation to environmental perturbations.

To probe the mechanism for depletion of cellular thiols during nutrient depletion, we generated a strain lacking γ -glutamyltranspeptidase (Ggt), an enzyme involved in glutathione degradation. However, analysis of the Δggt strain suggests that another pathway is involved in degradation of GSH following nutrient limitation. We found that the Δggt strain performed similarly to WT during sulfate starvation and GSH levels still decreased. However, we did find that the Δggt strain exhibited reduced fitness during stationary phase (Chapter 5, Figure 5 and 6) and apparently leaked more GSH into the culture medium (Chapter 5, Figure 7). These results suggest an important role for GSH

in maintenance of cellular fitness during stationary phase, a results supported by the finding that the $\Delta gshB$ mutant is less fit during stationary phase than the WT strain (Chapter 2, Figure S1 and S2).

Changes in light intensity and nutrient availability clearly influence the cellular thiol content by altering photosynthetic activity and substrate availability. We also find that the cellular GSH content could be modulated in other ways. For instance, we observed a significant increase in GSH content following addition of H_2O_2 to cells, a ROS species that is particularly reactive with cellular thiols (Chapter 2, Figure 4). Additionally, we showed that GSH content increases rapidly upon exposure to the antibiotic gentamicin (Chapter 3, Figure 1). In this case, however, we find an increase in GSH content corresponds to a decrease in growth rate. We suspect that this represents a rapid response to a formidable attack on cellular physiology that eventually ends up in death for the WT *Synechocystis* 6803 strain. Besides binding to and inhibiting ribosome function, aminoglycoside antibiotics stimulate the production of ROS that end up killing the cell (Kohanski et al., 2007; Kohanski et al., 2008; Dwyer et al., 2009; Kohanski et al., 2010). In a strain containing a gentamicin resistance cassette, we find that GSH is also a necessary component of antibiotic resistance (Chapter 4, Figure 2). We also found that growth in iron deplete conditions leads to increased GSH levels. Iron depletion can lead to production of increased ROS (Shcolnick et al., 2009). These results suggest that regardless of photosynthetic capacity or growth rate, certain conditions necessitate increased GSH content for protection of cellular components. Furthermore, our results

clearly demonstrate that GSH levels are not static, but highly responsive to multiple environmental stimuli in cyanobacteria.

GSH Protects Cells From Diverse ROS

Cyanobacteria are robust organisms capable of surviving in extreme conditions. This robustness is in part due to flexible metabolic networks that can quickly adjust to changing conditions (Singh et al., 2010; Wegener et al., 2010). Among the many strategies utilized by cyanobacteria to acclimate to a variety of harsh environments is a robust and extensive antioxidant network comprised of small molecules and proteins (Latifi et al., 2009). We find that despite the array of antioxidants available to the cell, GSH is critical for protection against a diverse set of ROS.

To facilitate our studies on the role of GSH, we generated a mutant that lacks the terminal step of GSH biosynthesis (Chapter 2, Figure 1). The $\Delta gshB$ mutant no longer makes GSH, but instead accumulates the precursor compound γ -EC (Chapter 2, Figure 2). The γ -EC molecule is structurally similar to GSH and can functionally replace GSH under some conditions. In fact, Halobacteria contain γ -EC as their major low-molecular weight thiol (Sundquist and Fahey, 1989). This is likely due to the differences in stability of γ -EC versus GSH. GSH is more resistant to metal induced oxidation than γ -EC, except in high salt environments such as the cytoplasm of halobacteria (Sundquist and Fahey, 1989). Therefore, the $\Delta gshB$ strain is partially sensitized, allowing us to probe conditions requiring GSH but not another similar thiol. It is possible that at one point in the

evolutionary history of cyanobacteria, γ -EC was the primary thiol. Cyanobacteria are credited with the evolution of GshA, the first enzyme in glutathione biosynthesis. However, evolution of GshB likely evolved independently many times, generating a more stable compound (Copley and Dhillon, 2002).

We subjected the $\Delta gshB$ strain to multiple different environmental and redox perturbations. We found that this strain is sensitive to diverse ROS (Chapter 1, Figure 3). This is significant because different ROS are formed through different mechanisms and are reactive with different cellular components. We found that the $\Delta gshB$ mutant was sensitive to hydrogen peroxide (H_2O_2), singlet oxygen (1O_2) and superoxide ($\cdot O_2$). The major site for production of $\cdot O_2$ is at the acceptor side of PSI where electrons reduce cytoplasmic redox carriers. Superoxide dismutase is an enzyme that participates in the metabolism of $\cdot O_2$ and generates H_2O_2 , which is metabolized by catalase and other peroxidases. Despite these other detoxification mechanisms, GSH is still absolutely essential for protection from these compounds. Furthermore, we found that GSH is required for protection from 1O_2 , a high-energy spin state of O_2 that can be quenched by carotenoids. We also found that the $\Delta gshB$ strain was extremely sensitive to Cd, a heavy metal that induces ROS formation in the cell by disrupting sulfur metabolism (Houot et al., 2007). These results implicate GSH as a basal antioxidant that has crucial functions despite many other cellular antioxidants, possibly by buffering dramatic cellular redox changes that disrupt the function of the enzymatic components.

Stability of Photosynthetic Reaction Centers and the Light Harvesting Complex

Optimization of photosynthesis begins with the ability of the cell to harvest and funnel light energy toward the photosystems. In cyanobacteria, this also requires precise positioning of the light harvesting antennae (phycobilisome) and stoichiometric balancing of the photosynthetic reaction centers. Adjustment of PSI to PSII stoichiometry is especially important during redox perturbations such as high light (Muramatsu et al., 2009). Downregulation of photosynthesis and energy metabolism is found to be important during many environmental and redox perturbations and likely represents a strategy to minimize damage induced by ROS during non-optimal conditions (Singh et al., 2010).

We find that GSH is involved in facilitating PSI stability during redox stress caused by application of the antibiotic gentamicin (Gm) (Chapter 4, Figure 4). Our results suggest that Fenton reactions involving PSI iron-sulfur clusters participate in the generation of ROS upon application of Gm. This result parallels the findings that in heterotrophic bacteria, TCA cycle enzymes are the likely source of iron-cluster centers involved in these reactions (Kohanski et al., 2007; Kohanski et al., 2008). While PSII is the source of O₂ within the photosynthetic cell, PSI is involved in driving high-energy electrons into the cytoplasmic space through solvent-exposed iron-sulfur clusters. Our results suggest that GSH may be involved in protection of PSI from ROS induced damage.

Besides altering photosystem stoichiometry, cyanobacteria are able to modulate the light-harvesting antenna complex (phycobilisome) to optimize photosynthesis. Expression of phycobilisomes is highly correlated with light levels, but is also highly regulated during many diverse perturbations (Singh et al., 2010). We found striking differences in the levels of phycocyanin (PC), the major pigment in the phycobilisome, between the WT and $\Delta gshB$ strains during many different experiments. In fact, the $\Delta gshB$ strain maintains a higher PC:Chl ratio under most conditions, but this difference is exaggerated during conditions such as high light (Chapter 6, Figure 4) and after extended growth into stationary phase (Chapter 1, Figure S3). While we have not identified a mechanism for this observation, we speculate that GSH or the cellular redox status could be involved in regulation of the phycobilisome. As support for this hypothesis, several phycobilisome subunits have been identified as targets of glutaredoxin in *Synechocystis* 6803 (Li et al., 2007).

Coordination Between Redox Pathways

Cyanobacteria are often faced with undesirable conditions to which they must acclimate or die. Strikingly, cyanobacteria are able to cope with many different perturbations due to their flexible metabolism. For instance, during conditions where reducing power is limited, cyanobacteria shift their metabolism in favor of utilizing alternative nitrogen sources that require less energy (Singh et al., 2008; Wegener et al., 2010). Therefore it is not surprising that many different pathways are involved in protection of the cell from ROS. We have shown the GSH is critical for this process in cyanobacteria. However,

we were surprised that the $\Delta gshB$ mutant did not exhibit reduced growth compared to the WT during exposure to high light. It is possible that during these conditions, many other pathways are involved in cellular protection during this condition (Singh et al., 2008). One pathway that is particularly interesting is the reduction of O_2 to H_2O . In cyanobacteria, flavodiiron proteins (Flv) catalyze this reaction using NADPH as an electron donor (Helman et al., 2003). Importantly, this reaction does not result in the formation of ROS. To determine whether GSH and Flv proteins cooperate to protect the cells from ROS, we generated and characterized the $\Delta gshB/\Delta flv3$ double mutant (Chapter 6). Initial results suggest some cooperativity between these pathways because growth of the double mutant is extremely reduced on solid media compared to the single mutants and WT strains (Chapter 6, Figure 2). However, our results also suggest that under the conditions tested, GSH contributes more than Flv to the observed phenotypes.

IMPLICATIONS OF THIS WORK

Redox Homeostasis

Overall, this work implies that the cellular redox environment is modulated under many different conditions. While the cellular redox environment can be modified by changes in the ratio of GSH:GSSG, we found that the levels of GSSG were maintained under 10% of the total pool during many different perturbations. We did find large differences in the total pool size during many different conditions. We were able to estimate the redox potential of the 2GSH/GSSG couple based on the quantification of the reduced species and an estimation of the cellular concentrations (Figure 1). We found that the 2GSH/GSSG redox state changed significantly during conditions that lead to decreased GSH levels. However, these estimates must be interpreted with caution. A major assumption for these calculations is the actual molar concentration of the reduced and oxidized species within the cell. To calculate this parameter, the cell volume must be accurately determined. In our estimates, we calculated the cell volume based on the measured diameter of the cell and assuming a perfect sphere. However, the actual cytoplasmic volume is most likely quite different from this estimation due to the packing of cellular components including the thylakoid membrane. Furthermore, small changes in the cell diameter can drastically change the cell volume and therefore, the GSH concentration. The 2GSH/GSSG couple is also influenced by temperature and pH. Therefore, it is difficult to accurately quantify this parameter. Recently, a redox sensitive GFP (roGFP) has been used to estimate the redox state of the GSH/2GSSG (Dooley et

al., 2004; Hanson et al., 2004; Cannon and Remington, 2006; Jiang et al., 2006; Meyer et al., 2007; Gutscher et al., 2008; Wolf et al., 2008; Meyer and Brach, 2009). However, to date this methodology has not been successfully applied to a photosynthetic organelle or cyanobacterial cell.

During our studies of the $\Delta gshB$ mutant, we found that this strain accumulates γ -EC to levels at least 4-fold higher than the WT strain accumulates GSH. While feedback inhibition of GshA by GSH has been well documented (Jez et al., 2004; Ashida et al., 2005), it is interesting to speculate whether the altered redox potential of γ -EC compared to GSH necessitates an increase in cellular concentration. While we have not directly measured the redox potential of γ -EC, estimations based on auto-oxidation in the presence of transition metals suggest that it is in between cysteine/cystine ($E_h = -160$ mV) and GSH/GSSG ($E_h = -240$ mV) (Sundquist and Fahey, 1989; Schafer and Buettner, 2001). It is possible that if regulation of γ -EC biosynthesis is not controlled, the cellular redox environment in the $\Delta gshB$ strain might be more reducing than in the WT.

Acclimation to Environmental Perturbations

Our results implicate GSH as a multifunctional and important molecule in cyanobacteria. Besides functioning as a redox buffer, it also functions in many other biochemical pathways. In fact, our results implicate GSH as a key intermediate in nitrogen and sulfur metabolism. It is possible that sulfate is assimilated into cysteine and then immediately conjugated into GSH. In accordance with this, we found that the intracellular cysteine

concentrations were maintained very low compared to GSH and γ -EC. During conditions when sulfate became limiting, the cellular GSH levels dropped drastically within several hours. During normal metabolism, it is possible that cysteine is constantly siphoned out of the GSH pool. This strategy would make sense because free cysteine can be toxic to the cell because it can participate in reducing transition metals and promoting Fenton chemistry and ROS induced cell damage (Park and Imlay, 2003). Moreover, we have recently shown that ROS are likely generated during many different genetic and environmental perturbations in cyanobacteria (Appendix I) (Singh et al., 2010). Therefore GSH likely plays a role in cellular protection during acclimation to many of these perturbations.

Metabolic Flexibility

When cells experience a perturbation, there is an initial response at the transcriptional level that eventually dampens over time. As the perturbation continues, the cells reach a metabolic homeostasis that is tuned to the new environment. This is true of a genetic and environmental perturbation. Upon deletion of the $\Delta gshB$ gene, the cells likely underwent a time of stress that dictated a rewiring of existing transcriptional networks. After a while, the strain adjusted to this challenge by making numerous metabolic changes. One change that we have directly measured is the increase in the PC:Chl ratio. While we are uncertain of all the implications of this change at the metabolic level, initial measurements suggest that this could result in increased non-photochemical quenching of PSII.

Our results imply that several pathways that utilize GSH must be able to function to a degree with only γ -EC. One pathway that is particularly interesting and intriguing is the interaction of GSH with iron-sulfur homeostasis in *Synechocystis* 6803. Recently, GSH was determined to be a ligand for an iron-sulfur cluster bound to a monothiol glutaredoxin in *Synechocystis* 6803 (Picciocchi et al., 2007; Iwema et al., 2009). We speculate that γ -EC could replace GSH in this role in the $\Delta gshB$ mutant. However, our results demonstrating that GSH facilitates PSI stability, while γ -EC doesn't, could suggest a defect in an iron-sulfur cluster regulatory pathway.

Photosynthetic Electron Transport

We previously found that the $\Delta gshB$ strain could not support PSI-mediated electron transport in the presence of electron donor/acceptor pairs in whole cells. However, we found that PSI activity was higher in isolated membranes of the $\Delta gshB$ strain compared to the WT. In order to fully understand this phenomenon, we have currently begun to analyze photosynthetic electron transport reactions in vivo using a pulse-probe spectrophotometer. Using this technique, we can monitor the redox state of the PSI P700 reaction center during actinic illumination and upon transfer to the dark. During illumination, P700 is oxidized to the radical cation, P700⁺. When the light is turned off, P700⁺ is reduced back to P700. The steady state levels of the P700/P700⁺ redox couple reflect the rate of electron flow into and out of PSI. We found that the rate of dark recovery of P700 was significantly faster in the $\Delta gshB$ strain compared to the WT during conditions when electron transport from PSII was blocked (Chapter 6, Figure 5). These

results imply a difference in the amount of electrons upstream of PSI and could suggest differences in linear vs. cyclic electron flow between these strains. However, further studies are necessary to fully characterize the mechanism behind the observation.

The role of GSH in Diazotrophic Cyanobacteria

Synechocystis 6803 is a unicellular cyanobacterium that is able to assimilate nitrate from the environment. There are other classes of cyanobacteria that are able to assimilate nitrate from the environment and fix atmospheric dinitrogen (N_2) into ammonia (NH_3). Among the nitrogen fixing cyanobacteria, *Cyanothece* are interesting because they are able to fix N_2 within a single cell. This is remarkable because the nitrogenase enzyme that catalyzes this reaction is very sensitive to oxygen, a byproduct of oxygenic photosynthesis. Therefore, *Cyanothece* separate photosynthesis and nitrogen fixation diurnally. This separation requires strict coordination of metabolic processes that can be seen at the transcriptional and protein level in *Cyanothece* 51142 (Stöckel et al., 2008; Stockel et al., 2011). Compared to *Synechocystis* 6803, many more redox reactions are occurring during the night in *Cyanothece* to provide reducing equivalents and ATP used in nitrogen fixation. Therefore, it is likely that GSH could play a critical role in *Cyanothece* during the diurnal cycle. In fact, the genes involved in GSH biosynthesis and degradation exhibit robust diurnal oscillations (Figure 2). Interestingly, the genes involved in glutathione degradation are co-regulated with the genes involved in biosynthesis. Also noticeable is the upregulation of the biosynthetic genes at night. Perhaps this is in anticipation of the oncoming light reactions that provide reducing

power for assimilation of nutrients such as sulfur. Recently, *Cyanothece* 51142 has been found to exhibit significant rates of nitrogenase-mediated H₂ production under aerobic conditions (Bandyopadhyay et al., 2010). There are likely many different redox related processes essential for this observation that await discovery.

FUTURE DIRECTIONS

Glutathione is a multifunctional molecule that functions not only as a redox buffer and antioxidant, but also in numerous other metabolic pathways. Over time, many specialized processes have been built on the chemistry of GSH. This is especially true in photosynthetic organisms such as plants. While the research presented in this work has shed light on many aspects of GSH in cyanobacteria, there are still many unanswered questions.

As implied in other sections, the redox state of the GSH/GSSH couple contributes to the cellular redox environment. However, it is notoriously challenging to accurately measure this parameter *in vivo*. Even more challenging are dynamic measurements of the cellular redox potential. These are the types of changes that can turn on signaling cascades and influence cellular physiology. Rapid and accurate measurements of the cellular redox environment could allow one to analyze specific redox circuits and networks within the photosynthetic cell. There has been some promising research on this topic using redox sensitive GFP (roGFP), however, there are still many hurdles before this technology can be utilized to estimate the redox state of a photosynthetic cell.

Beyond cellular measurements of cellular redox poise, there are many open questions as to what processes are directly regulated by GSH. In one scenario, a protein can be regulated through equilibration with a specific redox couple such as in the case with the

thioredoxin system. Alternatively, many proteins have been shown to be glutathionylated. While there have been some targets of glutaredoxin identified in *Synechocystis* 6803 (Li et al., 2007), the physiological relevance of these targets have not been verified. One area that is of importance is the regulation of the light-harvesting antennae. We find that the PC:Chl ratio is consistently altered in the $\Delta gshB$ mutant compared to the WT strain. As several subunits of the phycobilisome were identified as targets of glutaredoxin, we speculated that this process could be regulated by GSH or by the redox state of the cell. However, these hypotheses need to be tested using rigorous biochemical methods.

During our analysis, we predicted that the γ -glutamyltranspeptidase enzyme was responsible for the degradation of cellular GSH during nitrate and sulfate depletion. However, analysis of Δggt mutants suggest otherwise. Recently, a *ggt* independent pathway was shown to be important for GSH degradation in plants (Ohkama-Ohtsu et al., 2008). However, although activity for the first enzyme in the pathway could be detected in plants, the gene product has not yet been identified. We hypothesize that a similar pathway is utilized in *Synechocystis* 6803 during nutrient depletion. This pathway involves a γ -glutamylcyclotransferase (*ggc*) and a 5-oxoprolinase. While there is a gene annotated as a 5-oxoprolinase in the *Synechocystis* 6803 genome, a *ggc* gene has not been identified. Characterization of this pathway could have significant implications in the fields of plant biology and photosynthesis.

Finally, our results suggest that GSH modulates photosynthetic electron transport mechanisms. We found that P700 recovery rates in the dark are altered in the $\Delta gshB$ mutant. These results could imply a difference in linear vs. cyclic electron transport pathways. Balancing photosynthetic electron transport with metabolic pathways is crucial for survival. It is possible that GSH is involved in regulation of this process in cyanobacterial and other photosynthetic organisms. However, further studies will be required to test this hypothesis.

REFERENCES

- Ashida H, Sawa Y, Shibata H** (2005) Cloning, biochemical and phylogenetic characterizations of γ -glutamylcysteine synthetase from *Anabaena* sp. PCC 7120. *Plant Cell Physiol* **46**: 557-562
- Aurora R, Hihara Y, Singh A, Pakrasi H** (2007) A Network of Genes Regulated by Light in Cyanobacteria. *OMICS* **11**: 166-185
- Bandyopadhyay A, Stockel J, Min H, Sherman LA, Pakrasi HB** (2010) High rates of photobiological H₂ production by a cyanobacterium under aerobic conditions. *Nat Commun* **1**: 139
- Cannon MB, Remington SJ** (2006) Re-engineering redox-sensitive green fluorescent protein for improved response rate. *Protein Sci* **15**: 45-57
- Copley SD, Dhillon JK** (2002) Lateral gene transfer and parallel evolution in the history of glutathione biosynthesis genes. *Genome Biol* **3**: 25.1-25.16
- Dooley CT, Dore TM, Hanson GT, Jackson WC, Remington SJ, Tsien RY** (2004) Imaging dynamic redox changes in mammalian cells with green fluorescent protein indicators. *J Biol Chem* **279**: 22284-22293
- Dwyer DJ, Kohanski MA, Collins JJ** (2009) Role of reactive oxygen species in antibiotic action and resistance. *Curr Opin Microbiol* **12**: 482-489
- Gutscher M, Pauleau A, Marty L, Brach T, Wabnitz G, Samstag Y, Meyer A, Dick T** (2008) Real-time imaging of the intracellular glutathione redox potential. *Nat Methods* **5**: 553-559

- Hanson GT, Aggeler R, Oglesbee D, Cannon M, Capaldi RA, Tsien RY, Remington SJ** (2004) Investigating mitochondrial redox potential with redox-sensitive green fluorescent protein indicators. *J Biol Chem* **279**: 13044-13053
- Helman Y, Tchernov D, Reinhold L, Shibata M, Ogawa T, Schwarz R, Ohad I, Kaplan A** (2003) Genes encoding A-type flavoproteins are essential for photoreduction of O₂ in cyanobacteria. *Curr Biol* **13**: 230-235
- Hihara Y, Kamei A, Kanehisa M, Kaplan A, Ikeuchi M** (2001) DNA microarray analysis of cyanobacterial gene expression during acclimation to high light. *Plant Cell* **13**: 793-806
- Houot L, Floutier M, Marteyn B, Michaut M, Picciocchi A, Legrain P, Aude J-C, Cassier-Chauvat C, Chauvat F** (2007) Cadmium triggers an integrated reprogramming of the metabolism of *Synechocystis* PCC6803, under the control of the Slr1738 regulator. *BMC Genomics* **8**: 350
- Iwema T, Picciocchi A, Traore DAK, Ferrer J-L, Chauvat F, Jacquamet L** (2009) Structural basis for delivery of the intact [Fe₂S₂] cluster by monothiol glutaredoxin. *Biochemistry* **48**: 6041-6043
- Jez JM, Cahoon RE, Chen S** (2004) *Arabidopsis thaliana* glutamate-cysteine ligase: functional properties, kinetic mechanism, and regulation of activity. *J Biol Chem* **279**: 33463-33470
- Jiang K, Schwarzer C, Lally E, Zhang S, Ruzin S, Machen T, Remington SJ, Feldman L** (2006) Expression and characterization of a redox-sensing green

- fluorescent protein (reduction-oxidation-sensitive green fluorescent protein) in Arabidopsis. *Plant Physiol* **141**: 397-403
- Kohanski MA, Dwyer DJ, Collins JJ** (2010) How antibiotics kill bacteria: from targets to networks. *Nat Rev Microbiol* **8**: 423-435
- Kohanski MA, Dwyer DJ, Hayete B, Lawrence CA, Collins JJ** (2007) A common mechanism of cellular death induced by bactericidal antibiotics. *Cell* **130**: 797-810
- Kohanski MA, Dwyer DJ, Wierzbowski J, Cottarel G, Collins JJ** (2008) Mistranslation of membrane proteins and two-component system activation trigger antibiotic-mediated cell death. *Cell* **135**: 679-690
- Kopriva S, Rennenberg H** (2004) Control of sulphate assimilation and glutathione synthesis: interaction with N and C metabolism. *J Exp Bot* **55**: 1831-1842
- Latifi A, Ruiz M, Zhang C-C** (2009) Oxidative stress in cyanobacteria. *FEMS Microbiol Rev* **33**: 258-278
- Li M, Yang Q, Zhang L, Li H, Cui Y, Wu Q** (2007) Identification of novel targets of cyanobacterial glutaredoxin. *Arch Biochem Biophys* **458**: 220-228
- Meyer AJ, Brach T** (2009) Dynamic Redox Measurements with Redox-Sensitive GFP in Plants by Confocal Laser Scanning Microscopy. *Methods Mol Biol* **479**: 1-15
- Meyer AJ, Brach T, Marty L, Kreye S, Rouhier N, Jacquot J-P, Hell R** (2007) Redox-sensitive GFP in *Arabidopsis thaliana* is a quantitative biosensor for the redox potential of the cellular glutathione redox buffer. *Plant J* **52**: 973-986

- Muramatsu M, Sonoike K, Hihara Y** (2009) Mechanism of downregulation of photosystem I content under high-light conditions in the cyanobacterium *Synechocystis* sp. PCC 6803. *Microbiology* **155**: 989-996
- Ohkama-Ohtsu N, Oikawa A, Zhao P, Xiang C, Saito K, Oliver DJ** (2008) A γ -glutamyl transpeptidase-independent pathway of glutathione catabolism to glutamate via 5-oxoproline in *Arabidopsis*. *Plant Physiol* **148**: 1603-1613
- Park S, Imlay J** (2003) High Levels of Intracellular Cysteine Promote Oxidative DNA Damage by Driving the Fenton Reaction. *J Bacteriol* **185**: 1942-1950
- Picciochi A, Saguez C, Boussac A, Cassier-Chauvat C, Chauvat F** (2007) CGFS-type monothiol glutaredoxins from the cyanobacterium *Synechocystis* PCC6803 and other evolutionary distant model organisms possess a glutathione-ligated [2Fe-2S] cluster. *Biochemistry* **46**: 15018-15026
- Schafer FQ, Buettner GR** (2001) Redox environment of the cell as viewed through the redox state of the glutathione disulfide/glutathione couple. *Free Radic Biol Med* **30**: 1191-1212
- Shcolnick S, Summerfield TC, Reytman L, Sherman LA, Keren N** (2009) The mechanism of iron homeostasis in the unicellular cyanobacterium *Synechocystis* sp. PCC 6803 and its relationship to oxidative stress. *Plant Physiol* **150**: 2045-2056
- Singh A, Elvitigala T, Bhattacharyya-Pakrasi M, Aurora R, Ghosh B, Pakrasi H** (2008) Integration of carbon and nitrogen metabolism with energy production is

crucial to light acclimation in the cyanobacterium *Synechocystis*. *Plant Physiol* **148**: 467-478

Singh AK, Bhattacharyya-Pakrasi M, Elvitigala T, Ghosh B, Aurora R, Pakrasi HB (2009) A systems-level analysis of the effects of light quality on the metabolism of a cyanobacterium. *Plant Physiol* **151**: 1596-1608

Singh AK, Elvitigala T, Cameron JC, Ghosh BK, Bhattacharyya-Pakrasi M, Pakrasi HB (2010) Integrative analysis of large scale expression profiles reveals core transcriptional response and coordination between multiple cellular processes in a cyanobacterium. *BMC Syst Biol* **4**: 105

Stockel J, Jacobs JM, Elvitigala TR, Liberton M, Welsh EA, Polpitiya AD, Gritsenko MA, Nicora CD, Koppenaar DW, Smith RD, Pakrasi HB (2011) Diurnal rhythms result in significant changes in the cellular protein complement in the cyanobacterium *Cyanothece* 51142. *PLoS One* **6**: e16680

Stöckel J, Welsh EA, Liberton M, Kunnvakkam R, Aurora R, Pakrasi HB (2008) Global transcriptomic analysis of *Cyanothece* 51142 reveals robust diurnal oscillation of central metabolic processes. *Proc Natl Acad Sci USA* **105**: 6156-6161

Sundquist A, Fahey R (1989) The function of gamma-glutamylcysteine and bis-gamma-glutamylcysteine reductase in *Halobacterium halobium*. *J Biol Chem* **264**: 719-725

Wegener KM, Singh AK, Jacobs JM, Elvitigala TR, Welsh EA, Keren N, Gritsenko MA, Ghosh BK, Camp DG, Smith RD, Pakrasi HB (2010) Global proteomics

reveal an atypical strategy for carbon/nitrogen assimilation by a cyanobacterium under diverse environmental perturbations. *Mol Cell Proteomics* **9**: 2678-2689

Wolf AM, Asoh S, Ohsawa I, Ohta S (2008) Imaging mitochondrial redox environment and oxidative stress using a redox-sensitive fluorescent protein. *J Nippon Med Sch* **75**: 66-67

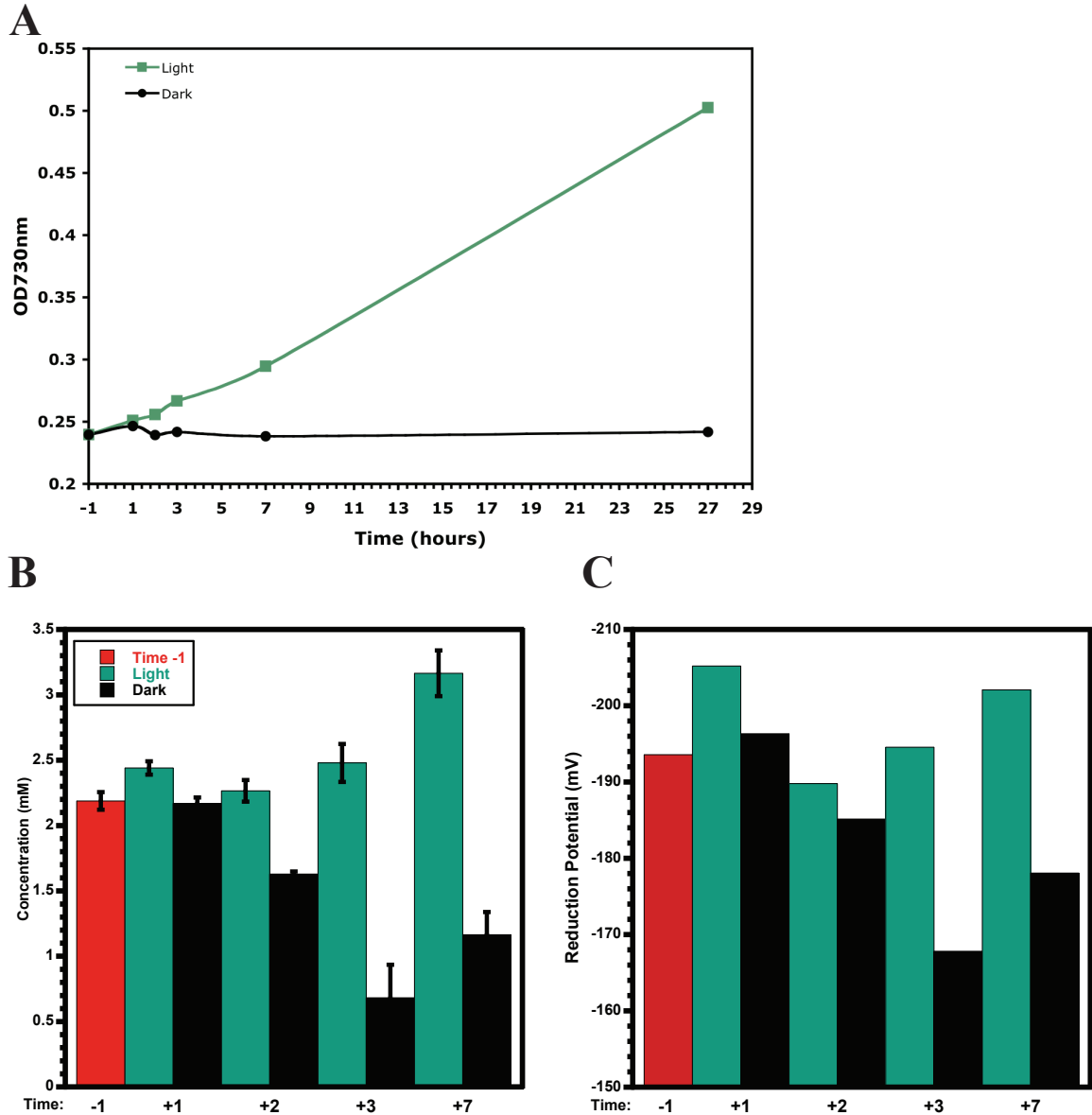


Figure 1. Growth, GSH content and estimation of 2GSH/GSSG redox potential.

WT *Synechocystis* 6803 cells were transferred from continuous light into either continuous light or dark (A). At specific time points, cells were harvested for measurement of GSH and GSSG by the GR-DTNB recycling assay (B). The reduction potential of the 2GSH/GSSG couple at 30°C, pH 7.0 was calculated using the Nernst equation (C).

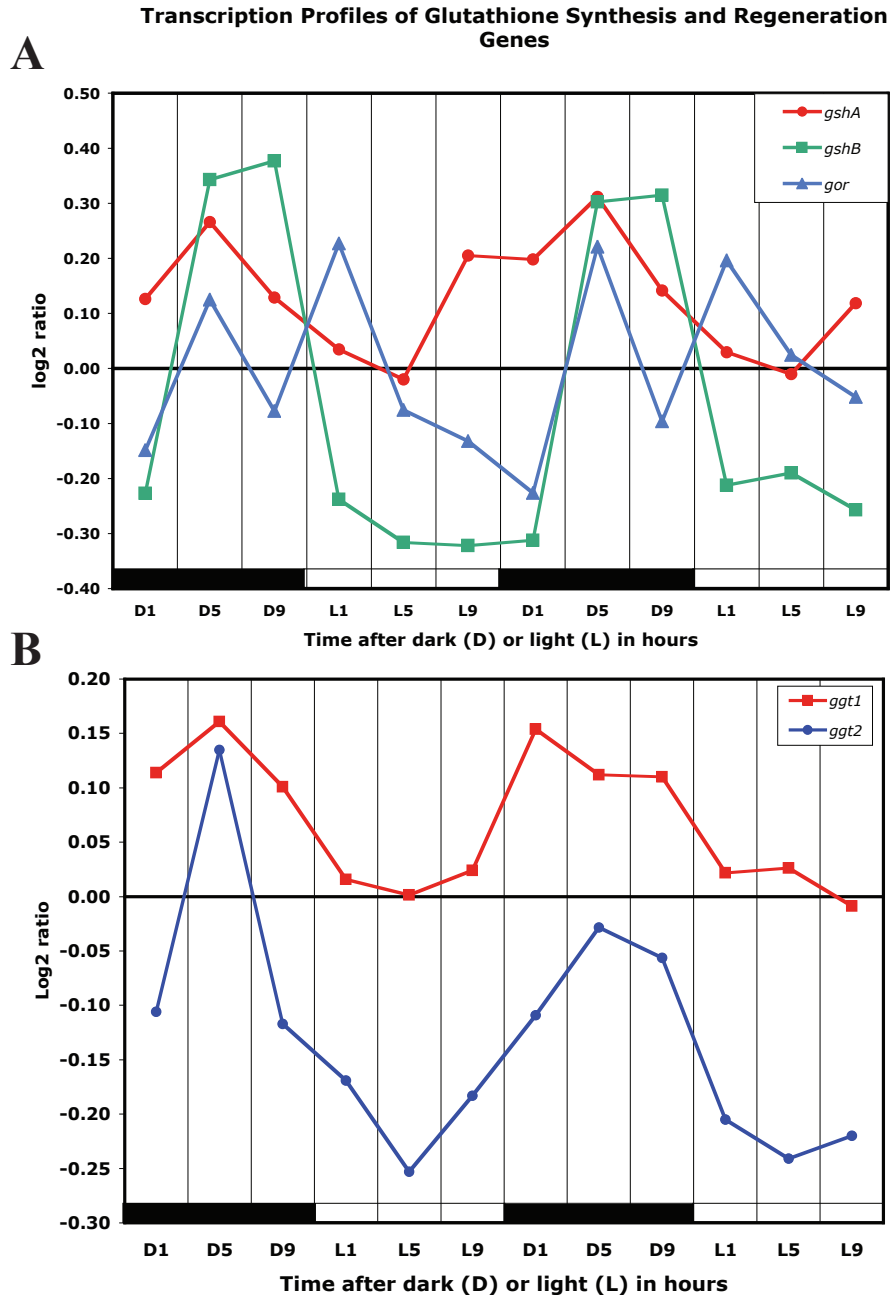


Figure 2. Diurnal regulation of transcripts involved in GSH metabolism in *Cyanothece* 51142.

(A). Expression profile of genes involved in GSH biosynthesis and redox cycling. GshA and GshB catalyze the biosynthesis of GSH, while glutathione reductase (Gor) maintains the GSH/GSSG redox state. (B) Expression profile of the two γ -glutamyltranspeptidase (*ggt*) genes encoded in the *Cyanothece* 51142 genome. Ggt is involved in GSH degradation.

Appendix I

Integrative Analysis of Large Scale Expression Profiles Reveals Core Transcriptional Response and Coordination between Multiple Cellular Processes in a Cyanobacterium

Adapted from:

Abhay K Singh, Thanura Elvitigala, Jeffrey C Cameron, Bijoy Ghosh, Maitrayee Bhattacharyya-Pakrasi, Himadri B Pakrasi (2010). Integrative Analysis of Large Scale Expression Profiles Reveals Core Transcriptional Response and Coordination between Multiple Cellular Processes in a Cyanobacterium. *BMC Sys Biol* 4: 105

All supplemental material can be found at:

<http://preview.biomedcentral.com/1752-0509/4/105/additional>

Gene expression database can be accessed at:

http://www.fibr.wustl.edu/synecho6803_database/

SUMMARY

Cyanobacteria are the only known prokaryotes capable of oxygenic photosynthesis. They play significant roles in global biogeochemical cycles and carbon sequestration, and have recently been recognized as potential vehicles for production of renewable biofuels. *Synechocystis* sp. PCC 6803 has been extensively used as a model organism for cyanobacterial studies. DNA microarray studies in *Synechocystis* have shown varying degrees of transcriptome reprogramming under altered environmental conditions. However, it is not clear from published work how transcriptome reprogramming affects pre-existing networks of fine-tuned cellular processes.

We have integrated 163 transcriptome data sets generated in response to numerous environmental and genetic perturbations in *Synechocystis*. Our analyses show that a large number of genes, defined as the core transcriptional response (CTR), are commonly regulated under most perturbations. The CTR contains nearly 12% of *Synechocystis* genes found on its chromosome. The majority of genes in the CTR are involved in photosynthesis, translation, energy metabolism and stress protection. Our results indicate that a large number of differentially regulated genes identified in most reported studies in *Synechocystis* under different perturbations are associated with the general stress

response. We also find that a majority of genes in the CTR are coregulated with 25 regulatory genes. Some of these regulatory genes have been implicated in cellular responses to oxidative stress, suggesting that reactive oxygen species are involved in the regulation of the CTR. A Bayesian network, based on the regulation of various KEGG pathways determined from the expression patterns of their associated genes, has revealed new insights into the coordination between different cellular processes.

We provide here the first integrative analysis of transcriptome data sets generated in a cyanobacterium. This compilation of data sets is a valuable resource to researchers for all cyanobacterial gene expression related queries. Importantly, our analysis provides a global description of transcriptional reprogramming under different perturbations and a basic framework to understand the strategies of cellular adaptations in *Synechocystis*.

INTRODUCTION

Genomic scale measurements of cellular components such as RNA, protein, and metabolites have been instrumental in unraveling the complexity of cellular functions in *E. coli*, yeast and other model organisms [1-9]. One group of organisms, namely cyanobacteria, lag behind in the use of these technologies, despite its evolutionary, ecological, environmental and biotechnological importance. Cyanobacteria are the only known prokaryotes capable of oxygenic photosynthesis and they play a significant role in global biogeochemical cycles [10]. It is estimated that cyanobacteria may be responsible for more than half the total primary production essential for sustaining life on Earth [11]. These organisms are credited with the transition of the Earth's atmosphere from an anaerobic state to the aerobic condition, the evolution of planetary primary production, and as being the progenitor of chloroplasts in higher plants [12-14].

A systems level understanding of changes in cellular components, and coordination among elaborate networks of fine-tuned cellular processes in cyanobacteria is of the utmost importance for many reasons. For example, cyanobacteria have recently attracted significant interest due to its crucial role in carbon capture, and its ability to produce renewable carbon-neutral biofuels. Additionally, cyanobacteria are good model systems to understand the impact of changing conditions on an organism's physiology. This is because cyanobacteria have successfully survived broad changes in environment including temperature, pH, nutrient availability, redox, CO₂ and O₂ throughout evolution

[15]. Similarly, the exquisite dependence of these organisms on sunlight for the generation of energy for their entire metabolism necessitates constant modifications of the cellular machinery, such that light energy can be efficiently harvested under natural conditions. These characteristics have enabled cyanobacteria to acquire diverse arrays of physiological characteristics which are necessary for survival under changing environmental conditions. Identification of key factors and understanding their role in the acquisition of phenotypic states under changing environmental conditions has been an active area of research in cyanobacteria for many years. Among cyanobacterial strains, *Synechocystis* sp. PCC 6803 (hereafter *Synechocystis*) has been extensively used as an experimental organism for physiological, biochemical and molecular studies. The availability of the *Synechocystis* genome sequence, the first cyanobacterium and the third prokaryote to be sequenced [16], has allowed a spurt of large scale studies on measurements of RNA and proteins in this model organism.

Numerous gene expression data sets for *Synechocystis* under diverse environmental and genetic conditions (see additional file 1) have accumulated in the literature and public databases. However, these transcriptome studies in *Synechocystis* have not led to a full understanding of the interactions between cellular processes required to maintain a steady internal state (homeostasis) for optimal function and growth. A major reason for this is related to the use of a random cut-off approach in most studies to identify differentially regulated genes. As a result, genes with low transcript abundance or showing small changes in transcripts levels have not been identified in most of these studies. The

importance of the identification of such genes is being increasingly recognized, because organisms have stronger constraints on their expression patterns due to their involvement in crucial cellular functions [17]. Additionally, recent studies have shown that transcriptome reprogramming plays a central role in the acquisition of a phenotypic state under specific perturbations [1, 8, 18-20]. Thus, identification of all differentially regulated genes in *Synechocystis*, regardless of the amplitude of changes in transcript levels, is very important to understand cellular strategies when cells are perturbed.

Significant insights on integrated cellular response from omics data sets, especially transcriptomics, have been obtained by the integration of data sets generated under diverse genetic and environmental perturbations [4-7, 9, 21-23]. Such an approach offers many advantages over studies involving a single perturbation. For example, integration of data sets readily allows identification of genes with low transcript abundance or small changes in transcripts levels. Additionally, stress-specific and general responses can also be identified by the integration of data sets. The availability of large data sets also makes it possible to derive a realistic, systems level network based on the regulation of metabolic pathways identified from the expression patterns of their associated genes. Such a network provides the framework to identify coordination and interactions between various cellular processes under different perturbations, and is key to an overall understanding of how various cellular functions coordinate to develop appropriate adaptation strategies. In this study, we have integrated transcriptomics data sets obtained from *Synechocystis* under 163 different environmental and genetic perturbations. This has

led to the identification of genes differentially regulated in response to most perturbations. Furthermore, availability of large data sets enabled us to generate a Bayesian network based on KEGG pathways which has provided insights into the interactions among cellular pathways.

MATERIALS AND METHODS

Collection of transcriptomics data sets

A total of 163 DNA microarray data sets were obtained from different sources. These include 86, 33 and 45 experiments from NCBI-GEO [49], KEGG expression [50] and from individual authors of the related literatures (additional file 1), respectively. These data sets were generated using either environmental perturbations (95) or genetic modifications (69). The environmental perturbations include changes in light quantity and quality, oxidative stress, osmotic stress, high temperature, nutrients availability, treatments with DCMU and DBMIB. The additional file 1 provides the details of all environmental and genetic perturbations.

Identification of gene- and pathway-levels behaviors

Raw data were processed using the robust version of LOWESS normalization [24]. The resulting values were used for subsequent computational analyses. For some data sets, we did not have access to the raw data and in those cases, the normalized data from the corresponding analyses were utilized.

To avoid the effects of local technical and biological variations, the differential behaviors of any individual gene were identified using statistical significance tests only. The level of shift in the sample means of replicates of individual gene expressions in each experiment was quantified using one sample KS-test [43]. In KS-test, we determine

whether the observed log-ratio values were significantly different from a distribution with a zero mean. If the null hypothesis was rejected at a significance level of 5%, that gene was assigned +1 or -1 depending on whether the mean value was > 0 or < 0 , representing an up and down regulation, respectively. If the null hypothesis could not be rejected, we assigned that gene a value 0, indicating that it was not differentially expressed.

To obtain function level behaviors, genes were grouped based on their KEGG metabolic pathway classifications. For any given KEGG pathway, expression of individual genes were considered as population and pathways were assigned one of the three states (+1, 0 or -1) based on the KS-test. We further considered the number of genes in individual pathways and the percentage of differentially expressed conditions to select 51 pathways for further analysis.

Gene regulatory network

A co-expression network was generated to identify the regulatory genes that are co-expressed with the CTR genes. Similarity between expression patterns of the CTR and regulatory genes was measured using the Hamming distance [51]. Expression patterns that agree more than 60% of times were identified and connections were drawn between corresponding genes.

Derivation of associations between metabolic pathways using the Bayesian network approach

Selected 51 KEGG pathways were modeled using the Bayesian network approach. The Bayesian networks are graphical models representing the probabilistic relationships between different factors and have been extensively used in numerous fields [52]. The Bayesian Information Criteria (BIC) was used as performance measure in evaluating possible network structures. BIC is defined as,

$$BIC(S/D) = \log_2 P(D/\hat{\theta}_s, S) - \log_2(M) \times size(S)/2$$

where S is the structure of the network defining the nodes and the links between the nodes; θ_s is the set of estimated parameters; D is the observed data given as an $M \times N$ matrix with N as the number of nodes (pathways) and M as the number of observations (experiments). The network structure was discovered using the Greed Equivalence Search (GES) algorithm [53]. GES resulted in a network with a higher score compared to several other algorithms. More details of computational steps are provided in Elvitigala et al., [54].

Determination of Regulatory Links Strength: To quantify the connection strengths of different links in the network, we used the ‘True Link Strength Percentage’, introduced by [55]. True link strength percentage measures the reduction of uncertainty on the state of the child node due to knowledge of the state of a parent node. It is computed as the

ratio between reduction in entropy of the child node given the parent node and the original entropy of the child node.

Network Inference for Different Experimental Conditions: We used the ‘Junction Tree’ algorithm to perform Network inference as previously described [44]. For this purpose, we fed the states of one or more pathways, which are expected to get significantly affected by the given experiment condition, as evidence to the network, and the changes in probabilities of other nodes are evaluated.

RESULTS AND DISCUSSION

Analysis of the *Synechocystis* transcriptome under multiple perturbations

We initiated an examination of adaptation strategies in *Synechocystis* to various stress conditions by integrating transcriptome data sets from 163 environmental and genetic perturbations. These data sets were obtained from various public sources (see Methods for details). The complete description of experimental conditions, source(s) of transcriptome data sets and relevant references are provided in the additional file 1. Integration of transcriptome data sets obtained using differing microarray platforms/laboratories was challenging from a data analysis perspective. In addition, physiological conditions of *Synechocystis* cells in several of the studies under normal conditions as well as after the exposure to perturbations were not documented. This further complicated our analysis. We reasoned that if the adaptation strategies employed by *Synechocystis* under different perturbations are robust, it should be possible to identify them despite the above mentioned technical and biological challenges. Our analysis framework included normalization of raw data using a robust version of LOWESS [24], and the identification of differentially regulated genes using a statistical significance test on log-transformed ratios of changes in gene expression between cells under control and perturbed conditions. The amplitude of changes in transcript levels was ignored, largely because such changes are subject to the magnitude of the perturbations both in intensity and duration. For example, expression of heat shock proteins (HSPs) responds immediately to changes in increased growth temperature, whereas, for the same genes,

the response to changes in nutritional deficiency may be slower. In addition, the unknown physiological conditions of cells make selection of differentially regulated genes based solely on the amplitude of transcript level meaningless. We discretized the regulation of differentially expressed genes into three levels; upregulated (+1), downregulated (-1) and not regulated (0), such that the final conclusion is not biased by the contribution of individual experiments. This step was performed for each experiment separately to ensure that the analysis was independent of technical variations. We also removed genes present on the six plasmids in *Synechocystis* from further analysis because data on the regulation of plasmid encoded genes has been mostly studied only in our lab [25]. All 163 transcriptome data sets were considered for pathway-level analyses whereas gene-level analyses were based on 68 data sets due to the availability of sufficient number of replicates allowing statistical significance test of the data sets.

We could identify all but five genes (3259/3264) present on the *Synechocystis* chromosome that show differential regulation in at least one study (Fig. 1; additional files 2 and 3). As expected, integration of data sets readily allowed a separation of stress-specific genes from general-stress response. The comparative analysis of differentially regulated genes shows that a large number of genes respond in a stress-specific manner, showing differential expression that was limited to one or a group of stress conditions. These genes may play a direct role under a given perturbation or under certain conditions that have similar effects on cell physiology. It is also quite possible that a fraction of these stress-specific genes are identified purely based on the noise and/or technical issues

associated with the individual study. Nonetheless, we expect that compilation of the transcriptome data sets in the present study will be a useful resource towards understanding the functional roles of gene products in *Synechocystis* as well as in the functional annotation of hypothetical and unknown genes. We encourage readers to explore the regulation of genes provided in the additional file 2. We have found the transcriptome data sets useful in many ways. For example, one can easily identify genes or cellular processes that are specifically regulated in response to a certain stress.

Further analysis of the *Synechocystis* transcriptome shows that, a large number of genes were differentially regulated under a majority of perturbations. We could identify approximately 12% (399) of *Synechocystis* chromosomal genes that show differential regulation in more than 50% of transcriptome data sets (additional file 4). Since these genes exhibit consistent differential regulation in the majority of perturbations, we have designated these genes collectively as the ‘core transcriptional response (CTR)’ in *Synechocystis*. Expression of the CTR under diverse conditions attests to its significant role in adaptation strategies. In addition, regulation of the CTR is much more significant when only data sets obtained under environmental perturbations are examined. The regulation of the CTR in at least half of the perturbations suggests that changes in transcript levels of these genes may not be directly related to the primary stress but are secondary effects. In this scenario, it is likely that a combination of stress-specific and the CTR genes highlight the uniqueness of each transcriptional program utilized to choose a suitable phenotypic state under a given perturbation. Of the 399 genes, the majority are

involved in the photosynthetic process (79 genes), transcription and translation (30 genes), energy metabolism (22 genes), HSPs (10 genes), and nitrogen metabolism (8 genes). The remaining genes in the CTR encode proteins involved in other processes (79 genes) and for unknown functions (165 genes). Below, we provide a short description of the major processes present in the CTR and describe the impact of their regulation on the adaptation strategies during various perturbations.

Photosynthesis: All organisms need chemical energy for metabolic activities. For *Synechocystis*, photosynthesis is the sole source to generate chemical energy under photoautotrophic conditions. For this reason, there is a tight connection between the activity of the photosynthetic process and other principal metabolic pathways. It is not surprising therefore that photosynthesis was one of the major cellular functions represented in the CTR. More than 60% of all photosynthesis genes in *Synechocystis* were present in the CTR and they were downregulated across most perturbations. Of the various functional complexes, genes involved in ATP synthase (all genes), CO₂ fixation, phycobilisome, PSI and PSII were most affected under different perturbations. There were fewer genes encoding NAD dehydrogenase in the CTR and their regulation did not follow the pattern similar to the regulation of other photosynthetic complexes. In addition to its role in providing energy for cellular metabolism, the intermediates of photosynthetic electron transport chain have been suggested to monitor the overall physiological conditions through redox active intermediates [26, 27]. It has been suggested that the redox state of plastoquinone (PQ), an electron carrier that transfers

electrons from PSII to cytochrome b6f, is involved in the regulation of photosynthetic genes among other genes. In this scheme, oxidized PQ controls PSII genes whereas reduced PQ controls PSI genes. Our analysis shows that the majority of perturbations led to downregulation of both PSII and PSI genes, suggesting against the involvement of the redox state of PQ as the principal regulator of photosynthesis genes. Regardless of the factors involved in photosynthesis gene expression, it is evident from our analysis that downregulation of photosynthetic activity is key to acclimation under a majority of perturbations. Our analysis additionally shows that the regulation of photosynthesis genes in *Synechocystis* is associated with the general stress response.

Energy metabolism: *Synechocystis* contains active glycolysis/gluconeogenesis pathways. In most cases, reduced carbon generated from photosynthesis enters the glycolytic pathway and is subsequently utilized in many biosynthetic pathways. In some conditions, reduced carbon is stored in the form of glycogen which can be utilized later to provide energy, and as a carbon source for many biosynthetic pathways [28]. Our analysis shows that energy metabolism is another functional category for which a number of genes were present in the CTR. Most of these genes were also downregulated across the different experimental conditions. Thus, it is clear from our analysis that most perturbations lead to downregulation of energy production through the two major routes, photosynthesis and energy metabolism, in *Synechocystis*. These results are in accordance with studies from other organisms, where shutting down major energy producing pathways have been suggested to be important in acclimation under stress conditions.

Translation: Translation is another process for which several genes were present in the CTR, and in general, they were downregulated. Downregulation of ribosomal genes suggests that most perturbations in *Synechocystis* result in the transient translational/growth arrest similar to what has been suggested for several other organisms [4, 18, 21, 22]. It is noteworthy that expression of ribosomal genes in *Synechocystis* correlates with regulation of energy producing pathways (photosynthesis and energy metabolism). Thus, it can be suggested that regulation of genes involved in photosynthesis, energy metabolism and translation are controlled in anticipation of changes in growth under perturbations.

Stress proteins: Genes encoding a number of proteins with known functions in cellular protection and repair including HSPs, proteases, sigma factors, and antioxidant proteins were present in the CTR and they were upregulated across perturbations. Upregulation of genes encoding stress proteins are suggestive of two intertwined attributes; damage to proteins and increased production of reactive oxygen species (ROS) due to cellular redox imbalance caused by perturbation. The maintenance of redox balance is particularly challenging for oxygenic photosynthetic organisms like *Synechocystis* because photosynthesis inherently produces strong oxidants and reductants. Additionally, multiple redox active intermediates are used as electron carriers in the photosynthetic electron transport chain. Thus, any disturbance in the photosynthetic electron transport chain and/or activity of enzymes involved in photosynthesis significantly influences the redox poise leading to an increased production of ROS.

Regulatory genes: The CTR contains six regulatory and sensory genes. Four of these genes (*sll1742*, *slr1738*, *slr1285* and *sll1392*) were upregulated while two (*sll1555* and *sll1291*) were downregulated. Interestingly, known genes under the control of these regulatory proteins were also part of the CTR suggesting that the regulatory and their target genes may be co-regulated. For example, the *slr1285* (*hik34*) gene has been suggested to be involved in expression of HSP genes [29], and as described in the previous section, several HSP genes are part of the CTR. Both *hik34* and HSP genes were upregulated in most perturbations. Similarly, the *sll1392* gene has been named *pfsR*, an acronym for photosynthesis, Fe homeostasis, and stress response [30]. Although, little is known about genes under the control of PfsR, we find that numerous genes belonging to photosynthesis, Fe homeostasis, and stress response are part of the CTR. A third gene, *sll1291* (*rre12*), is part of a gene cluster involved in regulating chemotaxis. Chemotaxis is a general phenomenon found in bacteria, and is required for optimal growth under unfavorable conditions. In addition, we find that regulation of the *hik42* gene, a hybrid sensor and regulator, is conserved across perturbations suggesting an important role for its product in the development of appropriate adaptation strategies. Finally, the *slr1738* gene encoding PerR, was also present in the CTR. PerR is a transcriptional regulator belonging to the Fur family of regulators that negatively controls a set of genes responding specifically to oxidative stress [31, 32].

Genes with unknown functions: Nearly 40% of the genes in the CTR encode proteins with unknown functions. Some of these genes have orthologs in at least another

cyanobacterial strain while some are only present in *Synechocystis*. These specific *Synechocystis* genes may impart their unique signature features necessary for survival in the natural habitat. Identification of these unknown genes in the CTR provides a strong foundation to determine their functional roles in the development of adaptation strategies under perturbations. For example, we find that a gene cluster, *sll1783-sll1785*, is consistently regulated across perturbations. A literature survey shows that the *sll1785* gene has recently been implicated in the transport of copper [33]. We hope that the identification of the commonly regulated unknown genes will spur research work to identify their crucial role(s) in cyanobacterial physiology.

Other genes: In addition to the above described functional groups, genes involved in other cellular processes were also present in the CTR (additional file 4). However, the numbers of genes regulated in these pathways were not as large when compared to the functional groups described in the previous sections. A primary reason for the lesser number of genes could be related to our observation that the same gene(s) in a given pathway were not always regulated across various experimental conditions. It remains to be seen if these pathways are controlled by differential regulation of different set of genes specific to certain conditions.

Regulation of the CTR

We next asked whether transcriptome data sets can provide insights into the mechanism regulating the CTR. We considered two possibilities: (i) a single regulatory system

responding to an internal signal commonly generated under most perturbations, or (ii) a complex set of regulatory network systems responding to either internal or external signals. In the latter case, change(s) in the components and/or functional states of a regulatory system under a specific condition leads to an overall modulation of the network. This in turn triggers the regulation of the CTR. An indication of the potential mechanism(s) comes from regulation of genes involved in photosynthesis, energy metabolism, nutrient assimilation and translation described in previous sections. A majority of these genes showed similar pattern(s) of regulation, which is in agreement with the suggestion that photosynthesis is tightly connected with other metabolic pathways. Thus, it can be suggested that regulation of the CTR under perturbation is linked to the activity of the photosynthetic electron transport chain. Such a hypothesis has been considered previously. It has been suggested that the redox state of PQ is involved in communicating environmental signals to regulatory circuits such as the one that controls the CTR [26, 27, 34, 35]. However, our analysis shows that the regulation of photosystem genes is not dependent on the redox state of PQ. This finding is in accordance with a previous study which showed that treatment of *Synechocystis* with saturating amount of DCMU and DBMIB led to downregulation of photosynthetic genes [36]. We propose that regulation of the CTR is controlled by ROS. Evidence for the involvement of ROS comes from the identification of numerous upregulated genes involved in protection against ROS including superoxide dismutase, *aphC* (encoding a type-2 peroxiredoxin) and *perR*. Upregulation of superoxide dismutase provides support to our argument that most perturbations lead to increased production of hydrogen

peroxide in the cell. Additionally, expression of *aphC* and *perR* genes, both expressed from the same divergent promoter in *Synechocystis*, are known to be responsive to hydrogen peroxide [31, 32]. Our analysis also provides evidence for the involvement of multiple regulatory and sensory proteins in regulation of the CTR in *Synechocystis*. Evidence for this comes from the presence of several regulatory genes and their target genes in the CTR (additional file 4). These results together suggest that multiple regulatory network systems sense internal signal(s) in the form of ROS produced under various perturbations to regulate the CTR. We note that this conclusion is based entirely on the expression patterns of genes. Further experimentation based on these findings will be necessary to establish a role of ROS in the regulation of the CTR.

Large-scale transcriptomic data sets have been useful in identifying groups of genes showing similar patterns of expression. Such analyses have been used to predict functions of unknown genes based on coregulation with functionally known genes and for the identification of target genes of transcriptional regulators. The latter is based on the assumption that regulatory factors are themselves transcriptionally regulated such that their expression patterns are strongly correlated with target genes. To identify whether genes in the CTR are coregulated with any of the regulatory genes in *Synechocystis*, we developed a correlation matrix for 146 regulatory genes. We identified genes as being coregulated with a given regulatory gene, if their expression profiles correlate in at least 60% of the experiments. The use of this criterion is based on the expression profiles of two genes, *perR* (a regulatory gene) and *aphC* gene, divergently transcribed from a

common promoter. Transcription of these two genes is negatively controlled by PerR which binds to a single PerR site present in the promoters of these genes. Inactivation of PerR leads to simultaneous expression of both genes [31, 32]. Our analysis shows that expression profiles of these two genes were similar in 61% of the experiments. We found that expression patterns of 25 regulatory genes could be correlated with more than 85% of genes found in the CTR (Fig. 2). As can be expected, expression patterns of some genes were found to be correlated with multiple regulatory genes while others showed coregulation with a single regulatory gene (additional file 5). Interestingly, the expression patterns of several unknown genes were found to be correlated with multiple regulatory genes.

A correlation between expression patterns for regulatory and target genes provides the first step towards a full understanding about the existence of regulatory networks. This is especially true for *Synechocystis* where little is known about the existence of such networks. To begin with, we looked for the previously reported regulatory factors and their target genes and whether our analysis was able to capture them. We find that several HSP genes are coregulated with the *hik34* gene (Fig. 2; additional file 5). As previously mentioned, Hik34 has been suggested to be involved in the regulation of HSP genes in *Synechocystis* [29]. These results indicate that identification of coregulated genes could provide useful information on regulatory networks. Next, we attempted to determine whether target genes contain conserved cis-elements involved in the binding of transcriptional regulators. Unfortunately, not many cis-elements specific to

transcriptional regulators have been identified in *Synechocystis*. Of the regulatory genes selected, only the binding site of PerR is known. A 15-bp consensus sequence (TTATAATnATTATAA) is known to be required for the binding of PerR in *Bacillus subtilis* [37]. A similar binding site has been suggested in *Synechocystis* [32]. Our analysis shows that a total of 53 genes were coregulated with the *perR* gene. Interestingly, expression patterns of some genes were strongly correlated with the *perR* gene; even better than the correlation with the *aphC* gene. A survey of the PerR binding site in the upstream regions of all 53 coregulated genes showed that very few genes contain such a repeat. In fact, we were unable to find a canonical binding site for PerR in the upstream region of genes which showed stronger correlation to PerR than the divergently transcribed *aphC* gene. Whether the 15 bp binding site suggested in *B. subtilis* is also specifically needed for binding in *Synechocystis*, hence, needs further investigation. Additional mechanisms involved in possible gene regulation by the PerR regulator in *Synechocystis* cannot be ruled out at present.

Given the possibilities mentioned in the previous paragraph, we investigated regulatory gene(s) which were coregulated with a large number of genes. These genes include *sll1771* (coregulated with 113 genes), *rre12* (64 genes), *slr2024* (56 genes), *perR* (53 genes) and several others (see additional file 5). Some of these genes (*perR* and *rre12*) have been described in previous sections. The *sll1771* gene encodes PphA, a PP2C-type phosphatase suggested to be involved in dephosphorylation of the PII protein in *Synechocystis* [38]. The PII protein has been suggested to be involved in sensing the C/N

ratio in cyanobacteria [39]. Its activity is controlled by phosphorylation [38]. The large number of genes showing coregulation with the *pphA* gene was notable. Further analysis suggests a basis for correlation of the *pphA* expression along with its coregulated genes. As previously stated, cyanobacteria grown under photoautotrophic conditions acquire and fix carbon through the Calvin cycle using the energy generated by photosynthesis. The fixed carbon enters the glycolytic pathway and is utilized for nitrogen assimilation and for biosynthetic pathways. Assimilation of both C and N are energy intensive. Therefore, a tight correlation must exist on the expression patterns of genes involved in the various aspects of C and N metabolism. Because the PII protein is a global regulator of C/N assimilation and phosphorylation plays a key role in its activity, it is understandable that the expression patterns of so many genes coincide with that of the *pphA* gene. We also note that the expression pattern of the *glnB* gene, which encodes the PII protein, was correlated with the transcription of very few genes. These results suggest that regulation of C/N by the PII protein does not require significant changes in transcript levels of the *glnB* gene. Instead, a change in the transcript levels of the *pphA* gene is the key to regulating PII activity. We also found that expression patterns of a large number of ribosomal genes were correlated with the *nusG* (*sll1742*) gene. NusG is a regulator of gene expression known for complex and sometimes opposite effects on mRNA elongation [40].

Identification of KEGG pathways responsive to perturbations

Our analysis of the CTR has led to the identification of key functional groups that are regulated in a concerted manner to allow cells to adapt under different perturbations. However, it is not clear how changes in a few major cellular processes affect others. Recent studies have shown that coordination between cellular pathways is the key to developing an appropriate adaptive response under perturbations [1, 8, 19, 41]. During the analysis of transcriptome data sets, we noticed that some genes for a given cellular process were regulated in some data sets while a different set of genes for the same process were regulated in other data sets. It is highly possible that the regulation of a pathway is the same under diverse perturbations, although the changes are brought about by the regulation of different sets of genes in the pathway. Additionally, we observe that some KEGG pathways contain genes exhibiting negatively correlated expression dynamics. Such negative correlations of gene expression have been previously observed in other organisms, and may ultimately be related to interactions between various pathways [21, 42]. Therefore, we next determined the regulation of KEGG pathways across perturbations.

Based on Cyanobase annotations, there are currently 1582 genes (~45% (1582/3495)) with assigned functions in *Synechocystis*. Of these, 917 genes are associated with KEGG pathways, with some having multiple entries (1482 total entries). Accordingly, 60% of genes with known functions are currently associated with one of the 103 KEGG pathways listed for *Synechocystis*. In order to understand pathway level behaviors,

expression levels of genes belonging to a pathway from individual data set were considered together and subsequently collapsed into a single value using the one-sample ‘Kolmogorov-Smirnov (KS)’ test [43] as described in the Methods section. Figure 3 shows an example of how the transcript levels of genes belonging to the component ‘ribosome’ are distributed among various experiments. The histogram in figure 3A corresponds to values observed under the ‘Singh_nitrogen_starvation’ experiment (additional file 6). Based on the KS test, this distribution was identified as being significantly different from a population with a mean of zero. Therefore, we assigned the value -1 indicating that the component ribosome was downregulated. Similarly, figure 3(B) and 3(C) show the corresponding histograms for the two experiments ‘KEGG_Hihara_hl_15 min’ and ‘KEGG_Hihara_hl_15 h’, respectively (additional file 6). Distributions in figure 3(B) did not meet the significance criterion and were assigned a value of 0, indicating the component ribosome was not differentially expressed. In contrast, the population in 3(C) had a positive mean, significantly different from zero and therefore, we assigned to it a value of +1, representing upregulation. Initially, we considered all KEGG pathways for which a gene has been assigned in *Synechocystis* (additional file 6). Further manual examination revealed that 51 KEGG pathways showed significant regulation across the different experimental conditions (additional file 7). Such an examination was necessary to remove bias introduced by transcriptome data sets generated from any single laboratory. Of the remaining KEGG pathways that were removed from further analysis, some pathways had either only a small number of

Synechocystis genes in the pathway (less than 3 genes) or the number of differentially regulated genes was small.

Coordination between KEGG pathways

To understand the coordination between various KEGG pathways under different perturbations, we generated a Bayesian network based on 51 selected KEGG pathways. A Bayesian network is a graphical model representing probabilistic relationships between different factors (in our case pathways) [44]. The nodes in the network correspond to random variables in the system while links between nodes represent probabilistic relationships. The compendium of large data sets made it possible to derive a realistic, systems level Bayesian network for *Synechocystis*. Such an approach has several desirable properties including a solid probabilistic background behind the algorithms, including an ability to combine data from different conditions, and an ability to make inferences of network changes under perturbations which can be tested in subsequent experiments. As expected, links in the network do not account for the same level of influence by parent nodes to the child node. We therefore quantified the link strengths by using the ‘True Link Strength Percentage’ as described in the Methods section. Figure 4 shows the resulting network for the selected 51 KEGG pathways. The various colors of the links represent the influence of the corresponding parent node on the child. The link strength percentages for the network varied between 15.8% and 45.8% (additional file 8). In addition, the link between two pathways does not always suggest positive correlation.

It is quite possible that two pathways are linked together because the overall expression of the two pathways is consistently negatively correlated across various perturbations.

A powerful feature of the Bayesian network is making inferences on expected changes in the networks under different perturbations. This allows one to make predictions on possible modifications to the pathways so that a desired behavior is obtained from the system. There are several existing algorithms to perform inferences on Bayesian networks. Among these, the junction tree algorithm is one popular technique to get marginal probabilities of a Bayesian network given evidence(s) (see Methods for details). We have simulated several hypothetical perturbations using our network. We used three different scenarios: first, we downregulated the photosynthesis antenna system; second, we downregulated photosynthesis antenna system while simultaneously upregulating glycolysis, and finally, we downregulated both photosynthesis antenna system and glycolysis to understand how other KEGG pathways respond to these changes. Results of such conditional changes on the response of other pathways are shown and discussed in the additional file 9.

The analysis of network shows many expected as well as novel coordination(s) between various pathways. Moreover, it demonstrates how a specific effect on a particular pathway will impact the function of other cellular processes in *Synechocystis* (additional file 9). On a long term basis (if the perturbation persists), even an effect on a single pathway will eventually have a ripple effect on all other pathways. In essence, no

pathway is an island. Since a significant amount of metabolic activity in *Synechocystis* is devoted to assimilation of C and N as well as protein synthesis, we have described in detail the coordination between KEGG pathways related to these metabolic activities, namely, glutamate metabolism, carbon fixation, and protein synthesis. The Bayesian network shows that glutamate metabolism in *Synechocystis* is probabilistically linked to the four other KEGG pathways involved in nitrogen assimilation i.e, nitrogen metabolism, arginine metabolism, urea cycle and metabolism of amino acids (Fig. 4). It is quite remarkable that a network derived from behavior of pathways based on transcriptional regulation shows close interdependence between various pathways involved in nitrogen metabolism. At the outset, the coordination between these pathways is significant because all these pathways are associated with the assimilation of nitrogen but utilizes different nitrogen sources such as nitrate, ammonium, urea, and arginine. It is also noteworthy that glutamate metabolism is the parent node connecting all other nitrogen pathways. This is significant, because all routes leading to the assimilation of N go through glutamate metabolism. The coordination between various pathways involved in nitrogen assimilation is also important given the fact that certain nitrogen assimilation pathways are energy intensive processes. It is therefore expected that the system would maximize resources under perturbation and utilize nitrogen sources that require minimal energy input. For example, the conversion of 1 mole of nitrate (present in the BG11 growth medium) to NH_4^+ by GS-GOGAT cycle requires 8 moles of reduced ferredoxin [45]. Any perturbation that affects the photosynthetic process leading to lesser production of reduced ferredoxin would lead to an activation of pathways involved in transport and

assimilation of other nitrogen sources. Indeed, we have recently found that illumination of *Synechocystis* with light that preferentially excites PSII leads to preferential utilization of an alternate nitrogen assimilation pathway over GS-GOGAT pathway [46].

A second node that is physiologically well understood involves carbon fixation. *Synechocystis*, like other photosynthetic organisms, utilizes energy produced from photosynthetic light reactions to fix atmospheric CO₂. It is expected that the rate of CO₂ fixation will be tightly linked to the activity of photosynthetic electron transport chain. The Bayesian network shows that carbon fixation is probabilistically linked to three KEGG pathways, namely glycolysis, pentose phosphate pathway and oxidative phosphorylation (Fig. 4). It is interesting to note that the transcriptional regulation of genes involved in carbon fixation is not correlated with expression of photosynthetic genes but to expression of genes involved in oxidative phosphorylation. In fact, the link strength between carbon fixation and oxidative phosphorylation was one of the strongest in the network. Thus, our analysis shows the expected relationship between the rates of ATP production to carbon fixation. The interaction of carbon fixation with glycolysis and the pentose phosphate pathway is expected since ribulose-1, 5-bisphosphate, the primary acceptor for CO₂, is regenerated by using the pentose phosphate pathway. Similarly, the product of carbon fixation, 3-phosphoglycerate, is channeled through glycolysis for either biosynthesis or glycogen accumulation. We also note that expression of glycolytic genes was not correlated with regulation of genes involved with the TCA cycle. It would be expected that flux changes in glycolysis will directly affect the flux through the TCA

cycle and therefore expression patterns of genes encoding proteins involved in the TCA cycle should correlate with those of glycolytic genes. This lack of an interaction may appear surprising, but it is not an unlikely scenario considering the function of the TCA cycle in cyanobacteria. Unlike other organisms, cyanobacteria have an incomplete TCA cycle. It has been suggested that the TCA cycle in cyanobacteria is primarily utilized as a source for the production of precursors for N assimilation and biosynthesis [47]. Additionally, we have recently observed in a quantitative proteome study under varying environmental conditions that few substrates of TCA cycle can be regenerated from sources other than the glycolytic pathway (Wegener et al., unpublished results).

A third node of significant interest to the maintenance of homeostasis in *Synechocystis* is the function of the ribosome. Synthesis of the ribosome has been linked with the growth rate of organisms [48]. The Bayesian network in the present study shows that ribosome is probabilistically linked to oxidative phosphorylation, RNA polymerase and aminoacyl-tRNA biosynthesis (Fig. 4). While the coordination of the ribosome activity with RNA polymerase and aminoacyl-tRNA biosynthesis are expected, the link between the ribosome and oxidative phosphorylation is indeed fascinating. Ribosome function often depicts the status of cellular activity with faster growth leading to more ribosome synthesis and vice versa. Our analysis suggests that the expression of ribosomal gene is linked to ATP generation in *Synechocystis*. To look closer at the similarity of expression patterns between the ribosomal and ATP synthase genes, we compared the expression of genes belonging to these two processes under several perturbations (Fig. 5). We chose

only those conditions where significant number of genes in these two processes was affected. Indeed, we found that the gene expression patterns in these two categories positively correlate to each other.

CONCLUSION

In summary, large-scale transcriptomics data sets obtained under diverse perturbations on a cyanobacterium have been integrated. A compelling rationale for the importance of the present study is embedded in the sources of the data sets. The data sets were generated in multiple laboratories using different platforms with mostly undocumented physiological conditions of the cells. Despite these limitations, we have found that a large number of *Synechocystis* genes found on chromosome (~12%) are commonly regulated upon changes in the existing conditions. A majority of genes in this group belong to photosynthesis, energy metabolism, and translation, suggesting that these functions respond mostly to internal perturbation secondary to the primary stress. Additionally, genes involved in the two major energy producing pathways (photosynthesis and energy metabolism) and translation are mostly downregulated. These results provide evidence that a major adaptation strategy in *Synechocystis* is the regulation of genes in the anticipation of changes in growth during altered environmental conditions. We also identified coregulation of the CTR genes with regulatory genes which has provided insights into the regulatory networks in *Synechocystis*. We further utilized these large data sets to generate a Bayesian network based on KEGG pathways. This network has provided new insights on the coordination and interaction between various metabolic pathways in *Synechocystis*. Overall, our study has significantly increased the understanding of cellular strategies through the lens of transcriptomics in a photoautotroph. We have provided all data sets generated in this study, which will be a

valuable resource to the entire cyanobacterial and plant research community for all gene expression related queries.

REFERENCES

1. R Bonneau, MT Facciotti, DJ Reiss, AK Schmid, M Pan, A Kaur, V Thorsson, P Shannon, MH Johnson, JC Bare, et al: **A predictive model for transcriptional control of physiology in a free living cell.** *Cell* 2007, **131**:1354-65.
2. LM de Godoy, JV Olsen, J Cox, ML Nielsen, NC Hubner, F Frohlich, TC Walther, M Mann: **Comprehensive mass-spectrometry-based proteome quantification of haploid versus diploid yeast.** *Nature* 2008, **455**:1251-4.
3. AM Feist, BO Palsson: **The growing scope of applications of genome-scale metabolic reconstructions using Escherichia coli.** *Nat Biotechnol* 2008, **26**:659-67.
4. F Girardot, V Monnier, H Tricoire: **Genome wide analysis of common and specific stress responses in adult drosophila melanogaster.** *BMC Genomics* 2004, **5**:74.
5. TR Hughes, MJ Marton, AR Jones, CJ Roberts, R Stoughton, CD Armour, HA Bennett, E Coffey, H Dai, YD He, et al: **Functional discovery via a compendium of expression profiles.** *Cell* 2000, **102**:109-26.
6. RG Jenner, RA Young: **Insights into host responses against pathogens from transcriptional profiling.** *Nat Rev Microbiol* 2005, **3**:281-94.
7. AR Joyce, BO Palsson: **The model organism as a system: integrating 'omics' data sets.** *Nat Rev Mol Cell Biol* 2006, **7**:198-210.

8. S Komili, PA Silver: **Coupling and coordination in gene expression processes: a systems biology view.** *Nat Rev Genet* 2008, **9**:38-48.
9. S Ma, HJ Bohnert: **Integration of Arabidopsis thaliana stress-related transcript profiles, promoter structures, and cell-specific expression.** *Genome Biol* 2007, **8**:R49.
10. PG Falkowski, LV Godfrey: **Electrons, life and the evolution of Earth's oxygen cycle.** *Philos Trans R Soc Lond B Biol Sci* 2008, **363**:2705-16.
11. ZI Johnson, ER Zinser, A Coe, NP McNulty, EM Woodward, SW Chisholm: **Niche partitioning among Prochlorococcus ecotypes along ocean-scale environmental gradients.** *Science* 2006, **311**:1737-40.
12. JF Kasting: **Earth history. The rise of atmospheric oxygen.** *Science* 2001, **293**:819-20.
13. T Cavalier-Smith: **Chloroplast evolution: secondary symbiogenesis and multiple losses.** *Curr Biol* 2002, **12**:R62-4.
14. JF Kasting, JL Siefert: **Life and the evolution of Earth's atmosphere.** *Science* 2002, **296**:1066-8.
15. JF Kasting: **When methane made climate.** *Sci Am* 2004, **291**:78-85.
16. T Kaneko, S Sato, H Kotani, A Tanaka, E Asamizu, Y Nakamura, N Miyajima, M Hirose, M Sugiura, S Sasamoto, et al: **Sequence analysis of the genome of the unicellular cyanobacterium Synechocystis sp. strain PCC6803. II. Sequence determination of the entire genome and assignment of potential protein-coding regions.** *DNA Res* 1996, **3**:109-36.

17. SA Rifkin, J Kim, KP White: **Evolution of gene expression in the *Drosophila melanogaster* subgroup.** *Nat Genet* 2003, **33**:138-44.
18. MJ Brauer, C Huttenhower, EM Airoidi, R Rosenstein, JC Matese, D Gresham, VM Boer, OG Troyanskaya, D Botstein: **Coordination of growth rate, cell cycle, stress response, and metabolic activity in yeast.** *Mol Biol Cell* 2008, **19**:352-67.
19. L Lopez-Maury, S Marguerat, J Bahler: **Tuning gene expression to changing environments: from rapid responses to evolutionary adaptation.** *Nat Rev Genet* 2008, **9**:583-93.
20. Y Jiao, OS Lau, XW Deng: **Light-regulated transcriptional networks in higher plants.** *Nat Rev Genet* 2007, **8**:217-30.
21. AP Gasch, PT Spellman, CM Kao, O Carmel-Harel, MB Eisen, G Storz, D Botstein, PO Brown: **Genomic expression programs in the response of yeast cells to environmental changes.** *Mol Biol Cell* 2000, **11**:4241-57.
22. JI Murray, ML Whitfield, ND Trinklein, RM Myers, PO Brown, D Botstein: **Diverse and specific gene expression responses to stresses in cultured human cells.** *Mol Biol Cell* 2004, **15**:2361-74.
23. A Tanay, I Steinfeld, M Kupiec, R Shamir: **Integrative analysis of genome-wide experiments in the context of a large high-throughput data compendium.** *Mol Syst Biol* 2005, **1**:2005 0002.
24. J Quackenbush: **Microarray data normalization and transformation.** *Nat Genet* 2002, **32 Suppl**:496-501.

25. AK Singh, T Elvitigala, M Bhattacharyya-Pakrasi, R Aurora, B Ghosh, HB Pakrasi: **Integration of carbon and nitrogen metabolism with energy production is crucial to light acclimation in the cyanobacterium *Synechocystis***. *Plant Physiol* 2008, **148**:467-78.
26. M Alfonso, I Perewoska, D Kirilovsky: **Redox control of psbA gene expression in the cyanobacterium *Synechocystis* PCC 6803. Involvement of the cytochrome b(6)/f complex**. *Plant Physiol* 2000, **122**:505-16.
27. T Pfannschmidt, K Brautigam, R Wagner, L Dietzel, Y Schroter, S Steiner, A Nykytenko: **Potential regulation of gene expression in photosynthetic cells by redox and energy state: approaches towards better understanding**. *Ann Bot (Lond)* 2009, **103**:599-607.
28. AK Singh, LA Sherman: **Pleiotropic effect of a histidine kinase on carbohydrate metabolism in *Synechocystis* sp. strain PCC 6803 and its requirement for heterotrophic growth**. *J Bacteriol* 2005, **187**:2368-76.
29. I Suzuki, Y Kanesaki, H Hayashi, JJ Hall, WJ Simon, AR Slabas, N Murata: **The histidine kinase Hik34 is involved in thermotolerance by regulating the expression of heat shock genes in *synechocystis***. *Plant Physiol* 2005, **138**:1409-21.
30. S Jantaro, Q Ali, S Lone, Q He: **Suppression of the lethality of high light to a quadruple HLI mutant by the inactivation of the regulatory protein PfsR in *Synechocystis* PCC 6803**. *J Biol Chem* 2006, **281**:30865-74.

31. M Kobayashi, T Ishizuka, M Katayama, M Kanehisa, M Bhattacharyya-Pakrasi, HB Pakrasi, M Ikeuchi: **Response to oxidative stress involves a novel peroxiredoxin gene in the unicellular cyanobacterium *Synechocystis* sp. PCC 6803.** *Plant Cell Physiol* 2004, **45**:290-9.
32. H Li, AK Singh, LM McIntyre, LA Sherman: **Differential gene expression in response to hydrogen peroxide and the putative PerR regulon of *Synechocystis* sp. strain PCC 6803.** *J Bacteriol* 2004, **186**:3331-45.
33. S Tottey, KJ Waldron, SJ Firbank, B Reale, C Bessant, K Sato, TR Cheek, J Gray, MJ Banfield, C Dennison, et al: **Protein-folding location can regulate manganese-binding versus copper- or zinc-binding.** *Nature* 2008, **455**:1138-42.
34. JF Allen: **Photosynthesis: the processing of redox signals in chloroplasts.** *Curr Biol* 2005, **15**:R929-32.
35. S Puthiyaveetil, JF Allen: **Chloroplast two-component systems: evolution of the link between photosynthesis and gene expression.** *Proc Biol Sci* 2009.
36. Y Hihara, K Sonoike, M Kanehisa, M Ikeuchi: **DNA microarray analysis of redox-responsive genes in the genome of the cyanobacterium *Synechocystis* sp. strain PCC 6803.** *J Bacteriol* 2003, **185**:1719-25.
37. M Fuangthong, AF Herbig, N Bsat, JD Helmann: **Regulation of the *Bacillus subtilis* fur and perR genes by PerR: not all members of the PerR regulon are peroxide inducible.** *J Bacteriol* 2002, **184**:3276-86.

38. A Irmeler, K Forchhammer: **A PP2C-type phosphatase dephosphorylates the PII signaling protein in the cyanobacterium Synechocystis PCC 6803.** *Proc Natl Acad Sci U S A* 2001, **98**:12978-83.
39. K Forchhammer: **Global carbon/nitrogen control by PII signal transduction in cyanobacteria: from signals to targets.** *FEMS Microbiol Rev* 2004, **28**:319-33.
40. RA Mooney, K Schweimer, P Rosch, M Gottesman, R Landick: **Two structurally independent domains of E. coli NusG create regulatory plasticity via distinct interactions with RNA polymerase and regulators.** *J Mol Biol* 2009, **391**:341-58.
41. T Koide, WL Pang, NS Baliga: **The role of predictive modelling in rationally re-engineering biological systems.** *Nat Rev Microbiol* 2009, **7**:297-305.
42. D Chen, WM Toone, J Mata, R Lyne, G Burns, K Kivinen, A Brazma, N Jones, J Bahler: **Global transcriptional responses of fission yeast to environmental stress.** *Mol Biol Cell* 2003, **14**:214-29.
43. FJ Massey: **The Kolmogorov-Smimov test for goodness-of-fit.** *J. Amer Statist Assoc.* 1951, **46**:68-78.
44. FV Jensen, TD Nielsen: **Bayesian Networks and Decision Graphs.** New York: Springer-Verlag Inc.; 2007.
45. A Herrero, AM Muro-Pastor, E Flores: **Nitrogen control in cyanobacteria.** *J Bacteriol* 2001, **183**:411-25.

46. AK Singh, M Bhattacharyya-Pakrasi, T Elvitigala, B Ghosh, R Aurora, HB Pakrasi: **A systems level analysis of the effects of light quality on the metabolism of a cyanobacterium.** *Plant Physiol* 2009.
47. E Flores, A Herrero: **Nitrogen assimilation and nitrogen control in cyanobacteria.** *Biochem Soc Trans* 2005, **33**:164-7.
48. RL Gourse, T Gaal, MS Bartlett, JA Appleman, W Ross: **rRNA transcription and growth rate-dependent regulation of ribosome synthesis in Escherichia coli.** *Annu Rev Microbiol* 1996, **50**:645-77.
49. R Edgar, M Domrachev, AE Lash: **Gene Expression Omnibus: NCBI gene expression and hybridization array data repository.** *Nucleic Acids Res* 2002, **30**:207-10.
50. M Kanehisa, S Goto, S Kawashima, A Nakaya: **The KEGG databases at GenomeNet.** *Nucleic Acids Res* 2002, **30**:42-6.
51. RW Hamming: **Error Detecting and Error Correcting Codes.** *Bell System Technical Journal* 1950, **26**:147-160.
52. O Pourret, P Naim, B Marcot: **Bayesian Networks: A practical Guide to Applications:** John Willey and Sons Ltd; 2008.
53. DM Chickering: **Optimal structure identification with greedy search.** *Journal of Machine Learning Research* 2002, **3**:507-554.
54. T Elvitigala, AK Singh, HB Pakrasi, B Ghosh: **Bayesian Network Approach to understand Regulation of Biological Processes in Cyanobacteria.** In: *IEEE Conference on Decision and Control*; 2009; Shanghai, China.

55. I Ebert-Uphoff: **Measuring Connection Strengths and Link Strengths in Discrete Bayesian Networks**. In: *Book Measuring Connection Strengths and Link Strengths in Discrete Bayesian Networks* (Editor ed.^eds.). City: Georgia Institute of Technology; 2007.

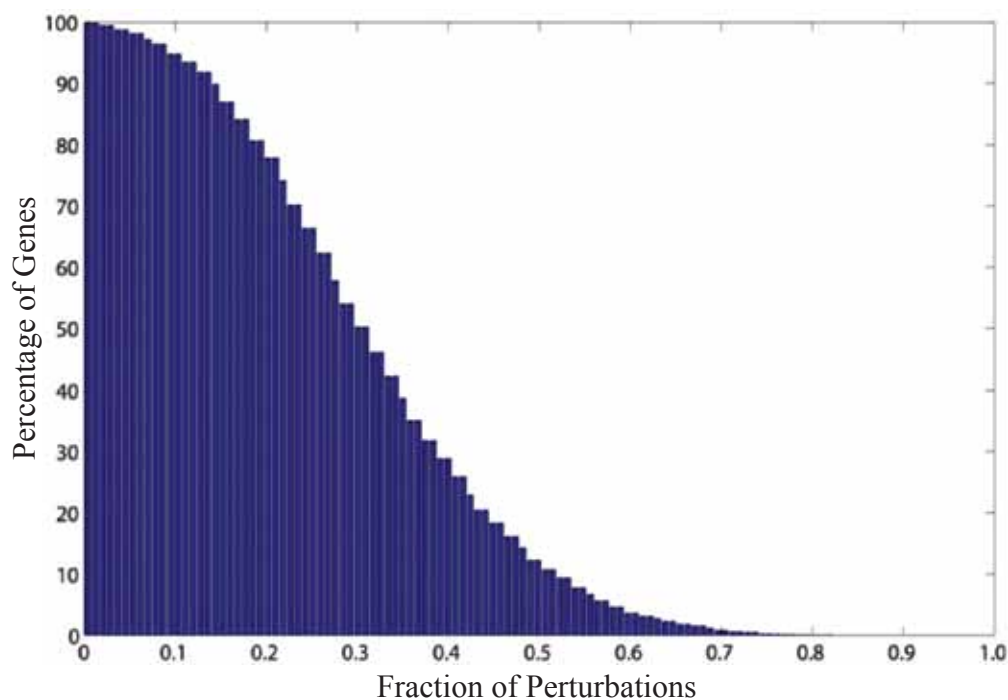


Figure 1. Differential regulation of *Synechocystis* genes across multiple perturbations. Differential regulation of genes was assessed by using a statistical significance test. Only 68 data sets generated under various environmental and genetic perturbations had sufficient number of replicates to be considered for the determination of such differential regulation of genes. All but 5 genes present on chromosome (3259/3264) were identified as differentially regulated in at least one experimental data set. The complete data sets with their respective fold changes are provided in the additional file 2.

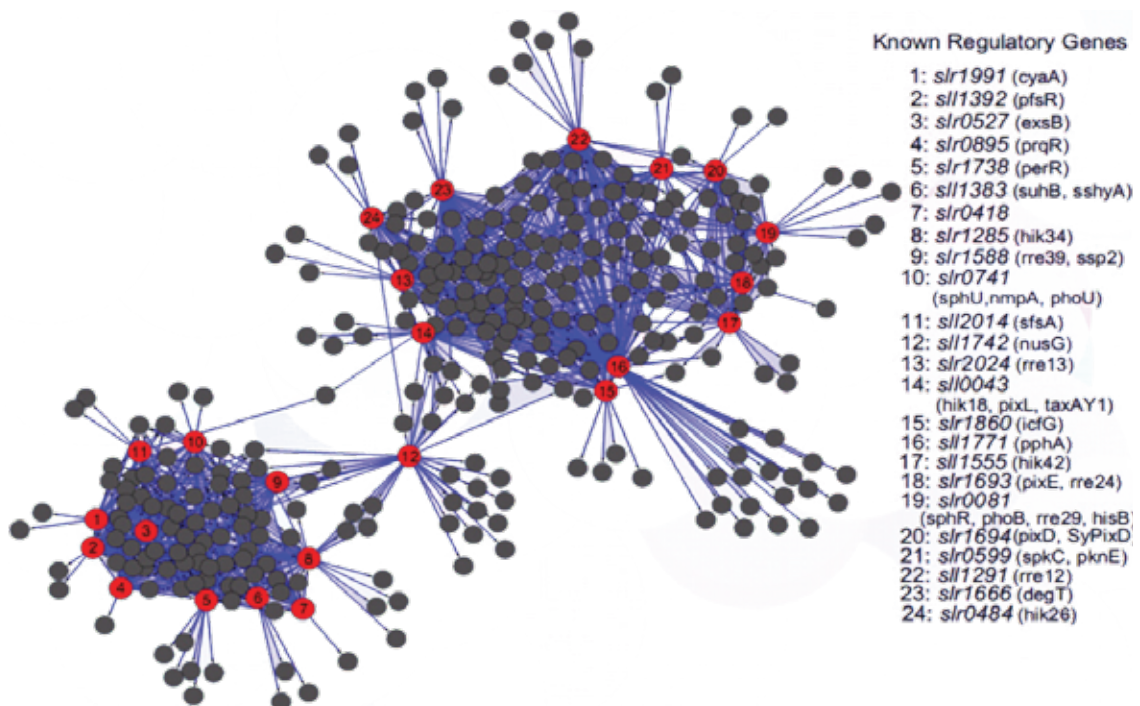


Figure 2. Coregulation of regulatory and CTR genes.

A correlation matrix was generated for the 146 regulatory genes and 399 genes present in the CTR by using the Hamming distance. Based on previous experimental results, we used 60% agreement as a cut-off to identify coregulation. Using this criterion, we could identify 25 regulatory genes (red solid dots) that were coregulated with 85% of the genes present in the CTR (black solid dots). The relevant similarity measurement values are provided in the additional file 5.

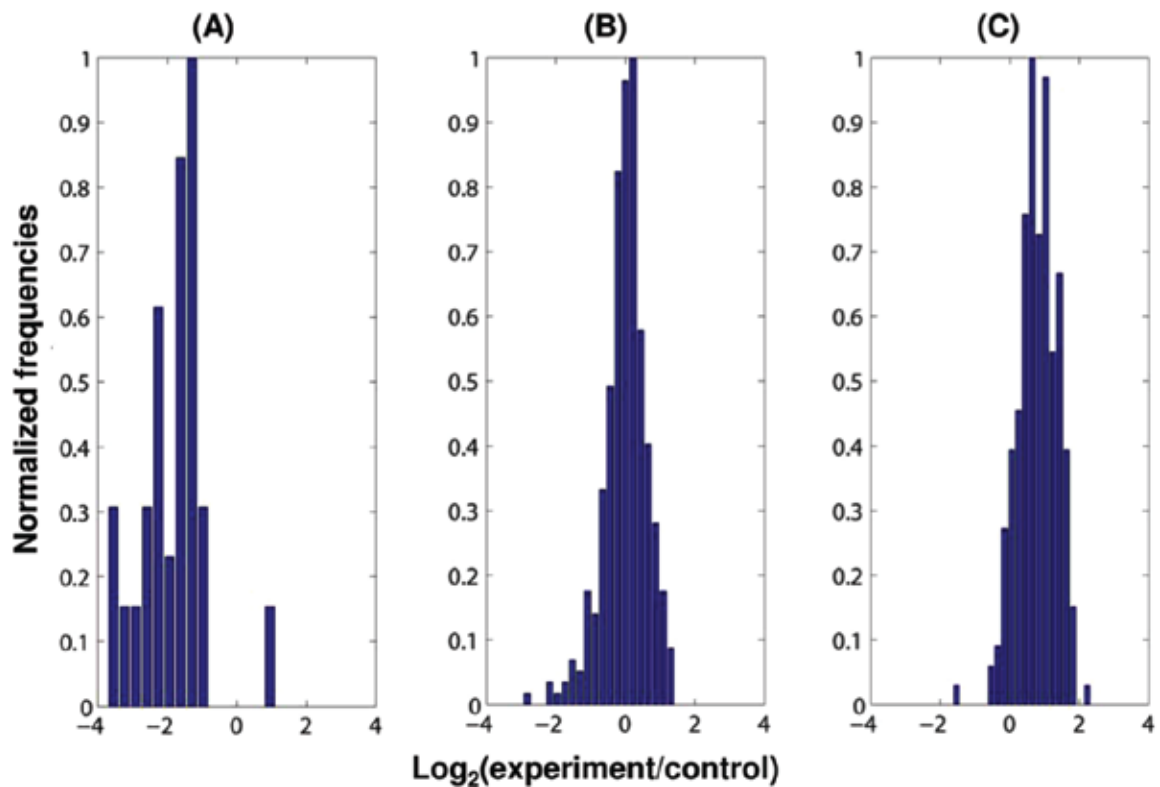


Figure 3. Regulation of the functional category “Ribosome” determined from its associated genes.

Distribution of \log_2 (target/control) values of individual genes for the functional category “ribosome” are shown for (A) Singh_nitrogen_starvation’, (B) ‘KEGG_Hihara_hl_15 min’ and (C) ‘KEGG_Hihara_hl_15 h’ (see additional file 6 for details). Based on the KS-test, “ribosomes” were either (A) downregulated, (B) not changed or (C) upregulated. Regulation of all KEGG pathways is provided in the additional file 6.

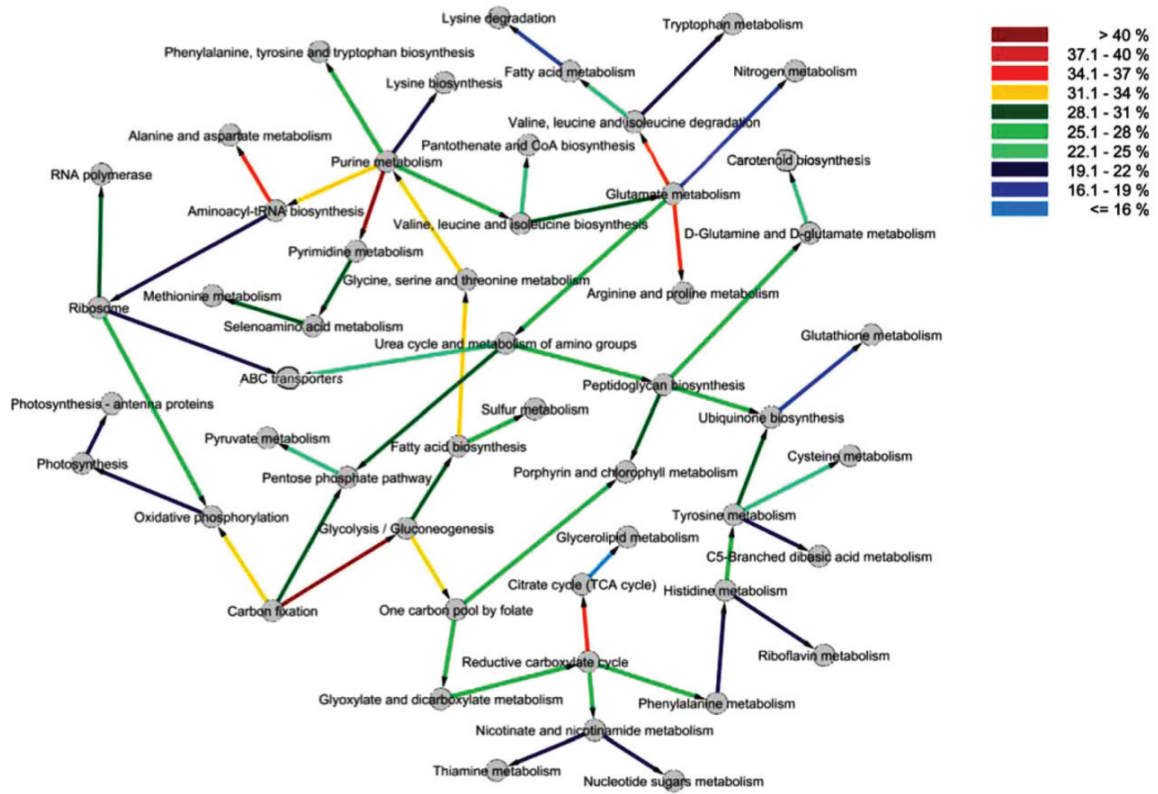


Figure 4. Bayesian network for 51 KEGG pathways derived using the GES algorithm.

Based on regulation of their associated genes, 51 KEGG pathways were identified as significantly regulated across multiple perturbations. The Bayesian approach was used to generate the network. The color of the arrows represent the strength of the links, quantified using the True Link Strength Percent 4 (see additional file 8).

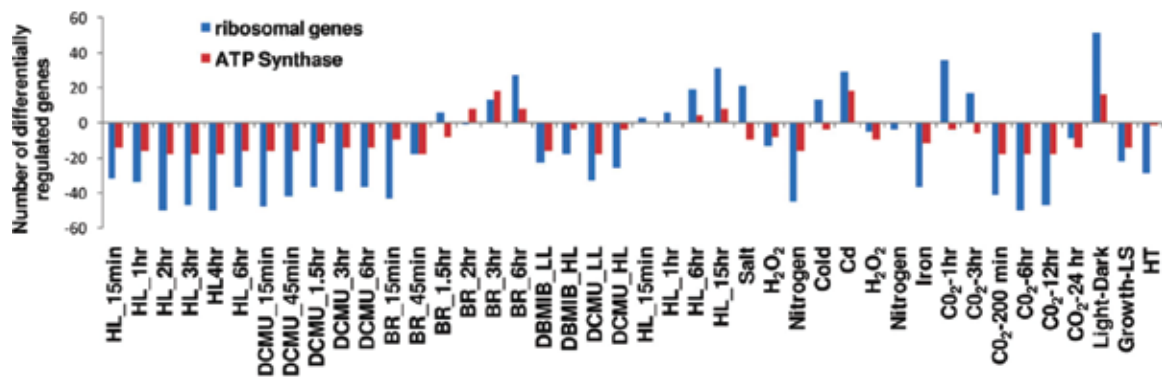


Figure 5. Coregulation of ribosomal and ATP synthase genes.

Data sets with the significant number of differentially regulated genes corresponding to functional categories “ribosome” and “ATP Synthase” were used to determine coregulation. The details of experimental conditions and differential regulation of genes corresponding of these two functional categories are provided in additional files 1 and 2, respectively. The various abbreviations used are HL = high light; DCMU = 3-(3,4-Dichlorophenyl)-1,1-dimethylurea; DBMIB = 2,5-dibromo-3-methyl-6-isopropyl-p-benzoquinone; BR = blue and red light; H₂O₂ = hydrogen peroxide; Cd = cadmium; LS = linear-stationary; and HT = high temperature.